Identifying and targeting defective immune surveillance mechanisms in myeloma using multi-parameter single cell profiling by mass cytometry

Frances Louise Seymour

August 2019

Submitted in partial fulfilment of the requirements of the Degree of Doctor of Philosophy

Centre for Haemato-Oncology

Barts Cancer Institute

Queen Mary University of London

Statement of originality

I, Frances Louise Seymour, confirm that the research included within this thesis is my own work or that where it has been carried out in collaboration with, or supported by others, that this is duly acknowledged below and my contribution indicated. Previously published material is also acknowledged below.

I attest that I have exercised reasonable care to ensure that the work is original, and does not to the best of my knowledge break any UK law, infringe any third party's copyright or other Intellectual Property Right, or contain any confidential material.

I accept that the College has the right to use plagiarism detection software to check the electronic version of the thesis.

I confirm that this thesis has not been previously submitted for the award of a degree by this or any other university.

Signature:

Date: 20/07/19

Collaborations

The work described in chapter 10 was performed in collaboration with Celgene Corporation. Celgene provided access to clinical samples and funded the work. I designed the mass cytometry panel, performed the optimisation work and performed mass cytometry on the clinical samples. The CITRUS algorithm was run by Mary Young of Celgene. I then performed data interpretation and further data analysis.

Meeting Abstracts

Seymour, F. Cavenagh, J. Gribben, J. Characterising the immunological microenvironment in newly diagnosed multiple myeloma. Blood 2018 132(Sup 1):58 Oral presentation at the 60th Annual Society of Haematology meeting, 1-4th December 2018, San Diego

Seymour, F. Young, M. Tometsko, M. Cavenagh, J. Thompson, E. Whalen, E. Danziger, S. Fitch, A. Fox, B. Dervan, A. Toy, T. Newhall, K. Gribben, J. Immune microenvironment analysis of bone marrow by mass cytometry and RNA sequencing in multiple myeloma patients treated with daratumumab and durvalumab. Blood 2018 132:3296 Poster presentation at the 60th Annual Society of Haematology Meeting, 1-4 December 2018, San Diego.

Truelove, E. Seymour, F. Matthews, J. Gribben, J. Deep phenotypic analysis reveals a monocyte subpopulation predictive of relapse/refractory diffuse large B-cell lymphoma. Blood 2018 132: 2863 Poster presentation at the 60th Annual Society of Haematology Meeting, 1-4 December 2018, San Diego

Seymour, F. Cavenagh, J. Gribben, J. Immunological profiling by mass cytometry reveals that TIM3 expression is reduced on NK cell subsets in newly diagnosed myeloma and is associated with loss of NK cell function and decreased survival. Haemasphere 2018 2(S1)219 Poster presentation at the 23rd Congress of the European Haematology Association, 14-17 June 2018, Stockholm

Seymour, F. Cavenagh, J. Gribben, J. Cytotoxic lymphocytes in newly diagnosed myeloma have reversible functional and phenotypic abnormalities that may offer therapeutic opportunities. Haematologica 2017 102(s1)498 ePoster presentation at the 23rd Congress of the European Haematology Association, 22-25 June 2017, Madrid

Abstract

Myeloma is a complex, incurable bone marrow malignancy of plasma cells with a diverse clinical course. Existing data suggests that abnormalities in T cell function and PD1 expression are present in myeloma and that immune subversion may be playing a role in progression of the disease. I hypothesise that characterisation of the cellular immunological landscape in myeloma will identify distinct functional populations which may offer therapeutic targets to restore immunological control of the disease.

Mass cytometry is a novel, single cell analysis technique which enables simultaneous assessment of more than 30 cell surface and intracellular antigens by utilising metal tagged antibody probes. Using this technology and an algorithmic based data analysis approach alongside traditional data analysis techniques I explored the bone marrow microenvironment in 9 control, 18 NDMM and 9 RRMM samples. RRMM samples were drawn from patients receiving dual targeting of CD38 and PDL1.

In NDMM I demonstrate that immune microenvironment changes include defects in antigen presenting populations, effector and helper lymphocyte populations and NK cells. These changes are present before treatment has been initiated and have prognostic significance. These functional defects are associated with upregulation of PD1 and PDL1 expression across multiple lineages.

In the RRMM setting treatment targeting PDL1 and CD38 results in early functional cytotoxicity and cytokine production signals.

Defective immunological responses correlate with poor clinical outcome and there is potential to restore immune function, providing a strong argument for considering multi-lineage immunological damage to represent a form of symptomatic myeloma.

Acknowledgements

The work presented in this thesis would not have been possible without the support and assistance of a number of people.

First I would like to thank my primary supervisor Professor John Gribben for giving me the support and freedom to pursue my interests in myeloma and create this project. His advice and mentorship has helped me to become a better clinician as well as researcher. I am also grateful for the opportunity to attend international meetings and conferences. I would also like to thank my secondary supervisor Professor Jamie Cavenagh for his support and advice.

There are many individuals within the Barts Cancer Institute who have provided invaluable help in finding my feet in the lab, planning experiments and troubleshooting problems. Particular thanks go to Joe Taylor, Robin Sanderson, Ed Truelove, James Aires and Jennifer Ball who have supported me through the highs and lows of this work and tolerated my own particular brand of humour.

I wish to thank the staff of the BCI Flow Core who assisted with the mass cytometry aspects of this work. Particular thanks go to Dr Becki Pike and Steve Lim who helped to get the project off the ground.

Thanks also to Dr Sameena Iqbal and the BCI tissue bank for access to the clinical samples that were so vital to this work. I am also indebted to the patients who allowed their blood and bone marrow to be used for clinical research.

This work was funded by the London Clinic Charity to whom I am very grateful for enabling me to carry out this project. Additional funding and access to clinical trial samples was provided by Celgene.

Finally I would like to thank Professor Guy Pratt for encouraging me to pursue my research dreams.

Table of contents

List of figures

List of tables

Abbreviations

AML	Acute myeloid leukaemia
ANOVA	Analysis of variance
BCI	Barts Cancer Institute
BCMA	B cell maturation antigen
BITE	Bi-specific T cell engager
BMMCs	Bone marrow mononuclear cells
C2D15	Cycle 2, day 15
CAR-T	Chimeric antigen receptor T cell
CDF	Cancer Drugs Fund
CI	Confidence interval
CITRUS	Cluster identification, characterisation and regression
CLL	Chronic lymphocytic leukaemia
CM	Central memory
CR	Complete response
CRAB	Hypercalcaemia, renal dysfunction, anaemia, bone pain
CFSE	Carboxyfluorescein succinimidyl ester
CT / PET-CT	Computed tomography / Positron emission computed tomography
CTD	Cyclophosphamide, thalidomide, dexamethasone
CTLA4	Cytotoxic T lymphocyte associated protein 4
CyTOF	Cytometry time of flight
DC	Dendritic cell
DLBCL	Diffuse large B cell lymphoma
DNA	Deoxyribonucleic acid
DNAM1	DNAX accessory molecule 1
DMSO	Dimethyl sufoxide

DVD	Daratumumab, bortezomib, dexamethasone
EBMT	European society blood and bone marrow transplantation
EBV	Epstein Barr virus
ECOG	Eastern cooperative oncology group score
EMRA	Terminally differentiated effector memory cell re-expressing CD45RA
FBS	Fetal bovine serum
FCS	Flow cytometry standard
FDA	US food and drug administration
FoxP3	Forkhead box P3
Gnz	Granzyme
GvHD	Graft versus host disease
HA	Health authority
HIV	Human immunodeficiency virus
HLA	Human leukocyte antigen
HR	Hazard ratio
IFNγ	Interferon gamma
Ig	Immunoglobulin
IGH	Immunoglobulin heavy gene
IL 2-35	Interleukin 2-35
IMiDs	Immune-modulatory drugs
IMS	Isopropanolol and methanol
Ir	Iridium
KIR	Killer cell immunoglobulin like receptor
KLRG1	Killer cell lectin like receptor G1
LAG3	Lymphocyte activating gene 3
LIR1	Leukocyte immunoglobulin like receptor 1

MGUS	Monoclonal gammopathy of uncertain significance
MHC	Major histocompatibility complex
MICA/B	MHC class1 polypeptide related sequence A/B
MM	Multiple myeloma
MMO	Metal minus one
MMM	Metal minus many
MPT	Melphalan, prednisolone, thalidomide
MSI	Mean signal intensity
MUC1	Mucin 1 cell surface associated
MW	Mann-Whitney
NDMM	Newly diagnosed multiple myeloma
NHS	National health service
NICE	National institute clinical excellence
NK	Natural killer
PBS	Phosphate buffered saline
PBMCs	Peripheral blood mononuclear cells
PCA	Principle component analysis
PD1	Programmed cell death protein 1
PDL1/2	Programmed cell death ligand 1/2
Perf	Perforin
PI	Proteasome inhibitor
PR	Partial response
RORγt	RAR related orphan receptor gamma
RPMI	Roswell Park Memorial Institute medium
RRMM	Relapsed refractory multiple myeloma
SAM	Significance analysis microarrays

SLAMF7	Signalling lymphocytic activation molecule 7
SPADE	Spanning-tree progression analysis of density normalised events
TCEP	tris(2-carboxyethy)phosphine
TCR	T cell receptor
TGFβ	Transforming growth factor beta
TH 1/2/17	T helper 1/2/17
TIM3	T cell immunoglobulin and mucin domain 3
TNFα	Tissue necrosis factor alpha
TRAIL	TNF related apoptosis inducing ligand
Treg	T regulatory cell
ULPB1	UL16 binding protein 1
VCD	Velcade, cyclophosphamide, dexamethasone
VDT	Velcade, dexamethasone, thalidomide

Note regarding terminology

The term myeloma is used when referring to the disease in general. The term NDMM and RRMM are used to refer to specific stages in the disease pathway.

1. The immune surveillance model of malignancy

1.1 Immune surveillance and immune dysregulation

1.1.1 Concept of immune surveillance and immune dysregulation in malignancy

The role of the immune system in recognising and destroying malignant cells was first proposed in 1909 by Paul Ehrlich [1]. In light of increasing evidence from murine models, in vitro analysis of human tumours and observations of human cancer behaviour this original model was incorporated into the three E's model of immune-editing [1], recognising the fact that when elimination of the malignant cells fails, the immune system continues to influence tumour growth and development. In this model the interaction between the immune system and the malignant cell are described be three phases; elimination, equilibrium and escape (Figure 1.1).

Stage 1: Elimination [1]. Elimination incorporates the classic immune-surveillance model and proposes that malignant cells are initially recognised and targeted by cells of the innate immune system. This initial response releases tumour antigens which recruit and drive the maturation of dendritic cells which are then able to prime and recruit antigen specific T cells. These tumour specific cells have direct cytotoxicity against the malignant cells. If this response is effective then the tumour clone will be eliminated. This is also known as the cancer-immunity cycle [2].

Stage 2: Equilibrium [1]. In situations where the tumour clone is not effectively eliminated a balance can be formed between tumour and immune cells. This equilibrium maintains the malignant population at macroscopically undetectable levels and may last for many years. Continued immunological response against the malignant cells will inevitably exert a Darwinian selective pressure which will drive the emergence of poorly immunogenic clones, in a process known as immune-selection [3]. This has been elegantly demonstrated in murine tumour transfer models where tumours from mice without an intact immune system are more immunogenic when transferred to wild type mice than those from mice with an intact immune system [4].

Stage 3: Escape. As the malignant cells become increasingly non-immunogenic they are able to proliferate unchecked by the immune system and clinically detectable disease becomes apparent. In addition to immune-selection a number of immune-subversion mechanisms contributing to tumour escape have been described including alterations in effector cells signal transduction [5], the release of tumour derived soluble factors such as MICA [1] which may function as a decoy molecule, modifications in tumour expression of MHC class I [6], expression of immunoregulatory ligands such as CD274 (Programmed death-ligand 1 (PD-L1) also known

as B7 homolog 1 (B7-H1) [7] and induction of immune regulatory cells [8]. In addition prolonged exposure of cytotoxic T cells to antigen which is not effectively cleared may result in a down regulation of cytotoxic activity as part of an evolutionary response to limit tissue damage [9].

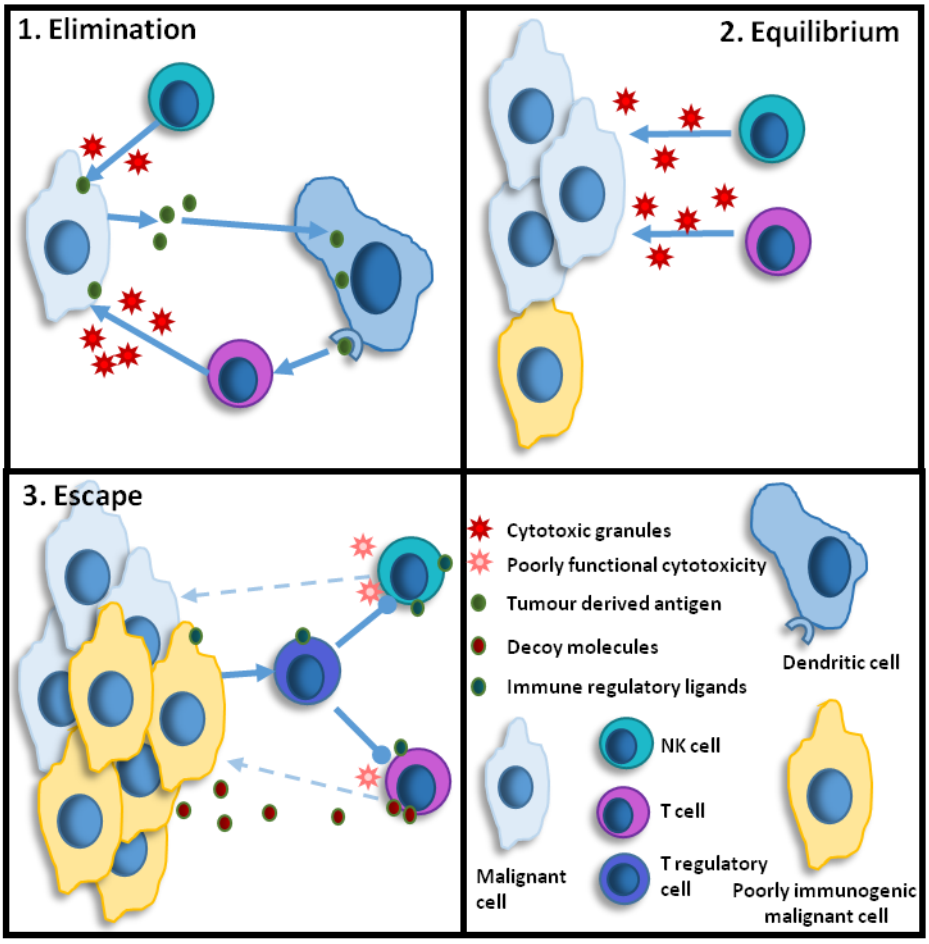

Figure 1.1: The immune surveillance model of malignancy

1.1.2 The body of evidence in support of the immune surveillance model

Observational support of the immune-editing concept includes the link between aging, with its associated decline in immune function, and malignancy [10] and the increased prevalence of cancer in individuals with congenital [11] or acquired [12] immunodeficiency syndromes or receiving immunosuppressing drugs [13]. Plasma cell disorders including MGUS [14] and myeloma [12] are reported at higher rates in individuals who are immunocompromised due to HIV. These observations all suggest that when the immune system is compromised risk of malignancy rises. These associations have become increasingly apparent as life expectancy has improved.

In the Rag $2^{-/-}$ mouse model of immunodeficiency, which lack mature lymphocytes, an increased rate of both spontaneous tumours (12/12 $Rag2^{-/-}$ v. 0/11 wild type) and carcinogen

induced tumours ($RAG2^{-/-}$ 30/52, wild type 11/57 p=<0.0001) are observed [4]. In genetic models of malignancy, perforin deficient mice develop more cases of lymphoma than wild type controls ($perf^{-/-}$ 9/12 v. wildtype 1/16 p=0.0091) [15]. These mouse models demonstrate the importance of a functioning, cytotoxic immune system in resisting malignant transformation.

In human malignancy associations have been reported between the presence of tumour infiltrating lymphocytes in histological specimens and improved survival in breast [16], oesophageal [17] and small cell lung [18] cancer. NK cell tumour infiltration has also been associated with improved prognosis in breast [19], gastric [20] and lung [21] cancer.

$CD4^+$ T regulatory cells have also been implicated in the development of malignancy. While the usual role of T regulatory cells is to suppress cytotoxicity against self antigen and thereby prevent autoimmunity, in the context of malignancy this can result in suppression of immune surveillance. Histological infiltration of tumour with T regulatory cells is associated with a poor prognosis in a range of malignancies including diffuse large B cell lymphoma (DLBCL) [22], breast cancer [23], ovarian cancer [24], hepatocellular carcinoma [25] and non-small cell lung cancer [26].

Poorly functional T cells in malignancy are often described as either exhausted or anergic. Anergy occurs when a T cell receptor (TCR) signal is received in the absence of a co-stimulatory signal and may occur early in tumour development if a T cell recognises a tumour associated antigen but does not receive a supportive co-stimulatory signal [27]. In contrast, T cell exhaustion is a reversible state of progressive loss of effector functions which is associated with prolonged antigen exposure and inflammation [27]. In exhaustion, typically a hierarchical loss of function is described with loss of IL2 production occurring early and failure in IFNγ release a late feature [28]. Exhausted T cells become “addicted” to their antigen and require continued stimulation of the TCR for survival [29]. They express high levels of CD279 – programmed cell death protein 1 (PD1) on the cell surface in addition to other immune inhibitory molecules such as CD223 - lymphocyte activation 3 gene (LAG3) [29]. In haematological malignancies, exhausted phenotype T cells have been reported by our group [30]. In murine models, infusion of chronic lymphocytic leukaemia cells results in an exhausted phenotype [31] whereas addition of anti-PDL1 monoclonal antibody prevents development of disease (McClanahan et al., 2015).

The role of immune-editing in tumour development in haematological malignancy is a growing area of interest, both as a mechanism for understanding tumour development and growth kinetics but also as a source of therapeutic targets. Diseases such as multiple myeloma, which have a clearly defined pre malignant phase and remain currently incurable, may benefit from these therapeutic approaches.

1.2 Clinical importance of myeloma

1.2.1 Definition, epidemiology and diagnostic criteria

Multiple myeloma is a mature B cell neoplasm arising from plasma cells [33]. The malignant cells are thought to arise from long lived, post germinal centre plasma cells which have undergone both class switching and somatic hypermutation[33]. The plasma cells are described as clonal because they all produce the same immunoglobulin molecule.

The International Myeloma Working Groups diagnostic criteria for the diagnosis of symptomatic and asymptomatic myeloma have recently been updated to include key biomarkers in addition to clinical features [34]. The diagnostic criteria are summarised in table 1.1. These new criteria represent a departure from traditional management strategies as asymptomatic patients with biomarkers suggesting high risk of disease progression within 24 months are now considered symptomatic and eligible for treatment.

Multiple myeloma	**Smouldering multiple myeloma**
Clonal bone marrow plasma cells >10% or biopsy proven extramedullary plasmacytoma and any one or more myeloma defining events. **Myeloma defining events:** Evidence of end organ damage attributable to plasma cell disorder. 1. Hypercalcaemia >2.75 mmol 2. Creatinine clearance <40ml/min 3. Anaemia <100 g/L 4. Bone lesion, 1 or more on Xray, CT or PET CT Any one or more biomarker: 1. Clonal bone marrow plasma percentage >60% 2. Involved: uninvolved light chain ratio >100 3. More than one focal lesion on MRI	Both criteria: 1. Serum monoclonal protein >30g/L or urinary monoclonal protein >500mg per 24 hours and/or clonal bone marrow plasma cells 10-60% 2. Absence of myeloma defining events or amyloidosis

Table 1.1: Diagnostic criteria for myeloma and smouldering myeloma. Adapted from IMWG diagnostic criteria [34].

The terms smouldering myeloma and asymptomatic myeloma are used interchangeably.

1.2.2 Clinical features

While the malignant plasma cell in myeloma is predominantly confined to the bone marrow, the clinical features of the condition are diverse. The “CRAB” criteria of hypercalcaemia, renal impairment, anaemia and bone pain are used to define symptomatic disease, however clinical features are not restricted to these findings.

Monoclonal immunoglobulin, also referred to as paraprotein, or immunoglobulin light chains secreted by the malignant clone can usually be detected in either the peripheral blood or in urine. This circulating disease biomarker is frequently identified in asymptomatic patients as part of a routine health screen or during the investigation of non-specific symptoms. Non-secretory myeloma is a rare and difficult to diagnose entity with malignant plasma cells within the bone marrow compartment but no detectable serological biomarker.

The monoclonal paraprotein can cause renal impairment by disrupting the normal filtration of the kidney and becoming deposited within glomeruli. At high levels paraprotein increases the viscosity of the blood leading to confusion, bruising and organ ischaemia. In some circumstances the paraprotein can act as a paraneoplastic autoantibody, particularly targeting myelin and leading to peripheral neuropathy.

Malignant plasma cells interact with and disrupt normal cellular mechanisms within the bone marrow microenvironment. This includes disrupting the balance between osteoclasts, which resorb bone, and osteoblasts, which lay down new bone, resulting in the formation of lytic regions. These characteristic lytic lesions can result in pathological fractures and bone pain and can often be detected on radiological imaging. The calcium released by bone destruction leads to hypercalcaemia, with its associated clinical features, often worsening renal impairment and pain.

Physical infiltration of plasma cells into the bone marrow niche leads to the suppression of healthy haematopoetic cells resulting in anaemia, thrombocytopaenia and increased susceptibility to infection. In addition normal immune cell function is compromised, further increasing the infection risk. Patients with MGUS have a two fold increased risk of developing an infection over a 5 year period [35]while individuals with myeloma have a seven fold increased risk of bacterial infections and 10 fold increased risk of viral infections [36].

1.2.3 Treatment strategies and their limitations

To date myeloma remains a controllable but not curable haematological malignancy. Median life expectancy in the UK is 5 years [37]. The progression of the disease is characterised by

shorter responses to treatment with escalation of clinical symptoms, particularly pain and infection, with associated debilitation. This coincides with the evolution of diverse subclones with unique genetic hallmarks, with the eventual dominance of a chemotherapy resistant clone [38]. Current guidelines recommend that treatment is only started once patients fulfil the criteria for symptomatic disease. Historically, treating asymptomatic myeloma has not been shown to improve overall survival and risks exposing the patient to unnecessary toxicity risks [39], however with novel treatments, evidence is emerging that treating high risk asymptomatic patients early may delay disease progression and improve overall survival, with an acceptable toxicity profile [40]. This has not yet become incorporated into standard UK practice. Recent redefinitions of symptomatic disease, however, has broadened the number of patients eligible to receive treatment.

Current therapeutic strategies for myeloma are focused on combined modality treatment. For those patients with sufficient physical fitness initial induction treatment is consolidated by a melphalan conditioned autologous stem cell transplant. The use of autologous transplant is designed to induce a prolonged period of treatment free remission. When high dose melphalan autograft (melphalan dose 140mg/m^2) was first compared to alkylator based conventional treatment , five year survival improved from 12% with standard treatment to 52% following autograft [41].

The role of allogenic stem cell transplantation in myeloma is less certain but is sometimes used for young fit patients. When tandem autografts were compared to autograft followed by HLA matched sibling allografts in patients with newly diagnosed myeloma, the allograft group had longer event free survival (35 v. 29 months) and overall survival (80 v. 54 months) than the tandem autograft group, with a grade 4 GvHD rate of 4% [42]. EBMT registry data from the mid-nineties however reported a transplant related mortality of 47% with a relapse rate of 45% at 60 months [43] and allogeneic transplant is currently reserved for a small subset of individuals.

For frail or elderly patients the goal is disease control with minimal toxicity. Multi agent therapeutic combinations are used and are commonly continued until the time of progression when a change in agents is introduced.

The optimal combination and order of use of therapeutic agents remains uncertain and clinical practice is largely restricted by access to drugs. In the UK, treatment options are governed by the National Institute of Clinical Excellence (NICE). Current NICE technical appraisals (as of May 2019) allow the use of bortezomib and dexamethasone with or without thalidomide, followed by a melphalan autograft, for transplant eligible patients [44]. Transplant ineligible patients can receive thalidomide with an alkylator and steroid or, if this is contraindicated, bortezomib with

an alkylator and steroid (NICE, 2011). In the relapsed setting the situation is more complex as patients can access both NICE approved regimens and drugs funded via the Cancer Drugs Fund (CDF). Options at first relapse include bortezomib monotherapy (NICE, 2007) or daratumumab, bortezomib and dexamthasone (NICE, 2019). For second relapse and beyond a range of agents can be considered provided stringent eligibility criteria are met, with restrictions in their use dependent on which previous treatments have been used. Options include ixazomib, lenalidomide and dexamethasone (NICE, 2018), pomalidomide (NICE, 2017), lenalidomide (NICE, 2009), carfilzomib (NICE, 2017) and panobinostat (NICE), 2016). Daratumumab monotherapy is available fourth line (NICE, 2018a) in patients who have not previously been exposed to daratumumab. The use of bendamustine can also be considered via the CDF. Additionally a large portfolio of national and company sponsored clinical trials are available.

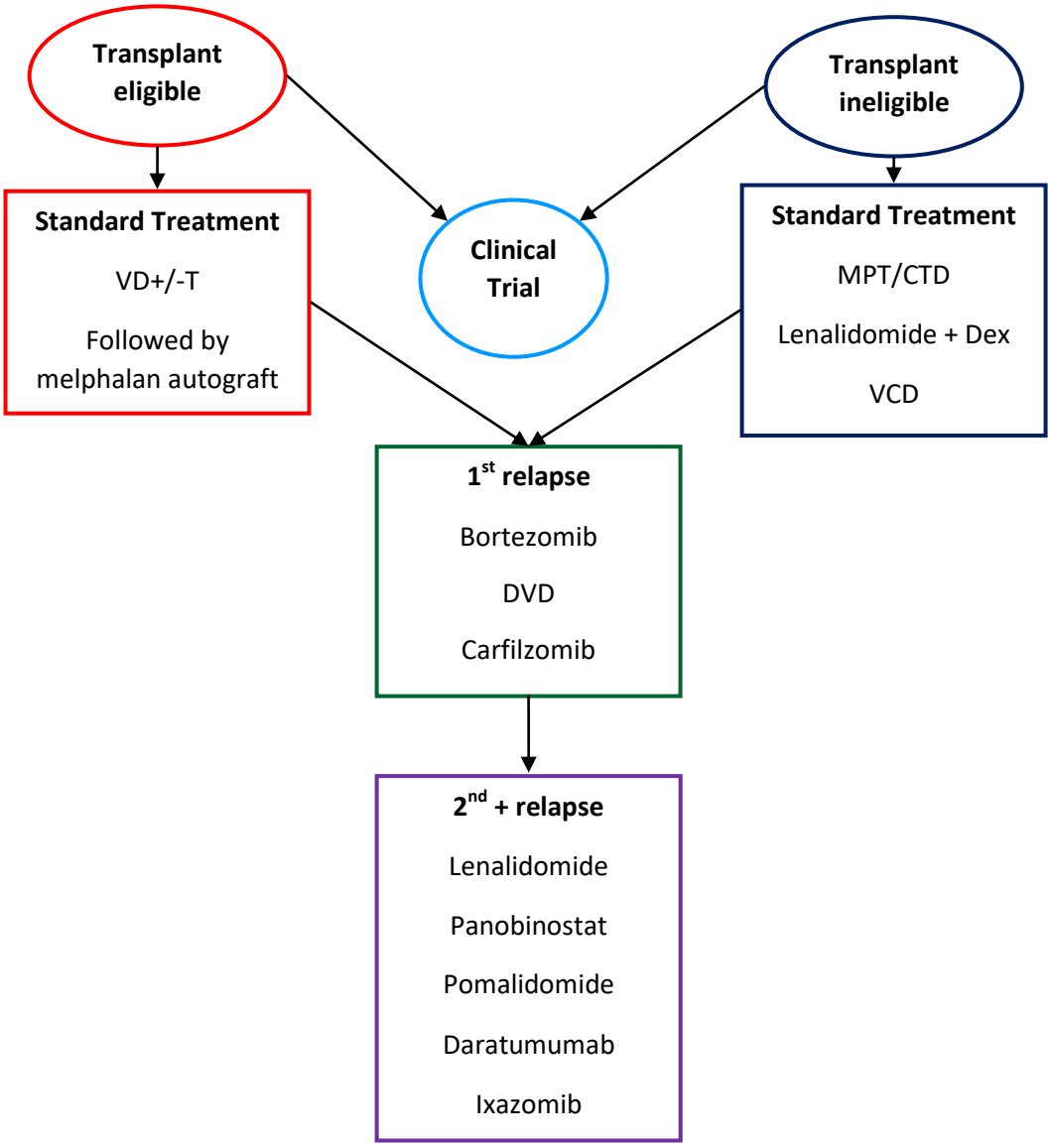

Figure 1.2: Standard myeloma treatment pathway in UK. Symptomatic patients are offered treatment based on transplant eligibility and according to treatment pathway approved by NICE and CDF. VDT = bortezomib, dexamethasone, thalidomide, MPT = melphalan, prednisolone, thalidomide, CDT = cyclophosphamide, dexamethasone, thalidomide, VCD = bortezomib, cyclophosphamide, dexamethasone, DVD = daratumumab, bortezomib, dexamethasone

Clinical trials have evaluated the role of maintenance therapy following autograft but consensus on this strategy has not been reached and trials are ongoing. In two separate meta-analysis of randomised controlled trials using lenalidomide post autograft [5455]a significant improvement in progression free survival (HR 0.49 95% CI 0.4-0.58 p<0.001) and OS (HR 0.77 95% CI 0.62-0.95 p=0.013) was observed, however significant toxicity was seen including a two fold increase in second malignancies [54].

1.3 Immune dysregulation in myeloma

1.3.1 The immune surveillance model and myeloma

Myeloma is an unusual malignancy because it has a well described pre malignant phase (MGUS) with an easily observable biomarker in the form of clonal immunoglobulin produced by malignant plasma cells. The stages of the immunoediting model can be correlated with the clinical stages of MGUS and myeloma progression. In addition to the original three E's, I propose a fourth stage, Evolution, which describes the emergence of drug and immunological resistant clones in response to ongoing selective pressures in the setting of an incurable malignancy (Figure 1.3).

1. Elimination: Clonal plasma cells are eliminated and no detectable disease is present
2. Equilibrium: MGUS. Clonal plasma cells are present but do not cause clinical disease. Continued immunological selection eventually leads to an increase in clonal plasma cells numbers until the diagnostic criteria for asymptomatic myeloma are reached. The rate of progression from MGUS to myeloma is 1% per year [56].
3. Escape: Loss of immunological control allows MGUS to progress to asymptomatic and then symptomatic myeloma. At this stage treatment is normally indicated. The disease, however, continues to follow a relapsing and remitting course in response to various therapeutic agents. Cytotoxic cells are expected to show progressive dysfunction with increasing markers of exhaustion.
4. Evolution: Continued clonal selection, via both immunological and therapeutic mechanisms [38], lead to increasingly drug and immune system resistant disease until current therapeutic options are exhausted. Cytotoxic T cells are expected to express anergic or exhausted phenotypes.

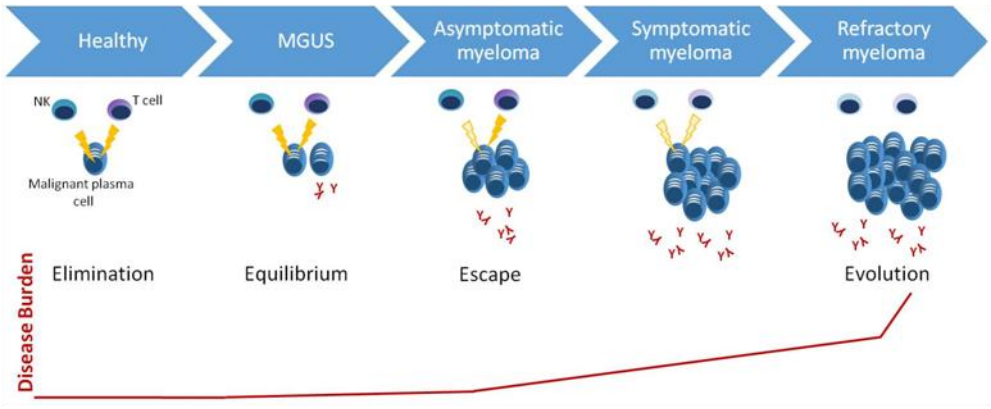

Figure 1.3: The immune surveillance model in myeloma

This model may also explain the diverse clinical course seen in individuals with myeloma, some of whom survive for many years with little or no treatment while others present with a rapidly progressive and treatment resistant disease. It is likely that those with slowly progressing disease are able to exert stronger immunological control over the malignant clone than those with more aggressive disease. In support of this theory, bone marrow derived T cells from patients with MGUS have been shown to produce more IFNγ in response to autologous plasma cell pulsed dendritic cells than those from patients with myeloma, demonstrating that cytotoxic T cells in MGUS are able to recognise and respond to the presence of malignant plasma cells but loose this feature as the disease progresses [57].

It is known that many of the cytogenetic changes associated with myeloma can be detected in plasma cells from patients with MGUS, suggesting that these recognised mutations are not sufficient to explain disease progression [58]. Within these cytogenetic groups however there remains heterogeneity with a shifting balance of genetic subclones seen as treatment progresses [38] suggesting that there is a role for accumulating genetic mutations in tumour escape and evolution. These genetic subclones may occur in response to immunological selective pressures as well as therapeutic pressures and may provide immune-evasion mechanisms.

In order to have an effective T cell response in myeloma the malignant plasma cells must express an antigen which can be recognised as foreign or abnormal by adaptive immune cells. Potential immune targets include;

1. Neoepitopes, formed by tumour specific DNA mutations arising from genetic instability resulting in novel amino acid sequences in expressed proteins [59].
2. Cancer testis antigen, proteins normally expressed on germline tissues which can become re-expressed when malignant cells revert to a more primitive phenotype [60]. As

cancer testis antigens are normally only expressed in immunologically privileged tissues, their expression at other sites can be immunogenic.

3. Idiotype antibodies arising from somatic mutations in the hypervariable region of the immunoglobulin variable domains [61]. In myeloma the monoclonal immunoglobulin characteristic of the disease forms the idiotype antibody. In normal plasma cell development B cells undergo somatic hypermutation in order to produce antibody with increasingly high antigen affinity, this continues in progeny cells. In the context of myeloma and other B cell malignancies this may lead to increased genomic instability and production of immunogenic proteins.

It is recognised that malignant plasma cells continue to express HLA class I and will therefore have the potential to display abnormal antigen to immune cells [62]. In order for expression of any of these potentially immunogenic proteins to be effective, however, they must be accompanied by an additional immune stimulating signal such as proinflammatory cytokines, to prevent immunological tolerance from developing [2]. Inherent immune suppression within the tumour microenvironment may prevent immune activation in response to these antigens from occurring and may explain why malignant cells are able to proliferate despite expressing immunological targets.

In myeloma, the peripheral blood cytokine environment is shifted towards a pro-tumour profile with increased IL17 and IL10 and decreased IFNγ. These changes are not restored to normal following treatment [63]. This pro tumour microenvironment may decrease dendritic cell numbers which in turn results in reduced antigen presenting capacity and therefore less opportunity for T cell activation. This will lead to a reduced response to immunogenic tumour derived peptides.

To date, much of the work investigating T cell dysfunction in myeloma has been carried out on peripheral blood and has been based on numeric assessment and a small panel of phenotypic markers. In some reports higher numbers of activated, suppressor and helper cells were seen in MGUS and myeloma compared to healthy controls [64], and higher lymphocyte numbers are positively correlated with improved survival [65]. Assessments of T cell cytotoxicity by chromium release assays demonstrated that T cell activity is reduced in myeloma compared to MGUS or healthy controls while good prognostic risk myeloma had T cell function similar to that of MGUS [66]. Together these findings support the hypothesis that T cell activity influences disease progression. This has been echoed by further studies of long term myeloma survivors which have identified both lower T regulatory cell numbers and the presence of non-anergic expanded T cell clones [67]. The T cell expansions have the phenotype of cytotoxic T cells and remain stable over many months [68–70]. These expanded T cell clones are likely to be

successfully maintaining the malignant clone in equilibrium, resulting in a better clinical outcome.

If myeloma follows the proposed immune editing model then it would be expected that immune checkpoint regulatory pathways are playing an important role in the disease. The best characterised immune checkpoint pathway in myeloma is the PD1 axis. PD1 expression is increased on both NK and T cells in myeloma [71–73] with up to 20% of myeloma T cells expressing PD1 in comparison with 6% of healthy T cells [72]. Other immune regulatory checkpoints are also recognised but their role in myeloma has not been fully investigated.

There is increasing evidence to suggest that within the PD1 expressing T cell populations there are distinct subsets with different functional capabilities. In murine chronic infection models two $CD8^+$ $PD1^+$ subsets have been defined. $PD1^{high}$ cells have higher proliferation but lower cytotoxicity than $PD1^{low}$ subsets [74]. This suggests that immune checkpoint receptor expression is highly complex with subtle functional differences between subpopulations and that exhausted T cells may retain more functional activity than previously thought. This will have implications for successful therapeutic targeting of these pathways.

The fact that malignant plasma cells have high PDL1 expression which is upregulated in response to IFNγ adds more weight to the importance of immune checkpoint pathways in myeloma [7]. Malignant plasma cells also secrete a range of immune regulatory molecules including MUC1 [75].

T regulatory cell numbers are increased in both peripheral blood and bone marrow from patients with myeloma when compared to healthy controls and MGUS [76–78] and higher numbers are associated with shorter survival [79,80]. This is in keeping with the suggestion that the tumour microenvironment can have an influence on the immune response. Interestingly, treatment with immune modifying drugs (IMiDs) appears to lead to an increase in T regulatory numbers [78,81], perhaps in a tissue protecting attempt to limit cytotoxic damage.

The accumulating evidence that immunological control has a key role to play in the evolution from MGUS to myeloma raises the possibility of targeting aspects of both the innate and adaptive immune system in an effort to control malignant cell escape and restore equilibrium or elimination. This would require the identification of appropriate combinations of molecular targets expressed by immune cells in myeloma as well as understanding which mechanisms are responsible for immunological escape in this disease.

1.3.2 Immunological therapies and their role in myeloma

Specific therapies targeting the immunological control of malignant plasma cells are being explored but have not been fully established and are either used in the setting of clinical trials or in a small subset of fit patients with poor risk disease. Given the growing body of evidence that immunological control is important in this disease numerous pre-clinical and early phase clinical trials are ongoing.

Immunological therapies for the management of haematological malignancy can be considered in four broad categories.

1. Monoclonal antibodies targeting plasma cells
2. Immune checkpoint regulation including PD1 and CD152 - cytotoxic T-lymphocyte-associated protein 4 (CTLA4) inhibitors
3. Cellular based therapies including CAR-Ts and vaccination strategies
4. Allogenic haematopoetic stem cell transplantation

1.3.2.1 Monoclonal antibodies

The transformation of B cell lymphoma treatment brought about by the introduction of the anti CD20 monoclonal antibody Rituximab [82] has led to great interest in the use of monoclonal antibodies for the treatment of other haematological malignancies. In the field of myeloma, antibodies targeting CD38 [83,84] and SLAMF7 [85] have been developed and demonstrated efficacy in the setting of relapsed refractory myeloma. These clinical studies led to the clinical approval of daratumumab , the first approved anti-CD38 mAb.

CD38 is highly expressed on malignant plasma cells but is also expressed across a wide range of haematological cells including the immune regulatory subset. Daratumumab is a human IgG1 monoclonal antibody targeting CD38, [Janssen] and has also been shown to have beneficial off target effects by reducing T regulatory numbers and allowing expansion of cytotoxic and helper T cell responses [86]. The targeting of a widely expressed antigen does, however, have some detrimental effects. In the case of anti-CD38 antibodies this includes antibody coating of red blood cells resulting in a positive antibody screen when attempting to source allogeneic blood for transfusion [87].

SLAMF7 (also called CS1) is expressed on plasma and NK cells. Elotuzumab [Humanised IgG1 monoclonal antibody targeting SLAMF7, Bristol-Myers Squibb] induces NK cell activation and antibody-dependant cell mediated cytotoxicity and has been shown to have a progression free survival benefit when used in combination with Lenalidomide and dexamethasone [85].

Bi-alleic (BITE) antibodies have been developed as a means of enhancing cytotoxic killing of malignant cells by ensuring their proximity. BITE antibodies consist of two FAB regions, one against a cytotoxic cell target and another against a malignant cell target. In myeloma BITE antibodies against CD3/ B cell maturation antigen (BCMA) [88,89] and CD3/CD38 [90] have shown in-vitro activity with lysis similar to that seen with CAR-T cells against the same targets.

1.3.2.2 Immune checkpoint regulation

The recognition of a role for malignant cells in down regulating immune surveillance mechanisms has renewed interest in targeting this pathway to treat haematological malignancy. In the context of the mature B cell neoplasm CLL exhausted T cells expressing the immune checkpoint inhibitor PD1 have been characterised [30] and drugs targeting the PD1 axis are being investigated in a range of haematological malignancies [91–93].

The role of PD1 inhibitors has been explored in mouse myeloma models which demonstrated a benefit for PD1 inhibition in combination with low dose radiation [94]. In vitro cell culture assays have also demonstrated improved T cell activity [72,95] and NK cell activity [73]. The addition of Lenalidomide to PD1 pathway inhibition further enhanced the anti-myeloma effect [73] suggesting a role for immune checkpoint regulators in combination with current therapeutic combinations.

In early phase clinical trials, single agent use of the anti-PD1 antibody nivolumab did not show significant activity in myeloma, with best response in 27 patients being stable disease with a median response of 10 weeks (range 1.6 to 126 weeks) [93]. When PD1 blockade was used in combination with lenalidomide and dexamethasone, however, clinical responses were seen [96] with 76% overall response rate after median follow up of 287 days. This phase one data includes individuals with IMiD refractory disease and demonstrates a higher response rate than might be expected in the relapsed refractory cohort. In the absence of randomised controlled trials however, it is unclear whether the response seen can be attributed to the PD1 blockade. Similar responses have been reported when the anti-PD1 antibody pembrolizumab and pomalidomide are used together [97]. The lack of single agent response but an effective response in combination with an IMiD is not well understood, but may relate to the immunosuppressive microenvironment in myeloma [93]. It is possible that a PD1 inhibitor alone is unsuccessful in the context of myeloma because it is only targeting a selective subset of T cells. The addition of an IMiD may enhance effectiveness by providing a more generalised T cell activation signal thereby overcoming additional inhibitory signals from the immunosuppressive tumour microenvironment. This observation highlights the importance of understanding the role of functional T cell subsets in order to optimise treatment strategies.

The combination of Pembrolizumab with IMiDs was explored in the phase 3 Keynote 183[98] (Pomalidomide and Dexamethasone +/- Pembrolizumab) and Keynote185[99] (Lenalidomide and Dexamethasone +/- Pembrolizumab) studies. The FDA paused both of these studies earlier due to excess deaths in the Pembrolizumab plus IMiD arms which also demonstrated increased toxicity compared to the control arms. The reasons for this increased mortality and toxicity is not fully understood but may relate to the T cell activation effects described above.

There is a concern that treating cells with PD1 inhibitors may lead to an increase in expression of other immune regulatory molecules such as CD366 - T-cell immunoglobulin and mucin-domain containing-3 (TIM3) or LAG3, with the danger that the response to checkpoint inhibition is only transient. In mice models the use of dual immune checkpoint inhibitors has synergistic effects and resulted in improved survival [100] and this is a potential mechanism to prevent drug resistance. The degree to which this occurs in myeloma is currently unknown, and a detailed understanding of the combinations of immune checkpoint regulators being expressed by different key cellular subpopulations will be vital as these immunological treatment strategies become established.

1.3.2.3 Cellular therapies

The presence of tumour specific antigens on malignant plasma cells raises the possibility of using targeted biological treatments directed towards these. The roles of dendritic cell vaccination, CAR-T (chimeric antigen receptor T cells) and expanded or modified NK cells have been investigated, both in mouse models and human clinical trials.

CAR-T cells targeting NKG2D [101], BCMA [102], SLAMF7 [103] and CD38 [104] have demonstrated efficacy against myeloma cell lines, while BCMA [102] and SLAMF7 [105] are effective in murine models of myeloma. In a human proof of principle clinical trial autologous CAR-T's against BCMA were found to be effective at producing clinical responses at high cell doses but this was accompanied by cytokine release syndrome and prolonged cytopaenias [106].

NK cells derived from patients [107,108], allogenic donors [107] or umbilical cord blood [109] can be expanded ex-vivo using cytokine cocktails or antigen feeder cells and infused as a cellular therapy alongside conventional myeloma treatment or with immunosuppressive therapy. Alternatively NK cells can be modified so that they express chimeric antigen receptors, in a process similar to the generation of CAR-T cells.

CAR-NK cells expressing the chimeric CS1 (SLAMF7) receptor have shown efficacy in mice models and against patient derived myeloma cells in vitro [103]. Ex-vivo expanded NK cells demonstrate lysis of in-vitro plasma cells [108–110] and in murine models [109] however clinical

efficacy has been less remarkable. When five patients received autologous ex-vivo expanded NK cells in a proof of principle study alongside standard myeloma treatment two patients achieved stable disease [108]. Phase one trials with umbilical cord blood derived NK cells are ongoing.

Experience of dendritic cell vaccination to prime an immunological reaction against specific tumour derived peptides has been drawn from malignant melanoma. In myeloma a range of different targets have been employed including MUC1 [111], BCMA [112] and Idiotype [113,114] antibody. Clinical responses in phase I trials have been disappointing with stable or slowly progressive disease frequently the best reported outcome [114,115]. In the post autograft setting however plasma cell-dendritic cell fusion vaccinations were able to convert a PR to CR or nCR in 24% of patients [116].

The role of cellular therapies in routine myeloma care has not been established, with mixed clinical response and costs making their use challenging. To date, these agents remain experimental and are not licensed for use.

1.2.3.4 Allogenic transplantation

Allogenic haematopoetic stem cell transplantation is a well established treatment for sufficiently fit patients, primarily in the setting of relapsed or high risk acute leukaemia or lymphoma. The aim of the treatment is to establish a non-host immune system with functioning immune surveillance (graft versus leukaemia effect) but with minimal activity against the host (graft versus host disease). It has previously been explored as a treatment strategy in myeloma, however as discussed in section 1.2.3, results were originally disappointing [43] and a large number of patients were not sufficiently fit to be candidates. There is renewed interest in this technique, however, particularly in the younger age group as a small number of patients appear to achieve durable remission following transplantation. As survival curves plateau it is possible that a small number of patients may have in fact achieved a cure. In one recent long term follow up of patients who underwent tandem autograft- reduced intensity allograft the progression free survival was 41% at 10 years [117].

An important benefit of all of these strategies is the potential to reinstate tumour immune surveillance and long term remission. While monoclonal antibodies and immune checkpoint inhibitors are likely to require prolonged treatment courses in order to achieve this, stable cellular therapies and allogenic transplantation have the potential to provide long term, treatment free remission. If treatment free remission can be induced with an acceptable toxicity profile then this has patient quality of life implications, in addition to cost savings and reduced morbidity.

Selecting the appropriate treatment strategy for the stage of a patient's disease will be crucial. Targeting the disease at an early time point before immune surveillance mechanisms become completely exhausted may only require the use of an immune checkpoint regulator, while a multiply relapsed patient may benefit from a combined approach with monoclonal antibodies, immune checkpoint regulations and cellular therapies in order to debulk the disease and restore immune function.

To optimise the use of immunological therapies it is vital to understand which therapies or therapeutic combination are best used for which patients and in what context. To this end the identification of novel biomarkers may help to identify which patient cohorts are most likely to benefit from a particular treatment, it is also essential to understand what immune dysregulation mechanisms are occurring in myeloma, at which disease time point they occur and whether resistance to treatment occurs.

1.3.3 Immune regulatory targets of therapeutic interest

A range of immune regulatory targets are of potential therapeutic interest.

1. **Immune checkpoint regulators:** TIM3 (CD336) [118], LAG3 (CD223) [119], PD1 (CD279)[120], PDL1 (CD274) [120], CTLA4 (CD152) [121]. These receptors can all be expressed on CD8 T cells, as well as other immunological cells, where they play a role in down regulating cytotoxic response
2. **Immune co-receptors:** OX40 (CD134) [122], NKG2D (CD314) [123], DNAM1 (CD226) [124]. These receptors, expressed on both CD8 T cells and NK cells, have a role as activating co-receptors, supporting positive signals received via the T cell receptor. Targeting these receptors in poorly responsive cells should lead to an antigen dependent increase in T cell activity.
3. **Context dependent receptors:** The T cell receptor 2B4 (CD244) is particularly interesting because its activity is context dependent [125]. In the presence of intracellular SAP, 2B4 signalling is cell activating. In the absence of SAP, 2B4 signalling down regulates the T cell response. This may make targeting the molecule for therapeutic purposes more challenging.

Examination of a broad range of immune regulatory targets requires embracing emerging technologies such as mass cytometry which permit multiple targets to be measured simultaneously. Understanding the pattern of receptor expression across different functional subsets and identifying which receptors are expressed together on the cell groups will be key to developing targeted therapeutic strategies

1.4 Knowledge can be drawn from other diseases

1.4.1 Malignant melanoma

Much of the early therapeutic interest in targeting immune surveillance was in the context of malignant melanoma. The immune checkpoint inhibitor ipilimumab, which targets CTLA4, was the first treatment to show a survival benefit in advanced melanoma [126]. Subsequently nivolumab, which targets PD1, and the combination of ipilimumab with nivolumab have been approved for use in advanced stage disease with superior responses to ipilimumab alone [126]. This groundbreaking research in melanoma is vital because, in addition to demonstrating proof of principle for immune checkpoint inhibition in advanced, previously untreatable malignancies, it also highlighted the diverse patterns of response and toxicities associated with the treatment.

As treatment with immune checkpoint inhibitors has become standard of care in melanoma the emergence of therapy resistant disease via induction of immune-evasion mechanisms has become an increasing problem [127]. It is likely that combined or multi-modality treatment strategies will be necessary to overcome the emerging resistance. Similar mechanisms are expected to come into play in myeloma.

1.4.2 Chronic lymphocytic leukaemia

Within haematological malignancies the role of T cell exhaustion in CLL has been well characterised. CD8 T cells from patients with CLL have been shown to have functional defects of immune synapse formation due to cytoskeleton abnormalities [128], inducible down-regulation in T cell expression of genes involved in vesicle transport, regulation of the cytoskeleton and cytotoxicity [129], increased expression of PD1, loss of proliferative capacity and cytotoxicity but increased production of IFNγ and TNFα [30]. Of note the immune synapse formation defects could be repaired with the addition of Lenalidomide [128]. In murine TCL1 model of CLL, the development of CLL corresponds with the development of a T cell exhaustion phenotype [31,130], furthermore blockade of PDL1 has been shown to prevent leukaemia engraftment and restore function of cytotoxic cells [32].

Since CLL is another chronic B cell malignancy with a recognised pre malignant phase it is likely that findings in CLL will be of relevance in myeloma with the beneficial effects of Lenalidomide being of particular interest as this is in established part of myeloma treatment.

1.5 Knowledge gaps and rationale for project

While the treatment options for myeloma have improved dramatically in the last 10 years with a correlated improvement in median survival, the disease remains incurable and treatment

resistance inevitably develops. The accumulating evidence that immune editing is an active selection force in myeloma and that immune subversion may be correlated with outcome makes this a key area for study and drug development. While there is some evidence to suggest abnormalities in T cell function and PD1 expression are present in myeloma, the functional potential of T cell subclones expressing varied markers of exhaustion and their potential as a therapeutic target has not been investigated. We can extrapolate the potential benefit of dual modality immune checkpoint blockade from other malignancies but need to determine its role in the field of plasma cell neoplasms.

This key avenue of research has the potential to transform myeloma care. Restoration of immune surveillance at the point of progression from MGUS to myeloma may avoid or delay the need for cytotoxic therapy, while restoration after autologous stem cell transplantation could be used to maintain a prolonged remission or MGUS like state.

1.6 Hypothesis

Characterisation of the cellular immunological landscape in myeloma will identify distinct functional populations which may offer therapeutic targets to restore immunological control of the disease

1.7 Aims

1. To interrogate the immune microenvironment in myeloma using single cell profiling techniques to establish activity of the major T cell and NK cell populations. There will be particular focus on:

    a. Patterns of expression of stimulatory and inhibitory receptors
    b. Functional activity

2. To integrate immunological subset information with clinical characteristics to establish patterns of immunological response and potential predictive biomarkers

3. To target immune subversion mechanisms in order to determine whether immunological surveillance can be restored

2: Mass Cytometry

2.1 The role of mass cytometry for single cell profiling of biological samples

Analysis of protein expression at a single cell level is a key way to explore the tumour microenvironment in haematological malignancies. This has been traditionally performed using flow cytometry which utilises fluorescent antibody tags to identify cellular targets. Antibody panels incorporating 10 fluorochromes are frequently employed and more complex panels can be developed by taking advantage of mutually exclusive antigens.

Flow cytometry has the advantage of being well established and relatively cheap to perform with a wide range of pre-conjugated antibodies available. If desired the sample can be retained following analysis to allow further work and specific cell populations of interest can be isolated from the sample. The technique has a number of disadvantages, however, including the need for compensation controls due to spectral overlap [131] which also restricts the number of antibodies which can be used per panel. Spectral overlap refers to the broad emission spectra associated with some fluorochromes with the result that the fluorescence from one antibody may be detected in a region expected to measure another antibody within the panel (Figure 2.1).

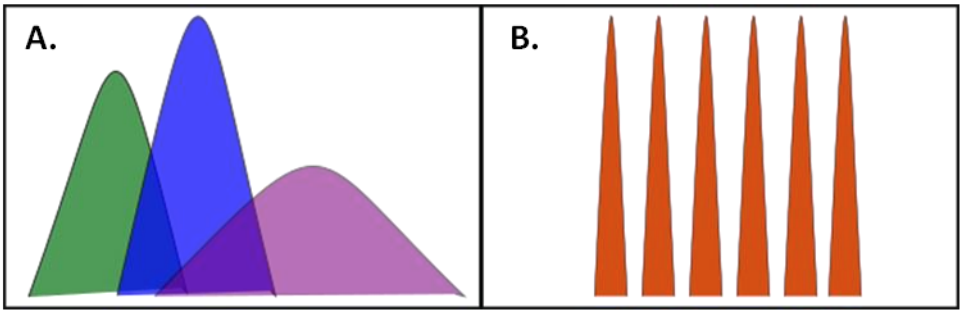

Figure 2.1 Spectral overlap

[A] Spectral overlap in flow cytometry. Signal from one flurochrome may overlap with another
[B] The metals used in mass cytometry have tight detection peaks which do not overlap

If multiple antigens of interest are to be studied by flow cytometry it is necessary to run multiple parallel panels with antibody redundancy, which may not be feasible if only small clinical samples are available. Baseline fluorescence may also make it difficult to discriminate small populations with accuracy.

Mass cytometry is a novel single cell profiling technique which utilises ultra-pure metal antibody tags in place of the fluorescent tags used in flow cytometry. This section will describe

this rapidly developing technology and discuss its role in interrogating the tumour microenvironment in plasma cell disorders.

2.2 The technology

Mass cytometry technology was developed in order to address some of the issue highlighted with flow cytometry and increase the number of antigens which could be assessed within a single panel. The technique combines features of flow cytometry with mass spectroscopy to allow multi-parameter single cell analysis.

In mass cytometry antibodies are attached to isotopically pure metals via a branching or linear polymer backbone (Figure 2.2). Most antibody clones used for flow cytometry are suitable for use in mass cytometry and it is possible to metal tag suitably pure antibody which have not been previously used for flow cytometry. It is not a requirement that the metals are antibody bound in order to be detected by a mass cytometer, leading to a range of novel techniques including the use of gold nanoparticles [132].

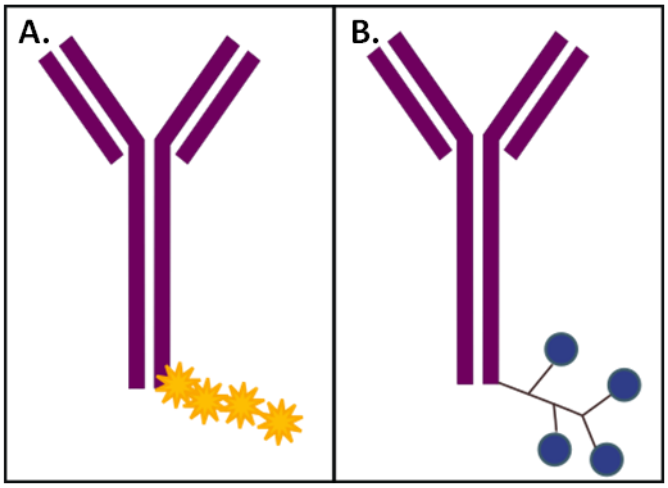

Figure 2.2 Antibody structure

[A] Flow cytometry antibody is conjugated to flurochromes
[B] In mass cytometry the same antibody can be conjugated to metal ions via a branching polymer

Cells which have been labelled with pure metal isotope tagged antibodies and re-suspended in water with a low metal content are then passed through a nebuliser to create a stream of droplets, each containing a single, labelled cell. Each droplet passes through a plasma coil which vaporises the cell, resulting in a cloud of cellular debris and metal isotopes. This cloud passes through a filter which removes cellular debris and applies a charge to the metal isotopes. Finally the purified cloud of ionised isotopes passes into a time of flight chamber, allowing the atomic weight of the tags to be determined (Figure 2.3) [133,134].

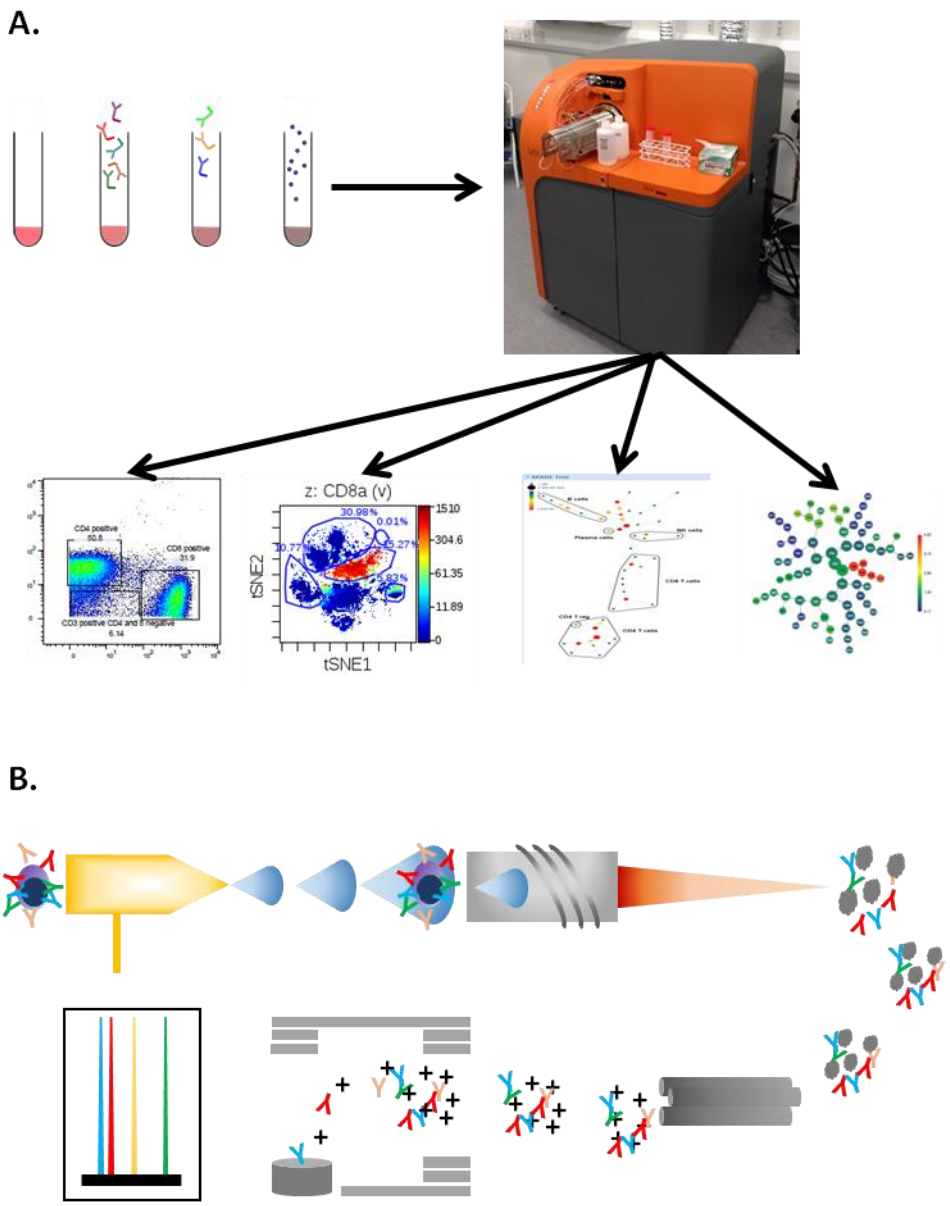

Figure 2.3 Mass cytometry workflow

[A] Samples are sequentially stained to label cell surface antigens, intracellular antigens and cellular DNA content. Samples pass through the mass cytometer and data can be visualised using a range of techniques
[B] Within the mass cytometer labelled cells are aerosolised, biological materials are vapourised by a plasma coil and debris is removed with an electromagnetic filter. Time of flight mass spectrometry is used to determine which metal tags are present.

2.3 Sample preparation workflow

The mass cytometry sample preparation workflow is similar to that used in flow cytometry. Samples are stimulated as desired, resuspended in appropriate buffers for viability and cell surface antibody staining, before being fixed and permeabilised for intracellular and nuclear antigen staining. Fluidigm, the company who distribute mass cytometry machine and reagents,

recommend the use of reagents particularly designed for mass cytometry in order to minimise the risk of heavy metal contamination.

2.3.1 Antibodies

The metal tags currently available are largely drawn from the lanthanide series as these have sufficient purity with low biological abundance [135]. The number of available metals continues to expand as new sources of pure metals are developed. At the time this panel was developed it was possible to incorporate 36 different markers into a single antibody panel. In addition separate markers are available for viability and cell identification via DNA intercalation.

Metal tagged antibodies can be targeted to a range of both phenotypic and functional markers both intracellularly and on the cell surface.

2.3.2 Controls

High purity metal isotopes have minimal spectral overlap when measured by mass cytometry. This removes the need for compensation controls which are routinely employed in flow cytometry, where fluorochrome overspill between channels can cause significant distortion of results if not corrected [136]. Attempts have been made to apply compensation to mass cytometry panels to further minimise cross talk, however the complexity of the panels makes this difficult without providing significant improvement in data. Recently mass cytometry compensation tools have been designed with the aim of allowing the use of less isotopically pure metal with higher levels of spill over, these tools, however, remain in the early stages of development [137].

EQ normalisation beads are used in each sample analysed in order to detect and compensate for signal decay, which is an inevitable consequence of the aging of mass spectroscopy detectors[138]. A normalisation algorithm, using the EQ beads as a standard, corrects signal within each .fcs file prior to further analysis. This ensures that direct comparisons can be made between samples analysed at different time points.

Isotype controls are not routinely used in mass cytometry as their value is unclear. The function of isotype controls are to determine the level of non-specific staining occurring with any given antibody [139]. For isotype controls to be effective they must match the antibody being assessed in terms of antibody class as well as tag [131]. In mass cytometry it is logistically very difficult to obtain appropriate isotype controls for every antibody in the panel.

Metal-minus-one (MMO) and metal-minus-many (MMM) controls can be used to help establish positive population cut off points when the resolution is unclear [140]. They are not required when discrete populations can be distinguished.

Biological controls should be implemented in the same way as in flow cytometry protocols.

2.4 Established research use

Since its development in 2002 and its commercial introduction in 2008, mass cytometry has been used to generate data from primarily immunological samples and in HIV research. More recently mass cytometry has started to be applied in haematological research, particularly in studying the clonal evolution of AML and the role of progenitor like cells in AML [141]. In the last three years there has been a dramatic increase in the number of research papers utilising the technology (Figure 2.4). While many of these early papers dealt with technical aspects of mass cytometry, increasingly it is being used as a research tool alongside other techniques including gene expression profiling and functional assays.

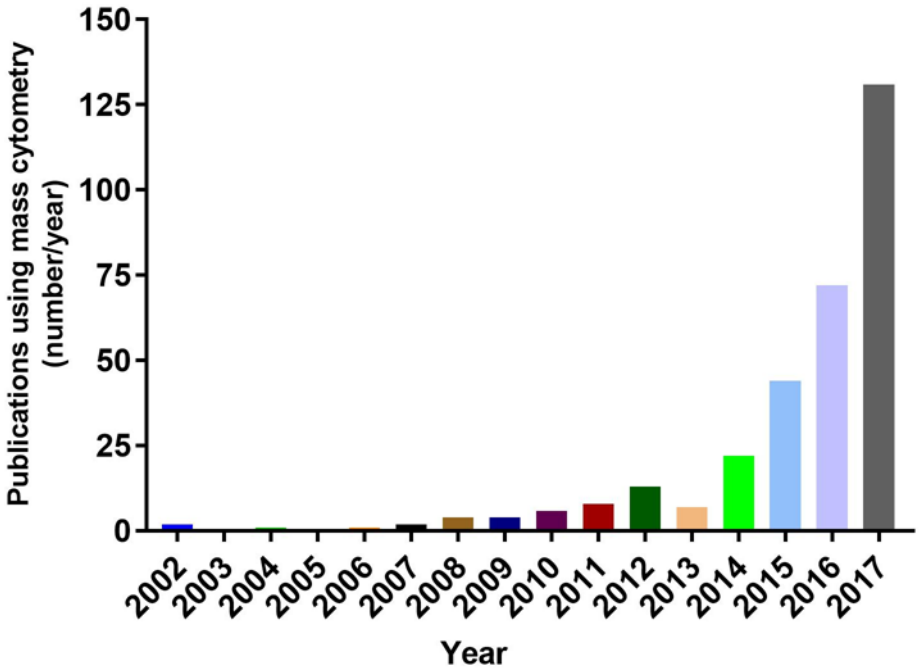

Figure 2.4 Mass cytometry publications

The number of publications in the scientific literature using mass cytometry have risen dramatically since 2014. Data obtained from PubMed literature search using "mass cytometry" and "CyTOF" as search terms.

In the field of myeloma research, mass cytometry has been used to characterise a bortezomib resistant cell line [142] and identify a novel expanded memory B cell population [143]. Furthermore a recent conference abstract has described using mass cytometry to study the effect of Daratumumab on immune activity [144].

2.5 Key strengths

2.5.1 Technical advantages

The key advantage of mass cytometry is that a single panel can be designed which includes up to 40 different cell surface and intracellular parameters, vastly increasing the amount of information which can be obtained from small biological samples. This includes signalling pathways [134], functional markers [145] as well as viability [134] and cell identification [134].

This can be achieved because the high purity metal isotope antibody tags have minimal spectral overlap and low biological abundance [135], meaning that there is low risk of background signal. As more metals are isolated at sufficient purity it is predicted that the number of available tags per panel may reach 100.

When designing a mass cytometry panel it is still necessary to avoid crosstalk of a high frequency antigen into a low frequency antigen channel. This can be achieved using the Fluidigm panel designer to ensure that there is less than 0.5% cross talk between each channel.

2.5.2 Data strengths

The data produced by mass cytometry can be used for hypothesis generation as well as hypothesis testing. The multi-parameter data produced can be analysed by a range of algorithmic based techniques, such as SPADE[146] and viSNE [147] which use spatial modelling to group cells with a similar phenotypes together. This can lead to the identification of novel and unexpected populations or can lead to the discovery of novel functional behaviour in established populations. Populations of interest can then be interrogated further using traditional data analysis techniques.

2.6 Potential pitfalls

Difficulties with mass cytometry are largely related to resources. There are also some technical issues which can affect data quality if not recognised and anticipated.

2.6.1 Resources

A commonly discussed concern regarding mass cytometry is one of cost. As this is a relatively new technique, there are only a limited number of companies producing mass cytometry compatible reagents. An antibody for mass cytometry costs 3-5 times that of the equivalent antibody for flow cytometry. In addition the machine can only be operated by specialist core facilities staff, meaning that machine time costs more than flow cytometry.

Sample acquisition times are significantly longer for mass cytometry compared to flow cytometry. The optimal flow rate for sample analysis is 500ul/660 seconds with a cell concentration of 2.5 – 5 x10^5/ml. This is primarily to ensure that the sample is aerosolised with one cell per droplet to reduce the incidence of doublets. This significantly limits the number of samples which can be processed in a day and greatly increases the costs of machine use. The problem is compounded by cell loss during processing and data acquisition which results in only approximately 30% of cells in the initial sample being available for data analysis [148]. It is therefore necessary to run the sample for longer in order to collect sufficient events for analysis. The introduction of an automated supersampler attachment which removes the need to inject aliquots of sample directly into the machine sample loops has streamlined the sample introduction process and reduced cell loss occurring due to settling within sample loops and sample loop switch over.

2.6.2 Technical issues

Mass cytometry is sensitive to heavy metal contamination of samples. Particular sources of contamination include barium in water or dust which can contaminate glassware, and lead, tin, mercury, iodine and barium in some commercially available buffers. It is therefore recommended that samples are stored and processed using plastic containers and with low metal reagents.

Signal decay is a recognised problem with mass spectroscopy as the inevitable consequence of aging detectors. This can prevent direct comparison of samples analysed at different time points. To reduce this problem standardised EQ normalisation beads are used in each sample in order to detect and compensate for signal decay [138].

Although fluorescence spill over does not occur in mass cytometry, crosstalk can occur between channels in certain circumstances. There are three potential sources of crosstalk: [149,150].

1. Abundance sensitivity: Identification of metal isotopes occurs using time of flight detection. Slight variations in the starting position and velocity of identical ions can result in broadened mass peak with signal detected in the mass +1 and mass -1 channels. The degree of spill over depends on instrument set up with daily tuning required to ensure that spill over into adjacent channels is less than 2%.
2. Oxide formation: As metal ions are vaporised by the plasma, metal oxides can form which are detected in the mass +16 channel. The tendency to oxidise varies between metals with lanthanum, cerium, praseodymium and neodymium having 2-3% spill over

into their mass +16 channel while europium has less than 0.1% spillover. The rate of oxidation is largely determined by the plasma flame temperature of the machine.

3. Isotopic purity: Naturally occurring elements are not isotopically pure and must be enriched in order to be suitable for use in mass cytometry. Most metals used in mass cytometry have a purity of greater than 98% but any residual alternative isotopes can cause cross talk into other channels. This is predictable and is taken into account when designing a mass cytometry panel to ensure that low abundance antigens are not labelled with antibodies which are susceptible to cross talk from isotopically impure metals.

Finally, sample loss is the inevitable consequence of this technique as the sample is vaporised. It is therefore not possible to perform cell sorting or further experimental work. It is also not currently possible to perform proliferation assays as these depend on fluorescent dyes, however cell surface Ki67 expression can be used as a surrogate marker and has been shown to correlate with CFSE proliferation studies [151].

2.6.3 Blessed with the curse of multidimensional data [152]

The size of a mass cytometry panel allows much more in depth sample interrogation with all functional and phenotypic markers being recorded across all cell types. While this raises the possibility of identifying novel populations, the complexity of data creates a challenge when it comes to analysis and interpretation. As the number of parameters are increased the number of dimensions across which data can be compared rises exponentially. In order to use traditional two dimensional plots to compare all parameters within a 40 parameter panel it would be necessary to review 780 plots, the same panel would contain over a trillion possible multi-parameter combinations [152]. This makes it necessary to use multidimensional data analysis algorithms and the input of bioinformaticians is crucial to most mass cytometry research.

2.7 Data analysis pathways

In order to optimise the analysis of mass cytometry data and overcome the “curse of multidimensionality”, it is necessary to employ a data analysis pipeline which includes dimensionality reducing algorithms alongside traditional gating strategies.

Initial data clean up steps include the exclusion of EQ beads and the identification of singlet, live cell events. This is best done with traditional two dimensional scatterplot analysis. An intensity signal of greater than 10^1 is considered the cut off for positivity as this excludes low level crosstalk [140]. A range of different algorithms can then be applied to the data.

2.7.1 SPADE

Spanning-tree Progression Analysis of Density-normalised Events (SPADE) [146] was developed at Stanford University specifically for the analysis of multi-parameter cytometry data sets. It employs an unsupervised approach to visualise multi-parameter data in a hierarchical clustered tree. The SPADE algorithm uses four computational models; density dependant down sampling, agglomerative clustering to identify cells with similar phenotypes, minimum spanning tree construction, up-sampling to map each cell in the data set to the tree [146]. Once the tree has been visualised different colours can be used to visualise the markers.

SPADE does not require user defined cell types which means that unexpected cell groups may be identified. It can also be used to identify rare populations since the density dependant down sampling prevents the most abundant cell types from dominating the analysis [146]. It does, however, present data as clusters of similar cells, meaning that single cell resolution is lost [147]. Each cluster can be interrogated further, using traditional gating strategies or an alternative multi-dimensional technique such as viSNE.

2.7.2 viSNE

viSNE is based on the t-Distributed Stochastic Neighbour Embedding algorithm (t-SNE) and has been designed to provide single cell visualisation of multi-parameter data [147] . The algorithm places individual cells on a map according to similar phenotypes across multiple dimensions. Cells are initially placed within a multi-dimensional cloud before a distance matrix is calculated between each pair of cells. This matrix is then transformed to a similarity matrix which can be plotted in two dimensions[147]. As with SPADE, a coloured overlay can then be used to assess the expression of various different markers. Gates can be applied to regions of the map to enable further data analysis.

2.7.3 CITRUS

Cluster Identification, Characterisation and Regression (CITRUS) was developed in order to identify subpopulations of cells which are associated with a pre-defined endpoint such as treatment status [153]. This is a different approach from viSNE and SPADE which are primarily designed to identify cell populations rather than to correlate specific populations with key endpoints.

CITRUS uses unsupervised clustering to identify phenotypically similar cells before applying supervised learning algorithms to identify subsets of clusters which are predictive of the pre-defined endpoints [153]. Cells from multiple samples are first combined and clustered in a semi-unsupervised manner, descriptive statistics characterising each cluster are extracted on a per-

sample basis, extracted cluster features are used alongside user-specified endpoints to train a supervised model, internal cross-validation evaluates model fit and finally model features are plotted as a function of endpoints of interest and clusters phenotypes are determined by the density plots of markers used for clustering [153]. In practical terms this means that CITRUS is ideal for comparing groups of samples, such as control and disease, or pre and post treatment.

2.7.4 PHENOGRAPH

Phenograph is a data driven, unsupervised, non-parametric approach which creates a nearest neighbour graph of interconnected nodes with similar phenotypes [141]. The graph is then partitioned into phenotypically coherent subpopulations using algorithms drawn from social networking. A tSNE based algorithm is then used to create a map to allow data visualisation in a similar way to viSNE.

2.7.5 Other visualisation techniques

A range of other visualisation techniques including principle component analysis (PCA) and heatmaps can be applied to mass cytometry data, as well as statistical techniques including significance analysis of microarrays (SAM).

2.8 The future

As mass cytometry technology continues to evolve the range of techniques available to researchers also expands. In addition to improvements to the mass cytometry machine, which is now onto its third generation, imaging mass cytometry now allows spatial information to be integrated with single cell profiling. This is anticipated to provide crucial information regarding the location of key distinct immunological subsets within the tumour microenvironment.

The numbers of publications incorporating mass cytometry has increased dramatically in recent years, in 2012 there were 13 publications per year citing mass cytometry, in 2015, when this project began, there were 44 and in 2017 the number had risen to 131 (PubMed Literature search Jan 2018). As mass cytometry becomes an increasingly well established technology the number of centres investing in its use has also increased. There are currently more than eight centres using mass cytometry at academic institutions in the UK alone compared with only three when this project started. This is leading to expanded networking and an increasing pool of expertise as well as paving the way for the development of novel applications.

Additionally an increasing number of companies are producing mass cytometry compatible reagents and antibodies resulting in increased catalogue of pre-conjugated antibodies as well as introducing price competition.

2.9 Summary points

1. Mass cytometry uses isotopically pure metal tagged antibodies to label cellular proteins, enabling 40 parameters to be assessed simultaneously within a single antibody panel with minimal spectral overlap
2. Potential technical limitations can be overcome with careful panel design, regular machine tuning and the use of appropriate controls
3. Algorithm based data analysis tools aid the interrogation of multi-dimensional data and can be used to identify novel populations
4. Continued developments are expanding the range of applications available to reasearchers

3. General materials and methods

3.1 Biological samples

3.1.1 Ethics

Ethical approval to obtain and study clinical samples was provided by the Health Research Authority NRES Committee (Reference 10/H0704/65) and East London and the City HA Local Research Ethics Committee (Reference 05/Q0605/140). All samples were obtained after receiving ethical approval and signed informed consent.

3.1.2 Isolation and cryopreservation of PBMCs

Healthy peripheral blood mononuclear cells were obtained in the form of leukocyte cones from the NHS Blood and Transplant. These are leukocyte rich blood generated as a result of platelet apheresis donation by healthy donors.

Mononuclear cells were isolated by density gradient separation. Cells were processed in a Class II biosafety cabinet. Each leukocyte cone was diluted to 150ml with sterile phosphate buffered saline. 30mls of diluted buffy coat were layered onto 15mls of Lymphoprep^{TM} (Fresenius-Kabi) in 50ml sterile conical tubes. Cell fraction separation was performed by centrifuging for 35 minutes at room temperature at 1500rpm with no break using an Allegra X-15R centrifuge (Beckman Coulter). The peripheral blood mononuclear cell layer was carefully removed by gentle pipetting, transferred to a fresh sterile 50ml conical tube and diluted with 20ml of sterile PBS. Samples were spun at 1200rpm for 10 minutes at room temperature with full break settings. Supernatant was discarded and cell pellets resuspended and pooled before being diluted with 30mls sterile PBS and spun at 1800 rpm for 10 minutes at room temperature. Red cells were lysed by incubation with 5ml of red cell lysis buffer dilution (1 in 10 dilution of red cell lysis concentrate buffer (Biolegend) in sterile water) for 5 minutes. Following incubation samples were diluted with 40mls sterile PBS and centrifuged at 1800 rpm for 10 minutes at room temperature. Cell number and viability was assessed using automated Vi-Cell XR haemocytometer (Beckman Coulter) at a 1 in 5 dilution.

Cells were suspended in freezing media (90% foetal bovine serum (FBS, Life Tech) and 10% dimethyl sulfoxide (DMSO, Sigma Aldrich)) at a concentration of $20x10^6$ per ml and immediately placed on ice before slow transfer of 1ml aliquots to cryovials. Vials were transferred to -80 ^{o}C freezer overnight in a controlled rate cooler (Mr. Frosty) before transfer to liquid nitrogen tank for long term storage.

3.1.3 Clinical sample identification and storage

All myeloma and MGUS tissue samples within the Bart's Cancer Institute Tissue Bank were identified. From this list all samples from time of first diagnosis were identified and clinical data relating to these samples was obtained via the Bart's Cancer Institute data managers.

Healthy bone marrow samples obtained after informed consent from individuals undergoing elective hip replacement were provided by Dr. John Riches and stored in liquid nitrogen until sample analysis. Further non myeloma control bone marrow samples from individuals with stage 1, non-bone marrow involved DLBCL patients were identified within the Bart's Cancer Institute Tissue Bank.

Myeloma patient samples and healthy bone marrow samples were collected, prepared and stored in liquid nitrogen by the Bart's Cancer Institute Tissue Bank. Samples were retrieved from long term storage and transferred to liquid nitrogen tanks within the laboratory area prior to analysis.

3.1.4 Sample thaw procedure

Cells were retrieved from liquid nitrogen storage and transported on dry ice. Thawing took place in pre heated waterbath at 37 ^{o}C. As soon as thawing occurred sample was transferred to Class II biosafety cabinet, and the outside of the vial was disinfected with 70% IMS. Cells were gently resuspended drop wise with 1ml of sterile, warmed FBS before being transferred to 10mls of pre warmed complete culture media. Cells were centrifuged at 500g for 5 minutes at room temperature. Cell number and viability was assessed using an automated Vi-Cell XR haemocytometer (Beckman Coulter) at 1 in 5 dilution, or a LUNA-FL^{TM} counter (Logo Biosciences).

3.2 Lanthanide labelling of antibodies

Where possible commercially available and validated antibody-lanthanide conjugates were purchased. When this was not possible, suitable antibodies were conjugated and validated in-house using appropriate, protein free buffer, purified antibodies.

MaxPar ready antibodies (BioLegend) were selected when available as these are validated for use by mass cytometry and are carrier protein free with optimised concentration. When these were not available for the markers of interest, highly purified, carrier free antibodies were used (BioLegend).

Target	Clone	Isotype	Source	Metal for conjugation
2B4	Cl.7	Mouse IgG1k	Biolegend (non MaxPar ready)	164Dy
CD38	HIT2	Mouse IgG1k	Biolegend MaxPar ready	161Dy
IL2	MQ1.17H2	Rat IgG2a	Biolegend MaxPar ready	148Nd
IL10	JES3-9D7	Rat 1gG1k	Biolegend MaxPar ready	141Pr
Ki67	Ki67	Mouse IgG1k	Biolegend MaxPar ready	153Eu
PD1	EH.12.2H7	Mouse IgG1k	Biolegend MaxPar ready	172Yb
PDL1	29E.2AS	Mouse IgG2k	Biolegend MaxPar ready	143Nd
TIM3	F38-ZE2	Mouse IgGk	Biolegend MaxPar ready	156Gd

Table 3.1: Antibody clones selected for in-house conjugation

Antibodies were prepared following the Fluidigm antibody labelling protocol. Initially when using MaxPar ready antibodies the buffer exchange steps were omitted, as advised by the manufacturer, however subsequently this step was reintroduced as it was found to improve antibody yield.

Filter tip pipettes were used throughout to prevent cross-contamination. X8 polymer antibody labelling kits containing x8 polymer, lanthanide metal solution, W-buffer, C-buffer, R-buffer were purchased from Fluidigm and stored as per manufacturer's instructions. Pre conjugation antibody concentration was verified by measuring absorbance at 280nm using a NanoDrop 1000 Spectrophotometer (Thermo Fisher Scientific).

3.2.1 Metal loading of polymer

Polymer tubes were pulsed for 10 seconds in an Eppendorf Microcentrifuge 5415 C (Brinkman Instruments). Polymer was resuspended with 95ul L-Buffer (Fluidigm) and mixed thoroughly by pipetting before adding 5ul of lanthanide solution (Fluidigm) and incubating at 37^{o}C in a waterbath for 40 minutes. 100ul of metal loader polymer was then added to 200ul of L-Buffer in a 3kDa 500ul V bottomed filter (Merck Millipore) and centrifuged at 12,000g for 25minutes at room temperature in Eppendorf Microcentrifuge 5415 C (Brinkman Instruments). 300ul C-buffer (Fluidigm) was added to the 3kDa filter containing the metal loaded polymer and centrifuged at 12,000g for 30 minutes at room temperature.

3.2.2 Buffer exchange and partial reduction of antibody

At the same time as polymer preparation, 100ug purified antibody was added to 300ul R-buffer (Fluidigm) in 50kDa 500ul V bottomed filter (Merck Millipore) and centrifuged at 12,000g for 10 minutes at room temperature using. Flow through was discarded. 4 mM TCEP

(Tris(2-carboxyethyl)phosphonium chloride) solution was prepared by diluting 0.5M TCEP stock (Life Technologies) in R-buffer (Fluidigm). 100ul of 4nM TCEP dilution was added to 50kDa filter containing purified antibody and incubated at 37 ^{o}C for 30 minutes in waterbath. 300ul of C-buffer (Fluidigm) was then added to the filter which was centrifuged at 12,000g for 10 minutes at room temperature. Flow through was discarded and a further 400ul of C-buffer was added and sample was centrifuged for 10 minutes at room temperature at 12,000g.

This step was timed to finish at the same time as polymer preparation.

3.2.3 Antibody conjugation with metal loaded polymer

Metal loaded polymer was re-suspended with 60ul c-buffer and mixed thoroughly by pipetting before being transferred to partially reduced antibody and mixed thoroughly by pipetting. Antibody-polymer-metal sample was incubated for 60-120 minutes in a 37 ^{o}C waterbath.

Following incubation, 200ul W-buffer was added to the conjugation mixture and centrifuged at 12, 000g for 8 minutes at room temperature. The wash was repeated five further times using 400ul of W-buffer each time. After the final wash, 50ul W-buffer was used to pipette sample and rinse walls of filter. Filter was then inverted over a fresh collection tube and centrifuged at 1000g for 2 minutes. The wash was repeated with a further 50ul W-buffer.

Antibody yield was determined using nanodrop against a W-buffer blank (Fluidigm). Antibody was diluted to a final concentration of 0.5 mg/ml in antibody stabilisation buffer (Candor) supplemented with 0.05% sodium azide (Sigma).

3.2.4 Validation of conjugated antibodies

The antibodies selected for conjugation had all been previously commercially validated for use in flow cytometry. In order to ensure that the conjugation process had been successful and had not damaged the antibody binding site it was necessary to validate each antibody for mass cytometry.

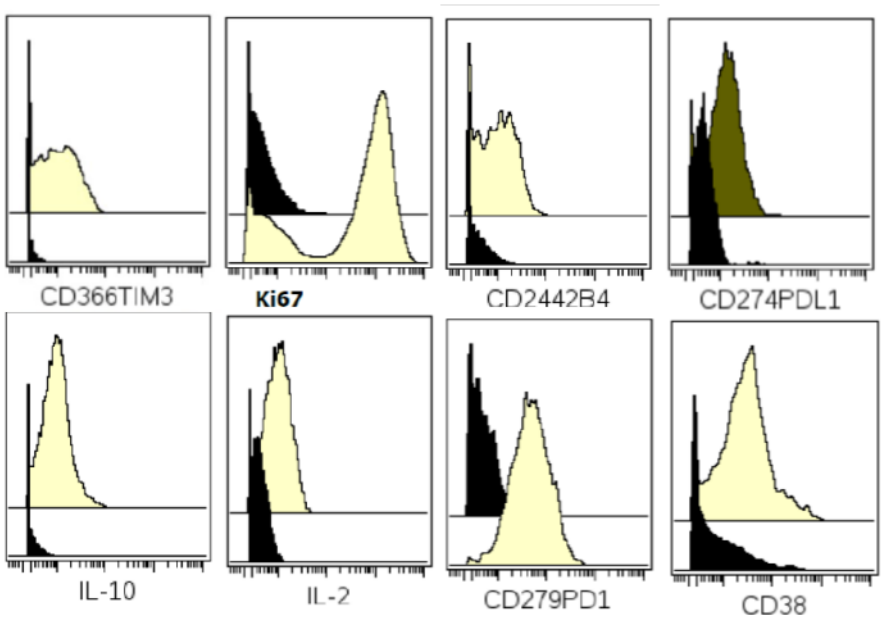

Figure 3.1 Antibody validation using known positive and negative controls

Antibodies were validated using known positive and negative populations (Figure 3.1) and, where available, were compared to a commercially available mass cytometry antibody of the same antibody clone but with a different metal tag (Figure3.2).

A.

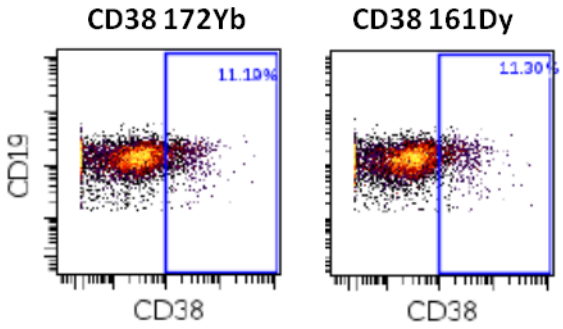

B.

	CD38 172Yb	CD38 161Dy
MSI	58.65	62.09
Percent in gate	11.19	11.30

Figure 3.2: Antibody validation by comparison to commercially conjugated antibody.

Healthy PBMC were stained with a lymphocyte phenotyping panel and either commercially conjugated CD38 172Yb (clone HIT2) or in house conjugated CD38 161Dy (clone HIT2).

[A] Cells were gated on CD19.

[B] MFI and percent in gate were compared between the two populations.

Subsequent runs of antibody production were validated against the positive and negative populations and against previously validated antibody conjugates (Figure 3.3).

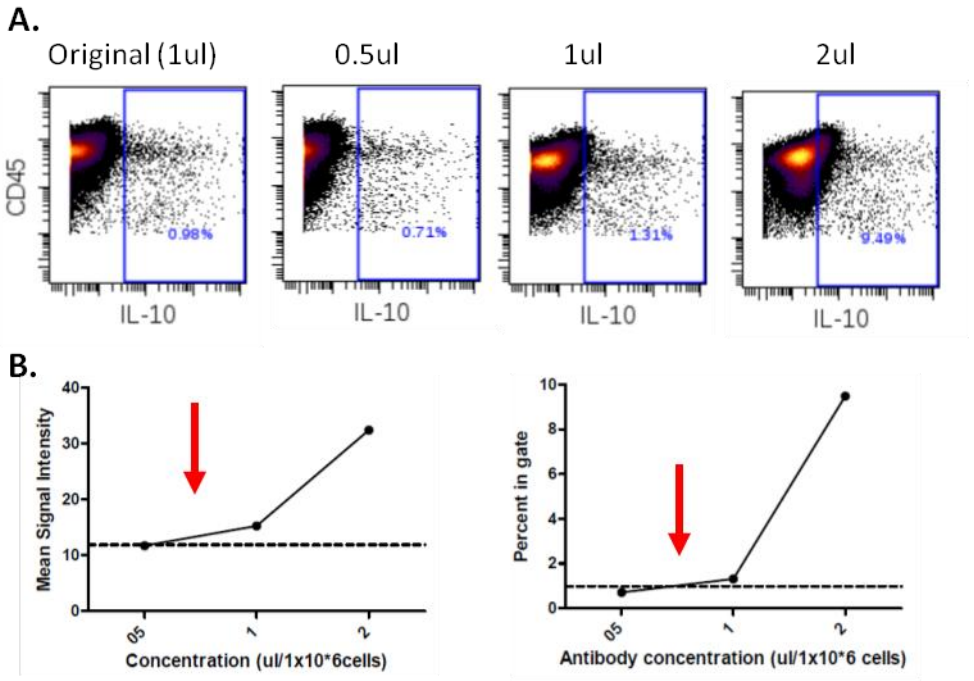

Figure 3.3 Validation of subsequent antibody conjugations

[A] Percent in gate data for IL10 antibody titration
[B] MSI and percent in gate data. Dotted line represent values from the original antibody batch

Target	Metal for conjugation	Positive population	Negative population	MSI on positive population	MSI on negative population
TIM3	156Gd	Stimulated CD4	Unstimulated CD4	13.09	1.79
PD1	172Yb	Stimulated Tregs	Unstimulated Tregs	68.1	5.51
PDL1	143Nd	Stimulated CD8 EM	Unstimulated CD8 EM	16.06	4.73
IL2	148Nd	Unstimulated CD8 EM	Stimulated CD8 EM	10.32	2.78
IL10	141Pr	Stimulated B cells	Unstimulated B cells	11.62	3.52
Ki67	153Eu	Stimulated CD4	Unstimulated CD4	924.03	7.3
2B4	164Dy	Stimulated CD8 EM	Unstimulated CD8 EM	12.33	3.22
CD38	161Dy	Unstimulated B cells	Unstimulated CD8	62.09	23.16

Table 3.2: Positive and negative controls for antibody titration and validation

3.2.5 Titration of conjugated antibodies

Antibodies were titrated across a range of concentrations between 0.25ul and 2ul per 1-3x10*6 cells. Mean signal intensity (MSI) was then plotted for each concentration to determine the minimum antibody required for adequate signal intensity. The stain index was calculated using the following formula:

(MSI positive population – MSI negative population)/2xSD negative population

A higher stain index indicates a better ability to distinguish between two populations. Optimal antibody concentration was determined on the basis of both MSI and stain index (Figure 3.4). For most antibodies a volume of 0.75ul was optimum, granzyme had a particularly strong signal and a concentration of 0.5ul was selected.

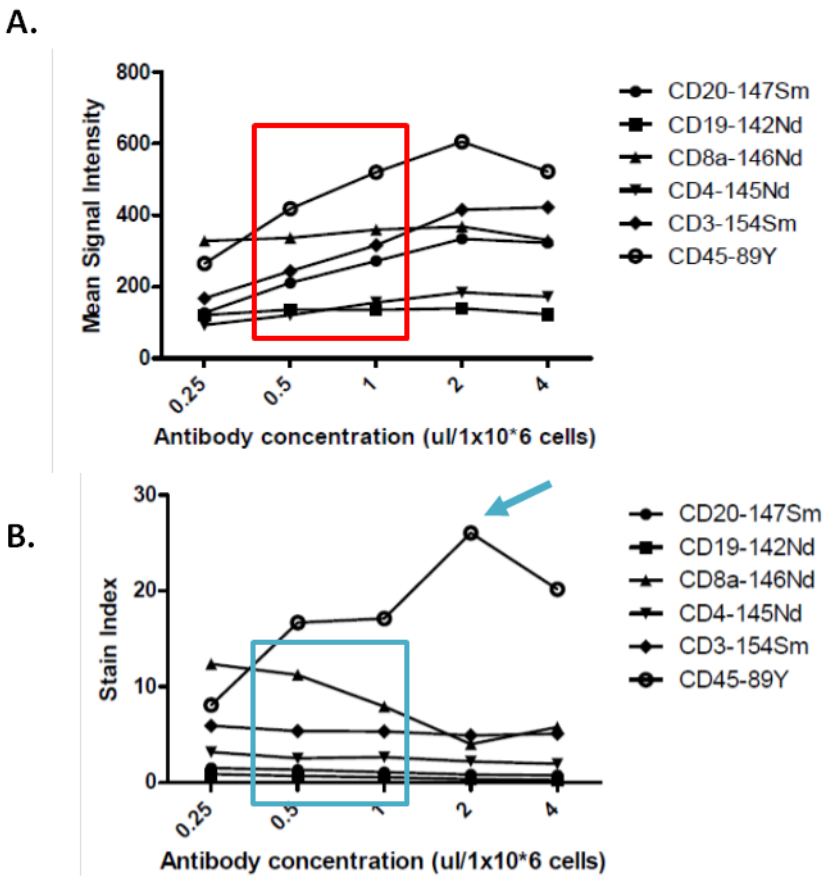

Figure 3.4: Determining optimal antibody concentration

[A] Mean signal intensity suggests an optimal antibody concentration of between 0.5 and 1ul per $1x10^6$ cells
[B] Stain index confirms the optimal antibody concentration of 0.5 to 1ul per $1x10^6$ cells with the exception of CD45 (blue arrow)

3.3 Sample stimulation

3.3.1 CD3 and CD28

Modifications to CD3 and CD28 stimulation were made for tube based versus plate based stimulation.

3.3.1.1 Tube based stimulation

Tightly covered polypropylene FACS tubes were incubated overnight with CD3 (clone OKT3, functional purified, e-biosciences) diluted 1 in 100 in sterile PBS. Control tubes were incubated with 100ul sterile PBS. The antibody solution was then removed and tubes were washed twice with sterile PBS before being blocked with complete culture media for 15 minutes.

Cells were thawed, rested overnight and re-suspended at a concentration of $3x10^6$ per ml. 200ul of cells were added to each tube and CD28 (clone CD28.2, functional purified, e-biosciences) was added at a concentration of 2ug per ml.

Cells were incubated in a humidified Galaxy 48S incubator (Ependorff) incubator for 72 hours at 37^oC with 5% CO_2.

Protein transport inhibitor (2ul/ml, e-biosciences) and metal tagged CD107a (2ul/ml, Fluidigm) were added for the final 4 hours of the stimulation.

3.3.1.2 Plate based stimulation

Wells in a 96 well, U bottomed plate were coated with 50ul of a CD3 (clone OKT3, functional purified, e-biosciences)/ PBS 1 in 100 dilution. The plate was wrapped tightly in parafilm and stored overnight at 4^OC. The antibody solution was then removed, wells were washed twice with PBS and blocked with complete culture media.

Cells were thawed, rested overnight and re-suspended at a concentration of $1x10^6$ per ml. 100ul of cells were added to each tube and CD28 (clone CD28.2, functional purified, e-biosciences) was added at a concentration of 2ug per ml.

Cells were incubated for 72 hours at 37^oC with 5% CO_2.

Protein transport inhibitor (2ul/ml, e-biosciences) and metal tagged CD107a (2ul/ml, Fluidigm) were added for the final 4 hours of the stimulation.

3.3.2 PMA

Cell stimulation cocktail containing PMA and Ionomycin (e-biosciences) was used at a concentration of 2ul per $1x10^6$ cells. Samples were stimulated for 4-5 hours in a humidified Eppendorf incubator at 37^oC with 5% CO_2.

3.3.3 Protein transport inhibition

When intracellular cytokine or cytotoxic granule formation was being measured following stimulation, protein transport inhibitor cocktail (e-biosciences) was added for the final four hours of incubation at a concentration of 2ul/ml.

3.4 Sample preparation and data acquisition: Mass cytometry

To optimise signal, CD107a antibody was added to samples during incubation at the same time as protein transport inhibitor. All other antibodies were used according to either cell surface staining or intracellular staining protocols. Cell staining protocols were adapted from those published by Fluidigm, and optimised to reduce cell loss while maintaining staining intensity.

All in-house conjugated antibodies were titrated to determine optimal staining concentration. Commercially available antibodies were only titrated if found to have a particularly high or low staining intensity during initial optimisation work.

To avoid heavy metal contamination mass cytometry ready reagents were used where possible. MilliQ water was used in place of MaxPar water when necessary. All reagents were stored in plastic not glass and sample analysis was carried out in polypropylene or polystyrene tubes. Cell loss during sample staining was found to be reduced by the use of 5ml polypropylene tubes (Falcon).

Antibody mastermixes were prepared such that a final volume of 50ul was added to each sample containing a cell concentration between 1x10*6 and 3x10*6. Mastermixes for cell surface staining were prepared in cell surface buffer (Fluidigm). Mastermixes for intracellular staining were prepared in nuclear antigen staining perm (Fluidigm).

3.4.1 Panel design and optimisation

3.4.1.1 Panel design

Designing a mass cytometry panel is complex due to the number of parameters involved. While spectral overlap or crosstalk is less of a problem than in flow cytometry is still necessary to plan a panel to avoid crosstalk of a high frequency antigen into a low frequency antigen channel [149]. The panel used for this work was optimised to ensure that there was <0.5% cross

talk between each channel using the MaxPAR panel designer which uses isotopic purity data, oxide formation tendency and antigen expression density information to calculate an optimum panel which minimises crosstalk (Figure 3.5).

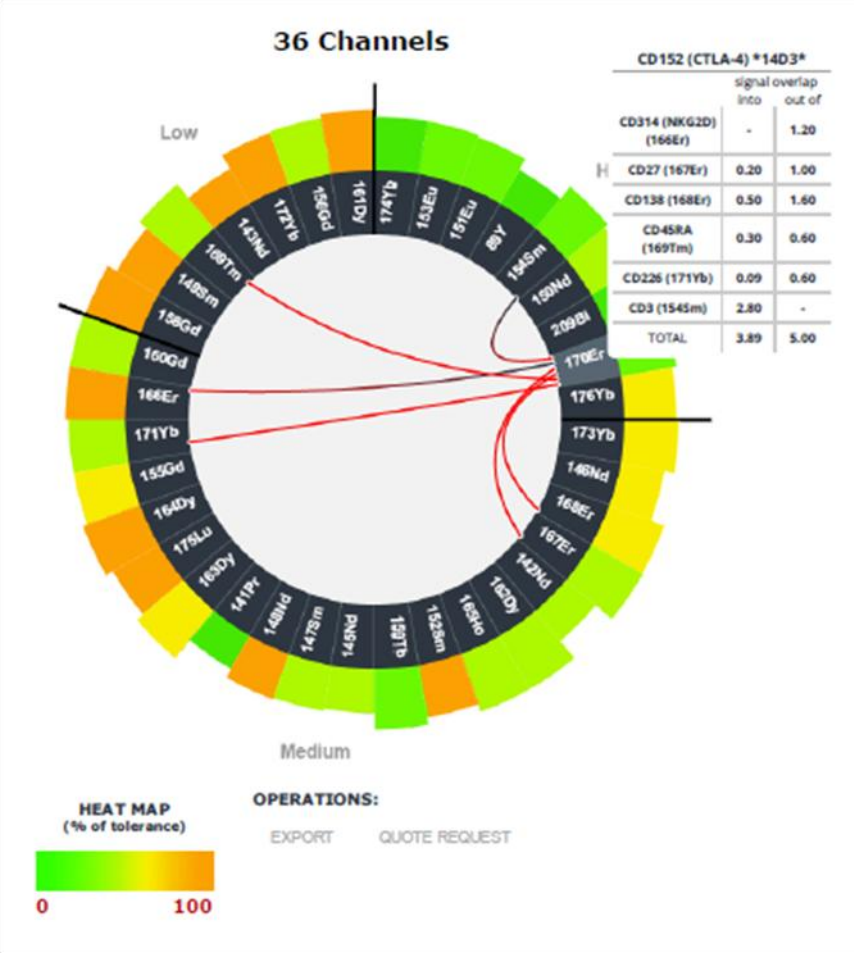

Figure 3.5: Mass cytometry panel design. The MaxPar panel designer allows you to visualise cross talk between different channels. The channels are grouped into three tolerance categories, low, medium and high which are arranged counter clockwise. The tile height for each tag represents the sensitivity of that channel and the colour represents the spill over into other channels.

3.4.1.2 Selection of antibody targets

When designing the antibody panel consideration was given to being able to identify the key cellular subsets of interest while being able to exclude potentially confounding cell types. It was particularly important to be able to exclude plasma cell from analysis as malignant plasma cells can aberrantly express a number of cell surface markers traditionally associated with other cell types, including CD56 [154].

Antibodies against nine immune regulatory receptors were included in order to identify potential therapeutic targets as well as to allow further characterisation of T cell subsets. Each

of these markers have previously been reported to be expressed by cytotoxic lymphocytes and to have a role in either immune tumour surveillance or the inhibition of the immune anti-tumour response.

Functional markers were selected to allow assessment of degranulation, cytokine production and proliferation. Granzyme, perforin and CD107a are well reported markers of degranulation in flow cytometry. Cytokines were selected according to reported cytokine production signatures of the different cell types of interest. Ki67 was a selected as a surrogate marker or proliferation and has previously been shown to correlate with CFSE based proliferation assays [151].

3.4.1.3 Optimisation of staining protocol

During the early stages of developing the mass cytometry panel a high level of cell loss was noted during the sample staining process. This was particularly problematic when considering the small sample size of many of the available clinical samples, which in some cases contain only $1x10^6$ cells. Steps were therefore taken to limit the number of washes required by combining compatible steps of the staining workflow. Viability staining was combined with cell surface staining and nuclear antigen staining was combined with intracellular cytokine staining. In addition a switch was made from using polystyrene tubes to polypropylene tubes for all stages of sample preparation. This resulted in an improvement in cell retention with satisfactory and appropriate staining intensity for all markers. The mean post staining cell recovery before these changes were made was 71%, following these changes it was 91%, however when using myeloma samples a mean cell recovery of 34% was seen. This is likely to reflect poor cell viability, particularly in the setting of stimulation.

The addition of an automated sample introducer, the supersampler, to the mass cytometer resulted in a 1.8 times increase in the number of CD45 positive event counts that could be analysed. The supersampler agitates the sample and maintains a forward flow through the machine tubing. This reduces cell settling and sticking to tubing.

Antigen	Clone	Metal Tag	Purpose	Source
CD45	HI30	89Y	Phenotyping - Pan leukocyte	Fluidigm
CD3	UCHT1	154Sm	Phenotyping - T cell	Fluidigm
CD4	RPA-T4	145Nd	Phenotyping - T cell	Fluidigm
CD8a	RPA-T8	146Nd	Phenotyping - T cell	Fluidigm
CD56	B159	155Gd	Phenotyping - NK	Fluidigm

CD16	3G8	209Bi	Phenotyping - NK	Fluidigm
CD19	HIB19	142Nd	Phenotyping - B cell	Fluidigm
CD20	2H7	147Sm	Phenotyping - B cell	Fluidigm
CD38	HIT2	161Dy	Phenotyping - Plasma cell	Biolegend*
CD138	DL101	168Er	Phenotyping - Plasma cell	Fluidigm
CD45RA	HI100	169Tm	Phenotyping - T cell subsets	Fluidigm
CD197 (CCR7)	G043H7	159Tb	Phenotyping - T cell subsets	Fluidigm
CD27	L128	167Er	Phenotyping - T cell subsets	Fluidigm
CD28	CD28.2	160Gd	Phenotyping - T cell subsets	Fluidigm
CD25	2A3	149Sm	Phenotyping - T regulatory	Fluidigm
CD127	A019D5	176Yb	Phenotyping - T regulatory	Fluidigm
FoxP3	PCH101	162Dy	Phenotyping - T regulatory	Fluidigm
HLA-DR	L243	174Yb	Phenotyping - B cell subsets	Fluidigm
CD244 (2B4)	C1.7	164Dy	Immune activatory receptor	Biolegend*
CD134 (OX40)	ACT35	158Gd	Immune activatory receptor	Fluidigm
CD314 (NKG2D)	ON72	166Er	Immune activatory receptor	Fluidigm
CD226 (DNAM1)	DX11	171Yb	Immune activatory receptor	Fluidigm
CD223 (LAG3)	874501	150Nd	Immune inhibitory receptor	Fluidigm
CD366 (TIM3)	F38-2E2	156Gd	Immune inhibitory receptor	Biolegend*
CD152 (CTLA4)	14D3	170Er	Immune inhibitory receptor	Fluidigm
CD279 (PD1)	EH12.2H7	172Yb	Immune inhibitory receptor	Biolegend*
CD274 (PDL1)	29E.2A3	143Nd	Immune inhibitory receptor	Biolegend*
Granzyme	GB11	173Yb	Functional - Degranulation	Fluidigm
Perforin	B-D48	175Lu	Functional - Degranulation	Fluidigm
CD107a	H4A3	151Eu	Functional - Degranulation	Fluidigm
IFNy	B27	165Ho	Functional - Cytokine	Fluidigm
TNFa	Mab11	152Sm	Functional - Cytokine	Fluidigm
IL2	Mq1-17H12	148Nd	Functional - Cytokine	Biolegend*
IL10	JES3-9D7	141Pr	Functional - Cytokine	Biolegend*
TGFB	TW4-6H10	163Dy	Functional - Cytokine	Fluidigm
Ki67	Ki-67	153Eu	Functional - Proliferation	Biolegend*
Cisplatin		198Pt	Viability	Fluidigm
DNA Intercalator		191/193Ir	Cell event identification	Fluidigm

Table 3.3: Antibodies selected for mass cytometry panel. * Purified antibody purchased from Biolegend and conjugated in-house using Fluidigm conjugation kits.

3.4.1.4 Determining threshold of detection

In order to determine the ability for mass cytometry to detect rare populations, spiking studies were carried out. A known number of CD45 labelled PBMCs were added to a known number of unlabelled PBMCs from the same donor. All cells were labelled with cisplatin and iridium to allow cell identification and exclusion of non-viable cells. Samples were then analysed by mass cytometry and the percentage of CD45 positive viable cells in each sample determined. Samples were run in triplicate with two sets of samples undergoing barcoding prior to analysis.

This demonstrated that it is possible to identify populations with a frequency 1%. At populations of less than 1% the spiked cells can still be identified but the actual detected population size is higher than the expected population size. This may relate to measurement error at low cell number or low level cross talk from another channel. (Figure 3.6)

A.

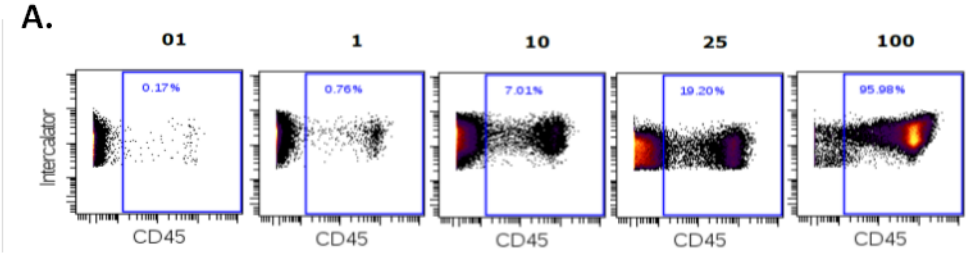

B.

Spiked (%)	Expected CD45 (%)	Actual CD45 (%)
100	95	95.89
25	23.75	19.2
10	9.5	7.01
1	0.95	0.76
0.1	0.095	0.17

Figure 3.6: Determining thresholds of detection. In order to assess threshold of detection for populations of varying frequency CD45 spiking experiments were performed. A known number of healthy PBMCs were stained with CD45-89Y before being spiked at different concentrations into unstained PBMCs. The entire sample was then stained with iridium to identify cell events and cisplatin to identify viable cells.

[A] CD45 expression of spiked samples

[B] Expected and actual CD45 expression of spiked samples

3.4.2 Cell surface staining

Samples were washed in 2mls of cell staining buffer (Fluidigm) for 5 minutes at room temperature at 500g using an Allegra X-15R centrifuge (Beckman Coulter). Supernatant was discarded and cells were re-suspended in residual volume by gentle vortex. 50ul of surface marker antibody master mix was added to each sample. Samples were gently vortexed and incubated for 30 minutes at room temperature. During the final 5 minutes of incubation 2ul of cisplatin stock (Fluidigm) diluted 1:10 in PBS was added. After incubation samples were washed twice using 2mls of cell staining buffer at 500g for 5 minutes at room temperature.

3.4.3 Intracellular and intranuclear staining

Intracellular and intranuclear staining steps were successfully combined using intranuclear staining reagents. Sample were vortexed thoroughly to re-suspend pellet in residual volume. 1ml on Nuclear antigen Staining Buffer (1 part concentrate with 3 parts diluents, both Fluidigm) was added to each sample and gently vortexed. Samples were incubated at room temperature for 30 minutes before being washed twice with 2mls of nuclear antigen staining perm (Fluidigm) at 800g for 5 minutes at room temperature. Following a second wash cells were resuspended in residual volume by vortex and 50ul of intracellular antibody mastermix was added. Samples were gently vortexed and incubated for 30minutes at room temperature. Samples were then washed twice with 2mls of Cell Staining Buffer (Fluidigm) at 800g for 5 minutes at room temperature.

3.4.4 Fixation and intercalation

Sample was re-suspended in residual volume and 1ml of FixI dilution (1-part FixI buffer to 4 parts MaxPar PBS), both Fluidigm) was added. Samples were stored for 12-72 hours at 4^{o}C. On the day of analysis 1ul of 1000x dilution of Ir intercalator was added to each sample and incubated for 20 minutes. Samples were washed twice with cell staining buffer, counted, and washed once with MaxPar water for 5 minutes at 800g at room temperature. Cells were left pelleted until run on mass cytometer.

3.4.5 Data acquisition

Samples were analysed using a CyTOF 2 mass cytometer (Fluidigm). Immediately prior to analysis samples were re-suspended to a concentration of 2.5x10^{5}/ml using MaxPar water (Fluidigm) containing EQ beads (Fluidigm) at a 1:10 dilution. Re-suspended sample was filtered prior to analysis using a 40 micron mesh filter (Falcon) to reduce debris and cell clumping. Samples were introduced using a supersampler (Victorian Airships) and run at a rate of 45

microliters per minute. Data files were normalised using the Helios Normaliser (Fluidigm) and stored using the .fcs format.

3.4.6 Data analysis

FCS files were analysed using Cytobank (Cloud based data analysis tool). Statistical analysis was performed in Prism (Graphpad version 5.4 and 7.2).

A data clean up approach was undertaken using Boolean manual gating. EQ beads, which were added to samples to allow data normalisation, were first excluded on the basis of cerium signal. Cell events were identified by dual expression of iridium 191 and 193 isotopes. Iridium is a cationic nucleic acid intercalator which is used to identify events containing DNA. Singlet cell events were then identified using 191Ir and event length. Finally live cell events were identified on the basis of low cisplatin signal (Figure 3.7).

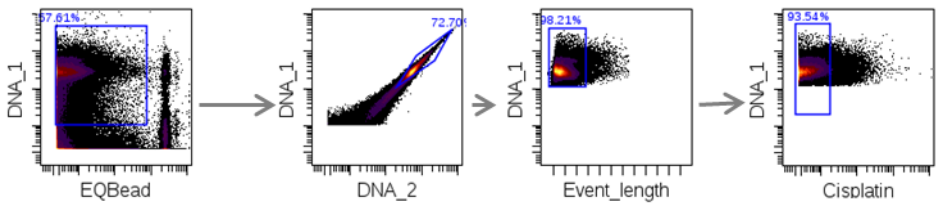

Figure 3.7: Gating strategy to identify live, singlet events

Boolean gating was used to identify cells populations according to their classically described phenotypes (Table 3.4). The expression of functional markers was also assessed using Boolean gating, with positivity cuts off determine by metal minus one controls where necessary.

Cell type	Phenotype
Cytotoxic T lymphocyte	CD45+CD3+CD8+
Naïve cytotoxic lymphocyte	CD45+CD3+CD8+CCR7+CD45RA+
Memory cytotoxic lymphocyte	CD45+CD3+CD8+CCR7+CD45RA-
Effector memory cytotoxic lymphocyte	CD45+CD3+CD8+CCR7-CD45RA-
EMRA cytotoxic lymphocyte	CD45+CD3+CD8+CCR7-CD45RA+
Natural killer cell	CD45+CD3-CD56+CD16+
Immature natural killer cell	CD45+CD3-CD56brightCD16+/-
Mature natural killer cell	CD45+CD3-CD56dimCD16+
Helper T cell	CD45+CD3+CD4+
Naïve helper T cell	CD45+CD3+CD4+CCR7+CD45RA+
Memory helper T cell	CD45+CD3+CD4+CCR7+CD45RA-
Effector helper T cell	CD45+CD3+CD4+CCR7-CD45RA+/-
T regulatory cell	CD45+CD3+CD4+CD25highCD127-FoxP3+
B cell	CD45+CD19+CD20+/-
Naïve B cell	CD45+CD3-CD19+CD20+/-CD27-HLADR-
Memory B cell	CD45+CD3-CD19+CD20+/-CD27+HLADR+
Plasma cell	CD45+CD3-CD19+CD20+/-CD38+CD138+
Malignant plasma cell	CD45+/-CD3-CD38brightCD138+CD56+/-

Table 3.4: Phenotypes used to identify cell populations

3.5 General statistical analysis

Data from .fcs files was assessed using both percent in gate and mean intensity signal parameters. For percent in gate analysis populations with fewer than 50 cells were excluded from further analysis to prevent skewing of percentage based statistics.

When two groups were being compared the t-test was used if data was parametric and the Mann-Whitney for non-parametric data. When multiple groups were being compared the Friedman test was used for non-parametric, paired data sets, the 1-way ANOVA for parametric, non-matched data sets and the repeated measures ANOVA for parametric, paired data sets.

Statistical analysis was carried out in Graphpad Prism versions 5.4 and 7.2

3.6 General reagents

3.6.1 Purchased reagents

Reagent	Details	Source
PBS	Dulbecco's Phosphate Buffered Saline	Sigma
FBS	Fetal Bovine Serum (Heat inactivated)	Life Technologies
RPMI	Rosewell Park Memorial Institute 1640	Sigma
Penicillin / streptomycin	10,000 units penicillin and 10mg streptomycin per ml	Sigma
Cell staining buffer	Buffered saline solution with blocking protein to minimise non specific binding	Fluidigm
Fix I	Buffer for cell fixation prior to permeabilisation	Fluidigm
MaxPar PBS	MaxPar Phosphate Buffered Saline	Fluidigm
MaxPar water	Metal contaminate free water	Fluidigm

Table 3.5: Purchased reagents

3.6.2 Reagents made in house

Reagent	Contents
FACS buffer	PBS + 2% FBS
Complete culture media	RPMI + 1% Pen strep + 10% FBS
Freezing media	FBS +10% DMSO

Table 3.6: Reagents made in house

4. Preface to chapters four to nine

Chapters four through nine describe the phenotypic and functional changes in key different immunological subsets as identified by mass cytometry from the same cohort of patient and control samples. Patient demographics and sample processing methodology are described here to avoid repetition.

4.1 Patient demographics

All single cell suspensions of myeloma tissue samples available within the Bart's Cancer Institute Tissue Bank were identified. Single, diagnostic bone marrow samples were selected for immunological characterisation by mass cytometry. Samples covered the range of myeloma types; IgG, IgA and light chain. Clinical features of the selected samples are shown in table 4.1.

Control bone marrow samples were obtained from elective hip replacements (n=6) and from stage one high grade lymphoma without any evidence of marrow involvement (n=3). It is understandably difficult to obtain sufficient quantities of age matched healthy bone marrow to act as controls. While the control samples used here are not truly healthy controls they are a readily available and chosen as best aged matched surrogate.

	Myeloma **N=18**	**Control** **N=9**
Age at sample collection (years) Median (range)	63.5 (41-90)	67 (40-85)
Male Number (%)	8 (45%)	4 (44%)
Sample type	IgA: 7 (39%) IgG: 7 (39%) Light chain: 4 (22%)	Hip replacement: 6 (66%) DLBCL stage 1: 3 (33%)
Survival (months) Median (range)	51.5 (1-144)	n/a

Table 4.1: Patient demographics

All samples were cryopreserved in liquid nitrogen, using a DMSO and FBS based freezing media, as per the SOP of the Barts Tissue Bank until time of analysis.

4.2 Specific methodology

Samples were processed for mass cytometry and analysed on a CyTOF2 mass cytometer as described in Chapter 3: General materials and methods: when sample size allowed, samples were stimulated in polypropylene FACS tubes with tube-bound CD8 and free CD28 as described in general materials and methods. Data was normalised against EQ bead standards. Data analysis took place in Cytobank.

4.2.1 Statistical analysis

During data analysis sub-populations with fewer than 50 cells were excluded from further percentage based analysis to prevent skewing of percentage based statistics.

All data was assessed for normality using the D'Agostino and Pearson omnibus normality test. When two groups were being compared the t-test was used if data was parametric and the Mann-Whitney for non-parametric data. When multiple groups were being compared the Friedman test was used for non-parametric, paired data sets, the 1-way ANOVA for parametric, non-matched data sets and the repeated measures ANOVA for parametric, paired data sets.

Statistical analysis was carried out in Graphpad Prism version 5.4 and 7.2.

5. Phenotypic and functional assessment of CD3+CD8+ T cells and subsets in newly diagnosed multiple myeloma

5.1 CD8+ lymphocytes and the immune response to malignancy

The immune surveillance model proposes that liberation of tumour antigen by innate immune cells drives recruitment and maturation of antigen presenting cells, which in turn prime and recruit antigen specific T cells. In this model, antigen specific CD8 cytotoxic T cells are then able to identify and target malignant cells. When this system fails or is overwhelmed then overt malignancy can develop.

CD8 T cells which encounter antigen in the absence of a second co-stimulatory signal become anergic [27], while those with a prolonged exposure to antigen in a pro-inflammatory state enter a reversible state of exhaustion [27] (Figure 5.1). T cell exhaustion is associated with a hierarchical loss of cytokine production, with early loss of IL2 and loss of IFNγ occurring later[28], and the expression of immune checkpoint inhibitors including PD1 [29]. The development of T cell exhaustion and its functional impact have been well described by our group in the B cell malignancy CLL [30], which, like myeloma, is a progressive and incurable malignancy. Unlike myeloma however, the bulk of malignant cells in CLL are circulating in peripheral blood while myeloma is largely a bone marrow based disease. Within the bone marrow microenvironment the interplay of structural cells, alongside antigen presenting cells and developing myeloid and lymphoid precursors creates a supportive niche which is hijacked by malignant plasma cells. CLL specific T cells which encounter their antigen in the peripheral circulation may not be subject to the same microenvironment influences as myeloma specific T cells which encounter their antigen in the bone marrow.

In murine models, the absence of mature lymphocytes or defects in lymphocyte cytotoxicity result in increased rates of spontaneous and induced tumour [4,15]. While in human solid tumours, including hepatocellular carcinoma [155], breast cancer [16] and small cell lung [18] cancer, the presence of tumour infiltrating lymphocytes is associated with improved survival, indicating the vital role lymphocytes play in immune surveillance.

Previous studies of the T cell landscape in myeloma have demonstrated that higher levels of circulating lymphocytes are positively correlated with improved survival [65]. Long term myeloma survivors have expanded populations of non-anergic clones [67] with a cytotoxic phenotype [70]. Functional assessment by chromium release assay reveals distinct differences in response between good and standard prognosis myeloma, with good risk individuals having more effective cytotoxicity [66]. Peripheral blood T cell PD1 expression is elevated in advanced myeloma compared to healthy controls [72].

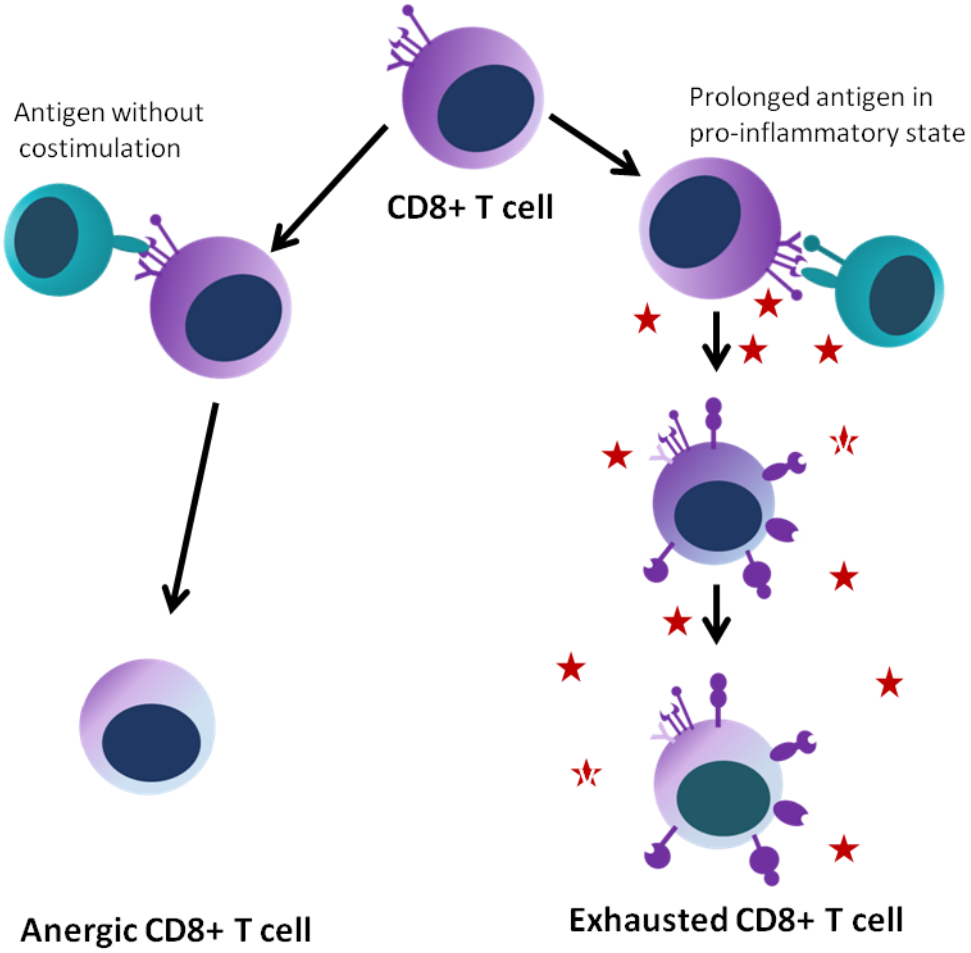

Figure 5.1: T cell anergy and exhaustion

CD8 positive lymphocytes which encounter antigen in the absence of a second co-stimulatory signal become anergic. Those with prolonged exposure to antigen in a pro-inflammatory state enter a reversible state of exhaustion associated with a hierarchical loss of cytokine production and the expression of immune checkpoint receptors.

Myeloma is a slowly progressive disease, characterised by a pre malignant phase followed by an asymptomatic, malignant phase which together may last many years. CD8 T cells are therefore exposed to tumour antigen for a prolonged period of time, with no effective clearance of the malignant cells. While no specific data is available about the immune microenvironment in NDMM, we postulate that features of T cell exhaustion rather than anergy will be seen, even at the time of diagnosis. As the disease progresses and plasma cell clones that are less immunogenic emerge the ability of CD8 T cells to target the malignant compartment is further compromised. It can therefore be expected that the CD8 T cell landscape in NDMM is distinct from that in relapsed refractory myeloma. Furthermore, targeting T cell defects at the time of relapsed refractory disease may be less effective due to the combination of T cell exhaustion and plasma cell immune-subversion. Identifying early

CD8 T cell changes may offer therapeutic opportunities early in the disease course to restore T cell function and control of the malignant plasma cells. For this reason only patients with newly diagnosed multiple myeloma are the focus of the chapter.

5.2 Aim

To compare the frequency and phenotype of CD8+ cytotoxic T lymphocytes in NDMM to non-myeloma controls

To compare the expression of functional markers of proliferation, degranulation and cytokine production of CD8+ cytotoxic T lymphocytes in NDMM to those seen in non-myeloma controls

5.3 Specific methodology

Patient demographics and specific methodology are described in the preface to chapter 4.

CD8 T cells were identified on the basis of the CD45+CD3+CD8+ phenotype. CD8 subpopulations were identified using expression of CD45RA and CCR7. (Figure 5.2)

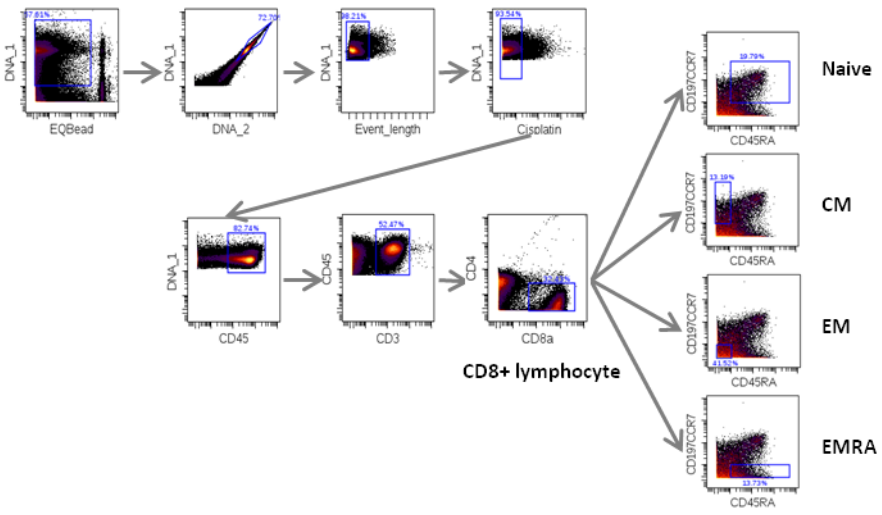

Figure 5.2: CD8 gating strategy

Dead cells, cell doublets and EQ beads were excluded from further analysis. CD8 positive T lymphocytes were identified on the basis of a CD45+CD3+CD8+ phenotype. CCR7 and CD45RA expression was then used to identify CD8 subpopulations.

5.4 Results

5.4.1 The proportion of CD8 positive cells is well preserved in NDMM however there is a reduction in the proportion of resting CD8 CM cells

In the resting state, no significant difference was seen in the proportion of CD3+ cells expressing CD8+ between control and NDMM samples (mean control 36.65%, NDMM 34.91% t-test p=0.7034) (Figure 5.3 A).

Within the CD8+ gate, cells were further categorised into naive, effector memory, central memory and EMRA populations on the basis of expression of CD45RA and CCR7. This demonstrated a relative loss of CM populations in NDMM (mean control 7.883%, NDMM 3.678% t-test p=0.0290). The reduction in CM cells in NDMM was accompanied by a non-significant relative expansion of naïve populations (mean control 23.72%, NDMM 29.27% t-test p=0.4859). There was also a non-significant loss of NDMM EMRA populations (mean control 26.06%, NDMM 16.83% t-test p=0.1042). Effector population proportions remained stable (mean control 18%, NDMM 21.51% t-test p=0.4171) (Figure 5.3 C). This shift towards naive populations differs from the observed changes in CLL where an expansion in effector subsets is seen [30]. These analyses are hampered by the relatively small number of samples analysed and will require validation with a larger cohort in the future.

While overall T cell numbers as a proportion of CD3+ cells are well preserved, the shift toward a naive phenotype in NDMM suggests that cytotoxic effector populations may be diminished, either due to, or resulting in, loss of immunological control of the malignant clone.

5.4.2 Stimulation with CD3 and CD28 restores CM cell proportions and results in an expansion in NDMM effector population proportions

Samples were stimulated with CD3 and CD28 in order to assess their capacity to generate cytokines, degranulate and proliferate. In the setting of exhaustion these cytotoxic functions are diminished [27,28]. When samples were stimulated with CD3 and CD28 for 72 hours, no difference was seen in the frequency of CD3+CD8+ populations between control and NDMM (mean control 24.86%, NDMM 26.26% t-test p=0.8387) (Figure 5.3 B). In contrast to resting samples, following stimulation NDMM CM population proportions were restored to normal levels (mean control 14.62%, NDMM 7.89% t-test p=0.1359) and a shift away from naïve populations was seen (mean control 20.59%, NDMM 15.6% t-test p=0.2264). Furthermore there was a significant relative expansion of effector cells in NDMM (mean control 21.94%, NDMM 42.82% t-test p=0.0298) accompanied by a non-significant reduction in EMRA populations (control 42.85%, NDMM 33.69% t-test p=0.1598) (Figure 5.3 D,E).

This suggests that, in the context of NDMM, the capacity to generate cytotoxic effector cells remains, providing that appropriate stimulatory signals are received. This is vital if therapeutic strategies targeting cytotoxic T cells are to be utilised effectively.

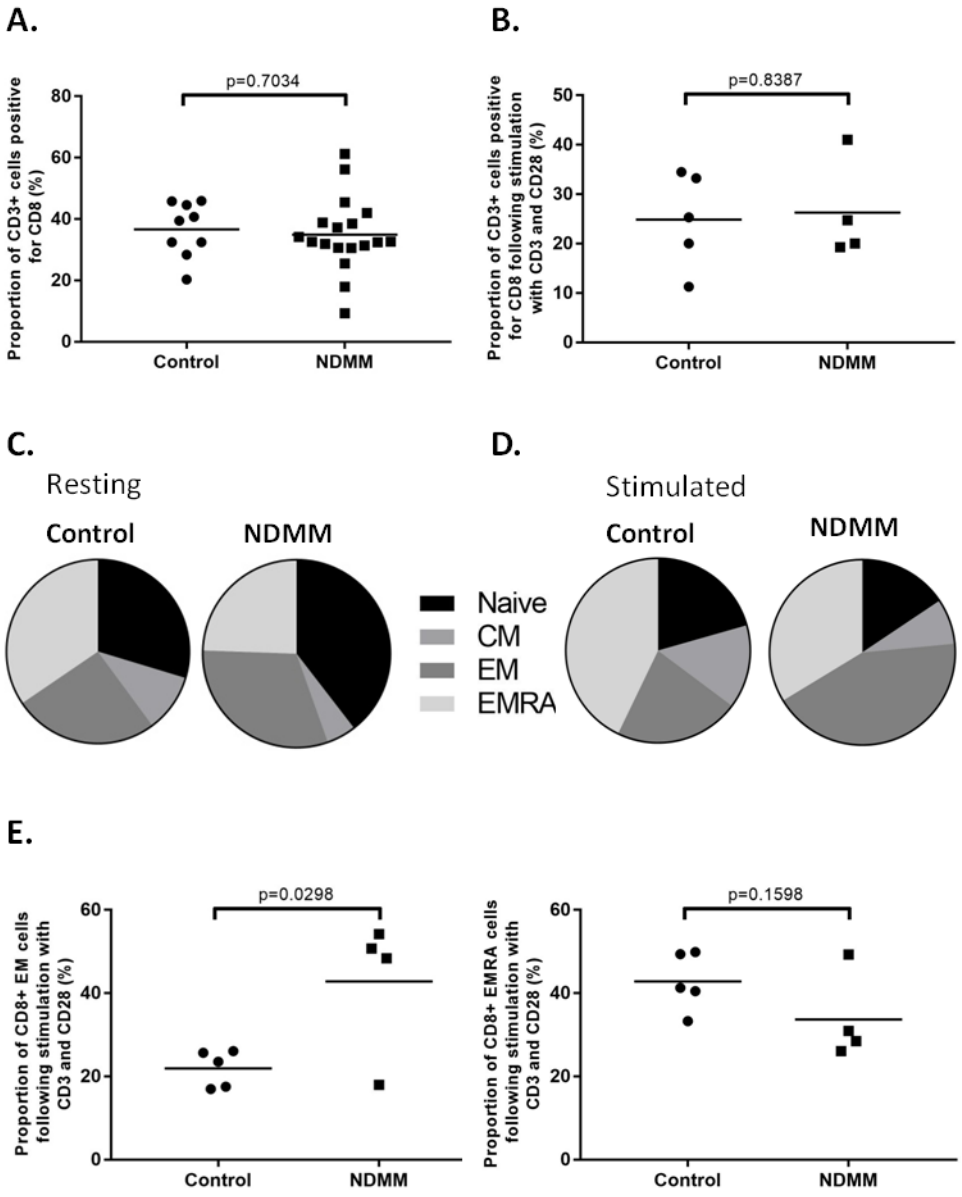

Figure 5.3: Frequency of CD8 populations.

[A] In the resting state no difference is seen between control and NDMM CD8 numbers.
[B] Following stimulation with CD3 and CD28 no difference is seen between control and NDMM.
[C] In the resting state there is a loss in CM populations in NDMM.
[D] Following stimulation with CD3 and CD28 CM populations are restored to normal levels
[E] Following stimulation with CD3 and CD28 with an expansion of EM but not EMRA populations.

5.4.3 CD8 populations in NDMM strongly up-regulate Ki67 expression in response to stimulation with CD3 and CD28

In the resting setting there is reduced Ki67 expression on NDMM naïve CD8 cells compared to controls (mean control 8.076%, NDMM 3.904% t-test p=0.0107). This suggests that the relative

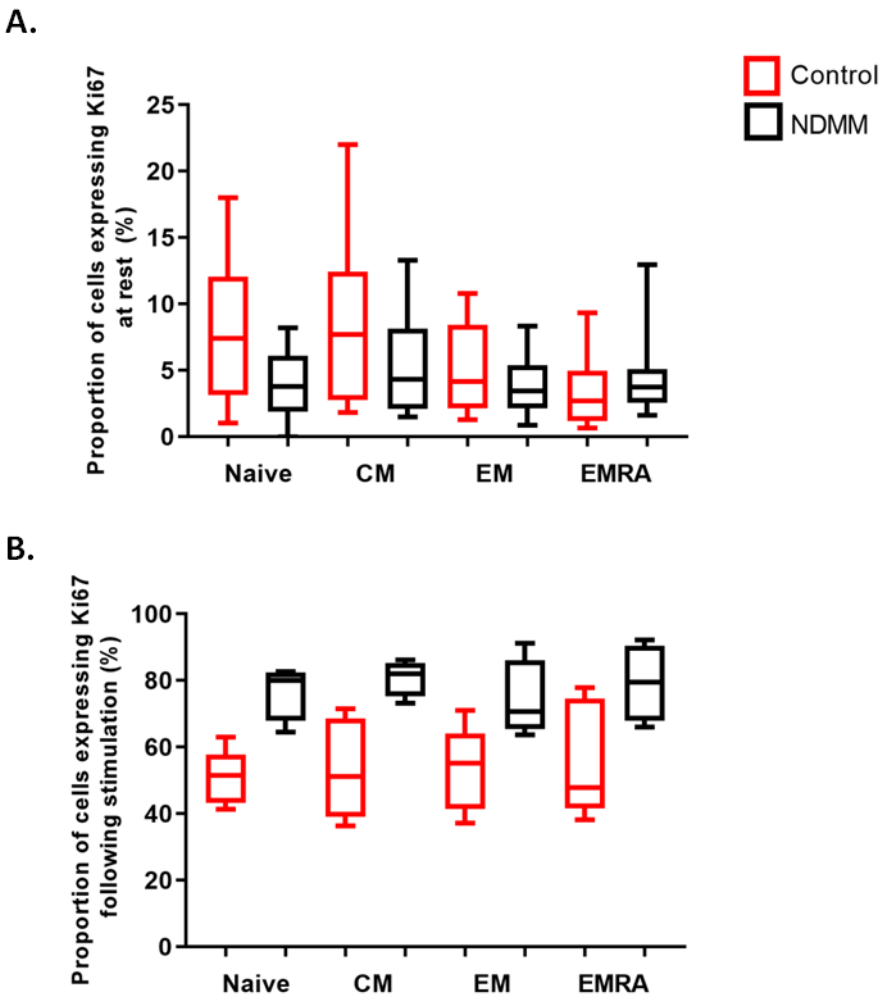

Figure 5.4: Proliferation of CD8 populations

[A] In the resting setting there is reduced Ki67 expression on myeloma naïve CD8 cells compared to controls (control 8.076% NDMM 3.904% p=0.0107) **[B]** Following stimulation with CD3 and CD28 no difference is seen in proliferation between control and NDMM.

expansion of the resting naïve subset described above is not due to proliferation of naïve subsets but is instead due to reduction in one or more other subsets (Figure 5.4 A).

Following stimulation with CD3 and CD28, Ki67 expression rises across all subsets with no difference in expression levels seen between the different subsets in control or NDMM samples. The proportion of cells expressing Ki67 following stimulation is higher in NDMM naïve (mean control 50.72%, NDMM 76.8% t-test p0.0023) and memory (mean control 53.34%,

NDMM 80.83% t-test p=0.0109) subsets than in control samples, suggesting that these populations have a high proliferative capacity. A similar pattern is seen with the mean expression intensity of Ki67 which is higher in NDMM across naïve (mean control 217.6, NDMM 691.6 t-test p0.0086), memory (mean control 217.6, NDMM 691.6 t-test p0.0086), effector (mean control 308.8, NDMM 782.4 t-test p0.0253) and EMRA subsets (mean control 311.4, NDMM 780.5 t-test p0.0206) (Figure 5.4 B).

This indicates that CD8 populations in NDMM retain their proliferative capacity.

5.4.4 CD8 subsets in NDMM are able to produce cytokines in response to appropriate stimulation, however an aberrant pattern of expression across subsets was seen for TGFb, IL2 and IL10

Resting cytokine expression was appropriately low in both control and NDMM samples. Following stimulation with CD3 and CD28 there was a rise in cytokine expression with no significant difference seen between control and NDMM (Figure 5.5).

Since IFNγ, which is lost late in the development of T cell exhaustion, continues to be expressed in NDMM, it is clear that a full T cell exhaustion profile is not present at the time of myeloma diagnosis (Figure 5.5 C).Work within our groups has previously reported that cytokine production was also relatively preserved in the setting of CLL, this was termed "pseudo-exhaustion" [30].

When expression of IL2 across the CD8+ subsets is considered, IL2 expression shows a broadly similar rise across all subsets in both control and NDMM samples. In control samples there was a statistically significant variation in expression (RM-ANOVA p0.0389) which was due to higher expression in memory and effector subsets. This was not significant in NDMM (RM ANOVA p=0.4301) (Figure 5.5 B).

Loss of IL2 production is considered to occur early in the development of T cell exhaustion while aberrant IFNγ production occurs later; in this data, overall intracellular expression of these cytokines is well preserved, suggesting that an established state of T cell exhaustion has not been reached. There is however, aberrant subset expression of IL2 in NDMM with loss of its expression in memory subsets which may indicate early evidence of T cell exhaustion.

The cytokines TGFβ and IL10 are often associated with a pro-inflammatory, pro-tumour cytokine environment. While overall intracellular expression of these cytokines does not statistically differ between control and NDMM, there are differences in which subsets are predominantly responsible in generating these cytokines, which may influence the secreted cytokine fingerprint within the tumour microenvironment. With TGFβ, a shift away from

production by naive subsets is seen, in a pattern distinct from expression in control samples (Figure 5.5 D).

IL10 expression in control populations shows a heterogeneous expression with highest peaks seen in the naïve and memory subsets (Control RM ANOVA p0.0055,). In NDMM subsets the expression is overall lower and more homogenous with a more modest rise in expression in memory and naïve subsets which does not reach significance (NDMM RM ANOVA p0.5450)(Figure 5.5 A).

Naive and effector subsets are expected to have differing spatial locations within the bone marrow microenvironment, with effector populations seen close to malignant plasma cells targets, this skew in pro-tumour cytokine production in NDMM CD8 subsets may therefore be delivering pro-tumour cytokines preferentially to the site of disease.

It is also worth noting that TGFβ and IL10 are present regardless of whether CD8 cells have undergone stimulation, while anti-tumour cytokines rise in response to stimulation. This suggests that providing T cells with an appropriate activating signal is sufficient to overcome the effects of these pro-tumour cytokines and generate anti-tumour cytokines.

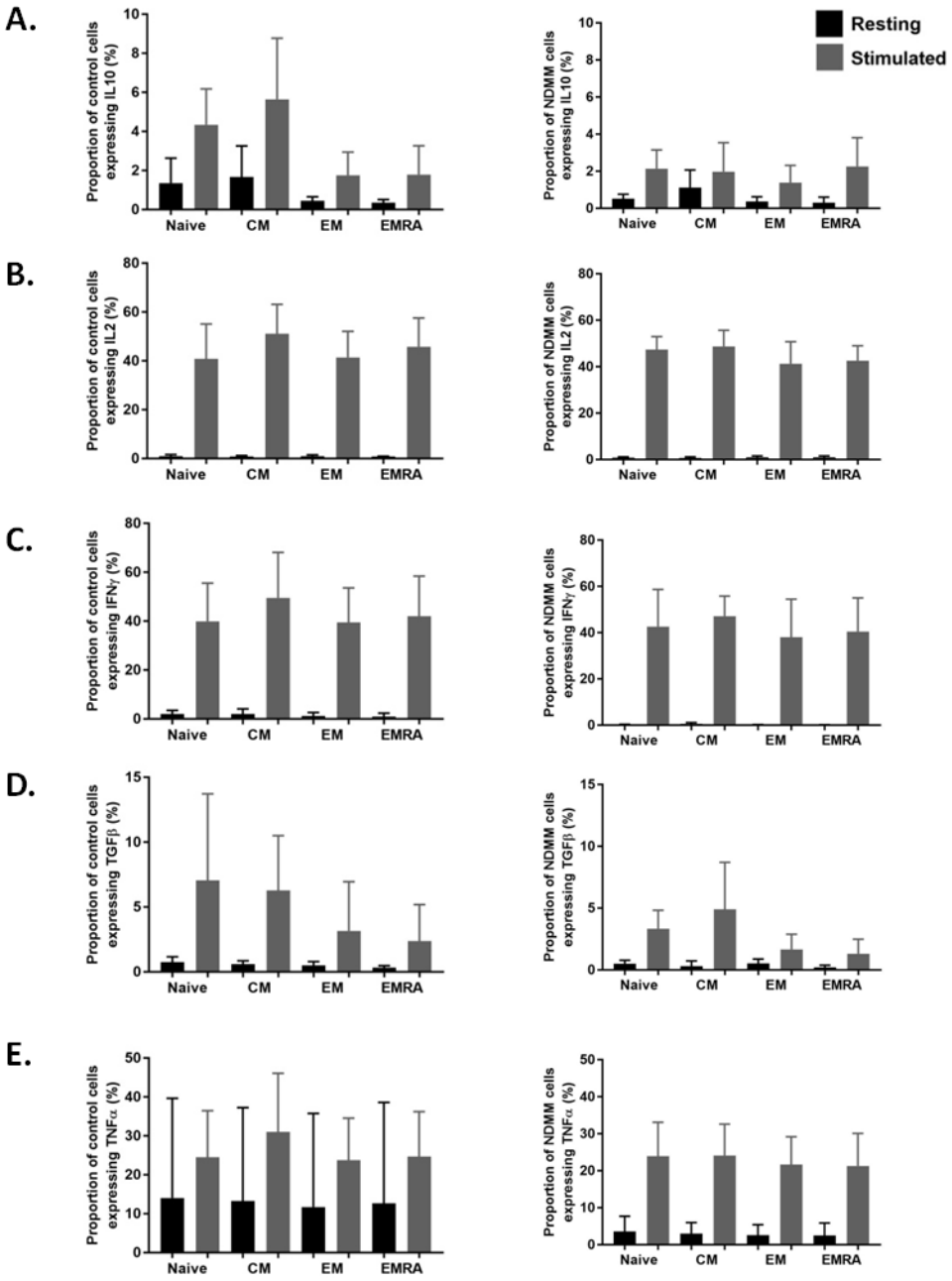

Figure 5.5: Cytokine expression across CD8 subsets in control and NDMM

[A] IL10 expression in NDMM shows a shift away from production by naive and CM subsets.
[B] IL2 expression rises across all subsets following stimulation with loss in variation of expression in NDMM.
[C] IFNγ production rises across all subsets following stimulation
[D] TGFβ expression is similar in pattern to IL10 with a shift away from naive populations.
[E] TNFα rises in expression levels following stimulation

5.4.5 Multi-cytokine producing CD8 subsets are present in NDMM

Since CD8 T cells are capable of producing multiple cytokine types simultaneously, the various cytokine producing subsets were examined.

When all five cytokines measured are considered together 32 different combinations of cytokine production can be identified. In both control and NDMM at rest only 21 of these 32 possible combinations are seen with the majority of these subsets producing only one or two cytokines (Figure 5.6 A). No significant difference between cytokine producing subsets is seen between control and NDMM.

Following stimulation with CD3 and CD28, all 32 cytokine populations become detectable in both control and NDMM samples, with no loss of diversity seen in NDMM. No significant difference between cytokine producing subsets is seen between control and NDMM (Figure 5.6 B).

While this technique can identify 32 cytokine producing subsets it is likely that this includes many populations which are not biologically meaningful. Therefore cytokines were then divided in to the categories pro-tumour and anti-tumour and the cytokines producing subsets in each group were examined (Figure 5.7). No difference was seen between cytokine producing subsets in the resting or stimulated state between control and NDMM samples.

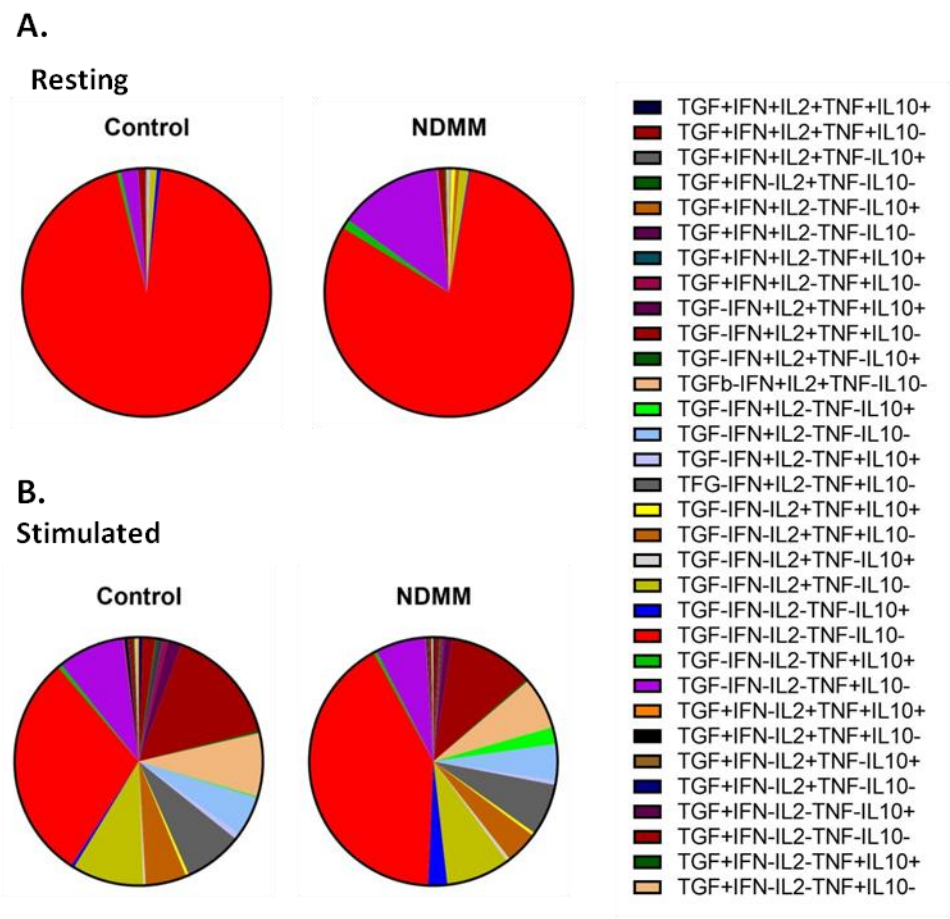

Figure 5.6: Multiple cytokine producing CD8 subsets

[A] At rest 21 of a possible 32 different cytokine producing subsets can be identified of which the majority produce one or two cytokines. No significant difference is seen between control and NDMM.
[B] Following stimulation with CD3 and CD28, all 32 cytokine populations become detectable in both control and NDMM samples, with no loss of diversity seen in NDMM. No significant difference between cytokine producing subsets is seen between control and NDMM.

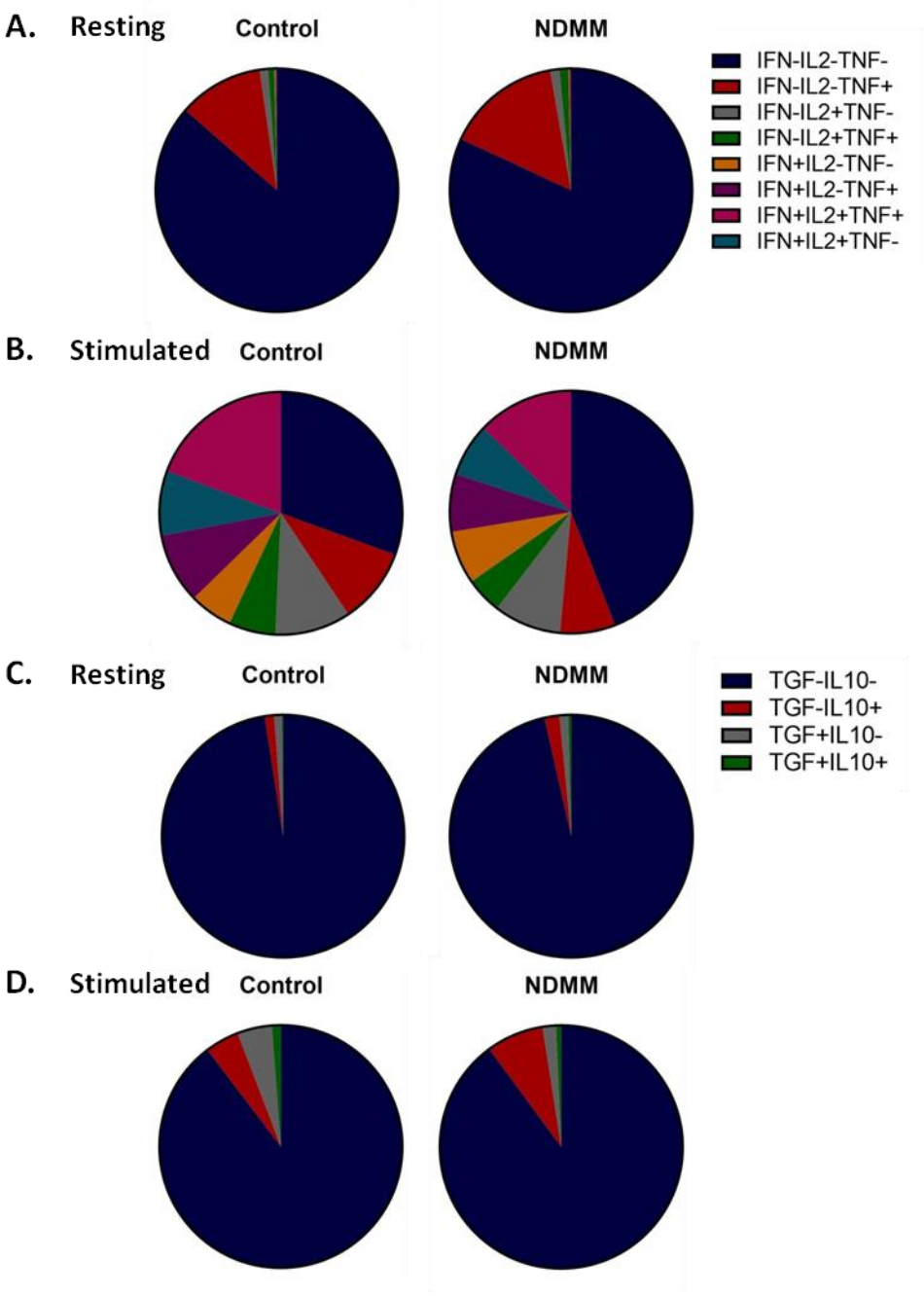

Figure 5.7: Pro and anti-tumour cytokine producing CD8 populations

[A][B] Anti-tumour cytokine producing subsets at rest and stimulation. No difference is seen between control and NDMM.
[C][D] Pro-tumour cytokine producing subsets at rest and stimulation. No difference is seen between control and NDMM

5.4.6 CD8 populations in NDMM express markers of degranulation which are most prominent on effector populations and are upregulated following stimulation with CD3 and CD28

In the resting setting, the proportion of CD8+ cells expressing CD107a is low, with a modest increase seen in NDMM when compared to control (median control 1.836% NDMM 7.156% MW p=0.0422)(Figure 5.8 B). This is echoed by the mean signal intensity which is higher on NDMM total CD8 (median control 0.8839 NDMM 5.884 MW p=0.0168), naïve (median control 1.318 NDMM 2.495 MW p=0.0236) and effector memory (median control 1.006 NDMM 2.056 MW p=0.0311) subsets compared to controls (Figure 5.8 B,C).

Expression of perforin and granzyme B appears higher in resting cells than that of CD107a with no significant difference in expression between control and NDMM samples (Figure 5.8 A). Expression of both markers is low in naïve and central memory subsets, peaks in effector memory subsets and shows a modest fall in EMRA subsets. The fall in expression in EMRA populations is more pronounced in control samples and, for granzyme, approaches statistical significance (mean control 24.45%, NDMM 53.95% t-test p=0.0513) (Figure 5.8 D,E).

Following stimulation with CD3 and CD28, expression of CD107a, granzyme and perforin rises across all subsets in both control and NDMM samples (Figure 5.8 C,D,E). There is no significant difference between the proportions of cells expressing these markers in control and NDMM.

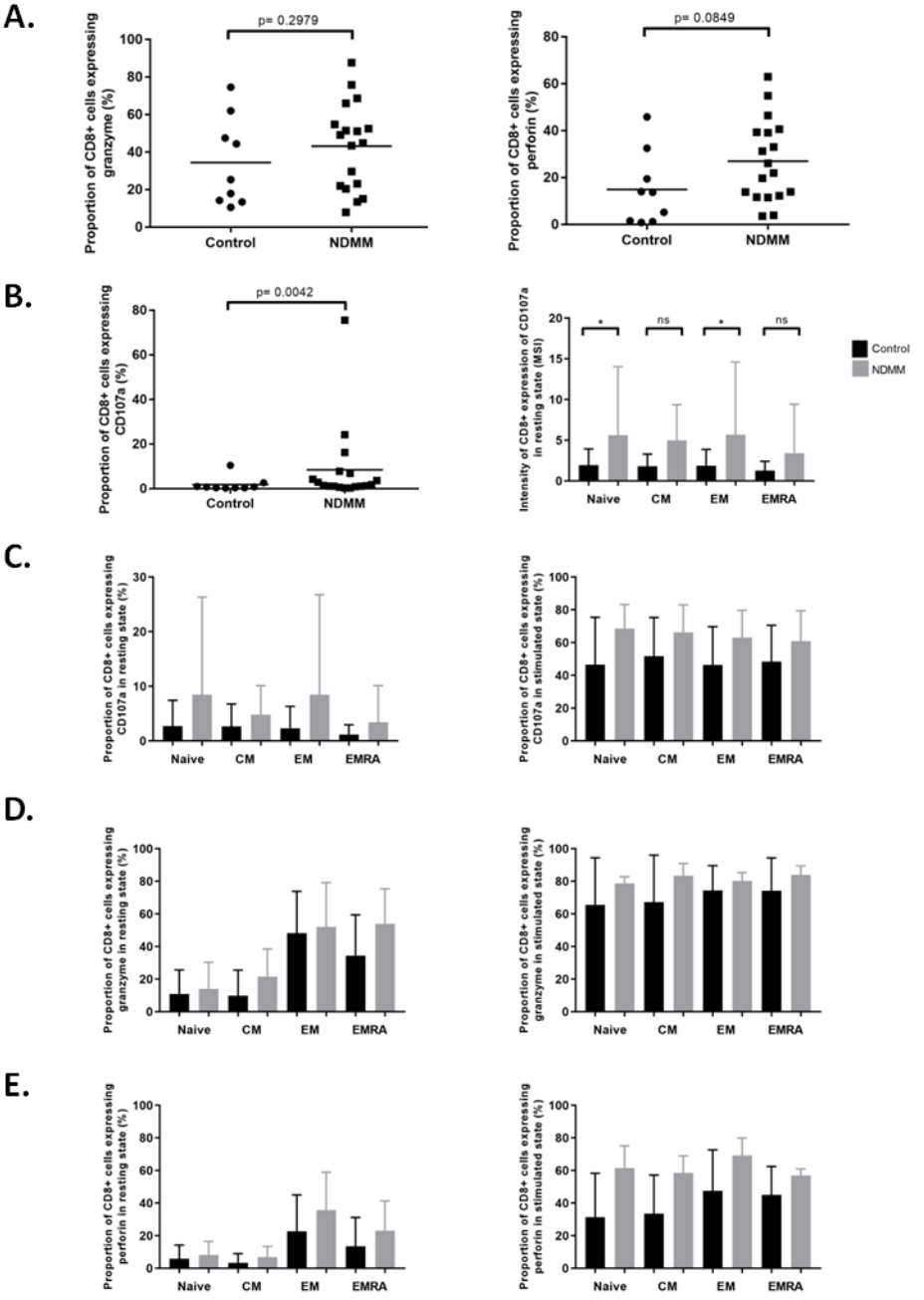

Figure 5.8: CD8 expression of markers of cytotoxicity

[A] Resting expression of granzyme and perforin shows no significant difference between control and NDMM

[B] Resting expression of CD107a is low with a modest increase in NDMM. This pattern is mirrored in mean signal intensity data.

[C] CD107a rises across all subsets following stimulation

[D] In the resting setting granzyme expression peaks in effector memory subsets. Following stimulation granzyme expression rises across all CD8 subsets.

[E] In the resting setting perforin expression peaks in effector memory subsets. Following stimulation perforin expression rises across all CD8 subsets.

5.4.7 DNAM1 , NKG2D, 2B4 and PD1 are present at detectable levels on resting CD8 cells in NDMM which may offer therapeutic opportunities

The co-activating receptors DNAM1 (NDMM 11.39%), 2B4 (NDMM 50.57%) and NKG2D (NDMM 42.73%) are all detectable on resting CD8 cells in NDMM at a level greater than 10% Figure 5.9 A). These remain detectable following stimulation with CD3 and CD28. NKG2D (resting NDMM 42.73%, stimulated NDMM 40.12%) levels remaining stable while 2B4 (resting NDMM 50.75%, stimulated NDMM 27.48%) levels fall (Figure 5.9 B). DNAM1 levels rise and will be discussed in more detail below.

In the resting state, 2B4 expression in naïve and memory populations is 20% while expression in EM and EMRA subsets is 70% and 50% respectively. The pattern is maintained in control and NDMM samples with a similar, albeit lower pattern seen following stimulation (Figure 5.10 D).

NKG2D expression is similar across all CD8 subsets in both control and NDMM samples with a similar pattern seen following stimulation (Figure 5.10 A).

Persistent expression of these receptors in the resting and stimulated state makes them interesting potential therapeutic targets. Using small molecule drugs or monoclonal antibodies to stimulate these receptors may upregulate the CD8 anti-tumour response. Since these ligands are also expressed on NK cells the activity of this population may also be optimised. This strategy carries the risk, however, of unregulated immune activation with the potential for autoimmune complications.

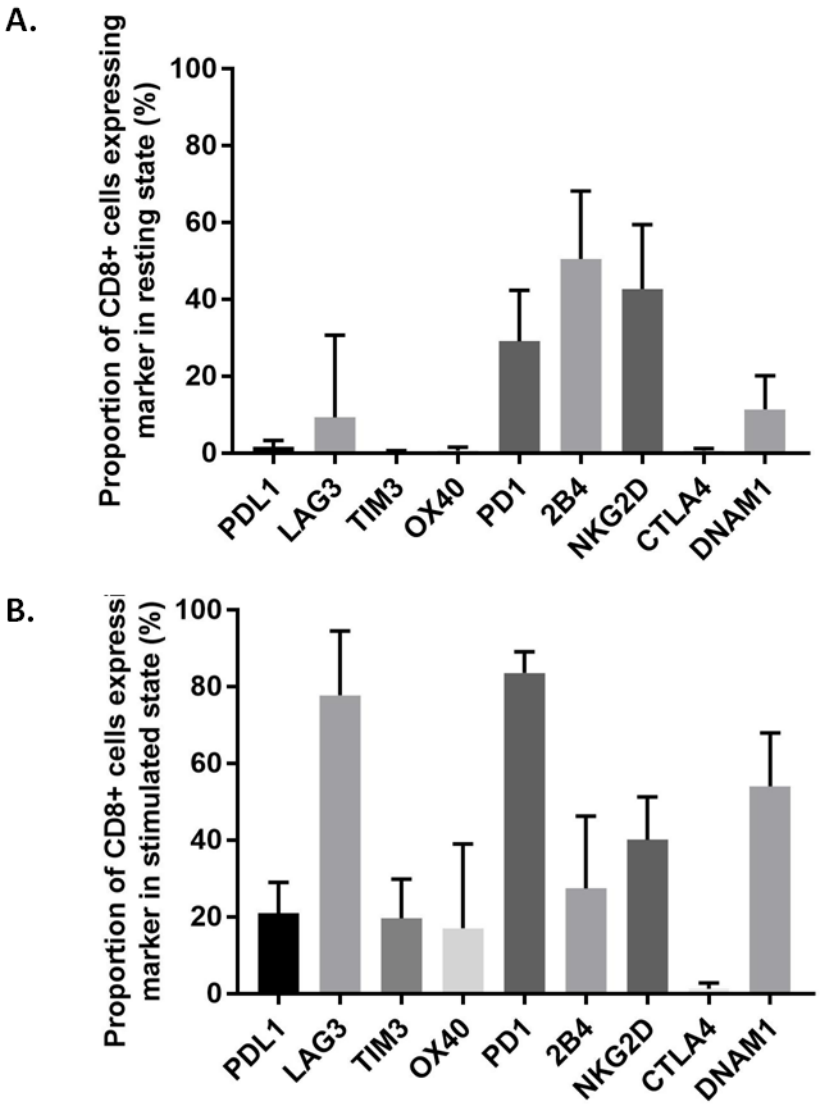

Figure 5.9: Expression of cell surface receptors by CD8 lymphocytes in NDMM

[A] At rest the co-activating receptors DNAM1, 2B4 and NKG2D are all detectable in NDMM at a level greater than 10%.
[B] Following stimulation with CD3 and CD28, NKG2D levels remain stable while 2B4 levels fall. DNAM1 levels rise.

5.4.8 Expression of DNAM1 on resting NDMM CD8 population is reduced in comparison to control samples

In the resting setting DNAM1 expression is reduced in NDMM compared to controls (mean control 18.79% NDMM 11.39% p=0.0463). Following stimulations DNAM1 levels rise and match those of healthy controls (mean control 51.48%, NDMM 54.07% p=0.7717). In the resting state control samples DNAM1 expression is low in naïve and EMRA subsets with peaks in EM and CM subsets (ANOVA p=0.0469). In resting NDMM samples this pattern of expression is lost, with a reduction in DNAM1 expression in CM and EM subsets (ANOVA p=0.1161) (Figure 5.10 C).

DNAM1 is a CD8 co-receptor which can provide the secondary signal necessary to fully activated lymphocytes whose TCR has been engaged by ligand. Loss of expression of the receptor in NDMM may hinder CD8 cell activation. The significance of this is uncertain as other co-stimulatory receptors are expressed at normal levels.

Expression of OX40 (CD134) (NDMM 17.02%), LAG3 (CD223) (NDMM 77.77%), TIM3 (CD366) (NDMM 19.59%) and PDL1 (CD276) (NDMM 20.93%) become detectable following stimulation with CD3 and CD28. In control samples OX40 expression is highest on naïve and central memory populations and falls on effector and EMRA populations (ANOVA p=0.0057) (Figure 5.10 G). Control LAG3 expression is consistent across all subsets (ANOVA p=0.5395) (Figure 5.10 H). Control TIM3 expression peaks in naïve and effector subsets (ANOVA p=0.0310) (Figure 5.10 E). Control PDL1 expression is stable across subsets (ANOVA p=0.2168) (Figure 5.10 F). Matching patterns are seen in NDMM samples.

Both TIM3 and LAG3 are reported to have immune regulatory functions when expressed by CD8 lymphocytes. Their expression is expected to rise following cell stimulation as a physiological mechanism to regulate and limit tissue damage during a cytotoxic response. The fact that their expression is undetectable in the resting state raises questions as to whether inhibitory monoclonal antibodies will be of benefit in NDMM.

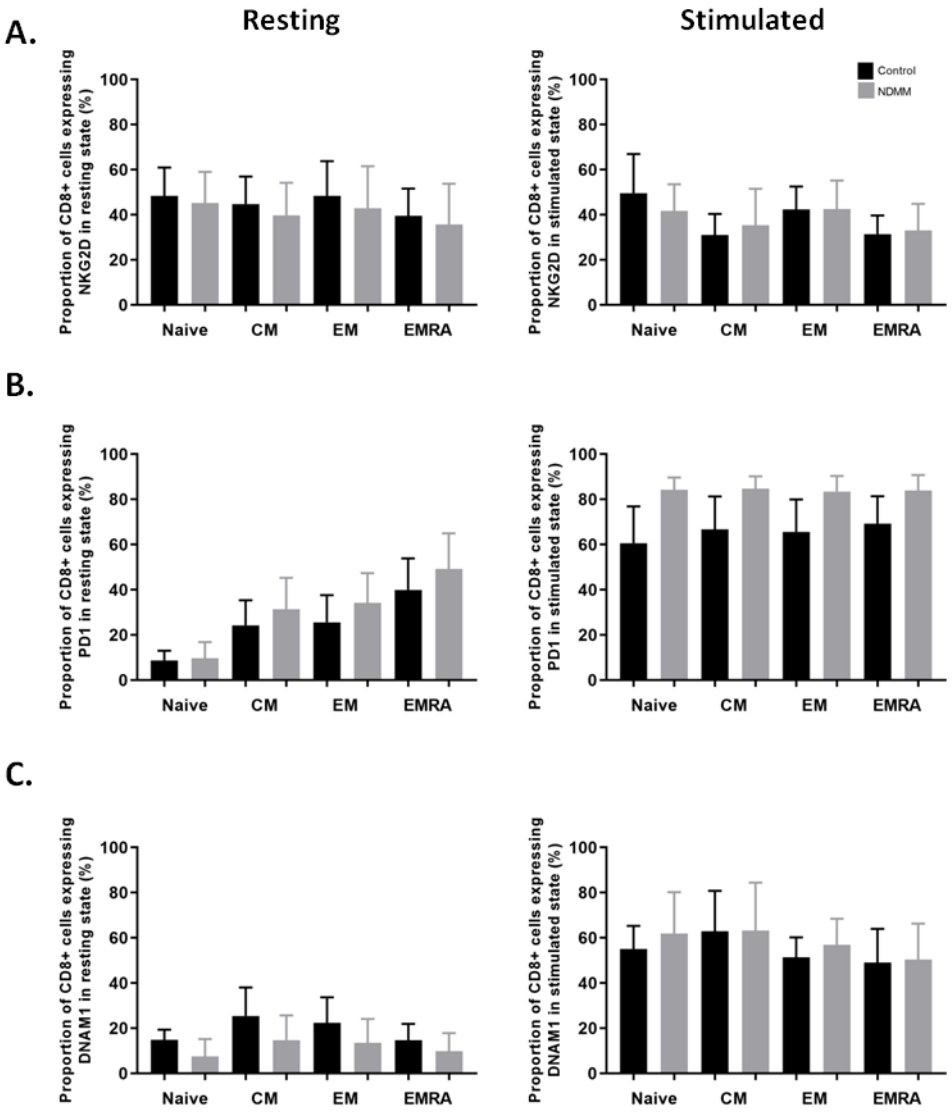

Figure 5.10: Cell surface receptor expression across CD8 subsets

[A] NKG2D expression is similar across all CD8 subsets in both control and NDMM samples and remains detectable following stimulation.
[B] PD1 expression is low on naive subsets and rises across memory and effector subsets in the resting state. Following stimulation there is equivalent expression across al subsets.
[C] DNAM1 expression is reduced in NDMM compared to control in the resting setting. In control samples expression peaks in effector populations but this pattern of expression is lost in NDMM. Following stimulation levels rise across all subsets in control and NDMM.

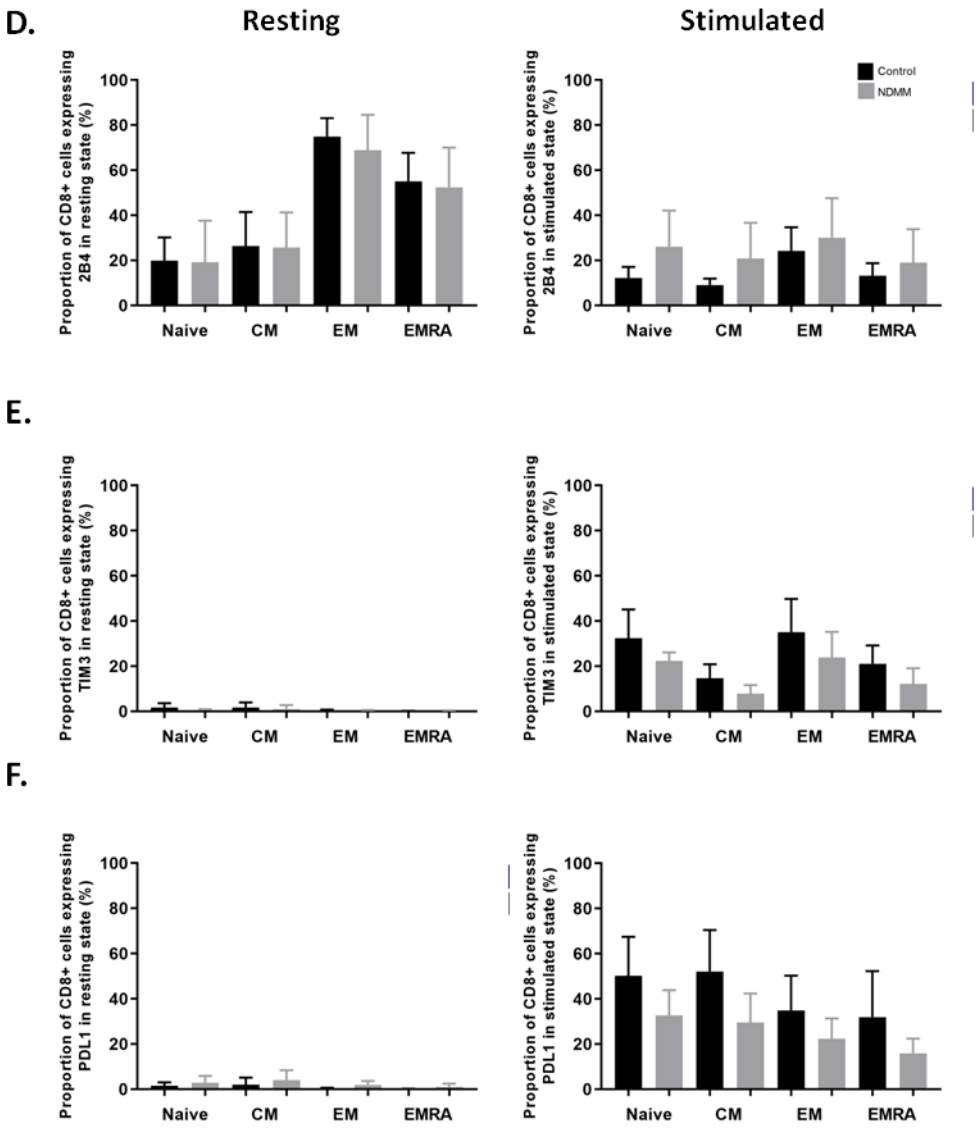

Figure 5.10 cont: Cell surface receptor expression across CD8 subsets

[D] 2B4 expression in naïve and memory populations is low while expression in EM and EMRA subsets is 70% and 50% respectively. Levels fall following stimulation.
[E] TIM3 expression at rest in undetectable. Following stimulation it peaks in naive and effector subsets.
[F] PDL1 expression at rest is low but rises across all subsets following stimulation.

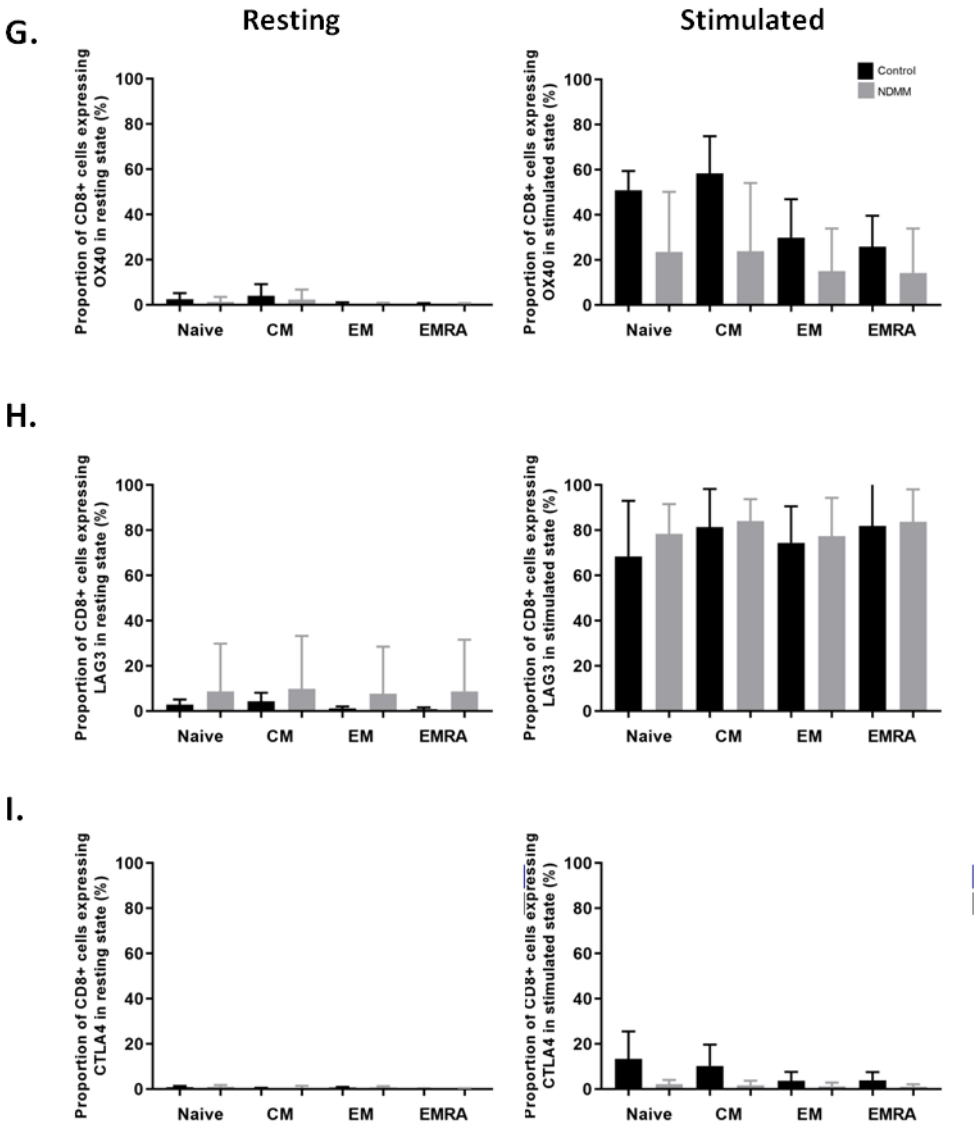

Figure 5.10 cont: Cell surface receptor expression across CD8 subsets

[G] OX40 expression is undetectable at rest. Following stimulation it peaks in naive and central memory subsets and is less marked in effector and EMRA populations.

[H] LAG3 expression rises following stimulation and is consistent across all subsets

[I] CTLA4 expression remains at a low level in both control and NDMM subsets at rest and following stimulation.

5.4.9 PD1 expression is increased in stimulated CD8 cells in NDMM when compared to controls

PD1 expression is detectable in the resting state (NDMM 29.1%) and rises with stimulation (NDMM 83.62%) with a significantly higher level reached in stimulated NDMM samples when compared to controls (mean control 65.54%, NDMM 83.62% t-test p=0.0455). In the resting setting, PD1 expression is low on naïve subsets and highest on EMRA subsets with both central memory and effector memory populations showing a modest expression. This pattern is seen in both NDMM and control populations (NDMM ANOVA p=<0.0001, control ANOVA p=<0.0001). Following stimulation there is equivalent expression of PD1 across all subsets (Figure 5.10 B).

5.4.10 PD1^{high} CD8 T cells are increased in NDMM and have an aberrant functional phenotype

When CD8+ cells are stratified according to PD1 expression levels three distinct populations can be considered, the PD1 low, intermediate and high subsets (Figure 5.11 A). In the resting setting, the proportion of cells with PD1^{high} expression is low, however it is significantly higher in NDMM samples (median control 0.44%, NDMM 1.05% MW p=0.0175) (Figure 5.11 B). When the PD1^{high} populations are compared, the NDMM PD1^{high} subset had a lower expression of DNAM1 (median control 17.31%, NDMM 2.726% MW p=0.0175) but higher expression of granzyme (median control 15.96%, NDMM 50.67% MW p=0.0379) compared to control samples (Figure 5.11 C).

When the pattern of expression is considered across PD1 low, intermediate and high populations in NDMM, granzyme and perforin expression is highest in PD1^{int} subsets (granzyme Friedman p0.0272 perforin Friedman p0.0207) (Figure 5.12). A similar pattern of expression is seen for DNAM1 (Friedman p0.0003) (Figure 5.13 B). In contrast NKG2D expression shows a modest increase in expression in PD1^{high} populations (Friedman p0.0272)(Figure 5.13 A), while 2B4 has equal expression between PD1^{high} and PD1^{int} subsets (Friedman p0.0162) (Figure 5.13 C). In control samples none of these markers show a significant variation in expression levels between PD1 subsets. This suggests that PD1^{high} subsets have lost cytotoxic activity, in keeping with the role of PD1 as a marker of immune cell exhaustion.

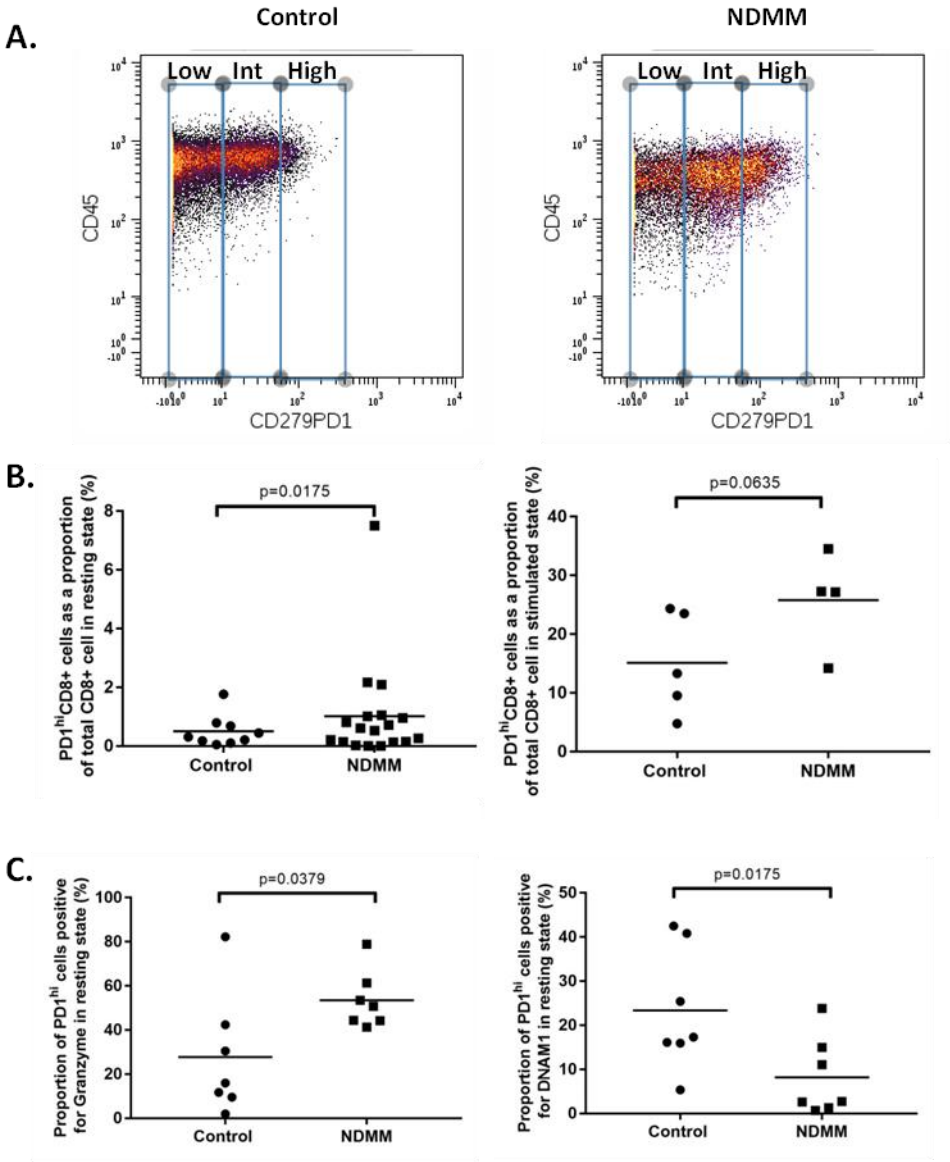

Figure 5.11: PD1 expressing CD8 populations

[A] Representative gating of PD1 expression by CD8 populations. Expression was divided into $PD1^{low}$, $PD1^{int}$ and $PD1^{high}$

[B] In the resting setting $PD1^{high}CD8+$ cells are increased in NDMM, this difference is not maintained following stimulation

[C] $PD1^{high}CD8+$ cells have different functional behaviour depending on whether they are from control or NDMM bone marrow samples. Granzyme expression is higher in NDMM while DNAM1 expression is reduced.

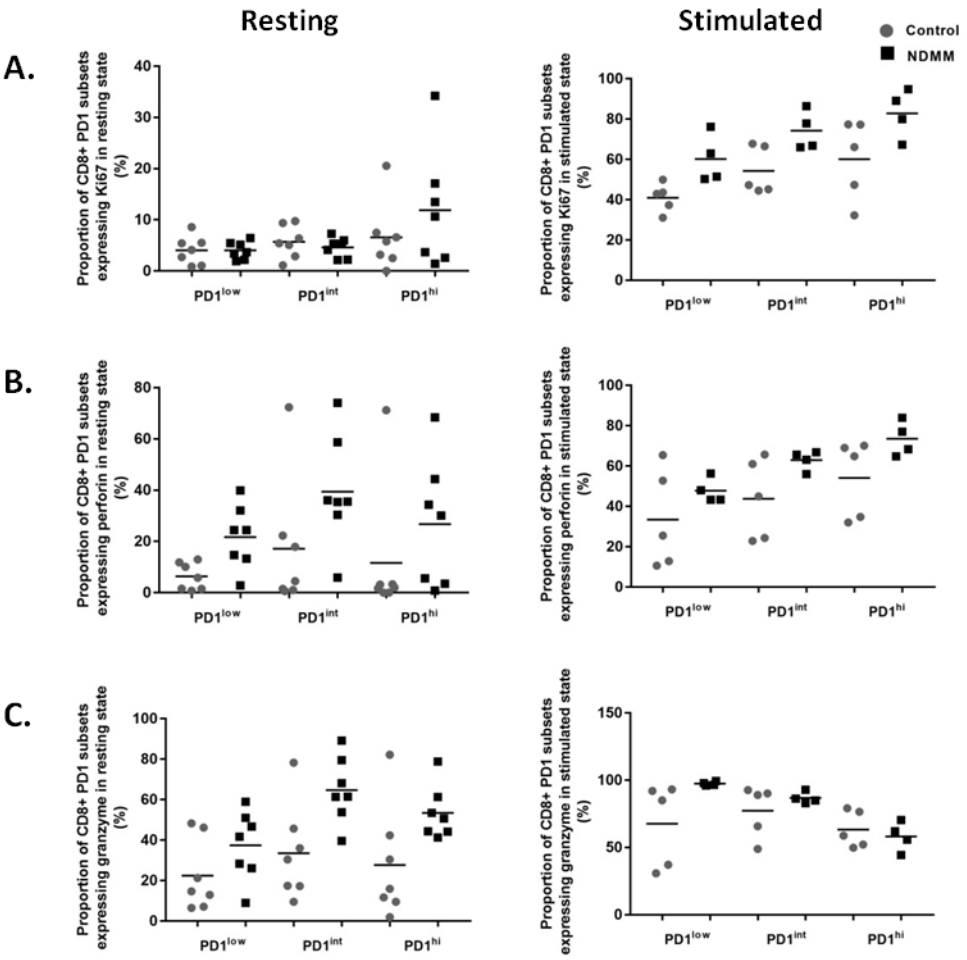

Figure 5.12: Proliferation and cytotoxicity in PD1 subsets

[A] Ki67 expression is highest in the PD1^{high} subset
[B] Perforin expression at rest is highest in the PD1^{int} subset. Following stimulation expression peaks in the PD1^{high} subset
[C] Granzyme expression at rest is highest in the PD1^{int} subset. Following stimulation expression drops in the PD1^{high} subset.

Following stimulation with CD3 and CD28, no difference is seen in the proportion of cells with $PD1^{high}$ expression between control and NDMM (Figure 5.11 B). There is, however, a shift in the pattern of marker expression across the NDMM PD1 subsets, with granzyme expression dropping in the $PD1^{high}$ subset compared to $PD1^{low}$ and $PD1^{int}$ subsets (Friedman p0.0046) (Figure 5.12 C). In contrast perforin expression increases with increasing PD1 expression level (Friedman p0.0046) (Figure 5.12 B). This suggests that the $PD1^{high}$ subset does retain some ability to respond to T cell stimulation.

Following stimulation, expression of Ki67 is highest in $PD1^{high}$ subsets (Friedman p0.0046), in keeping with previous published murine data [74] (Figure 5.12 A). Furthermore a distinct $PD1^{high}$ cytokine profile become apparent in NDMM, with increased expression of IL10 (Friedman p0.0417)(Figure 5.14 C), IL2 (Friedman p0.0046)(Figure 5.14 D) and TGFβ (Friedman p0.0046)(Figure 5.14 B) compared to other PD1 subsets. The $PD1^{high}$ subset also has distinct expression of other immune regulatory molecules with increased expression of LAG3 (Friedman p0.0046)(Figure 5.15 A), CTLA4 (Friedman p0.0046)(Figure 5.15 C), DNAM1 (Friedman p0.0046)(Figure 5.13 B) and NKG2D (Friedman p0.0046)(Figure 5.13 A) when compared to the other subsets. This suggests that the NDMM $PD1^{high}$ subset has an immune regulatory role.

In contrast to NDMM samples, a different $PD1^{high}$ cytokine profile is seen in control samples with both IL2 (Friedman p0.0008)(Figure 5.14 D) and TNFα (Friedman p0.0085)(Figure 5.14 A) levels being increased. In addition control samples show increased levels of TIM3 (Friedman p0.0008)(Figure 5.15 B) expression in the $PD1^{high}$ subset. Expression of LAG3, NKG2D, DNAM1 and perforin is similar to that described for NDMM samples (Figures 5.12, 5.13, 5.15). This pattern of activity suggests that the $PD1^{high}$ subset in control bone marrow has an activated, cytotoxic phenotype.

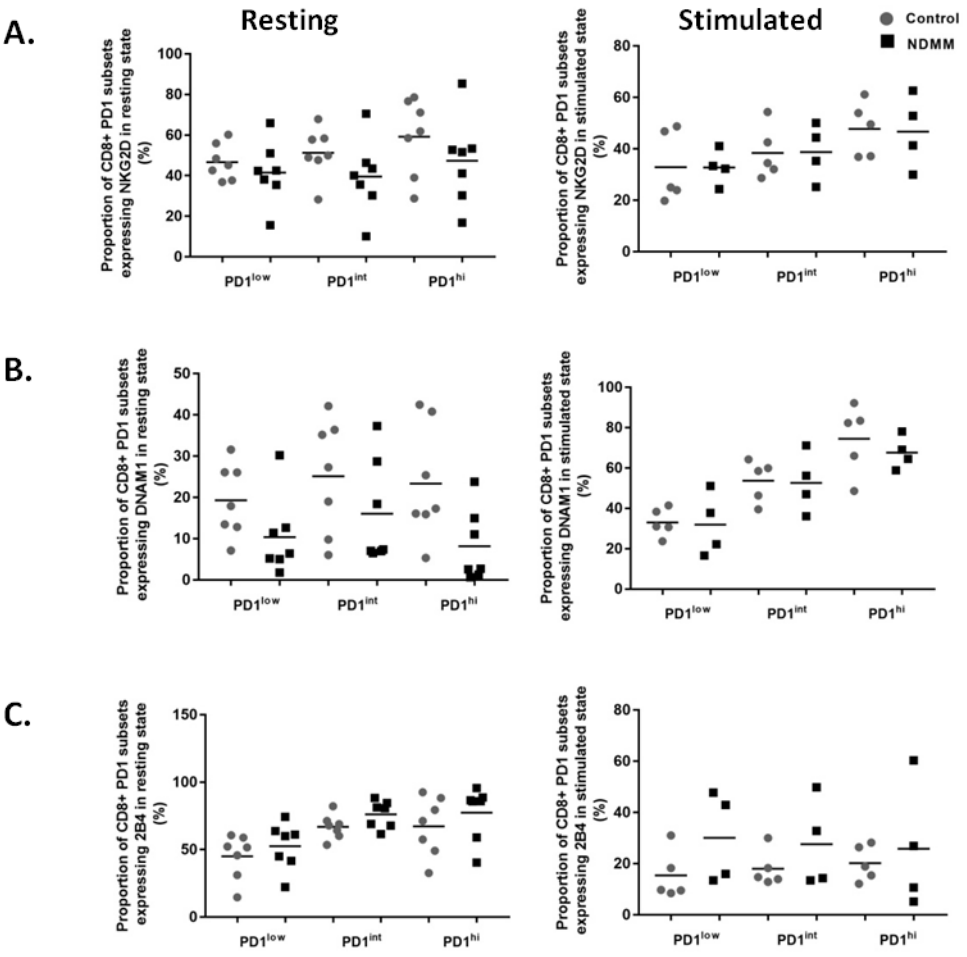

Figure 5.13: Co-receptor expression on PD1 subsets

[A] NKG2D shows a modest increase in $PD1^{high}$ subsets at rest. Following stimulation levels rise with increased PD1 expression.
[B] DNAM1 expression at rest peaks in the $PD1^{int}$ subset. Following stimulation levels rise with increased PD1 expression.
[C] 2B4 expression at rest is seen on both $PD1^{int}$ and $PD1^{high}$ subsets. Levels fall following stimulation.

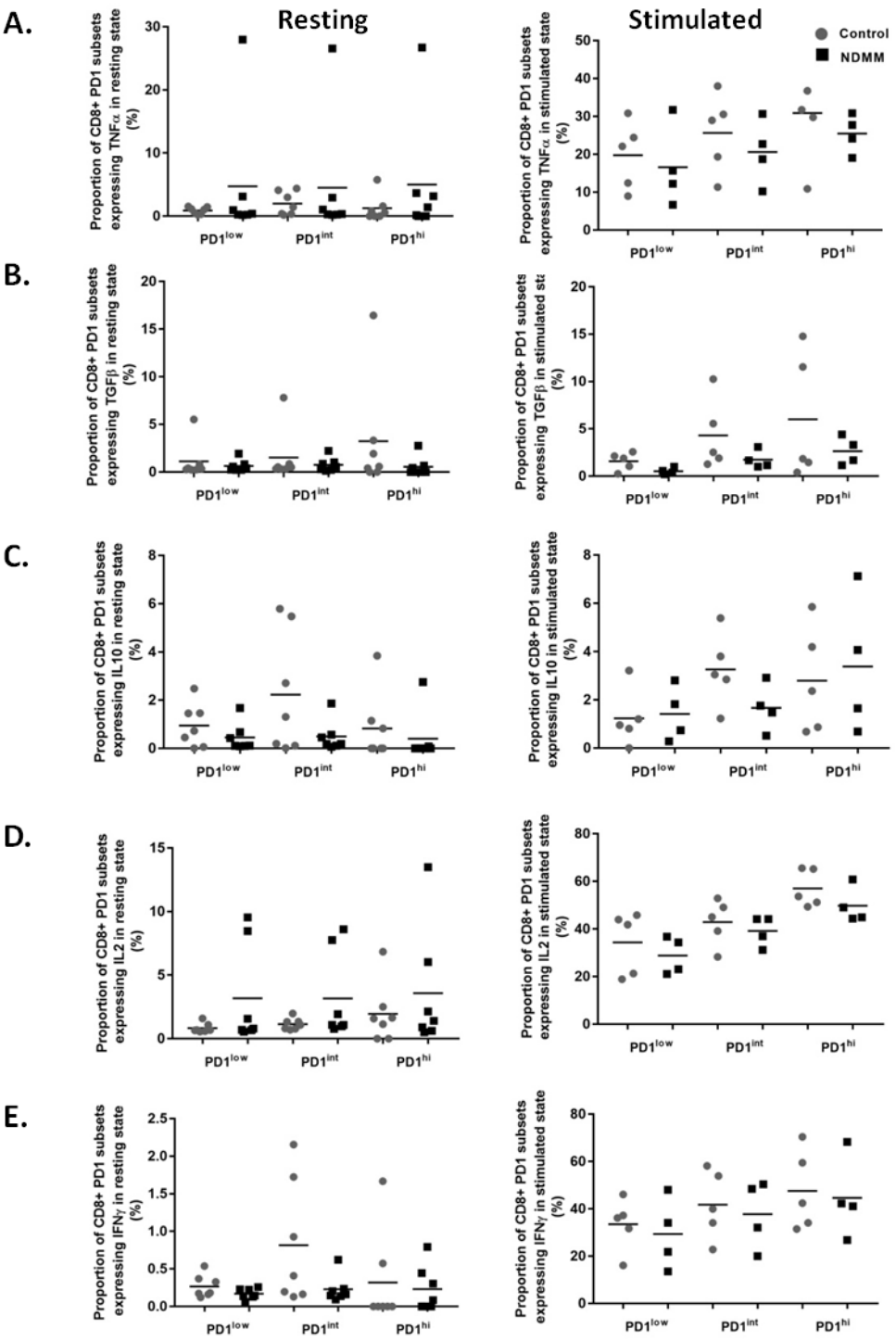

Figure 5.14: Cytokine expression by PD1 subsets

[A] TNFα expression is increased in the control PD1^{high} subset following stimulation

[B] TGFβ expression is increased with increased PD1 expression

[C] IL10 expression is increased in the NDMM PD1^{high} subset following stimulation

[D] IL2 expression is increased with increased PD1 expression

[E] IFNγ expression rises with increasing PD1 expression

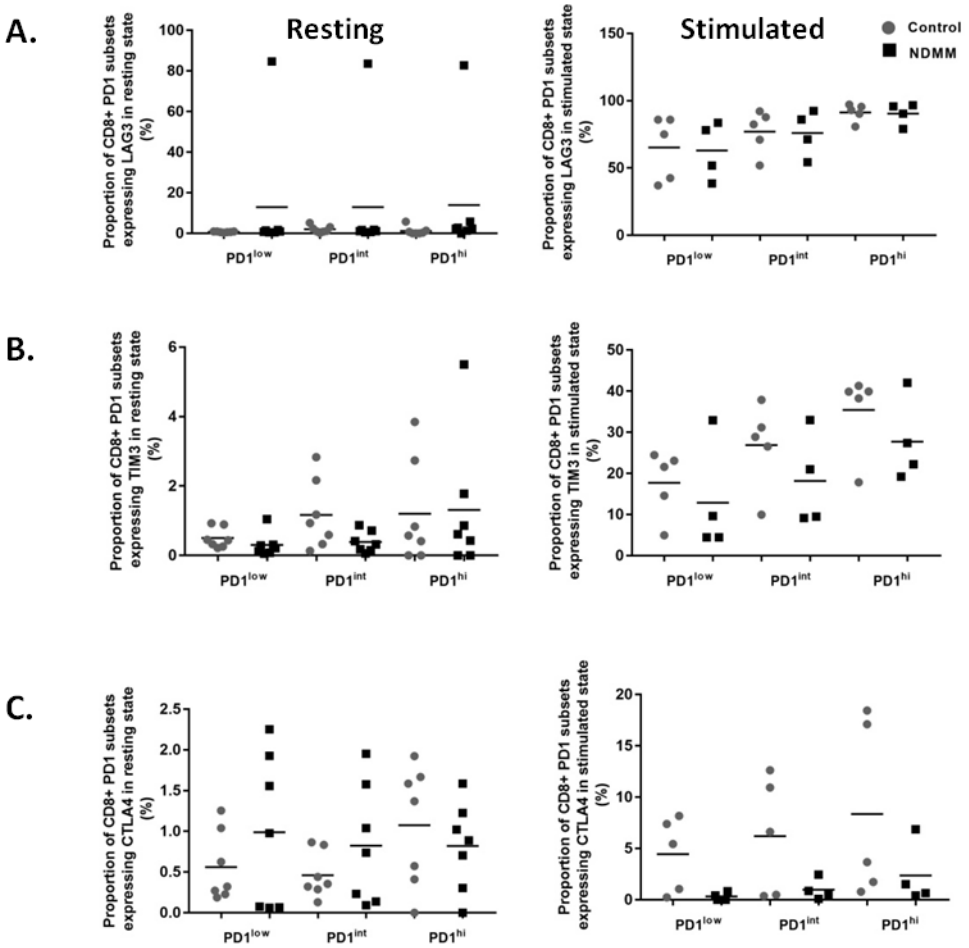

Figure 5.15: Immune checkpoint receptor expression by PD1 subsets

[A] LAG3 expression rises with increasing PD1 expression following stimulation
[B] TIM3 levels following stimulation show a more marked increase in control samples
[C] CTLA4 expression is very low across all subsets

PD1 expression is known to transiently rise when a T cell is activated and may have a role to play in the generation of memory subsets [117]. Previous work within the group has suggested that that $PD1^{int}$ expression may be a marker of cell activation while $PD1^{high}$ expression is a marker of pathological changes in T cells [32], this has also been reported in the context of human head and neck tumours [156]. Furthermore in murine models $PD1^{high}$ subsets retain proliferative activity but are less cytotoxic [74].

This data presented here supports the suggestion that in the setting of NDMM, resting T cells with intermediate PD1 expression are more cytotoxic than their $PD1^{high}$ counterparts and that, following stimulation, increased proliferation is seen in $PD1^{high}$ populations.

Following stimulation an interesting distinction is seen between control and NDMM $PD1^{high}$ subsets with a predominantly pro-tumour profile being seen in NDMM, whereas a more anti-

tumour pattern is seen in control samples. The NDMM PD1 populations also show aberrant expression of degranulation markers. This suggests that, while $PD1^{high}$ cells may be seen in both NDMM and control samples following stimulation, the environmental context is an important influence in the behaviour of these $PD1^{high}$ subsets following stimulation.

5.4.11 Dual checkpoint receptor expressing populations have distinct functional phenotypes

In order to explore the functional behaviour of CD8+PD1+ lymphocytes, population co-expressing a second immune regulatory receptor were assessed. No differences in the cell size of PD1+TIM3+, PD1+LAG3+ or PD1+2B4+ was observed between control and NDMM samples (Figure 5.16).

The PD1+TIM3+ population had increased expression of Ki67 in control populations (median control 32.39, NDMM 10.83 MW p=0.0354) suggesting that there is loss of proliferation in NDMM (Figure 5.17A). No differences in cytotoxic activity or cytokine production were observed. The CD8 PD1+TIM3+ population has been previously described in the context of tumour infiltrating lymphocytes in head and neck cancers [156], renal cell carcinoma [157] and schwannomas [158]. This subset is described as being more exhausted than PD1+TIM3- cells with defects in proliferation, cytokine production and perforin and granzyme expression reported.

CD8+ lymphocytes co-expressing PD1 and LAG3 demonstrated a shift towards a more cytotoxic phenotype in NDMM with both CD107a and perforin expression being increased (CD107a median control 5.524, NDMM 16.37 MW p=0.0062; perforin median control 31.82, NDMM 154.9 MW p=0.0462)(Figure 5.17 B,C). Low cell numbers do not allow distinction between PD1 high and PD1 intermediate expression in this analysis. It may be that PD1+LAG3+ cells have intermediate PD1 expression, which is associated with increased expression of cytotoxic molecules. Alternatively LAG3 may be acting to mitigate the functional impacts of high PD1 expression.

Previous reports regarding the role of dual PD1+LAG3+ cells in malignancy have been varied. In the setting of follicular lymphoma tumour infiltrating PD1+LAG3+ have been shown to have reduced cytokine producing and degranulation potential compared to PD1+LAG3- subsets [159].

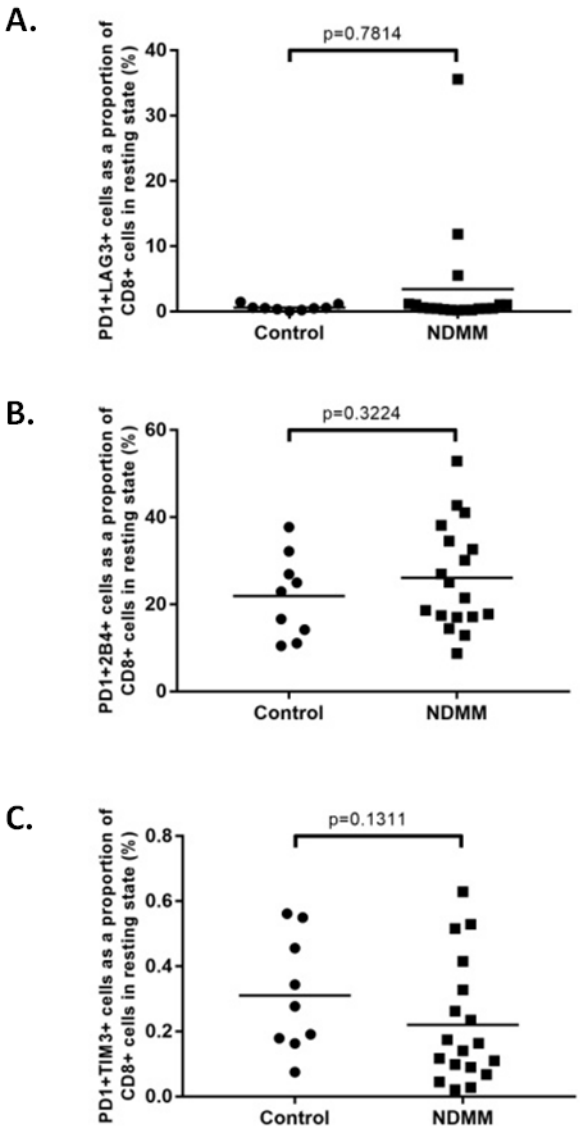

Figure 5.16: No difference was observed in populations sizes between dual checkpoint receptor expressing CD8 populations in control and NDMM

[A] PD1+LAG3+
[B] PD1+2B4+
[C] PD1+TIM3+

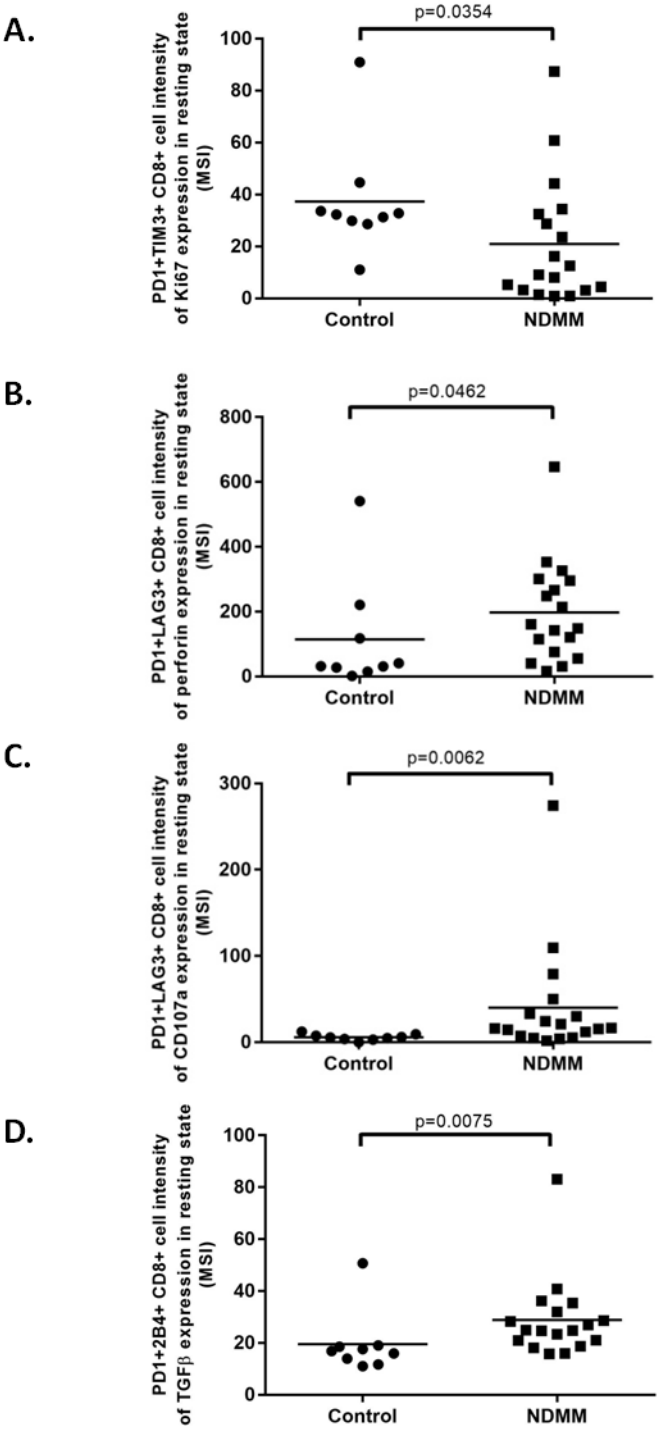

Figure 5.17: CD8 dual checkpoint expressing phenotype and function

[A] The PD1+TIM3+ population has loss of Ki67 expression in NDMM
[B][C] The PD1+LAG3+ population has increased expression of perforin and CD107a in NDMM
[D] The PD1+2B4+ population has increased expression of TGFβ in NDMM

In contrast, work in murine models has demonstrated subtle PD1+LAG3+ subsets where the degree of PD1 expression determines the impact of LAG3 co-expression [160]. The $PD1^{int}$LAG3+ subset had increased IFNγ, TNFα and CD107a expression compared to the $PD1^{int}$LAG3- subset, while LAG3 expression made no difference to the exhausted phenotype of $PD1^{high}$ expressing cells. This description of increased cytotoxic activity in dual expressing subsets is strikingly similar to the changes I have demonstrated in NDMM, suggesting that the changes I see may relate to a lower level of PD1 expression.

Finally the PD1+2B4+ population demonstrated increased expression of TGFβ in NDMM suggesting a shift towards a pro-tumour cytokine profile (median control 16.91, NDMM 24.87 MW p=0.0075)(Figure 5.17 C). Dual PD1+2B4+ expression has previously been reported in the setting of chronic viral infection when it was found to result in a less proliferative phenotype, cytokine expression was not examined [161].

When the functional activity of the three populations are compared in NDMM there is variation in expression of Ki67 (Ki67 Friedman p=0.0009), IL10 (Friedman p=<0.0001) and TGFb (Friedman p=0.0020) which are all expressed at lower levels by the PD1+2B4+ population (Figure 5.18).

This analysis of dual immune checkpoint inhibitor expressing cells suggests that the combination of inhibitory receptors being expressed by a CD8+ T cell is key in directing the nature of its response. Differences in cytotoxicity, cytokine production and proliferation are seen with different receptor combinations and may go some way towards explaining the diversity of response seen in PD1 positive cells. This is an example of the complexity of immune checkpoint regulation which can only be fully explored when multiple parameters are measured simultaneously at the single cell level.

A.

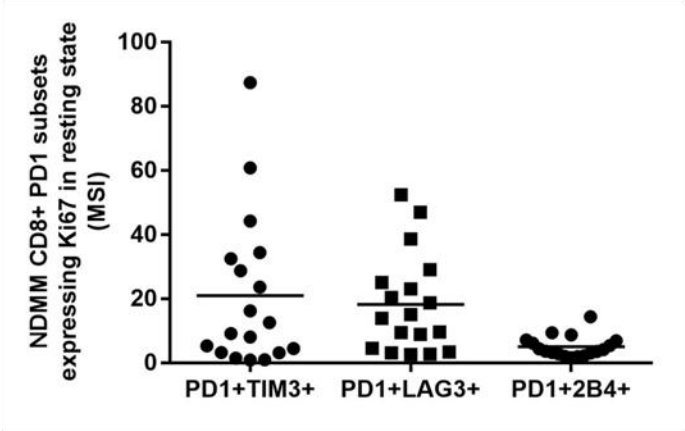

B.

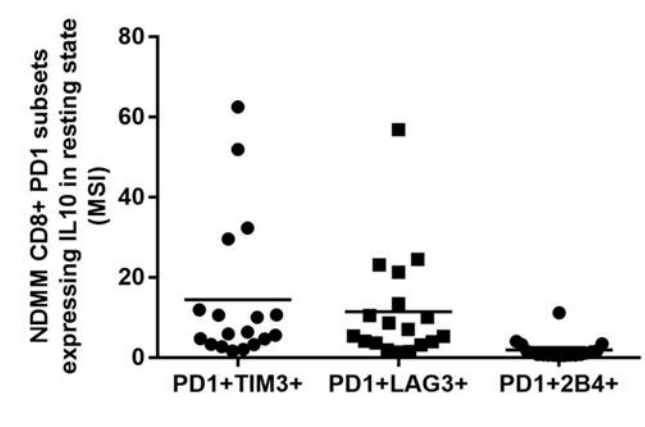

C.

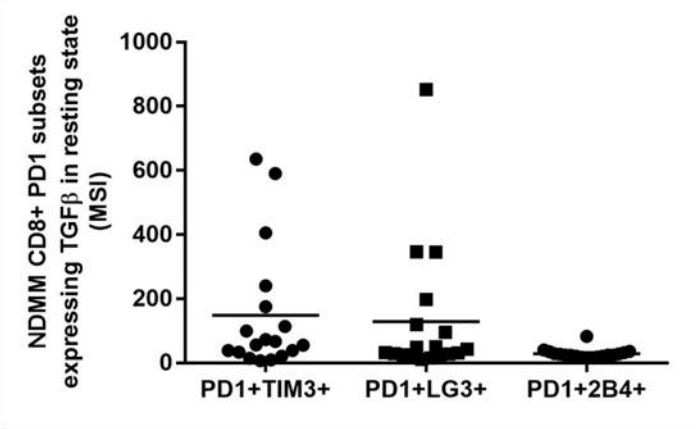

Figure 5.18: Patterns of marker expression by dual checkpoint receptor CD8 populations

[A] Ki67 expression is lowest in PD1+2B4+ populations
[B] IL10 expression is lowest in PD1+2B4+ populations
[C] TGFβ expression is lowest in PD1+2B4+ populations

5.5 Summary of results

1. CD8 T cell numbers are maintained in the bone marrow in NDMM
2. CD8 subsets in NDMM are able to produce cytokines in response to appropriate stimulation, however an aberrant pattern of expression across subsets was seen for TGFβ, IL2 and IL10
3. CD8 populations in NDMM express markers of degranulation which are most prominent on effector populations and are upregulated following stimulation with CD3 and CD28
4. CD8 populations in newly diagnosed NDMM strongly up-regulate Ki67 expression in response to stimulation with CD3 and CD28
5. DNAM1, NKG2D, 2B4 and PD1 are present at detectable levels on resting CD8 cells in NDMM which may offer therapeutic opportunities
6. Expression of DNAM1 on resting NDMM CD8 population is reduced in comparison to control samples
7. PD1 expression is increased in stimulated CD8 cells in NDMM when compared to controls
8. $PD1^{high}$ CD8 T cells are increased in NDMM and have an aberrant functional phenotype
9. Dual checkpoint expressing CD8 populations have diverse functional phenotypes

5.6 Discussion

This data identifies a number of important ideas surrounding CD8 lymphocyte function in NDMM. CD8 lymphocytes in this setting demonstrate phenotypic and functional changes across multiple subsets which can only be explored by measuring multiple parameters at the single cell level. Mass cytometry is particularly well suited to this type of in depth analysis as it allows these parameters to be measured simultaneously.

The first is of population skew within the tumour microenvironment with functional changes seen in cell subsets which would be expected to be engaging with the malignant cell population. This pro-tumour shift in function is characterised by aberrant loss of IL2, granzyme and co-activation potential accompanied by the increased expression of IL10 and TGFβ.

Lymphocytes which infiltrate a tumour will have repeated, direct exposure to tumour antigen and are therefore likely to become phenotypically and functionally distinct from their non-tumour infiltrating counterparts. In the setting of myeloma the malignant cells are often diffusely infiltrating the bone marrow, so all lymphocytes within the bone marrow compartment have the potential to have tumour infiltrating lymphocyte characteristics. Given

the persistence of tumour antigen in this setting it is therefore not unexpected that effector lymphocyte populations from within the bone marrow have features of dysfunction.

The second key theme identified by this data is the functional behaviour of PD1 expressing subsets. Firstly there is a distinction between $PD1^{int}$ and $PD1^{high}$ expression with $PD1^{int}$ cells having enhanced cytotoxic activity compared to other subsets. Secondly there are distinct differences in the $PD1^{high}$ subsets between control and NDMM, with NDMM subsets showing loss of cytotoxicity, pro-tumour cytokine responses and increased expression of inhibitory receptors.

The recognition that $PD1^{int}$ expression by CD8 cells indicates recent activation is increasingly being reported in the literature [162]. It has also been suggested that PD1 expression can be used to identify and isolate antigen specific T cells [163]. This highlights the importance of setting appropriate thresholds to define populations according to the biological question being asked, with more stringent threshold required if PD1 expression is being used to define exhausted populations.

The observation that there are functional differences between $PD1^{high}$ expressing CD8 populations in control and NDMM bone marrow samples demonstrates that PD1 expression alone is not sufficient to determine the behaviour of cells. This suggests that the microenvironment context is key, with $PD1^{high}$ cells from within a malignant environment demonstrating pro-tumour characteristics which are not found in cells from a non-malignant environment. This highlights the complexity of the immunological response to cancer, with multiple factors determining the function of cell subsets. This may explain the variation in response seen to immune checkpoint regulators as well as the varied clinical course in multiple myeloma. It can be hypothesised that individuals with longer durations prior to and between treatments are able to maintain immunological control despite a malignant microenvironment.

5.7 Relevance of work

1. Identifies defects in the CD8 populations which are expected to interact directly with malignant cells
2. Demonstrates that the level of PD1 expression is vital in predicting functional behaviour of CD8 subsets
3. Demonstrates that the functional impact of PD1 expression is modulated by the presence of other checkpoint inhibitors

6. Natural killer cell phenotype and function in NDMM

6.1 Natural killer cells and the recognition of tumour cells

Natural killer (NK) cells are innate lymphoid cells which, while sharing many phenotypic features with CD3+ lymphocytes, lack an antigen specific receptor that has undergone somatic hypermutation. They instead rely on the interplay between a range of activating and inhibitory signals to determine the behaviour of the cell.

There are two important pathways by which NK cells can recognise transformed cells:

1. **Loss of self** when transformed cells down regulate MHC class 1 expression
2. **Cellular stress** when target cells up regulate ligands of NK cell activating receptors including NKG2D and DNAM1

In health MHC class 1 is expressed on nearly all human cell types with the exception of red blood cells and platelets and is used to display peptides derived from normal cellular protein turnover. MHC containing normal self protein is not normally an immune target, however a transformed or virally infected cell will also display viral or tumour antigens which can then be recognised by antigen specific immune cells. NK cells, unlike antigen specific cells, detect the presence of MHC rather than the antigen it contains. A cell which is not expressing MHC class 1 is a target for NK cell cytotoxicity.

Alongside MHC expression, NK cells also respond to the levels of expression of a range of both NK cell inhibitory and NK cell stimulatory ligands (Table 6.1). The interplay between MHC expression and NK cell ligand expression is key in determining whether a cell becomes an NK target. A healthy cell expresses both MHC and low levels of NK cell activating ligands, however NK cells do not become activated as the inhibitory signals from MHC outweighs the activating signals. An excess of NK activating ligands will trigger NK cell activity regardless of MHC expression (Figure 6.1).

In addition to the key receptors involved in NK cell activation, NK cells also express a range of receptors that can modify the NK cell response. This includes LAG3 [164] and TIM3 [165] which are described as having inhibitory effects on $CD3^+$ lymphocytes, but their role in NK cell behaviour is less clearly defined. NK cell exhaustion, with loss of functional activity which parallels that described in CD8+ lymphocytes, has been described in the setting of chronic infection and malignancy [166][167].

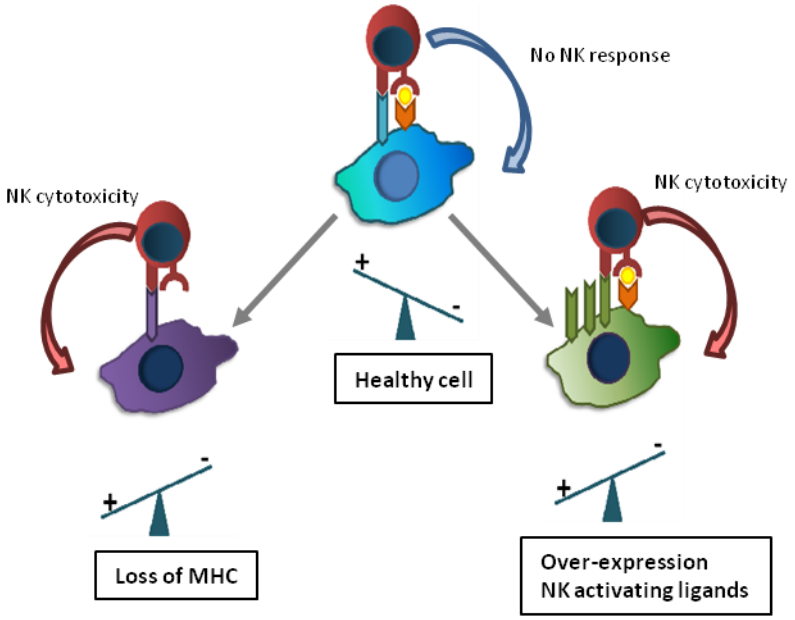

Figure 6.1: Routes to NK cell activation.

Healthy self cells express both MHC and low levels of NK cell ligands. The balance of signals to NK cells is in favour of no NK cell activation. Transformed cells which fail to express MHC shift the balance of signals to NK cells to favour NK cell activation and cytotoxicity results. Transformed cell over-expressing NK cell activating ligands also shift the balance of signal in favour of NK cell activation. (Image based on Raulet and Vance, Nature Reviews Immunology 2006)

An NK cell which has been activated can perform three key activities against target cells:

1. Direct cytotoxicity via the release of cytotoxic granules
2. Secretion of cytokines, including IFNγ and TNFα.
3. Expression of apoptosis ligands including TRAIL and CD95-L

NK cells are classically divided into two subpopulations based on their expression of CD56. CD56 is strongly expressed on immature NK cells and is lost as cells mature. The immature, NK 56^{bright} subset constitutes 10% of circulating NK cells while the NK 56^{dim} subset forms 90% of circulating NK cells. The NK $CD56^{bright}$ subset is classically described as being immature and predominantly secretes cytokines in response to IL12 and IL18 [168]. In contrast the NK 56^{dim} subset is considered more mature and releases cytotoxic granules in addition to cytokines following encounters with NK receptor ligands [168].

NK cell cytotoxicity is delivered via immunological synapse formation with a target cell. The synapse is used to deliver a targeted release of preformed lytic granules containing granzyme and perforin. This is an actin remodelling dependant process similar to that seen in CD8+ lymphocytes [169].

Receptor	Ligand
MHC class 1 specific	
CD94 – NKG2	MHC peptides with HLA-E
KIR	Various MHC class 1
LIR1	Various MHC class 1
NK activating	
NKG2D	ULPB, MIC A/B
2B4	CD48
DNAM1	CD122 / CD155
FCyR	Surface bound IgG
NK inhibiting	
2B4	CD48
KLRG1	Cadherins
NKR-P1B	CLR-B

Table 6.1: NK cell receptors and ligands

Healthy NK cells predominantly produce TNFα and IFNγ which are secreted via a non immunological synapse polarised pathway which is distinct from cytotoxic granules [170]. Peak cytokine production occurs six hours after cell activation [168]. The dominant cytokine produced is dependent on the nature of the activating stimulus received by the NK cells with TNFα production requiring engagement of fewer receptor classes than IFNγ production [168].

NK cells are known to express apoptosis ligands including FAS ligand [171] and TRAIL [172].Unlike granzyme dependent cytotoxicity, apoptosis ligand dependent target cell killing requires multiple NK cell – target conjugations which gradually activate caspase 8 resulting in target cell death [173]. Immature NK cells have been reported to utilise a predominantly TRAIL mediated cytotoxic pathway while mature $CD56^{dim}$ NK cells primarily use a FAS ligand dependant pathway alongside direct cytotoxicity[172].

It is known that malignant cells can exert a range of inhibitory effects on NK cells. This includes the expression of inhibitory ligands, the down regulation of MHC expression, the release of immunosuppressive cytokines, chemokines and other secretes molecules including adenosine, and modification of the stromal microenvironment [174].

Malignant plasma cells differ from many other transformed cells because they continue to express MHC class 1 [175] and therefore have a degree of protection against NK cell mediated lysis. Despite the continued expression of MHC, NK cells still have the potential to target

malignant plasma cells providing sufficient levels of NK cell activating ligands are expressed by the myeloma cells. Plasma cells express cell surface MICA, the ligand for the NK receptor NKG2D, however the level of expression decreases with progressive disease [176]. The NK cell activating receptors NKG2D [177178], DNAM1 [179] and 2B4 [178] are reduced in myeloma, suggesting that the response to plasma cell ligands will be suboptimal. This is seen functionally as NK cells in myeloma demonstrate reduced in-vitro cytotoxicity [180,181]. Furthermore NK cell expression of the immune checkpoint inhibitor PD1 is elevated and PD1 blockade has been shown to enhance NK cytotoxicity and IFNγ production[71].

The importance of NK cells in the initial anti-tumour response is demonstrated by the elevated risk of malignancies seen in those with genetic NK cell defects. There are a number of genetic immunodeficiency syndromes which predominantly effect NK cell function [182]. The best characterised of these are all associated with decreased lytic function and may also have abnormalities of proliferation and subset distribution. The most well described NK cell defect is GATA2 deficiency which associated with increased incidence of human pappilomavirus (HPV) associated cervical cancer and Epstein Barr virus (EBV) associated tumours[183]. It is unknown whether this increased risk of malignancy is due to failure of immune-surveillance or loss of control of oncogenic viruses.

There have also been reports that specific NK cell subsets may have a regulatory role. Cooper et al described an IL10 producing $CD56^{bright}$ subset induced by the presence of IL-15 [184]. This is in contrast to the IFNγ producing subset induced by IL-12. These distinct $CD56^{bright}$ cytokine producing subsets may have immune stimulatory and immune regulatory roles.

6.2 Aims

To compare the frequency and phenotype of NK cell subsets in NDMM to non-myeloma controls

The compare the expression of functional markers of proliferation, degranulation and cytokine production of NK cell subsets in NDMM to non-myeloma controls

To identify features of NK cells in NDMM which may predict duration of survival

6.3 Specific methodology

Cryopreserved bone marrow samples from patients with NDMM, who had not yet received any treatment, were identified within the Barts Cancer Institute tissue bank. These were processed for mass cytometry and analysed on a CyTOF2 mass cytometer as described in

chapter three. Data was normalised against EQ bead standards using the Helios normaliser (version 6.7).

NK cells were identified using the phenotype $CD45^{+}CD3^{-}CD16^{+/-}CD56^{+}$ and were further subdivided according to level of CD56 expression into $CD56^{bright}$ and $CD56^{dim}$ subsets (Figure 6.2).

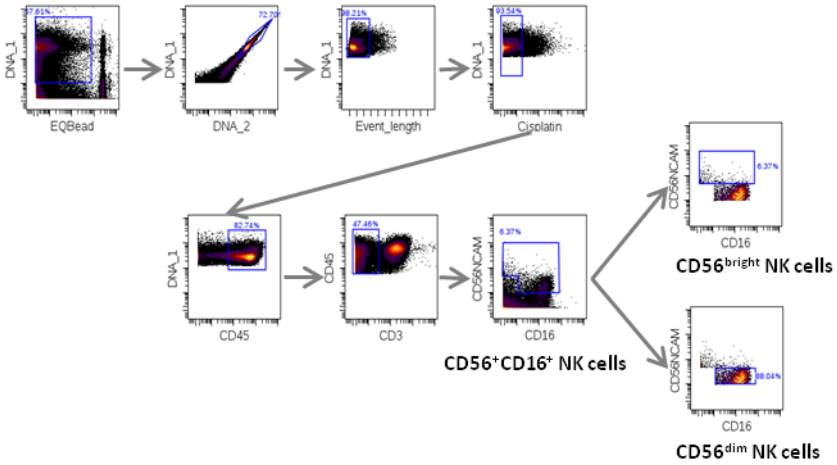

Figure 6.2: NK cell gating strategy.

In order to identify live, singlet NK cell events, EQ beads were first excluded. Cellular events were identified on the bases of dual iridium intercalator expression (DNA_1 and DNA_2). Singlets events were identified using event length and iridium expression (DNA_1). Low cisplatin expression was used to gate on live events. Next sequential gates on CD45+,CD3-, CD56+, CD16+ were used to identify NK cells. Finally intensity of CD56 expression defined NK cell subsets.

The use of CD56 as an NK cell marker in myeloma can be problematic as malignant plasma cells can also express CD56 [154], while NK cells are strongly positive for CD38 [185]. Low plasma cell CD138 expression as a result of cryopreservation is a further complication [186]. The fact that population frequencies across all cell types, including NK cells, in this analysis are close to expected values suggests that there is not a large problem with malignant plasma cells being detected within the NK cell gates. Backgating on B cell and plasma cell lineage markers was also used to ensure that CD56 positive plasma cells were not included within the NK cell gate.

6.4 Results

6.4.1 The NK cell population in NDMM is shifted toward a less mature, $CD56^{bright}$ phenotype

In both control and NDMM bone marrow samples the natural killer population made up 3% of total $CD45^{+}$ cells (mean control 3.377%, NDMM 3.152% t-test p=0.8709) (Figure 6.3 A). When the NK population was further subdivided according to expression of CD56, a significant shift towards the less mature $CD56^{bright}$ population was observed in NDMM when compared to

control samples (CD56^{bright} mean control 11.34%, NDMM 24.08% t-test p=0.0460; CD56^{dim} mean control 80.22%, NDMM 58.97% t-test p=0.0213)(Figure 6.3 B).

This pattern could be due to relative expansion of the NK CD56^{bright} subset or relative loss of the CD56^{dim} population.

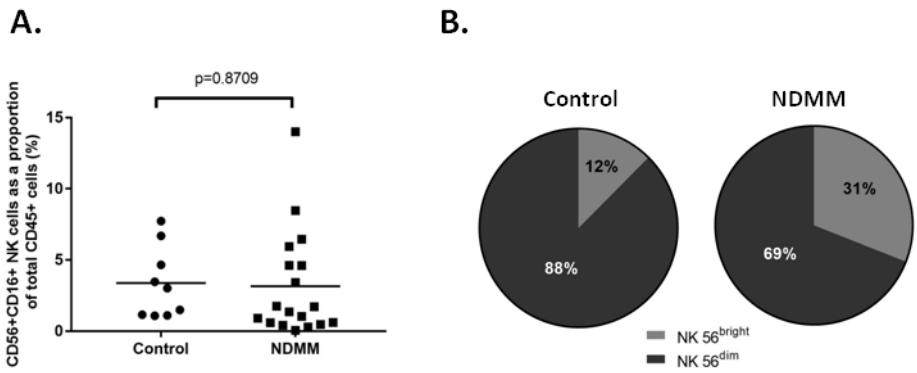

Figure 6.3: NK cell populations.

[A] Total bone marrow NK cell numbers were well maintained in NDMM
[B] When NK cell subsets were examined as a proportion of all NK cells, a shift towards the NK56^{bright} population was seen in NDMM.

6.4.2 NK cells in NDMM have lower expression of Ki67, with the CD56^{dim} population being least proliferative

Expression of Ki67 across the total NK cell population is two times higher in control samples compared to NDMM (mean control 29.57%, NDMM 15.5% t-test p=0.0721)(Figure 6.4 A). Within the NK56^{bright} subset no significant difference is seen in proliferation between control and NDMM samples (mean control 26.78%, NDMM 24.84% t-test p=0.8402), however in the CD56^{dim} subset Ki67 expression is significantly lower in NDMM (mean control 29.51%, NDMM 11.12% t-test p=0.0054)(Figure 6.4 B). This suggests that the relative expansion of the NK56^{bright} subset seen in NDMM is due to a failure of proliferation in the more mature NK56^{dim} subset, rather than due to expansion of the more immature fraction. This may indicate the development of NK cell exhaustion in the NK56^{dim} subset.

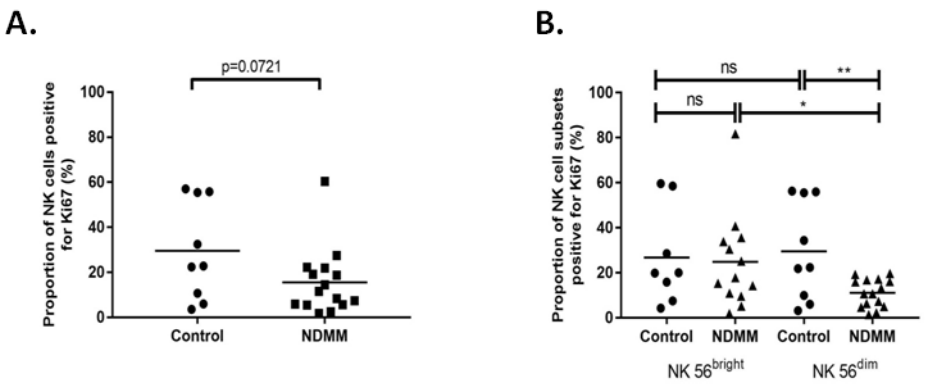

Figure 6.4: Proliferation in NK cell populations.

[A] No difference in Ki67 expression was seen when comparing the entire NK cell cohort
[B] A fall in Ki67 expression was seen on NK56^{dim} cells in NDMM

6.4.3 Granzyme and perforin expression is more intense in the NDMM NK56^{dim} subset but is not accompanied by a rise in CD107a

In order to assess the cytotoxic potential of NK cells in NDMM, intracellular expression of granzyme and perforin and cell surface expression of CD107a was examined in the resting state. No difference in the size of the population expressing the markers was observed between control and NDMM (Perforin mean control 50.02%, NDMM 63.50% t-test p=0.2701; granzyme mean control 53.29%, NDMM 61.84% t-test p=0.4851; CD107a median control 2.186%, NDMM 4.019% MW p=0.0955)(Figure 6.5 A). Of note there was a broad range of both granzyme and perforin expression between individuals in both control and NDMM groups.

While the proportion of cells expressing granzyme was not significantly different between disease and control groups, there was an increase in the intensity of expression in NK56^{dim} subset (median control MSI 153.4, NDMM MSI 497.1 MW p=0.0251) which is classically described as the more cytotoxic subset (Figure 6.5 B). Within the NK56^{dim} subset an increased intensity of perforin expression was also observed (median control MSI 200.3, NDMM MSI 915.8 MW p=0.0148)(Figure 6.5 B).

Since this increase in the constituents of cytotoxic granules intensity is not accompanied by CD107a expression it is unclear where this represents meaningful cytotoxic activity. It could instead represent generalised cellular activation, or a cytotoxic granule packaging defect similar to that reported in CLL [30]. Unlike CD8+ T cells, NK cells store pre-formed perforin and granzyme within cytolytic granules to enable a rapid response when cells are activated. The upregulation of granzyme and perforin expression may therefore represent an increase in stored granule content rather than an increase in cytolytic activity.

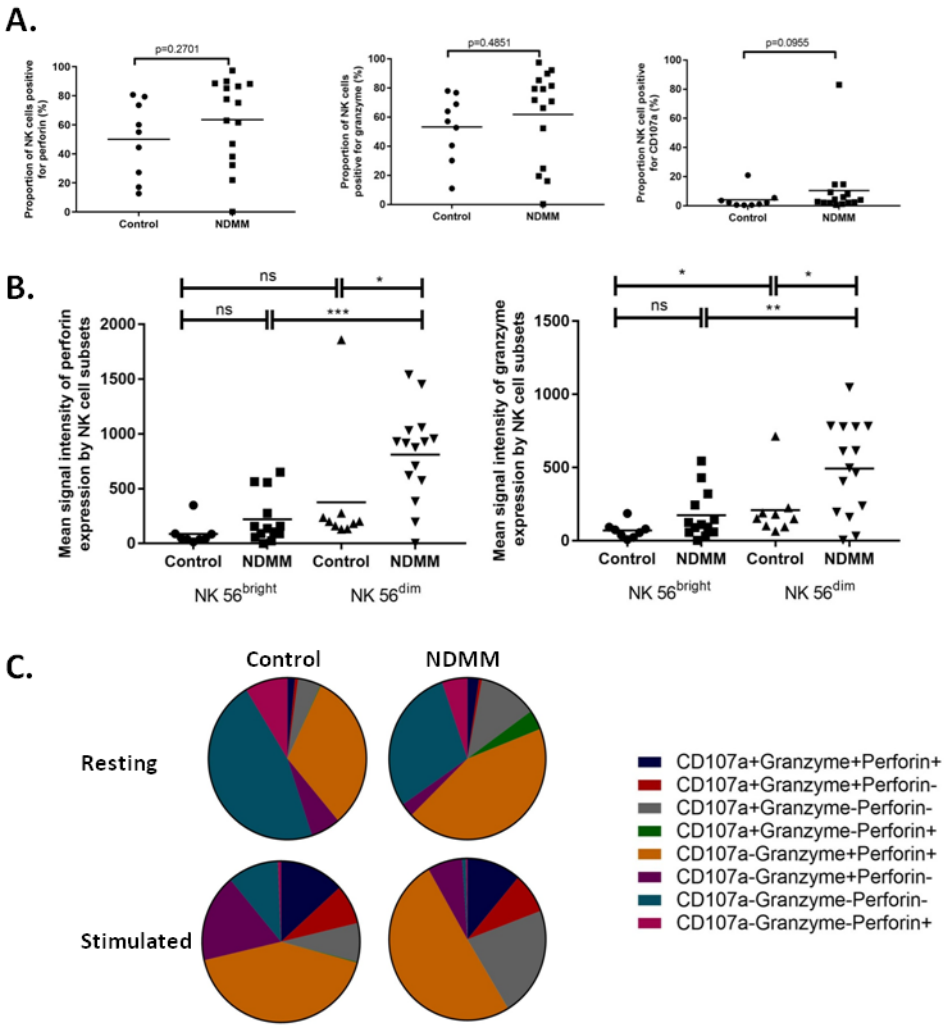

Figure 6.5: NK cell cytotoxicity.

[A] No difference in the size of the population expressing the markers was observed between control and NDMM
[B] There was an increase in the intensity of granzyme and perforin expression in the NK56^{dim} subset .
[C] The proportion of triple positive cells (dark blue segment) rose in both control and NDMM samples following stimulation. This was accompanied by a fall in triple negative cell populations (turquoise segment)

To address this observation, the proportion of cells of triple positive for granzyme, perforin and CD107a was assessed. The proportion of triple positive cells rose in both control (median resting 0.26%, stimulated 9.986% MW p=0.0120) and NDMM (median resting 1.582%, stimulated 8.537% MW p0.0445) samples following 72 hour exposure to autologous BMMC stimulated with CD3 and CD28. This was accompanied by a fall in triple negative cell populations (control median resting 44.36%, stimulated 2.189% MW p=0.0120; NDMM median resting 22.55%, stimulated 0.576% MW p=<0.0001). No difference in peak triple positive cell

numbers were observed between control and NDMM (median control 9.986% NDMM 8.537% MW p=0.8413)(Figure 6.5 C).

Given the ongoing presences of tumour antigen in NDMM an increase in cytotoxic activity compared to controls would have been expected if NK cells were fully functioning. Interestingly both NK cell perforin (Pearson correlation r=0.5737, p=0.0254)(Figure 6.6 A) and granzyme (Pearson correlation r=0.5506, p0.0334) (Figure 6.5 B)expression positively correlated with survival suggesting that persistent NK cell cytotoxicity it a key aspect of the immunological control of NDMM.

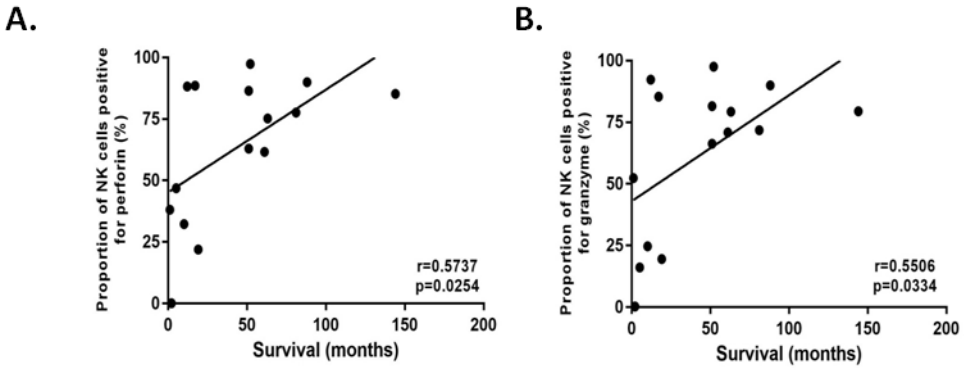

Figure 6.6: Correlation of degranulation markers with survival.

[A] NK cell perforin expression positively correlates with survival
[B] NK cell granzyme expression positively correlates with survival

6.4.4 Loss of intracellular IFNγ and IL10 is seen in NDMM NK cell populations

NK cells are classically described as producing the anti-tumour cytokines IFNγ and TNFα and the pro-tumour cytokine IL10. When each cytokine is considered separately in resting NK cells, intracellular expression of both IFNγ (mean control 2.07%, NDMM 0.53% t-test p=0.0305) and IL10 (mean control 7.09%, NDMM 1.44% t-test p=0.0114) is reduced in NDMM compared to controls (Figure 6.7 A). IL10 expression is lost across both the $CD56^{bright}$ (mean control 3.76%, NDMM 1.31%, t-test p=0.0024) and $CD56^{dim}$ (mean control 7.364%, NDMM 1.847%, t-test p=0.0242) subsets, while IFNγ expression is predominantly lost in the $NK56^{dim}$ subset (mean control 2.030%, NDMM 0.6164% t-test p=0.0403) (Figure 6.7 B). No difference in TNFα expression is seen. Following 72hour incubation with autologous bone marrow mononuclear cells which have been stimulated with CD3 and CD28, no difference is seen in single cytokine expression levels between control and NDMM NK cells and NK subsets (Figure 6.7 C).

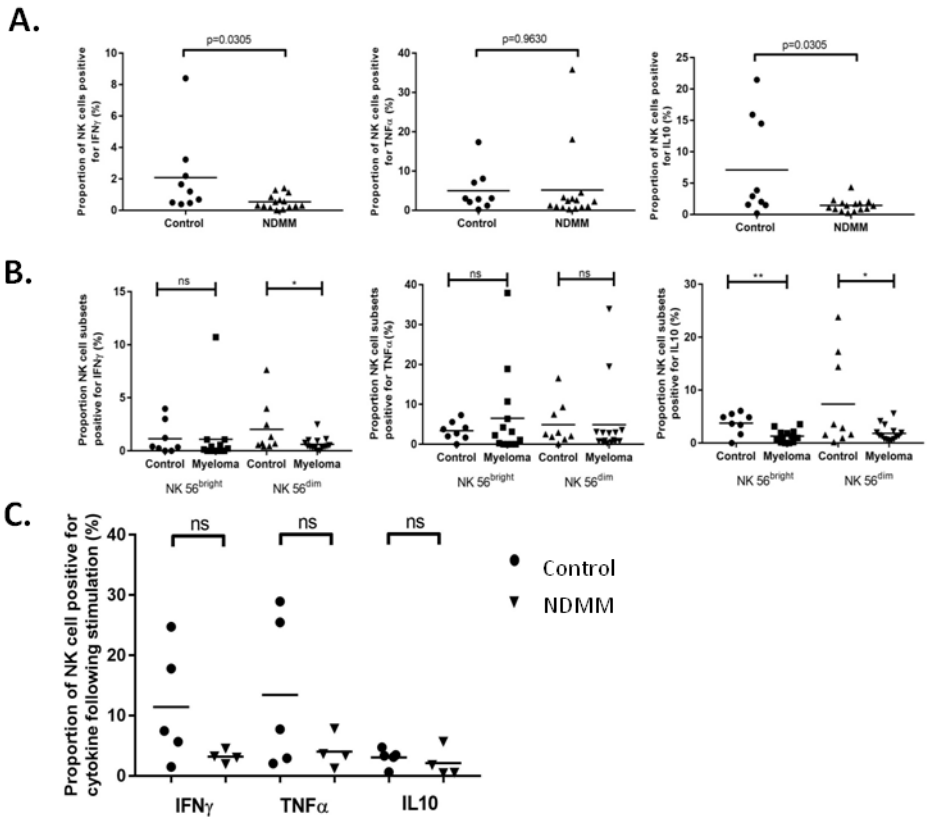

Figure 6.7: Cytokine expression by NK cells.

[A] Intracellular expression of both IFNγ and IL10 is reduced in NDMM compared to controls.
[B] IL10 expression is lost across both the CD56^{bright} and CD56^{dim} subsets, while IFNγ expression is predominantly lost in the NK56^{dim} subset. No difference in TNFα expression is seen.
[C] Following 72hour incubation with autologous bone marrow mononuclear cells which have been stimulated with CD3 and CD28, no difference is seen in single cytokine expression levels between control and NDMM NK cells .

The loss of IL10 expression in NDMM compared to controls at first appears unexpected. The CD56^{bright} IL10 producing subset in control samples may, however, represent the regulatory population described by Cooper et al [184] which may be suppressing tissue damaging NK cell activity in the absence of an appropriate activating signal.

Loss of NK cell IFNγ expression has previously been reported in the context of CLL [30] and is thought to represent NK cell exhaustion. IFNγ production by NK56^{dim} populations is known to require the engagement of more NK cell activating receptors than TNFα [168] implying that IFNγ production will be lost first when the driving mechanism is failure of NK cell receptor engagement. In contrast, cytokine production by CD56^{bright} NK cells is determined by the cytokine microenvironment. With this in mind, the pattern of cytokine loss identified here in NDMM suggests a failure of NK cell receptor engagement by CD56^{dim} subsets.

Since NK cells often secrete a combination of cytokines, the distribution of multiple cytokine phenotypes was examined in both the resting and stimulated state. As expected, in the resting state the majority of NK cells are triple negative for TNFα, IL10 and IFNγ (mean control 87.15%, NDMM 78.82%)(Figure 6.8 A). Following stimulation, control samples have a ten fold increase in IFN+TNF-IL10- and IFN+TNF+IL10- cell populations (INF+TNF-IL10- resting 0.3432% stimulated 3.177% MW p=0.0070; IFN+TNF+IL10- resting 0.4388% stimulated 3.066% MW p=0.0020)(Figure 6.8 C). In NDMM there is a much more modest increase in IFN+TNF+IL10- cells only (INF+TNF+IL10- resting 0%, stimulated 1.136% MW p=0.0049) (Figure 6.8 C). This pattern is replicated in the NK 56^{bright} subset which is expected since these are described as the predominant cytokine producing subset.

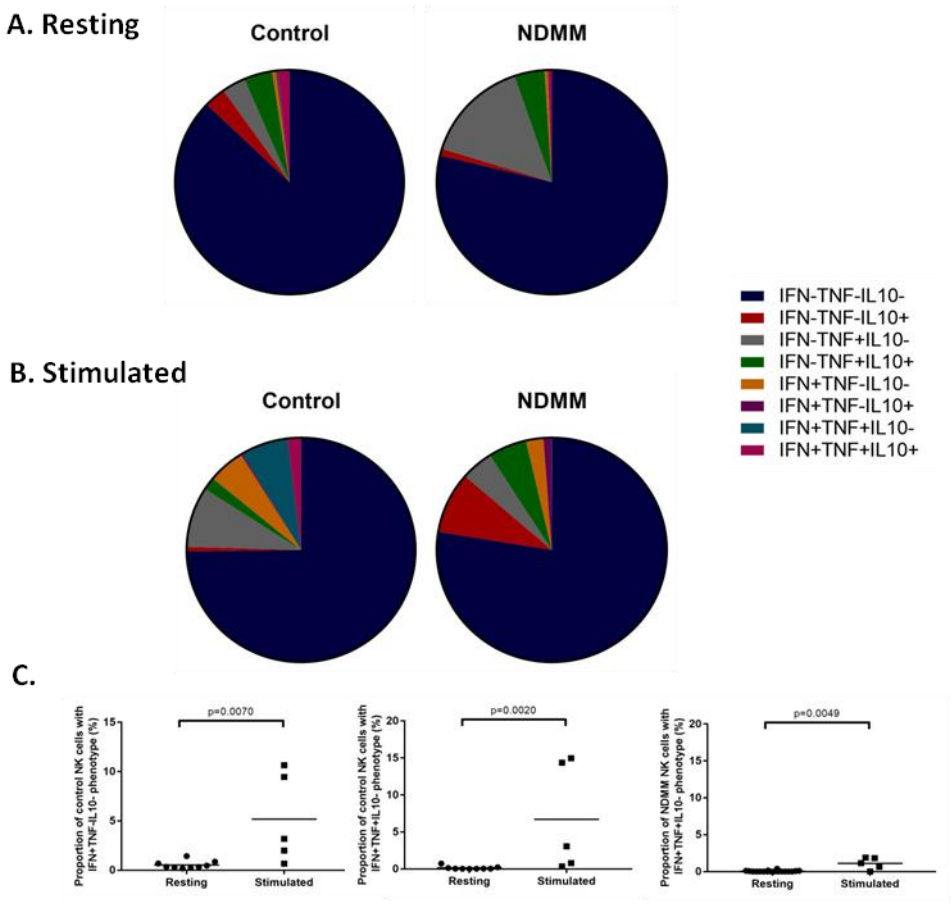

Figure 6.8: Multiple cytokine producing NK cell populations.

[A] In the resting state the majority of NK cells are triple negative for TNFα, IL10 and IFNγ
[B][C] Following stimulation, control samples have an increase in IFN+TNF-IL10- and TNF+IFN+IL10- cell populations. In NDMM there is a more modest increase in IFN+TNF+IL10- cells only

6.4.5 TIM3 expression is reduced in NK cells from NDMM and may represent loss of NK cell activation

Expression of TIM3 is significantly lower on NDMM NK cells than those of control samples (mean control 9.342%, NDMM 3.008% t-test p=0.0021) (Figure 6.9 A). This is predominantly due to a loss of expression on the $CD56^{dim}$ (mean control 9.620%, NDMM 3.228% t-test p=0.0019) subset (Figure 6.9 B), although a drop in intensity of expression (mean control MSI 9.864, NDMM MSI 2.320 t-test p=0.0397) but not proportion of cells expressing TIM3 is seen in the NK 56^{bright} subset (mean control 7.764%, NDMM 4.705%, t-test p=0.3904).

TIM3 expression is reported to increase with NK cell maturation and is considered to be a marker of NK cell activation [187]. As expected, TIM3 levels rise on control samples with NK cell maturity ($NK56^{bright}$ 7.764%, $NK56^{dim}$ 9.620%) however, they fall in NDMM ($NK56^{bright}$ 4.705%, $NK56^{dim}$ 3.228%)(Figure 6.9 B). Loss of NK cell TIM3 expression in NDMM may therefore represent the development of a less active or exhausted state. Expression of HLA-DR, another marker of NK cell activation, is also reduced on NK cells in NDMM adding weight to the proposal that there is a defect in NK cell activation in this condition (mean control MSI 255.2, NDMM MSI 117.1, t-test p=0.0165)(Figure 6.9 C). This shift in HLA-DR expression is also seen predominantly on the $NK56^{dim}$ subset (mean control MSI 246, NDMM MSI 97, t-test p=0.0102).

When NDMM patients are stratified according to survival, a higher level of TIM3 is seen in those surviving more than 36 months (mean <36 months 2.126%, >36 months 3.468% MW p=0.0311)(Figure 6.9 D), suggesting that NK cell activation is important for long term myeloma survival.

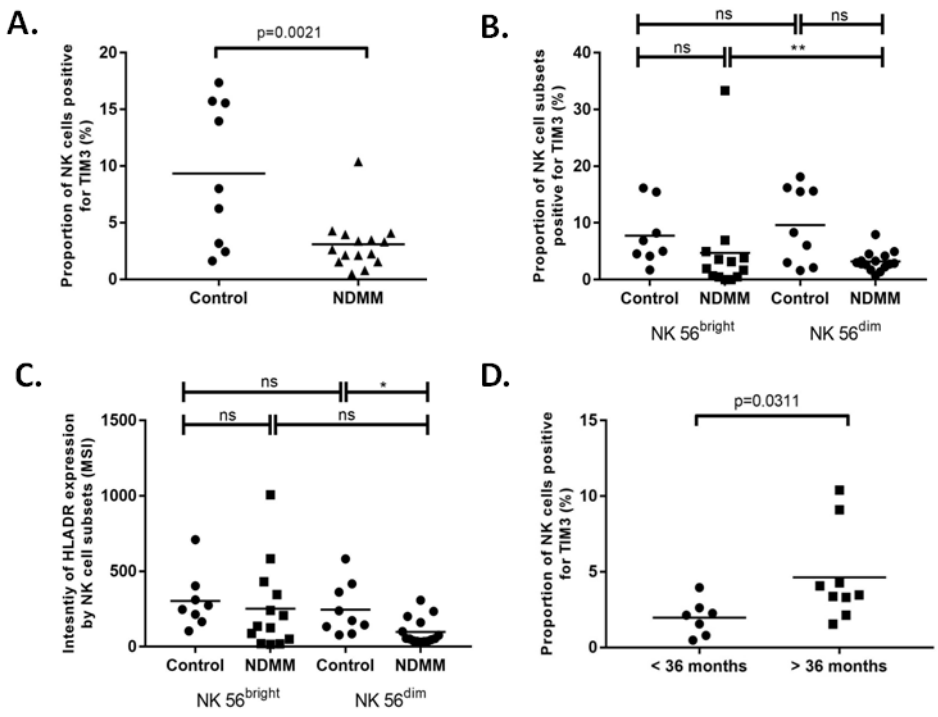

Figure 6.9: NK cell expression of activation markers.

[A] Expression of TIM3 is significantly lower on myeloma NK cells than those of control samples
[B] TIM3 expression is reduced on the CD56^{dim} subset. TIM3 levels rise on control samples with NK cell maturity, however they fall on NDMM
[C] Expression of HLA-DR is reduced on CD56^{dim} NK cells in a similar pattern to TIM3.
[D] When NDMM patients are stratified according to survival, a higher level of TIM3 is seen in those surviving more than 36 months, suggesting that NK cell activation is important for long term myeloma survival.

6.4.6 Receptors and ligands of the PD1 pathway are upregulated on NK cells from NDMM

Expression of both PD1 and PDL1 are two times higher on NDMM NK cells compared to control NK cells (PD1 mean control 7.5%, NDMM 15.85%; PDL1 mean control 4.852%, NDMM 11.88%). PD1 expression increases as cells mature with higher PD1 expression seen on both control and NDMM NK56^{dim} cells compared to NK 56^{bright} subsets (Figure 6.10A). Up regulation of PD1 expression in NDMM is more pronounced on CD56^{dim} populations (mean control 7.991%, NDMM 20.04% t-test p=0.0392) populations while PDL1 expression is predominantly seen on CD56^{bright} subsets (mean control 4.848%, NDMM 23.49% t-test p=0.0260)(Figure 6.10 B). This differential expression of PD1 and PDL1 across NK cell subsets may represent differing roles for PD1 and its ligand in NK cell maturity and activation.

Interestingly when cells are gated on PD1 high and low expression, higher granzyme (mean PD1^{low} 45.5%, PD1^{high} 81.54% t-test p=0.0046)(Figure 6.10 C) and DNAM1 (mean PD1^{low} 8.2% PD1^{high} 16.92% t-test p=0.0460)(Figure 6.10 D) expression is seen in the PD1^{high} subset

suggesting that PD1 may be a marker of NK cell activation rather than exhaustion in this context. As described earlier, however, the significance of elevated granzyme expression in NDMM NK cells is uncertain.

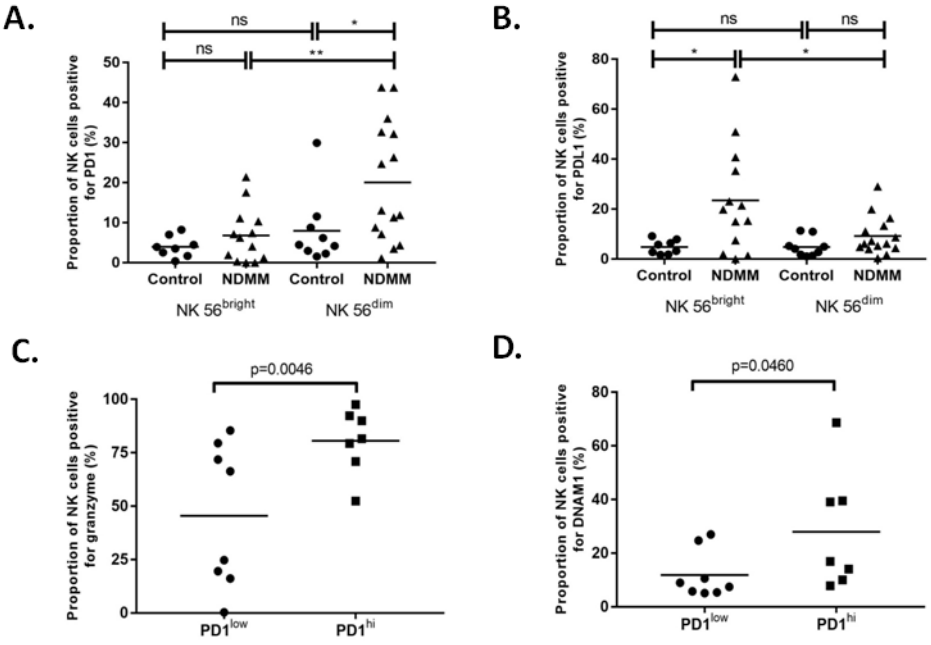

Figure 6.10: PD1 and PDL1 expression by NK cell subsets.

[A] PD1 expression increases as cells mature with higher PD1 expression seen on both control and myeloma NK56^{dim} cells compared to NK 56^{bright} subsets.
[B] Up regulation of PD1 expression in myeloma is more pronounced on CD56^{dim} populations while PDL1 expression is predominantly seen on CD56^{bright} subsets
[C] Granzyme expression is increased on on the PD1^{high} subset
[D] DNAM1 expression is increased on the PD1^{high} subset

6.4.7 NK cell activating receptors are expressed at normal levels in NDMM

NK cells can receive activating signals from a range of non-MHC ligands which may be expressed on tumour cells. The NK cell activating receptors DNAM1 (control 28.65%, NDMM 19.39 t-test p=0.1580), NKG2D (control 16.14, NDMM 21.35 p=0.3716) and 2B4 (control 79.15, NDMM 74.06 p0.6285) are all expressed at normal levels in NDMM (Figure 6.11). The immune checkpoint regulator LAG3 is also present at low levels on both control and NDMM cells (control 5.551, NDMM 8.483 p=0.7103)(Figure 6.11). No difference is seen when BMNCs are stimulated with CD3 and C28 and no difference is seen between NK CD56^{bright} and CD56^{dim} subsets.

A.

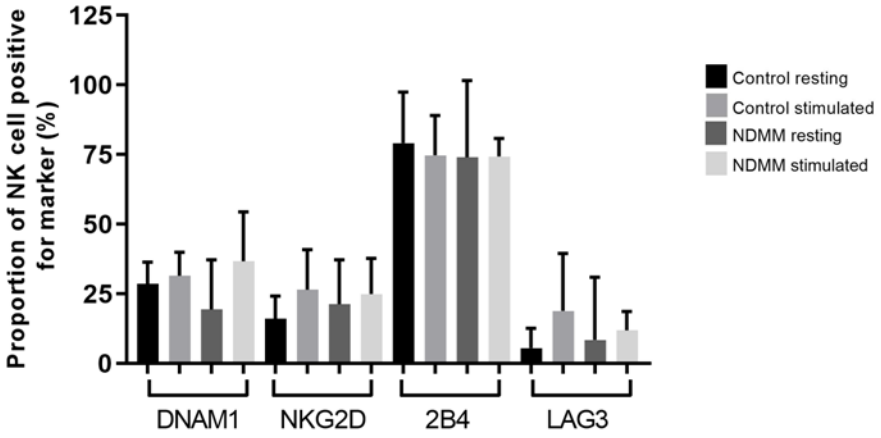

Figure 6.11: NK cell receptor expression.

[A] The NK cell activating receptors DNAM1, NKG2D and 2B4 are all expressed at normal levels in NDMM. The immune checkpoint regulator LAG3 is also present at low levels on both control and NDMM cells. No difference is seen when BMNCs are stimulated with CD3 and C28 and no difference is seen between NK 56 bright and dim subsets.

This is an important observation as NKG2D [177,178], DNAM1 [179] and 2B4 [178] have previously reported to have reduced expression in unselected myeloma patients. This data suggests that loss of these receptors may be a later feature of the disease, providing a therapeutic window to target these receptors at an early disease time point.

6.5 Summary of results

1. NK cell population proportions are shifted towards $CD56^{bright}$ phenotype in NDMM
2. Population shifts due to loss of proliferation in $CD56^{dim}$ subset
3. No differences in CD107a+Gnz+Perf+ cell numbers are seen between control and NDMM NK cells, however increased intensity of granzyme and perforin is seen in the 56^{dim} subset
4. Loss of IFNγ production by non-stimulated $CD56^{dim}$ subset
5. Failure to increase IFN+TNF-IL10- and TNF+IFN+IL10- NK cell populations following stimulation in NDMM
6. Reduced expression of markers of activation TIM3 and HLA-DR by $CD56^{dim}$ subsets in NDMM
7. Increased TIM3 expression seen on NK cell of those surviving more than 36 months

8. Increased PD1 and PDL1 expression in NDMM with higher PD1 expression on $CD56^{dim}$ subset
9. Normal levels of NK cell activating receptors in NDMM

6.6 Discussion

This data establishes that multiple NK cell defects are present at the time of myeloma diagnosis. These defects predominantly effect the $NK56^{dim}$ population and have multiple functional effects. Importantly this data also indicates that there is a survival advantage in having features of NK cell activation.

The $CD56^{dim}$ defects identified result in reduced proliferation, loss of IFNγ production, loss of NK cell activation and elevated PD1 expression. The consequences of increased granzyme and perforin expression in the absence of CD107a expression remain uncertain.

Similar shifts towards $CD56^{bright}$ NK cell populations have been reported in other malignancies. In the setting of non-small cell lung cancer several studies have identified that the predominant tumour infiltrating NK cell is $CD56^{bright}$, compared to being predominantly $CD56^{dim}$ in non-cancerous lung tissue[188]. Furthermore these $CD56^{dim}$ tumour infiltrating NK cells have defects in degranulation[188,189] and IFNγ production [189].

In haematological malignancies, Vari et al reported that NK cells in the peripheral blood of Hodgkin lymphoma (HL) patients are shifted towards a NK $CD56^{bright}$ subset. In HL, however, it is these $CD56^{bright}$ cells which have abnormal expression of PD1 with levels increased above that seen on the $CD56^{dim}$ subset. A similar shift in NK cell population was seen in DLBCL but changes in PD1 expression were less marked [190].

The NK $CD56^{dim}$ changes I have reported here are similar to those reported in tumour infiltrating lung cancer. This is consistent with the source of NK cell I have studied which have been collected from the bone marrow compartment where they will have been interacting directly with the malignant cell population, in a similar way to NK cells infiltrating lung tumours. It is possible that circulating NK cells in NDMM may have a phenotype more similar to those described by Vari et al.

The observation that several different markers of NK cell activation are seen at the time of myeloma diagnosis in those with superior long term survival highlights the key role NK cells are playing in tumour surveillance in this disease. A similar link between cell activation and prognosis could not be identified in CD8+ lymphocyte populations.

The role of PD1 expression by NDMM NK cells is uncertain as the highest PD1 levels are seen on NK cells which also have higher expression of granzyme and DNAM1, an observation inconsistent with NK cell exhaustion. When the entire data set is considered, however, PD1 expression is highest on the NK cell subset which also has loss of IFNγ production and proliferation, which is consistent with an exhausted cell population.

This data has important implications for optimising therapeutic strategies for NDMM. Traditionally individuals with NDMM are only offered treatment once symptomatic disease has become apparent. This data, however, clearly indicates that NK cell defects which may impact prognosis, are already detectable at the time of myeloma diagnosis. Focusing on repairing these defects at an early disease time point may allow long term myeloma control to be established, avoiding or delaying the need for more intensive therapeutic strategies and preventing end organ damage. Possible therapeutic options would include the use of Lenalidomide, which has been show to restore IFNγ production in NK cell from individuals with CLL [30]. Since this drug already has an established use in myeloma, is usually well tolerated and is an oral treatment this would be a practical choice for many patients. Alternative strategies would be to target the PD1-PDL1 axis using monoclonal antibodies such as Nivolumab or Durvalumab or to directly stimulate NK cell activity via stimulation of NKG2D or DNAM1. These strategies have the disadvantage of requiring regular infusions. PD1 axis blockade carries the risk of autoimmune complications while activating NK cells may lead to similar off target effects, for this reason this risks of these drugs may outweigh the potential benefits in otherwise well patients.

The early loss seen here of NK cell immune surveillance also raises the interesting question; is NK cell exhaustion responsible for progression from MGUS to myeloma? The immune surveillance model proposes that prolonged antigen exposure after initial failure to clear the malignant clone leads to lymphocyte exhaustion. This in turn allows the malignant clone to proliferate unchecked. This data in NDMM however suggests that loss of NK cell activity may be key at an early disease stage and that CD8 exhaustion may have a role to play later in the disease. The multiple NK cell defects identified are in contrast to CD8+ lymphocytes which, while having an increase in PD1 expression, maintain many of their functional attributes at this early disease stage.

In summary, this data demonstrates that NK cells in NDMM exhibit multiple features of NK cell exhaustion which disproportionately affect the cytotoxic $CD56^{dim}$ subset. Lack of NK cell activation is associated with inferior long term survival. The NK cell subset may serve as a useful therapeutic target at this early disease stage.

6.7 Relevance of work

1. Identifies NK cells as key in long term myeloma survivorship
2. Demonstrates that key immunological changes have already taken place at the time of myeloma diagnosis, raising questions about optimal treatment timings and strategies
3. Identifies a range of potential therapeutic targets to restore NK cell function

7. The phenotype and function of CD4+ lymphocytes in NDMM

7.1 CD4 lymphocytes and the coordinated immune response

CD4 lymphocytes are responsible for the coordination of other aspects of the immune response, via the production of cytokines and chemokines and through direct cell activation. The secreted cytokines can act as stimulatory or inhibitory signals to antigen presenting cells and cytotoxic cells depending on the microenvironment context. CD4 lymphocytes also provide the second activatory signal to B cells to induce antibody production [191].

CD4 cells are antigen specific, like CD8 lymphocytes, and require the presence of the antigen they recognise plus additional co-stimulatory signals in order to become activated. Unlike CD8 lymphocytes, however, they recognise antigen displayed in MHC Class II.

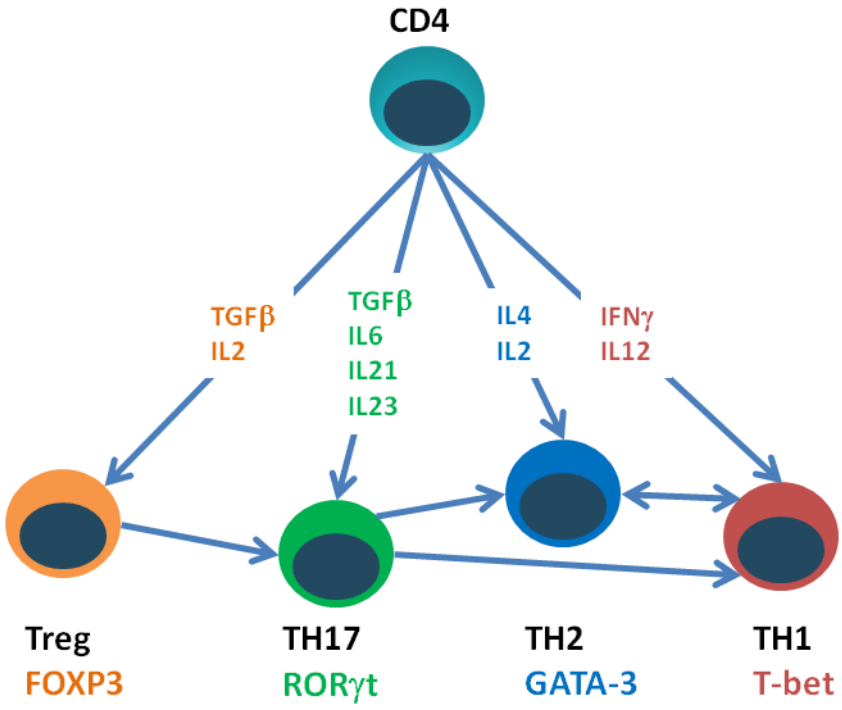

Figure 7.1: CD4 T cell subsets and plasticity

Naive CD4 T cells can differentiate into one of several effector phenotypes. Differentiation is driven by cytokine signalling and effector cells can also exhibit a degree of plasticity.

Naive CD4 lymphocytes can differentiate into one of several different effector subsets. This differentiation is driven by cytokine signalling and is dependent on the activation of specific transcription factors. There are currently four key, biologically relevant CD4 T cell subsets described [192]. These are summarised in table 7.1. CD4 populations also exhibit plasticity, with cells able to move between subsets in response to specific cytokine signals (Figure 7.1).

	Induced by	Function	Cytokines produced	Characteristic transcription factor
TH1	IFNγ IL12	Intracellular pathogens via activation CD8, macrophages, recruit NK cells	IFNγ IL2	T-bet
TH2	IL4 IL2	Extracellular parasites	IL4 IL5 IL13 IL25 IL10	GATA-3
TH17	TGFβ IL6 IL21 IL23	Extracellular bacteria and fungi	IL21 IL17a IL22	RORγt
Treg	TGFβ IL2	Immune tolerance and homeostasis	TGFβ IL35 IL10	FoxP3

Table 7.1: CD4 subsets

Within the setting of the cancer immune surveillance model, CD4 lymphocyte subsets have diverse roles. The TH1 subset can recruit cytotoxic NK and CD8 populations in addition to the production of IFNγ which may have direct anti-tumour effects [193]. The roles of both the TH2 and TH17 subsets are less clear cut. The TH17 subset is associated with a chronic inflammatory response which may suppress the activity of cytotoxic cells, however murine models using adoptive transfer of high number of TH17s have suggested an anti-tumour response [193].

The role of the T regulatory (Treg) subset is better defined. This subset comprises 5-10% of circulating CD4 T cells and mediates peripheral tolerance by suppressing self responsive T cells [8]. In the context of malignancy, however, this can result in the suppression of tumour recognising T cell populations. Unlike most CD4 subsets, Tregs have direct killing mechanisms via perforin and granzyme release, in addition to signalling via T cell inhibitory pathways and the production of TGFβ and IL10 [8].

Histological infiltration of tumour with Treg cells is associated with a poor prognosis in a range of malignancies including DLBCL [22], breast cancer [23], ovarian cancer [24], hepatocellular carcinoma [25] and non-small cell lung cancer [26].

Treg cell numbers are increased in both peripheral blood and bone marrow from patients with myeloma when compared to healthy controls and MGUS [76–78] and higher numbers are associated with faster time to progression [72] and with shorter survival [79,80]. This is in keeping with the suggestion that the tumour microenvironment can have an influence on the immune response. Not all reports confirm this however, with lower Treg numbers and poorly functional Treg cells also being described in myeloma [194]. Interestingly, treatment with IMiDS appears to lead to an increase in Treg numbers [78,81], perhaps in a tissue protecting attempt to limit cytotoxic damage.

7.2 Aim

To establish phenotype and function of CD4 Treg populations in NDMM and compare these to controls

To describe the phenotype and function of CD4 naive, effector and memory subsets

7.3 Specific methodology

CD4+ lymphocytes were identified by the phenotype CD45+CD3+CD4+ and then further subdivided on the basis of CD45RA and CCR7 expression. T regulatory cells were identified by the phenotype CD45+CD3+CD4+CD25highCD127-FoxP3+ (Figure 7.2).

CD4 markers were incorporated into the panel to enable the CD4 Treg population to be identified since this population has been shown to correlate with survival and prognosis in other studies. The incorporation of these markers also allows CD4 naive, memory and effector populations to be defined, however this was not the primary focus of the panel. As a result the markers for TH1, TH2 and TH17 subsets have not be included and these subsets cannot be identified. This limits the biological relevance of exploring the CD4 sunsets but some general observations can be made.

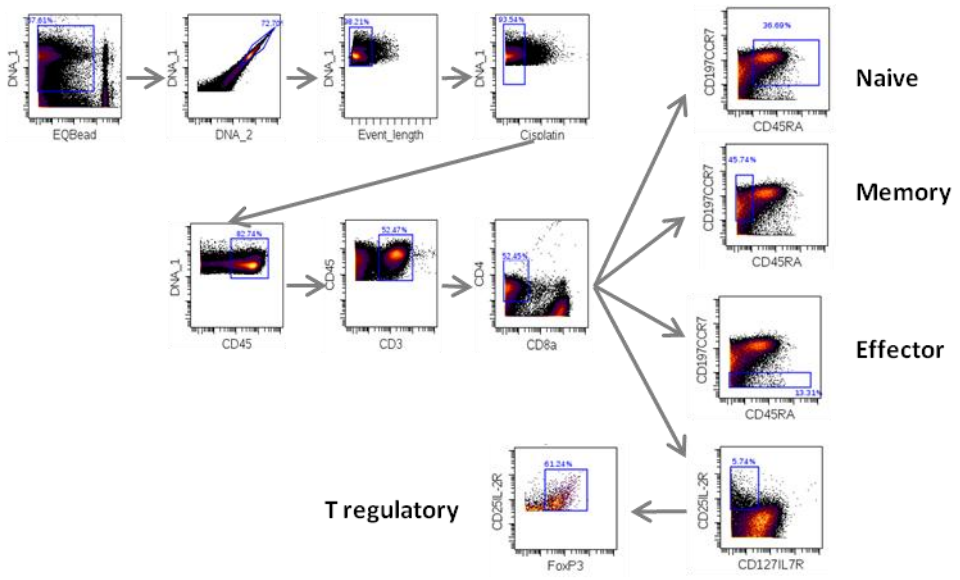

Figure 7.2: CD4 gating strategy

Dead cells, cell doublets and EQ beads were excluded from further analysis. CD4 positive T lymphocytes were identified on the basis of a CD45+CD3+CD4+ phenotype. CCR7 and CD45RA expression was then used to identify CD4 subpopulations. CD25, CD127 and FoxP3 were used to define T regulatory cells.

7.4 Results

7.4.1 There are no numerical differences between CD4 subsets in control and NDMM bone marrow

No numerical differences were identified in CD4 populations and their subsets, including Tregs, between control and NDMM (Figure 7.3 A). Furthermore no differences were seen in the CD8:CD4 ratio between control and NDMM (Figure 7.3 B).

The lack of increase in the Treg subset is at odds with much of the published data in myeloma, but may reflect differences in the stage of disease being studied, the use of appropriate age matched controls (which is not always done) and the different methodology to identify the population.

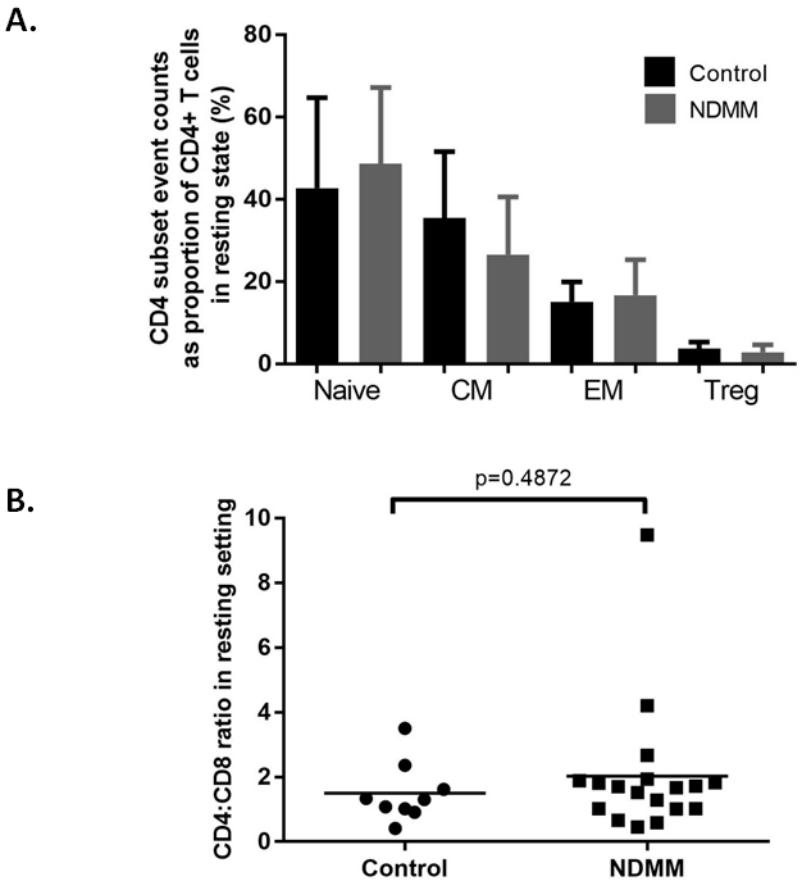

Figure 7.3: CD4 event counts

[A] No numerical differences were identified in CD4 populations and their subsets between control and NDMM. Median values; naive control 37%, naive NDMM 52%, CM control 43%, CM NDMM 23%, effector control 15%, effector NDMM 16%, Treg control 4%, Treg NDMM 3%.
[B] No differences were seen in the CD8:CD4 ratio between control and NDMM

7.4.2 CD4+ lymphocytes in NDMM are poorly proliferative, express PDL1 and generate TGFβ and perforin

Within the resting total CD4 population a small population of cells was observed to express PDL1 in control samples which was significantly higher in NDMM (median control 0.183%, NDMM 1.275% MW p=0.0043)(Figure 7.4 A) with a similar pattern seen for intensity of PDL1 expression (control MSI 1.417, NDMM 2.469 p=0.02)(Figure 7.4 B).

A shift towards a pro-tumour cytokine environment was noted in NDMM with increased intensity of TGFβ expression (median MSI control 11.74, NDMM 16.73 MW p=0.0146)(Figure 7.4 B) which was accompanied by an increase in perforin expression (median MSI control 2.961, NDMM 12.6 MW p=0.0308)(Figure 7.4 D) but not of granzyme (median MSI control 10.18, NDMM 19.84 MW p=0176)(Figure 7.4 H). CD107a was undetectable (Figure 7.4 G).

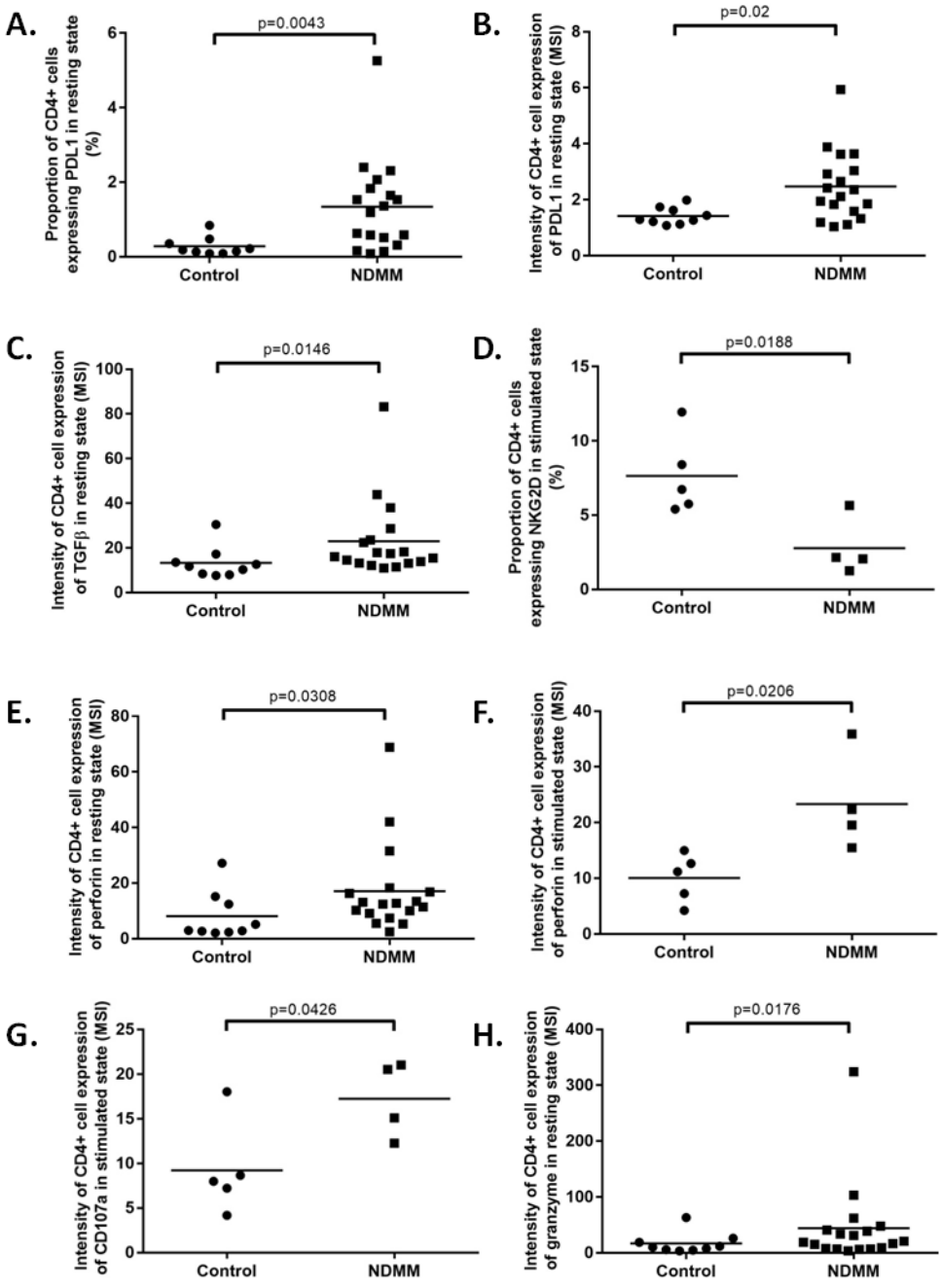

Figure 7.4: CD4+ lymphocytes in NDMM express PDL1 and generate TGFβ and perforin

[A][B] The proportion of cells expressing PDL1 and the intensity of PDL1 expression are higher in NDMM in the resting state
[C] TGFβ intensity is increased in resting NDMM.
[D] NKG2D levels were decreased following cell stimulation.
[E][F] Resting and stimulated perforin expression intensity was increased in NDMM
[G][H] CD107a but not granzyme expression intensity was increased in NDMM

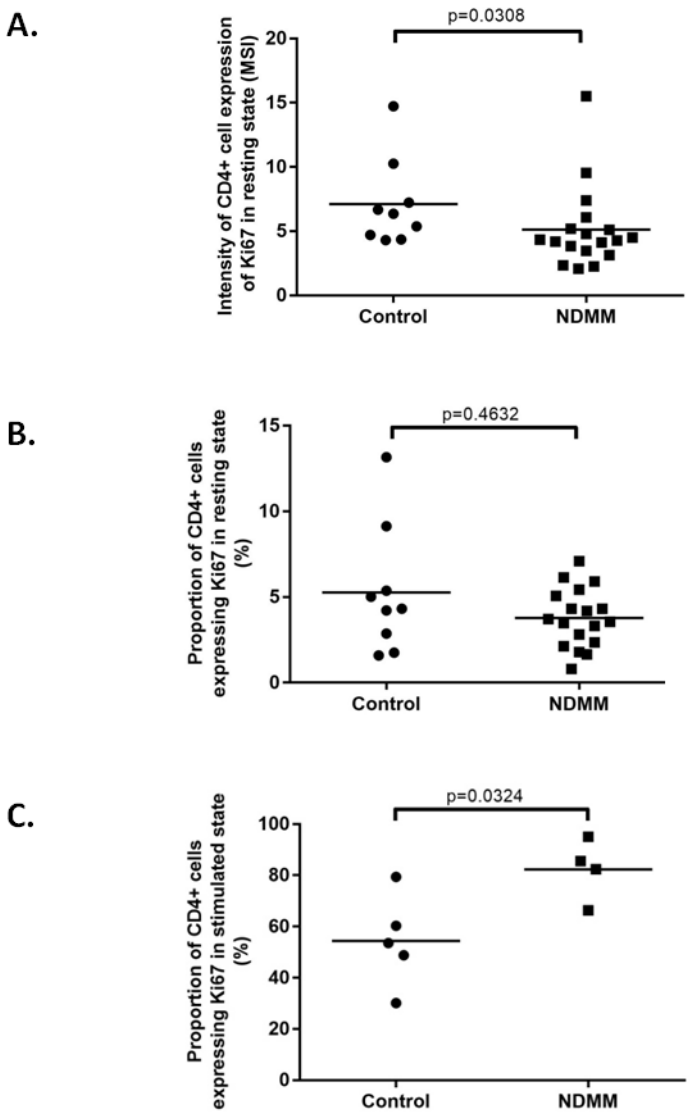

Figure 7.5: CD4+ lymphocytes in NDMM are poorly proliferative

[A] Intensity of resting Ki67 expression is lower in NDMM
[B] The proportion of cells expressing Ki67 in the resting state is no different between control and NDMM
[C] Following stimulation the proportion of cells expressing Ki67 was higher in NDMM

Intensity of Ki67 expression was lower in NDMM indicating a loss of proliferation (median MSI control 6.359, NDMM 4.309 MW p=0.0308)(Figure 7.5 A) however this did not translate into a difference in the proportion of cell positive for Ki67 (Figure 7.5 B).

Following stimulation with CD3 and CD28 there was a significantly larger Ki67 expressing CD4 population in NDMM (control 54.41%, NDMM 82.33% p=0.0324)(Figure 7.5 C), which also demonstrated an increase in Ki67 expression intensity (control MSI 296.8, NDMM 910.9 p=0.0089).

Despite the apparent increase in proliferation following stimulation, the CD4 population remains functionally abnormal with a smaller NKG2D expressing population (mean control 7.648%, NDMM 2.777% t-test p=0.0188). Interestingly there was also an increased intensity of CD107a (MSI mean control 9.216, NDMM 17.23 t-teat p=0.0426) and perforin (MSI mean control 10.06, NDMM 23.31 t-test p=0.0206) in NDMM CD4 cells following stimulation. These perforin and CD107a expressing CD4+ lymphocytes may represent a cytotoxic CD4 subset.

CD4 cytotoxic cells are a recognised entity [195–197] which are defined as CD4+ lymphocytes which express one or more of granzyme A, granzyme B or perforin. They have been shown in murine models to have anti-tumour activity in a similar way to CD8 lymphocytes [198]. Recently CD4+ cytotoxic cells have been identified at increased numbers in the peripheral blood of patients with NDMM. These cells were able to target plasma cells during in-vitro modelling and expressed lower PD1 than their CD8 counterparts [199].

7.4.3 The T regulatory population in NDMM has a more immune suppressive phenotype compared to control samples

The resting Treg population had a larger PDL1 expressing population in NDMM compared to control (mean control 0.2833%, NDMM 2.483% t-test p=0.0160), this was accompanied by an increase in PDL1 expression intensity (control 0.9247%, NDMM 2.825% p=0.0041) (Figure 7.6 A).

The expression of TGFβ (median MSI control 12.11, NDMM 17.66 MW p=0.0032)(Figure 7.6 B) was also elevated in NDMM as was perforin (median control 2.417%, NDMM 9.988% MW p=0.0194)(Figure 7.6 D) and CD107a expression (median control 0.6601%, NDMM 1.772% MW p=0.0401)(Figure 7.6 E).

Following stimulation, the proportion of Treg cells positive for Ki67 (mean control 61.85%, NDMM 91.83% t-test p=0.0394) was higher in NDMM, accompanied by increased intensity of expression (mean control MSI 327.1 NDMM 951 t-test p=0.0086)(Figure 7.6 F). They also have a decreased expression of NKG2D (mean control 11.9%, NDMM 2.183% t-test p=0.0114)(Figure 7.6 C). The intensity of CD107a (mean control MSI 10.58, NDMM 18.84 t-test p=0.0471)(Figure 7.6 E) and perforin (mean control MSI 12.66, NDMM 26.85 t-test p=0.0414)(Figure 7.6 D) expression was also increased.

Despite not identifying a numerical difference in Treg subset numbers between control and NDMM, it is clear that the functional differences describe a more immune suppressive subset in NDMM with evidence for immune regulation via cytotoxic mechanisms.

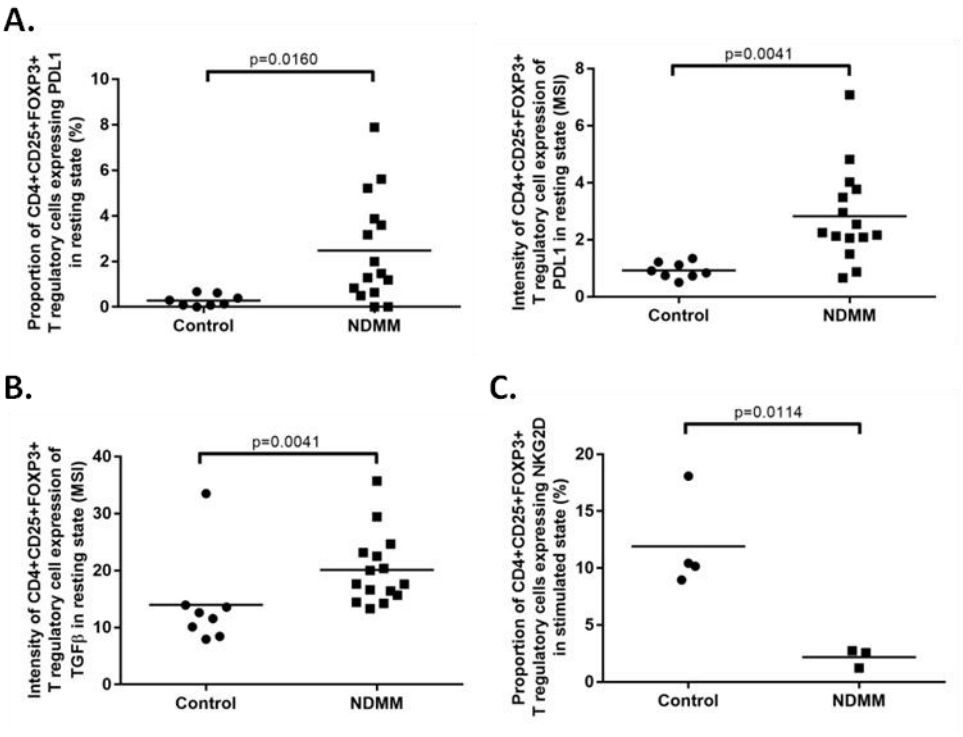

Figure 7.6: The T regulatory population in NDMM has a more immune suppressive phenotype compared to control samples

[A] PDL1 expression and intensity is higher on NDMM CD4 Tregs compared to controls
[B] TGFβ expression is elevated in CD4 Tregs in NDMM at rest
[C] NKG2D expression is decreased in NDMM CD4 Tregs following stimulation

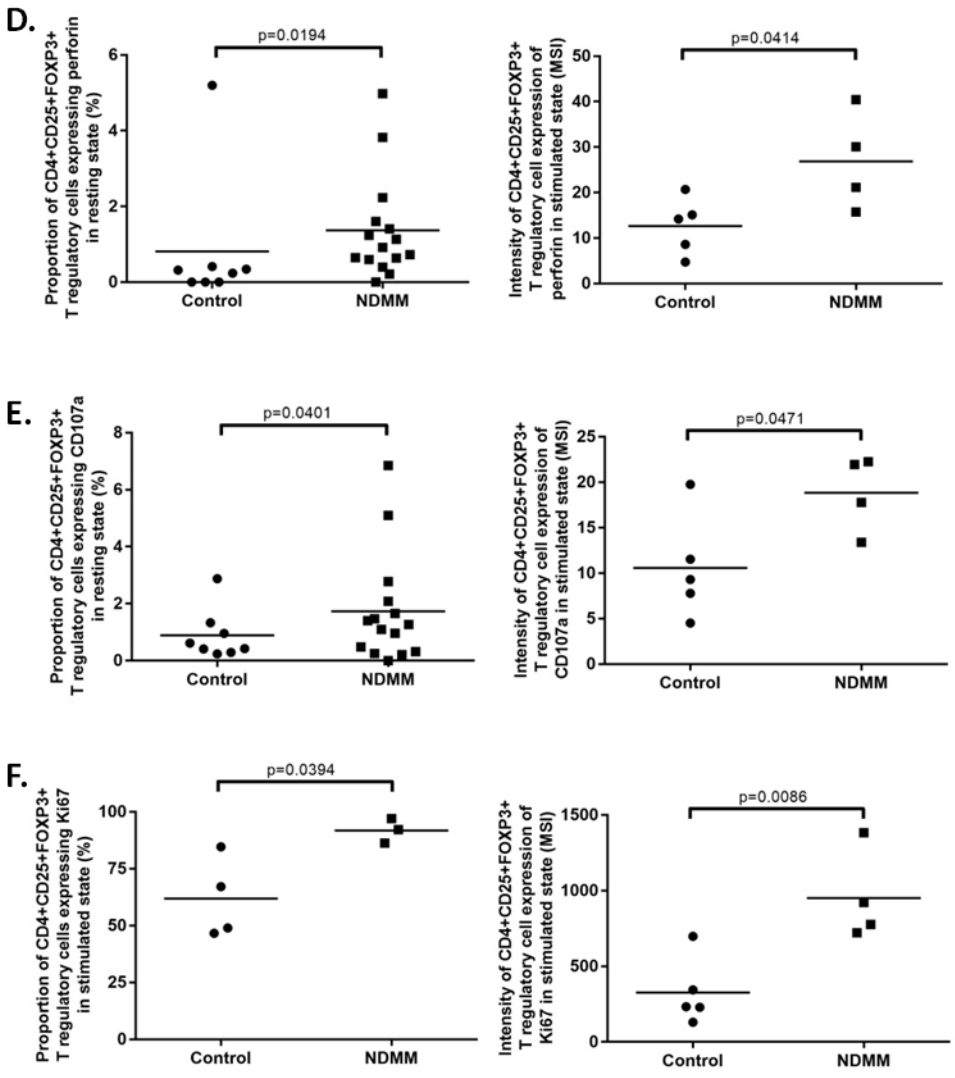

Figure 7.6 cont: The T regulatory population in NDMM has a more immune suppressive phenotype compared to control samples. Cont.

[D] Perforin expression is elevated in CD4 Tregs in NDMM at rest and remains increased following stimulation

[E] CD107a expression is elevated in CD4 Tregs in NDMM at rest and remains elevated following stimulation

[F] Ki67 expression and intensity is increased in CD4 Tregs in NDMM following stimulation

7.4.4. Naïve CD4 cells in NDMM are poorly proliferative and express PDL1

The resting naive CD4 population had a small proliferative population in control samples which was significantly smaller in NDMM (Ki67 mean control 5.45%, NDMM 3.129% t-test p=0.0390)(Figure 7.7 A). The expression of PDL1, while low in both disease and control samples, was significantly higher in NDMM (PDL1 control 1.374%, NDMM 2.602% p=0.0293)(Figure 7.7 B).

Stimulation with CD3 and CD28 results in an increase in the size of CD107a (control 21.77%, NDMM 49.96% p=0.0349)(Figure 7.7 D) and a decrease in NKG2D (control 21.4%, NDMM 8.388% p=0.0098)(Figure 7.7 C) expressing populations. This was accompanied by increased intensity of Ki67 (mean MSI control 256.5 NDMM 819.8 t-test p=0.0111)(Figure 7.7 A), PD1 (mean MSI control 39.13 NDMM 75.65 t-test p=0.0348)(Figure 7.7 F), perforin (mean MSI control 8.162 NDMM 26.85 t-test p=0.0421)(Figure 7.7 E) and CD107a (mean MSI control 9.03 NDMM 18.1 t-test p=0.0222)(Figure 7.7 D). This suggests that the CD4 naive population in NDMM is a poorly proliferative subset with a cytotoxic response following activation.

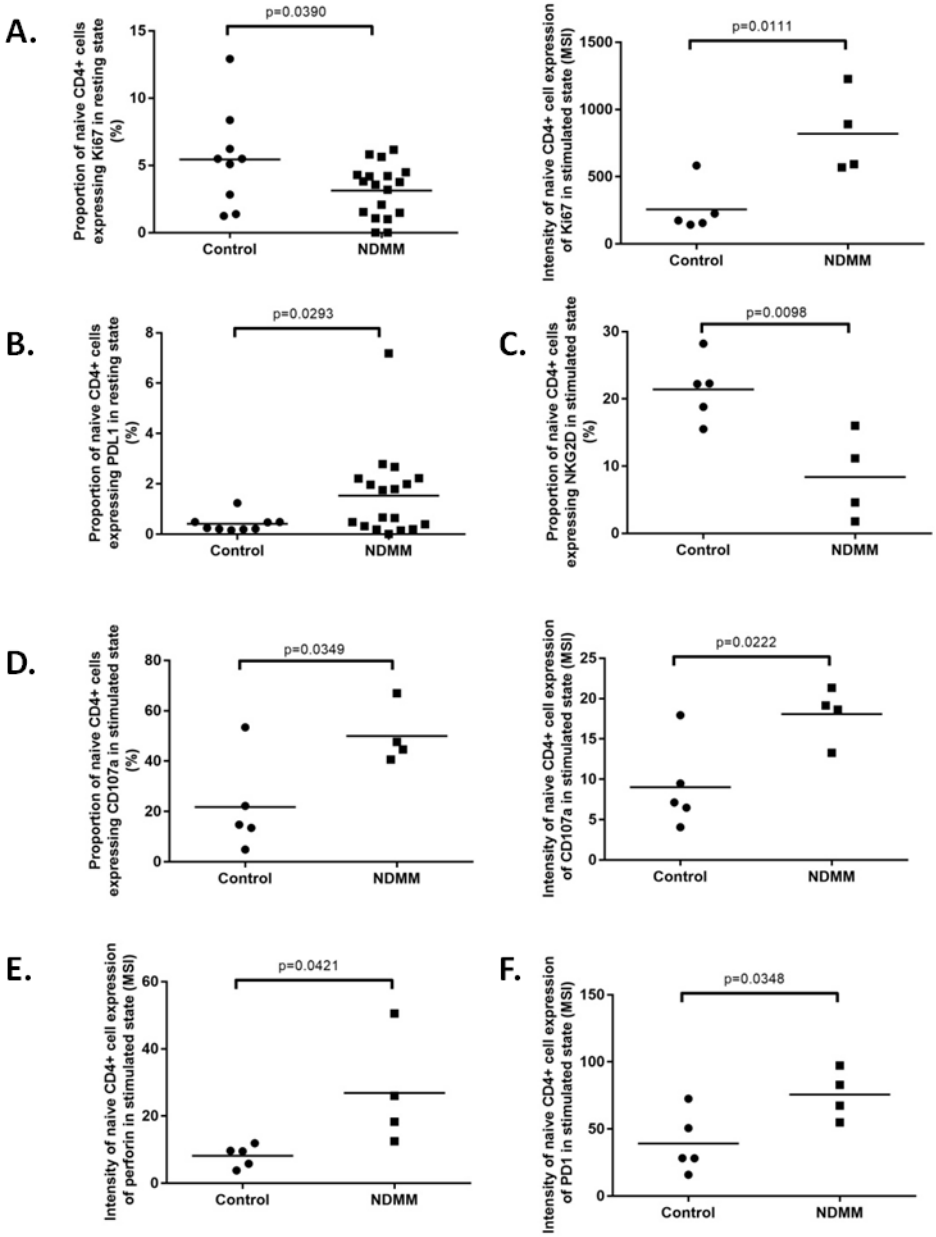

Figure 7.7: Naïve CD4 cells in NDMM are poorly proliferative and express PDL1

[A] The resting naive CD4 population had a small proliferative population in control samples which was significantly smaller in NDMM. Following stimulation there was an increase in Ki67 expression intensity.
[B] The expression of PDL1 in the resting state was significantly higher in NDMM
[C] A decrease in NKG2D is seen in NDMM following stimulation
[D] The proportion of naive CD4 cells positive for CD107a and intensity of CD107a expression was higher in NDMM following cell stimulation
[E] Perforin expression is increased in stimulted naive CD4 cells in NDMM
[F] PD1 expression is increased in increased in stimulated naive CD4 cells in NDMM

7.4.5 The memory CD4 subset in NDMM has a pro-tumour cytokine profile

The resting memory population demonstrated loss of DNAM1 expressing populations in NDMM (mean control 30.06%, NDMM 17.67% t-test p=0.0494)(Figure 7.8 A) with an increase in intensity of TGFβ expression (mean control 12.34%, NDMM 19.19% t-test p=0.0348)(Figure 7.8 B).

Stimulated CD4 memory populations had a higher proportion of Ki67 positive cells (mean control 48.54%, NDMM 77.64% t-test p=0.0347)(Figure 7.8 C) and granzyme positive cells (mean control 43.76% NDMM 90.5% t-test p=0.0390)(Figure 7.8 D) in NDMM.

The CD4 memory subset therefore has a pro-tumour cytokine profile.

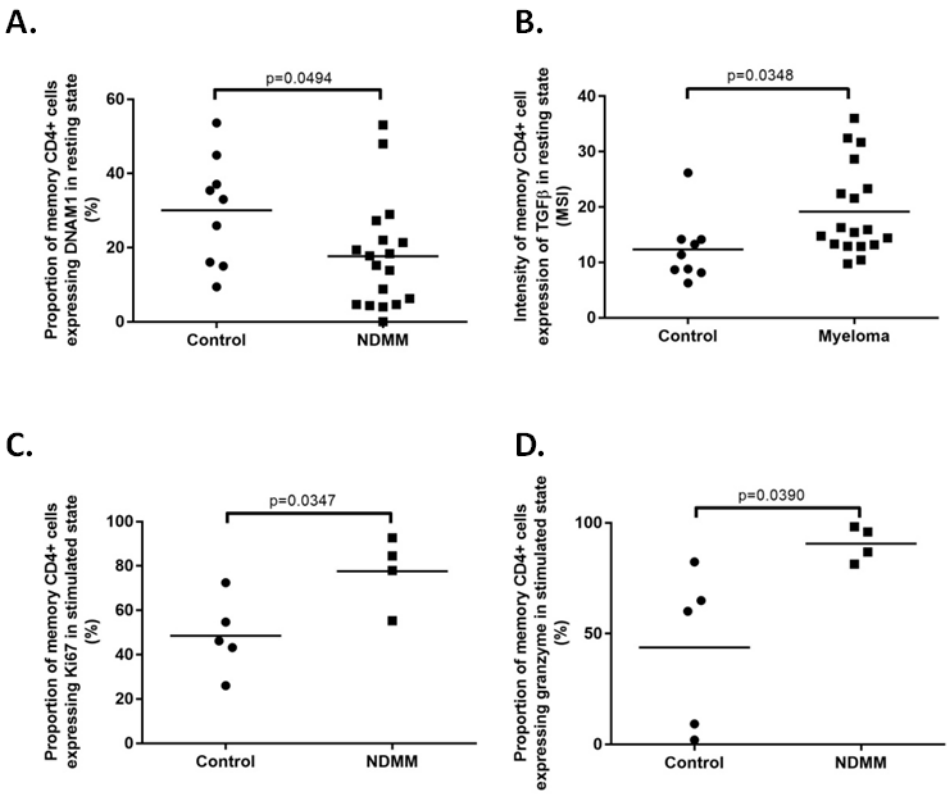

Figure 7.8: The memory CD4 subset in NDMM has a pro-tumour cytokine profile

[A] DNAM1 expression is lost on resting NDMM CD4 memory cells
[B] TGFβ expression is increased in resting NDMM CD4 memory cells
[C] Ki67 expression is increased on stimulated CD4 memory subsets in NDMM
[D] Granzyme expression is increased in stimulated CD4 memory populations in NDMM

7.4.6 The effector CD4 population has a pro-tumour phenotype

The resting effector CD4 population had an increase in intensity of both PDL1 (mean MSI control 1.451%, NDMM 2.223% t-test p=0.0085)(Figure 7.9 A) and TGFβ (median MSI control 8.518%, NDMM 16.3% MW p=0.0064)(Figure 7.9 B) expression suggesting a shift towards a pro-tumour environment.

Following stimulation effector CD4 populations had increased expression of Ki67 in NDMM (mean control 367, NDMM 982.4 t-test p=0.0153)(Figure 7.9 C) but this did not translate to a population size difference.

CD4 population phenotypes do not correlate with improved survival in NDMM.

7.5 Summary of results

1. No numerical differences were identified in CD4 populations and their subsets, including Tregs, between control and NDMM.
2. CD4+ lymphocytes in NDMM are poorly proliferative, express PDL1 and generate TGFb and perforin
3. The T regulatory population in NDMM has a more immune suppressive phenotype compared to control samples
4. Naïve CD4 cells in NDMM are poorly proliferative and express PDL1
5. The memory CD4 subset in NDMM has a pro-tumour cytokine profile
6. The effector CD4 has a pro-tumour phenotype
7. CD4 population phenotypes do not correlate with improved survival in NDMM.

A.

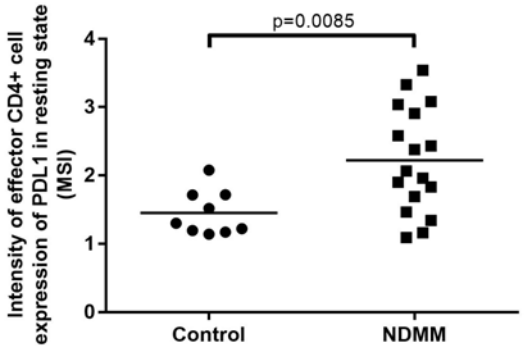

B.

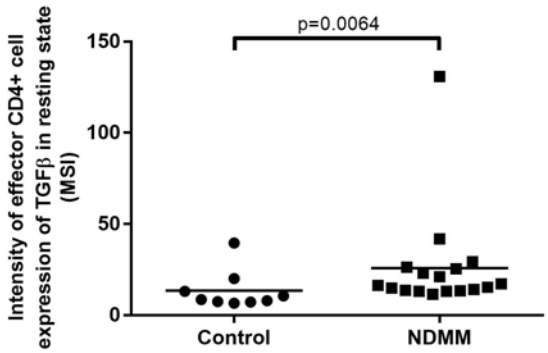

C.

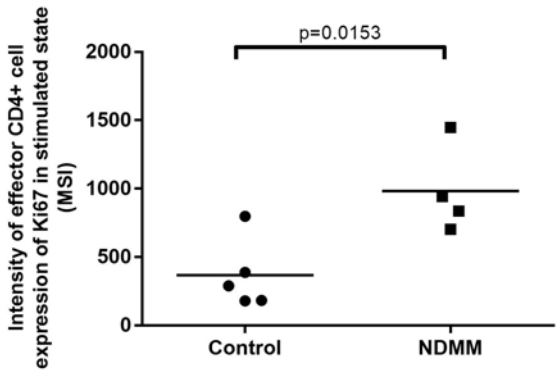

Figure 7.9: CD4 effector populations have a pro-tumour phenotype

[A] PDL1 expression on resting CD4 effector populations is increased in NDMM
[B] TGFβ expression on resting CD4 effector populations is increased in NDMM
[C] Ki67 expression on stimulated CD4 effector populations is increased in NDMM

7.6 Discussion

Across all CD4 subsets examined there was a recurring theme of increased PDL1 and TGFβ expression, suggesting a pro-tumour response. This was accompanied by a reduction in the proliferating fraction and the suggestion of a shift towards a CD4 cytotoxic phenotype.

Taken together, these data support our hypothesis that the CD4 ability to recruit an anti-tumour response is impaired, with function being polarised towards a regulatory response. While the CD4+perforin+ subset identified in the total CD4 cohort might represent an anti-tumour CD4 cytotoxic response, this may also represent an immune suppressive T regulatory subset with cytotoxicity directed toward anti-tumour immune cells rather than the tumour clone. This idea is supported by the fact that the pattern of perforin and CD107a expression is replicated within the T regulatory subset but not within the CD4 effector subset.

The data highlights the importance, once again, of the PDL1-PD1 axis in NDMM. PDL1 expression by T regulatory cells is an expected feature since one method of immune suppression by this subset is the engagement of immune regulatory receptors on cytotoxic lymphocytes. The increased expression of PDL1 across other CD4 subsets is perhaps more surprising, however it should be remembered that CD4 cells can act as antigen presenting cells and may therefore be able to deliver immune checkpoint signals to cytotoxic subsets.

There have been conflicting reports regarding the numbers of CD4 T regulatory compartment in myeloma, the data presented here confirms that, in the setting of the NDMM bone marrow compartment, T regulatory cells are not increased. They do, however, have a more immunosuppressive phenotype than their control counterparts with high expression of both TGFβ and PDL1 seen accompanied by activation of cytotoxic pathways. This is evidence that, while numerically normal, NDMM Tregs have immune suppressive potential.

An important limitation of this data is the lack of ability to discriminate between TH1, TH2 and TH17 subsets. These subsets are being increasingly recognised as vital in driving an anti-tumour response and understanding the numerical, phenotypic and functional characteristics would aid our understanding of the biology of the disease and potential pitfalls when using immune targeting therapy. Unfortunately mass cytometry panels are not yet complex enough to allow in depth characterisation of all immunological subsets!

7.7 Relevance of work

1. Demonstrates that T regulatory cells have a more immune suppressive phenotype in NDMM despite a lack of numerical difference

8. Plasma cell and the non-myeloma B cell population phenotype and function

8.1 Plasma cells and the non-myeloma B cell population

B cells form part of the adaptive immune system which can function as antigen presenting cells, generate cytokines and produce immunoglobulin. Naive B cells circulate until they meet their specific antigen. They then move to the germinal centre where they undergo somatic hypermutation and heavy chain class switching, generating long lived plasma cells with high affinity antibody and memory B cell subsets [33]. Mature memory B cells circulate within the peripheral blood, while plasma cells home to the bone marrow [33]. Following secondary exposure to their antigen both B cell subsets are able to rapidly proliferate and generate immunoglobulin in the case of plasma cells or re-enter the germinal centre in the case of memory B cells.

Myeloma is a malignancy of long lived, post germinal centre plasma cells which produce immunoglobulin. In myeloma, control of proliferation is a lost and, in most cases, immunoglobulin secretion is dysregulated. This results in production of the characteristic paraprotein which is responsible for many of the clinical features of myeloma, including renal impairment and hyperviscosity. The bulk of malignant disease occurs within the bone marrow although discrete plasmacytomas are sometimes seen. Heavy bone marrow infiltrations results in suppression of normal haematopoesis. Malignant plasma cells also induce changes to the stromal microenvironment, angiogenesis and induction of immune regulatory cytokines.

Molecular analysis of the IGH gene in myeloma has demonstrated that mature circulating B cells do not share the clonal IGH gene rearrangement of the malignant plasma cells [200] suggesting that the memory B cell compartment is not involved in the disease. B cell subset proportions have been reported to not be different between MGUS and myeloma [200], however there is a reduction in IgD+CD27+ unswitched memory cells [201] and a shift towards mature, post germinal centre B cell subsets [202] have been reported in myeloma compared to healthy controls

8.2 Aim

To describe non-malignant B cell lineage cells and malignant plasma cell phenotype in NDMM

To correlate malignant plasma cell changes to characteristics of other immunological subsets

8.3 Specific methodology

8.3.1 Identification of plasma cells

Plasma cells proved to be challenging to identify using traditional Boolean gating due to lack of a consistent phenotype and downregulation of CD138 expression due to cryopreservation [186]. In order to overcome this difficulty the viSNE dimensionality reducing algorithm was performed on the single cell gate of all NDMM and control unstimulated samples. 15000 cells were sampled per file and viSNE was performed with iterations set at 3000 and perplexity at 70.

The algorithm was run twice, once using basic phenotyping markers for dimensionality reduction and once using all markers. In both versions of the viSNE it was possible to place a plasma cell gate which incorporated varying malignant cell phenotypes while minimising incorporation of cells in control samples. The gate was predominantly placed on the basis of CD38 expression with the exclusion of other lineage markers. When the two viSNE versions were compared the malignant plasma cell proportions were matched between paired samples (paired t-test p=0.1967. Mean basic 24.16%, mean all 26.04%), however significantly more cells in control samples were located within the malignant plasma cell gate when only basic phenotyping markers were used to generate the viSNE (paired t-test p=0.0305 mean basic 2.204, mean all markers 1.111%). The viSNE incorporating all markers was therefore selected as the preferred option for further analysis.

Incidentally the all markers analysis also allowed identification of NK cells by viSNE which has previously been challenging.

8.4 Results

8.4.1 The non malignant B cell compartment is less proliferative in NDMM and expresses higher levels of IL2

When considering the non-myeloma B cell compartment no difference in event counts between control and NDMM samples was seen (Figure 8.1 A).

Proliferation was reduced in non-myeloma B cells in NDMM (mean control 13.79% NDMM 6.386% t-test p0.0336)(Figure 8.1 B) while IL2 expression is increased (median control 1.535% NDMM 3.923% MW p=0.0405)(Figure 8.1 C).

B cells are known to have the potential to produce a wide range of cytokines in response to various stimuli. IL2 producing B cell may have a role to play in polarisation towards the CD4

TH2 subset, as well as recruitment of NK cells and generation of CD4 T regulatory subsets [203]. It is not known whether the net result is a pro-tumour or anti-tumour response.

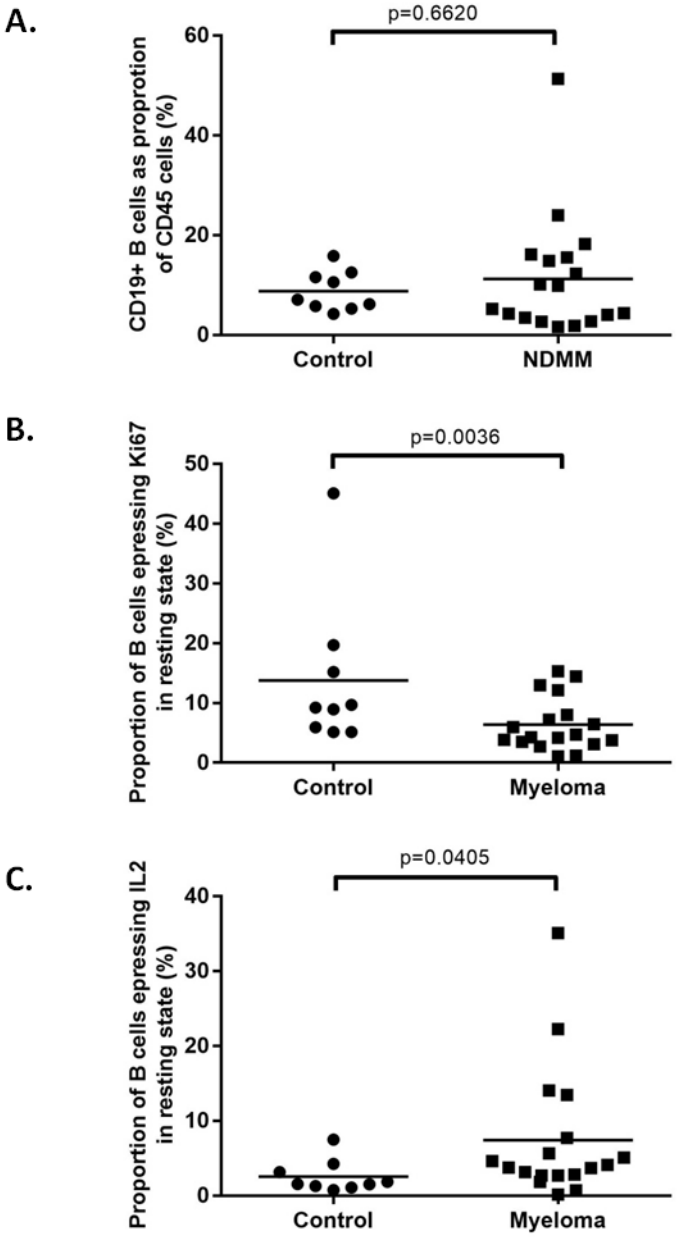

Figure 8.1: The non malignant B cell compartment is less proliferative in NDMM and expresses higher levels of IL2

[A] There is no difference in B cell event counts between control and NDMM
[B] Ki67 expression is reduced in non-myeloma B cells in NDMM
[C] IL2 expression is increased in non-myeloma B cells in NDMM

8.4.2 NDMM plasma cell populations as detected by mass cytometry vary widely in size between individuals

Using the complete phenotype viSNE gate the mean plasma cell event count in NDMM was 26.04% % (range 0.5933-95.18), compared to 1.11% (range 0.0867-2.513%) in control samples (Figure 8.2).

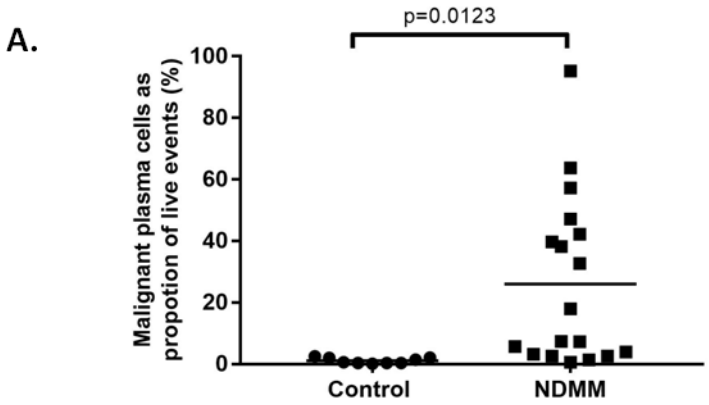

Figure 8.2: Myeloma plasma cell populations as detected by mass cytometry vary widely in size between individuals

[A] viSNE allows identification of plasma cells in NDMM which are significantly higher than in controls

Within the plasma cell gate a range of patterns of cell distribution could be identified. In some cases all cells were closely clustered together, indicating that these cells were phenotypically very similar and likely to be a single plasma cell clone (Figure 8.3 A). A second pattern was a tight clustering of a large proportion of cells, with other cells scattered throughout the gate (Figure 8.3 B). Finally some individuals had a diffuse spread of cells throughout the plasma cell gate (Figure 8.3 C). These differences in cell clustering within the plasma cell gate is likely to represent differences in the clonal behaviour of the malignant plasma cells, with some individuals having one dominant clone while others have multiple sub clones. Similar patterns of clonal behaviour have previously been reported in the context of genetic subclones [38].

Within these different patterns of plasma cell distribution there is also variation seen in PDL1 expression, with some individuals having no or minimal expression (Figure 8.4 A), while others have expression in a proportion of cells (Figure 8.4 B). Interestingly, even within a tight cluster of plasma cells there was variation in the levels of PDL1 expression.

The marked variation in plasma cell numbers may reflect true differences in disease burden, however it is well recognised that bone marrow aspirate samples often underestimate plasma cell burden compared to bone marrow trephines and the degree to which this is a problem

varies between individuals. Disproportionate loss of plasma cells in the samples analysed by mass cytometry due to poor viability and epitope downregulation following cryopreservation may also have an impact on total plasma cell numbers. For these reasons it has not been possible to assess the impact of plasma cell burden on the numbers and function of other immunological subsets.

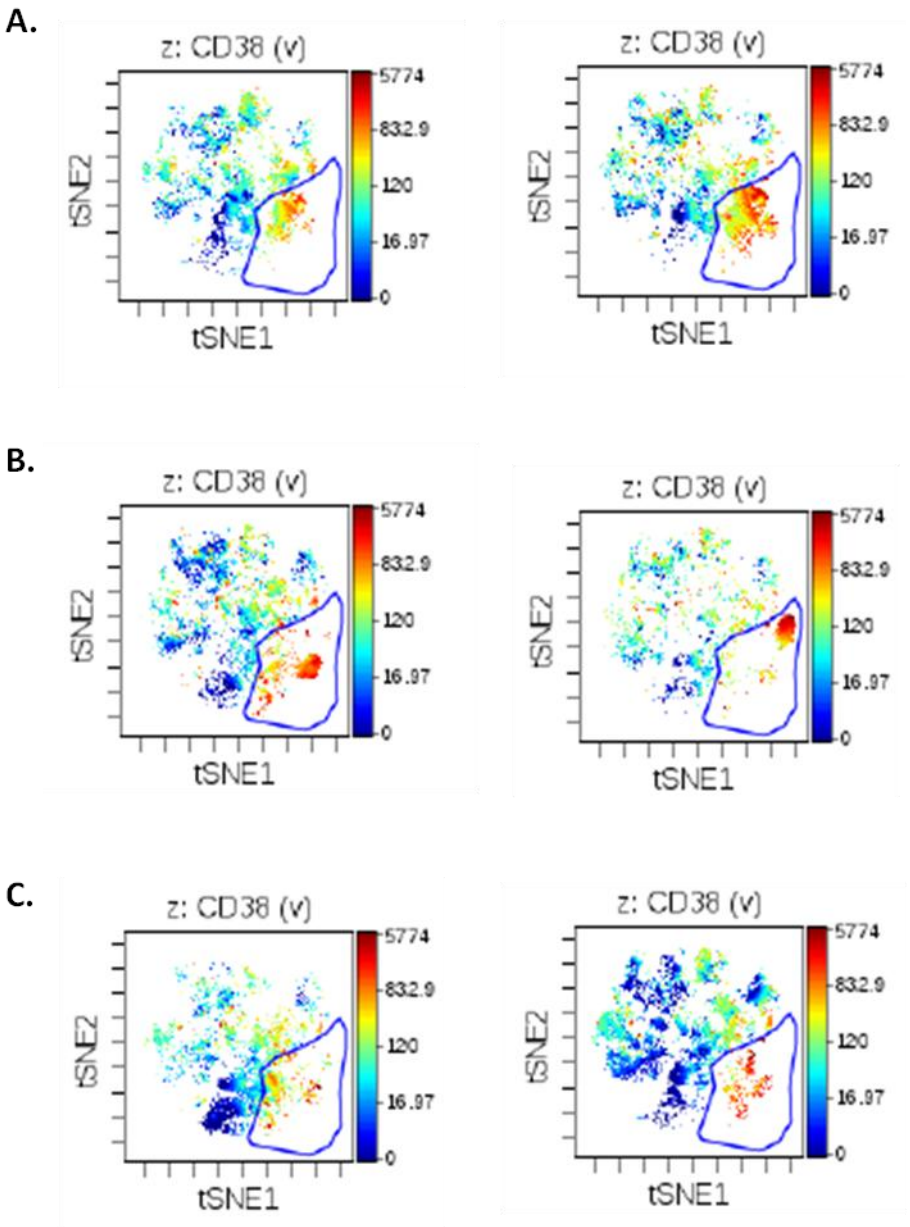

Figure 8.3: Plasma cells in NDMM demonstrate a range of patterns of distribution

[A] Localised
[B] Diffuse and localised
[C] Diffuse

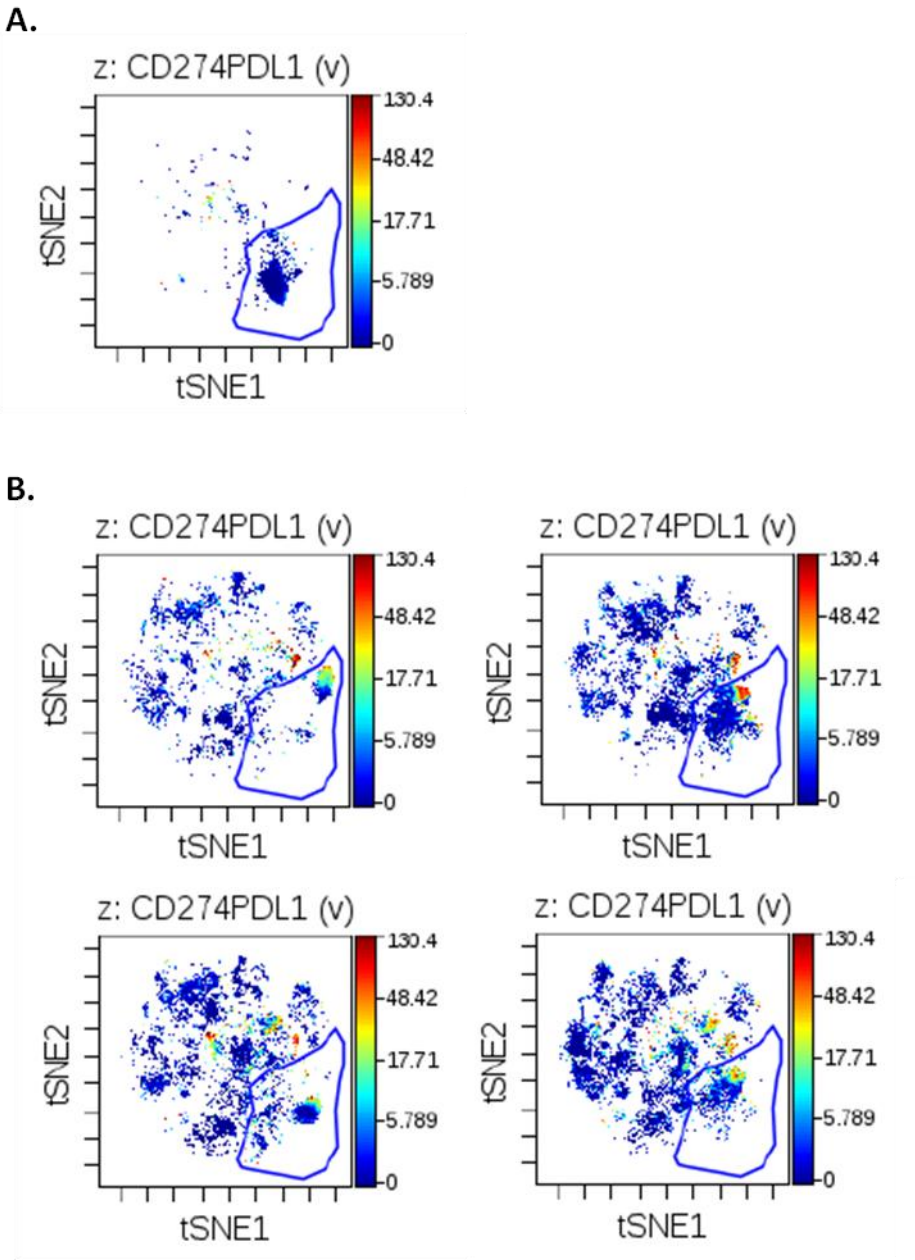

Figure 8.4: Variations in plasma cell expression of PDL1 are seen within the plasma cell gate

[A] Absent PDL1 expression
[B] Partial PDL1 expression

8.4.3 Plasma cell populations in NDMM express PDL1, LAG3 and 2B4

The plasma cell population in NDMM expressed PDL1 (15.71%), LAG3 (13.07%) and 2B4 (13.93%), with lower level expression of PD1(3.83%), OX40 (3.1%) and DNAM1 (3.7%) (Figure 8.5 A).

Plasma cell PDL1 expression is reported to be between 5 and 96% with average of 20% [204]. In murine studies LAG3 was expressed on 50% of plasma cells and was thought to represent a B

regulatory subset [205]. 2B4 is not normally expressed on B cells [206]. No data is available regarding PD1, OX40 and DNAM1.

When functional markers were assessed 20% of plasma cells were expressing Ki67, indicating proliferation in this subset. IFNγ was undetectable, a low level of IL2 (3.75%) and IL10 (5.96%) production was seen (Figure 8.4 B). TNFα production had a mean expression of 20%, however the median was 3.9% with just four individuals having elevated TNFα levels (Figure 8.5 B). TNFα expression by B cells [203] and plasma cells [207] has been previously reported but the biological consequences of this is unknown. TNFα has been reported to promote plasma cell survival in vitro [208] but is also a key part of the anti-tumour response.

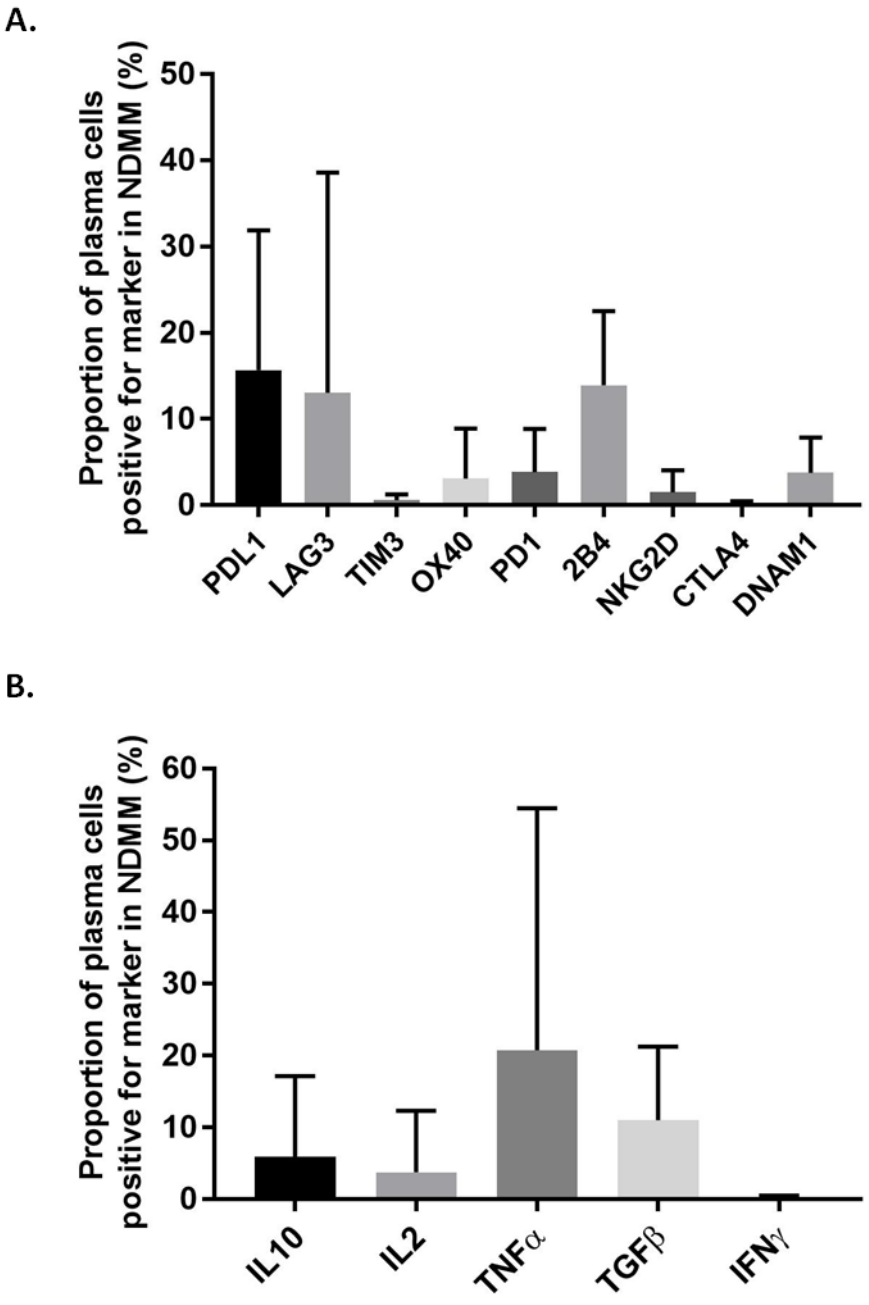

Figure 8.5: Plasma cell populations in NDMM express PDL1, LAG3 and 2B4 and produce TGFβ

[A] The plasma cell population in NDMM expressed PDL1 (15.71%), LAG3 (13.07%) and 2B4 (13.93%), with lower level expression of PD1(3.83%), OX40 (3.1%) and DNAM1 (3.7%).
[B] IFNy was undetectable, a low level of IL2 (3.75%) and IL10 (5.96%) production was seen. TNFa production had a mean expression of 20%, however the median was 3.9% with just four individuals having elevated TNFa levels.

8.4.5 High plasma cell TGFβ expression is associated with co-expression of immune checkpoint ligands and decreased CD8 subset cytotoxicity

Across the total population the mean expression of TGFβ was 6%, however expression was much higher (>20%) in four individuals. Plasma cells in those with higher TGFβ levels had three times higher expression of LAG3 (mean low 8.902% high 27.68%)(Figure 8.6 A) and double the expression of PDL1 (mean low 12.29% high 27.68%)(Figure 8.6 B). These changes, however, were largely driven by one individual who had very high LAG3 and PDL1 expression.

Level of plasma cell TGFβ expression showed a positive correlation with CD4 T regulatory cells TGFβ expression (r=0.5604, p=0.0295)(Figure 8.6 C). No correlation with survival was seen.

When PDL1 expression was stratified by mean expression, an increase in TGFβ expression was seen in those with higher PDL1 expression (MSI TGFβ low 7.438, high 18.13, t-test p=0.0325)(Figure 8.7 A). There was no correlation between plasma cell PDL1 expression and survival, however, a positive correlation was seen between plasma cell PDL1 expression and CD8 PDL1 expression (r=0.8219,p=<0.0001)(Figure 8.7 B). A negative correlation between plasma cell PDL1 expression and CD8 EMRA perforin was also seen (r=0.5529, p=0.0285)(Figure 8.7 C).

This suggests that plasma cells with a TGFβ+ or immune checkpoint regulatory phenotype may be exerting suppressive influences on CD8 cytotoxic function.

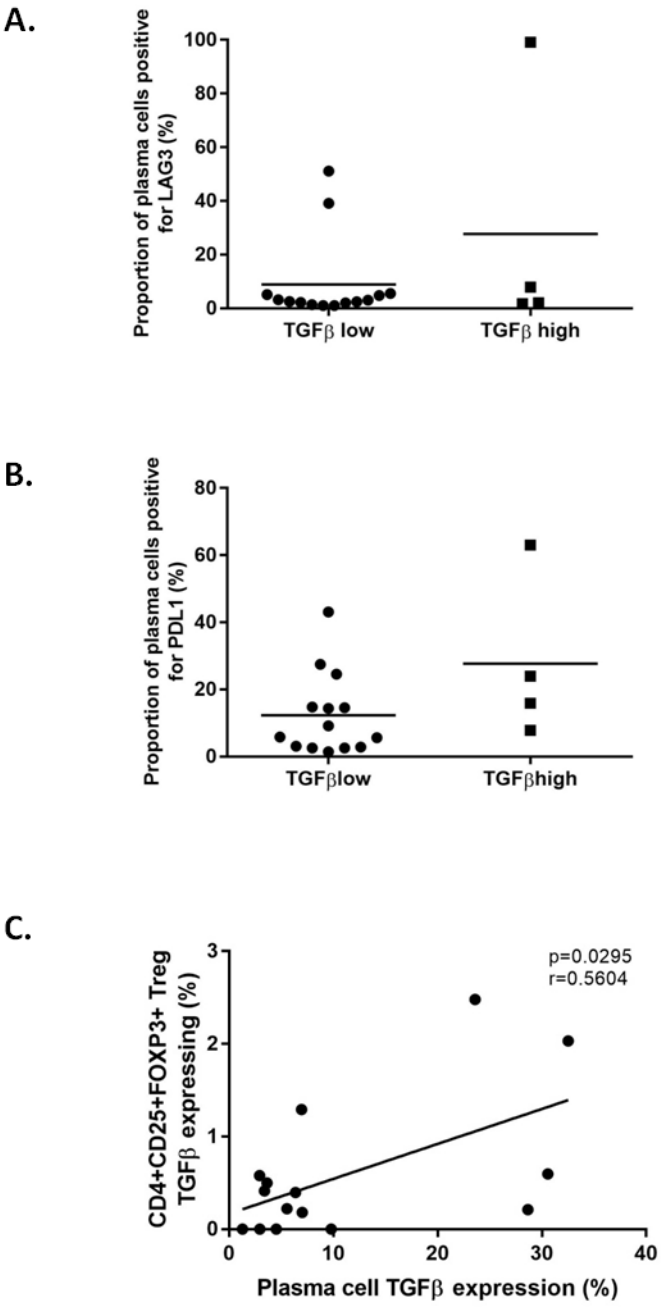

Figure 8.6: High plasma cell TGFb expression is associated with co-expression of immune checkpoint ligands

[A] Plasma cells in those with elevatedTGFb levels had three times higher expression of LAG3
[B] Plasma cells in those with elevated TGFb levels had double the expression of PDL1
[C] Level of plasma cell TGFb expression showed a positive correlation with CD4 T regulatory cells TGFb expression

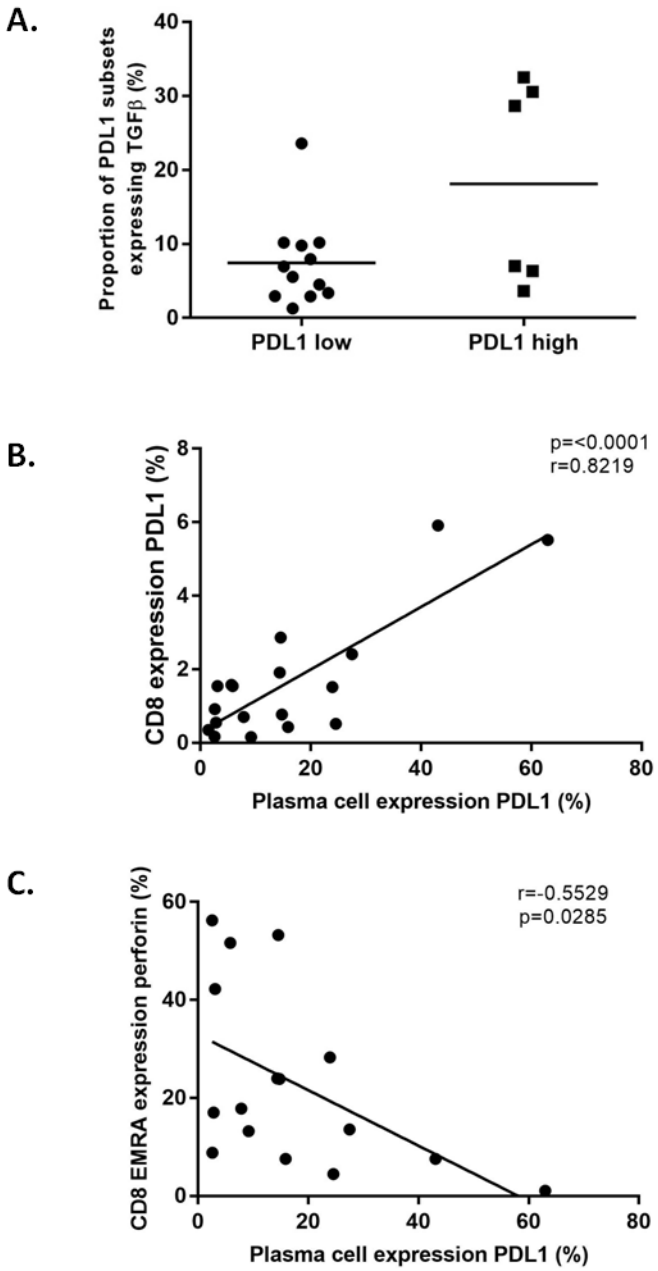

Figure 8.7: High plasma cell PDL1 expression is associated with decreased CD8 subset cytotoxicity

[A] An increase in TGFβ expression is seen in those with PDL1 expression above the mean
[B] A positive correlation was seen between plasma cell PDL1 expression and CD8 PDL1 expression
[C] A negative correlation was seen between plasma cell PDL1 expression and CD8 EMRA perforin was also seen

8.5 Summary of results

1. The non malignant B cell compartment is less proliferative in NDMM and expresses higher levels of IL2
2. NDMM plasma cell populations as detected by mass cytometry vary widely in size between individuals
3. Plasma cell populations in NDMM express PDL1, LAG3 and 2B4 and produce TGFβ
4. High plasma cell TGFβ expression is associated with co-expression of immune checkpoint ligands and decreased CD8 subset cytotoxicity

8.6 Discussion

Flow cytometry has traditionally relied on a set of sequential gates to identify plasma cells, based on strong expression of CD38 and CD138. Previous reports have suggested that this risks missing important malignant populations due to variation in plasma cell phenotype both between and within individuals [154]. I have shown that viSNE can be utilised to successfully identify plasma cell populations with diverse characteristics and distinguish them from healthy B cell populations. This technique is not dependent on a single phenotype and is successful despite loss of CD138 expression in these samples.

Deep characterisation of malignant plasma cells has several possible benefits; firstly it may identify new therapeutic targets and broaden our understanding of malignant plasma cell biology, secondly it may identify markers which predict response to treatment and finally it may allow the analysis and tracking of subclonal evolution. The data presented here has shown the both LAG3 and 2B4 are present on malignant plasma cells, this has not previously been reported in humans. It has also shown that plasma cells produce both TGFβ and TNFα which may drive plasma cell proliferation and suppress the anti-tumour response.

The loss of proliferation by non-myeloma B cells demonstrates that normal B cell function is inhibited by the presence of malignant plasma cell. IL2 producing B cell have been reported previously but their significance is unknown. Much of the work surrounding the immune microenvironment in myeloma has focused on cytotoxic cell populations. This data suggest that functional aberrations are also present within non-myeloma B cell populations. This may be contributing to the known increase in infection related mortality seen in myeloma patients, but may also be skewing the T cell response towards a potentially less anti-tumour response. This subset is therefore worthy of further future investigation.

This data demonstrates the key strengths of mass cytometry. Firstly is allows the exploration of the expression of markers beyond the subsets with which they are usually associated, thereby

providing new biological insights into disease mechanisms. Secondly the assessment of multiple cell types simultaneously allows the identification of patterns of response within individuals which may be of biological or prognostic significance when it comes to optimising treatment strategies. While the small numbers of patients examined in this work limits the power of this cross subset data analysis, it does provide evidence that mass cytometry is an appropriate tool to enable this approach which should be considered in future clinical trials.

8.7 Relevance of work

1. Demonstrates that viSNE can be used to identify plasma cells even when traditional gating has failed
2. Identified LAG3 and 2B4 expression on malignant plasma cells
3. Demonstrates the potential role of mass cytometry for deep profiling of immunological populations in therapeutic studies

9. Identifying a global bone marrow signature of multiple myeloma

9.1 Myeloma and global signatures of disease

Myeloma is a disease which, while originating within the plasma cell compartment, also involves the bone marrow microenvironment. This includes the supportive cellular network, the cells of bone remodelling and haematopoietic cells.

The recruitment of so many supportive cells into the disease pathogenesis may lead to a global, immunological, signature which is characteristic for the disease and distinguishes it from non myeloma bone marrow. As well as offering potential diagnostic techniques, the presence of such a signature may provide insights into the dominant drivers of the immunological aspects of the disease.

Ludwig et al have previously demonstrated a metabolomic signature that separates myeloma and MGUS from control bone marrow samples. This was characterised by loss of the essential amino acids isoleucine and threonine and their breakdown products in the disease setting, accompanied by a rise in urea and creatine and the presence of an oxidative environment [209]. Ludwig proposes that the progression from MGUS to myeloma is determined by cells from the microenvironment rather than intrinsic plasma cells changes and that these microenvironment changes also drive the metabolomic landscape.

Peripheral blood cytokine arrays have also demonstrated global aberrant microenvironments changes in MGUS and MM with Zheng et al describing increases in IL-4 and IL-10 accompanied by a fall in IFNγ in myeloma compared to age and sex matched controls [63]. Interestingly these cytokine aberrations did not return to normal after treatment, suggesting a sustained pro-tumour environment causing susceptibility to relapse.

9.2 Aim

To use mass cytometry data across all live cells to determine whether a global immunological cellular signature of multiple myeloma is present.

To determine whether an immunological signature correlates with clinical disease progression and survival

9.3 Specific methodology

9.3.1 CIRTUS algorithm

Chapters five to eight describe the phenotyping and functional changes seen when mass cytometry data was analysed according to traditional Boolean dot-plots. In order to identify

novel populations and confirm manually identified changes, an algorithmic approach was undertaken.

The CITRUS (Cluster Identification, Characterisation and Regression) algorithm is an unsupervised clustering approach which was designed to identify cell populations which are associated with a specific endpoint.

CITRUS was applied to the live cell gate of all control and NDMM samples. The selected endpoint was disease status (Control versus NDMM). The algorithm was set to determine clustering on the basis of marker abundance and all lineage and functional markers were included. An equal number of events were sampled from each individual. The false discovery rate was set to 5%. CIRTUS applied the correlative Significance Analysis of Microarrays (SAM) model to determine which populations were associated with a given endpoint.

The CIRTUS algorithm was run three times in parallel on the same data set to confirm findings were reproducible (Figure 9.1).

The output of CITRUS is a clustered map of cell populations with each cell population "node" being numbered to allow cross referencing with abundance and phenotype data. Each node represents a daughter of the proceeding node. A unique .fcs file is generated for each node on a per sample basis and can be exported to enable further interrogation and statistical analysis.

Statistical analysis was performed using non-parametric testing with Mann-Whitney for non-paired samples and Wilcoxon for paired samples.

It must be remembered when interpreting CITRUS plots that the data represents only the down sampled cells from each population and that peripheral CITRUS nodes may represent only a small number of cell events.

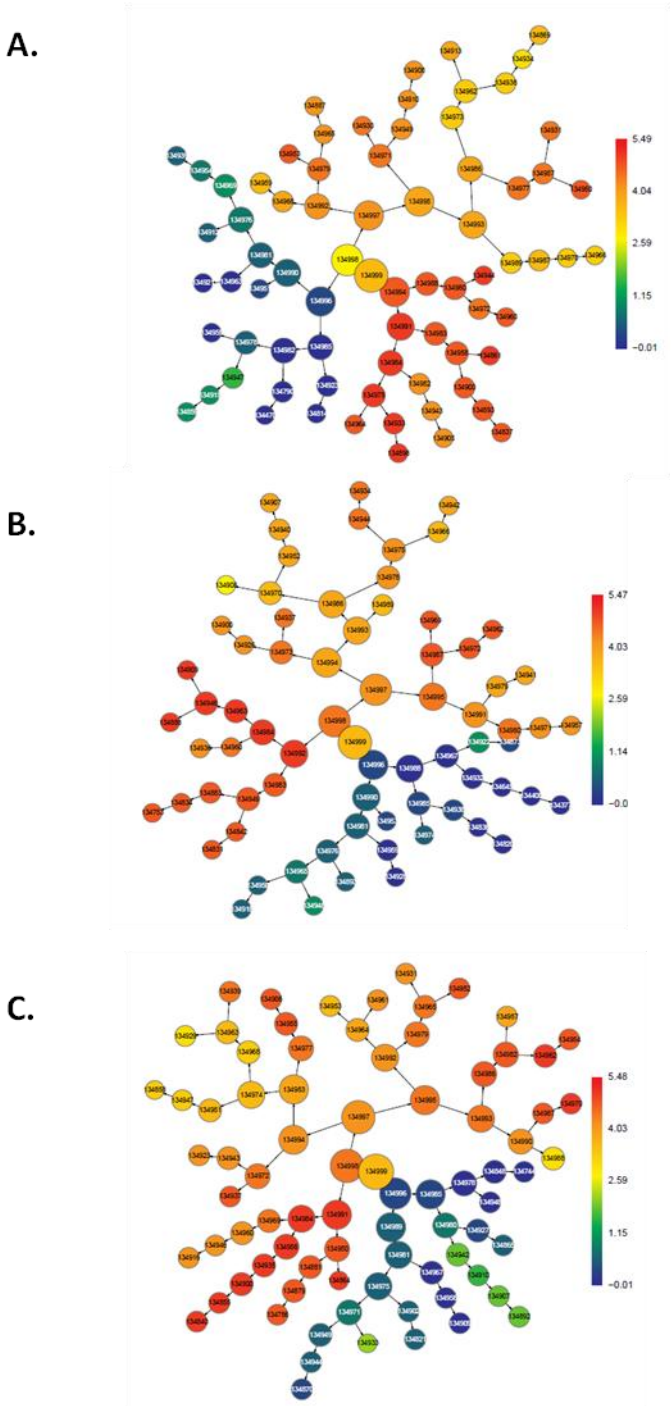

Figure 9.1: The CIRTUS algorithm was run three times in parallel on the same data set to confirm findings were reproducible

The output of CITRUS is a clustered map of cell populations with each cell population "node" being numbered to allow cross referencing with abundance and phenotype data . While the maps generated by each run are not identical, the same populations can be identified.
[A] CITRUS run 1
[B] CITRUS run 2
[C] CITRUS run 3

9.4 Results

9.4.1 Identification of cell populations

Using the CIRTUS map and marker expression data it was possible to identify seven distinct cell populations which were present in all three iterations of the CITRUS analysis. These could be further divided into sub-populations with unique phenotypic or functional characteristics (Table 9.1).

Cell type	**Phenotype for CITRUS identification**
B lymphocytes	CD19+CD20+OX40+TGFb+CD45RA+
CD 4 T lymphocytes	CD45+CD3+CD4+
NK cells	CD45+CD3-CD16+CD56+
Plasma cells	CD45-CD3-CD56+CD38+CD138+PDL1+FOXP3+TGFb+
Dendritic cells	HLADR+TGFb+
Population 1 (DC^{TOL})	PDL1+Ki67+
Population 2 (DC^{16})	CD16+PDL1+LAG3+TIM3+CCR7+2B4+DNAM1+
CD8 T lymphocytes	CD45+CD3+CD8+
Population 1 (Cytotoxic)	Granzyme+Perforin+DNAM1+
Population 2 (Cytokine)	IL2+NKG2D+

Table 9.1: Phenotypes of populations identified by CITRUS

The core populations identified were; B lymphocytes, CD4 T cells, two distinct CD8 T cell populations, plasma cells, NK cells and dendritic cells (DCs)(Figure 9.2).

Of the cellular populations identified, CIRTUS highlighted five populations or subpopulations which had a significant difference in population abundance between control and NDMM samples. These were plasma cells, two DC populations, a CD4 subpopulation and a CD8 subpopulation (Figure 9.3).

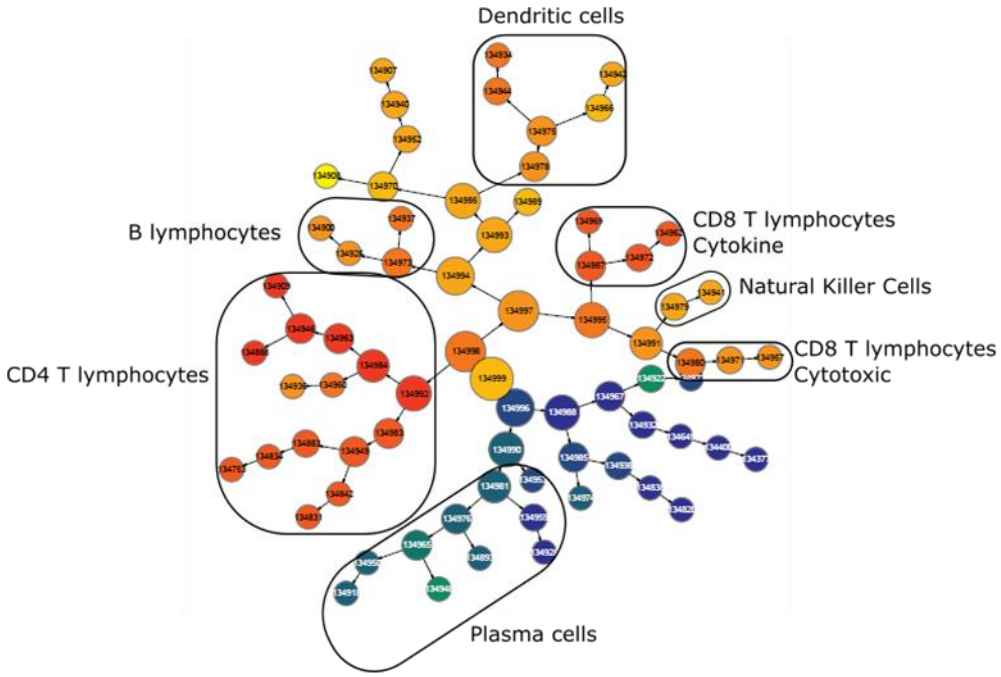

Figure 9.2: Populations identified by CITRUS analysis

Using the CIRTUS map and marker expression data it was possible to identify seven distinct cell populations which were present in all three iterations of the CITRUS analysis. The core populations identified were; B lymphocytes, CD4 T cells, two distinct CD8 T cell populations, plasma cells, NK cells and dendritic cells (DCs).

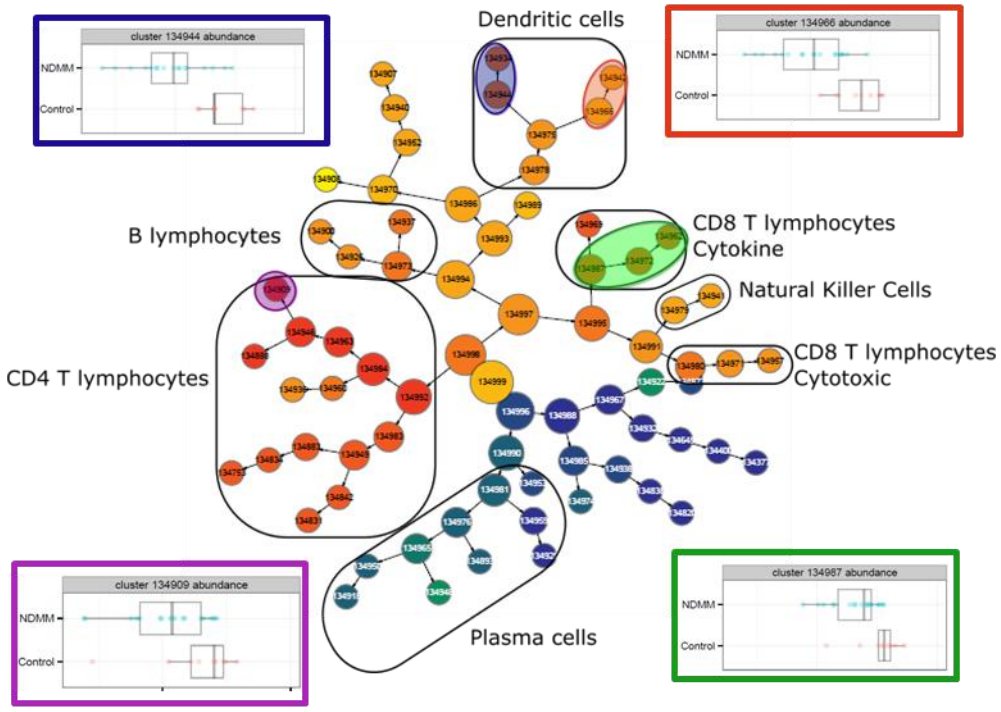

Figure 9.3: Nodes identified by CITRUS with significant abundance difference between control and NDMM

Significant differences in population abundance between control and NDMM were seen in plasma cells, two DC populations [blue and orange], a CD4 subpopulation [purple] and a CD8 subpopulation [green].

9.4.2 Dendritic cell populations are lost in NDMM and a shift towards tolerogenic activity is seen (Figure 9.4)

The ability to identify dendritic cells is of particular note since the mass cytometry panel was not designed with this cell population in mind. While specific DC markers were not included in the panel, it was possible to infer the DC cell population on the basis of exclusion of other cell types and the expression of cell surface receptors associated with DCs. Strong HLA-DR expression by CD45+ cells which did not express B cell markers or CD3 was considered consistent with a DC phenotype. Furthermore this population co-expressed a range of markers found on DCs including PDL1 and TIM3.

Within the DC cell cluster two distinct populations could be identified. The first was strongly CD16 positive and co-expressed a range of markers associated with DC maturity and activation including CCR7, TIM3 and 2B4. CD16 expression on DCs is described on monocyte derived DCs [210]. This mature, active population is termed DC[16]. The second population with strongly PDL1 positive and also expressed Ki67 suggesting that it is a proliferative population.

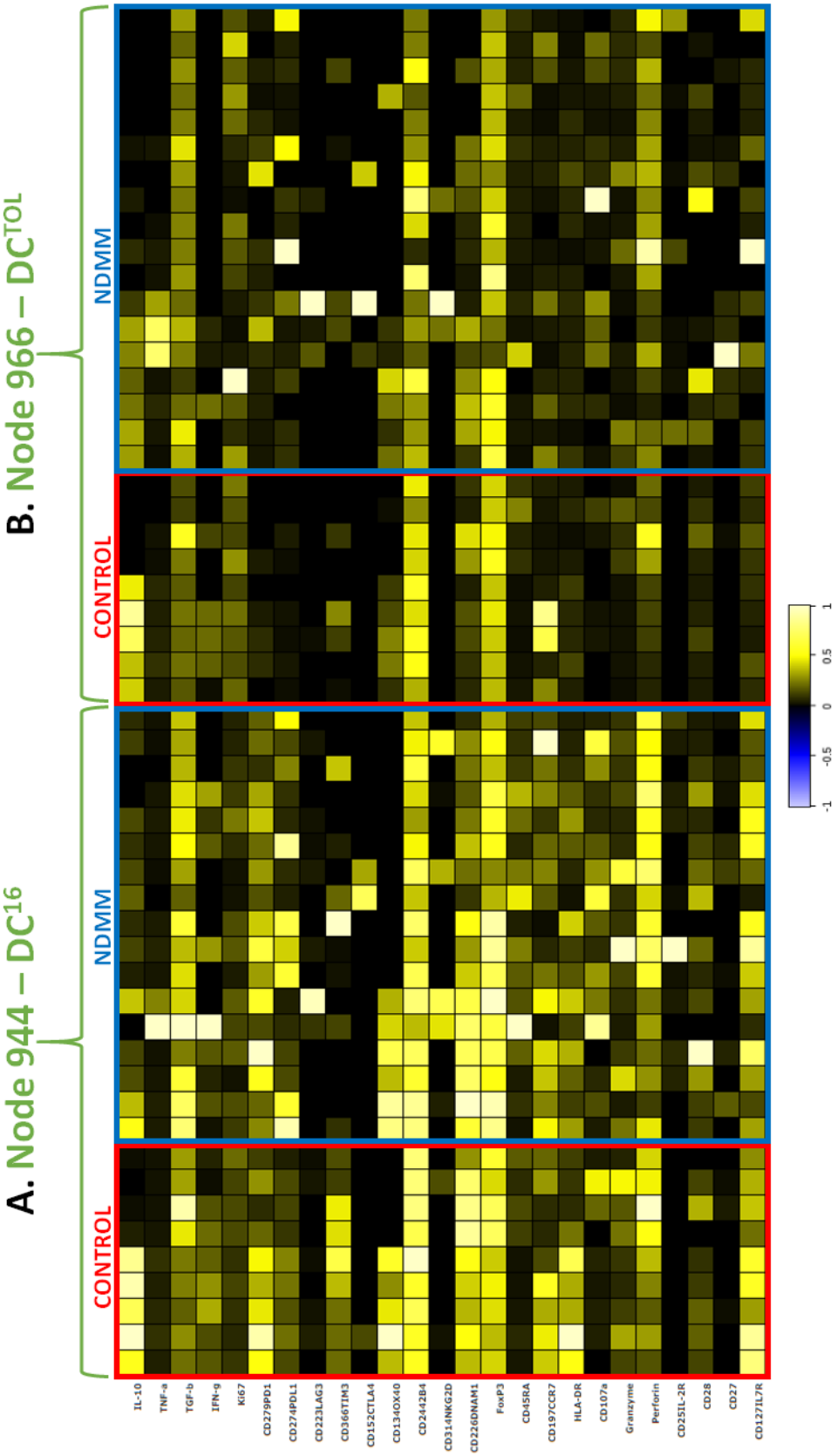
A. Node 944 – DC16
B. Node 966 – DCTOL
CONTROL
NDMM
CONTROL
NDMM
IL-10
TNF-a
TGF-b
IFN-g
Ki67
CD279PD1
CD274PDL1
CD223LAG3
CD366TIM3
CD152CTLA4
CD134OX40
CD2442B4
CD314NKG2D
CD226DNAM1
FoxP3
CD45RA
CD197CCR7
HLA-DR
CD107a
Granzyme
Perforin
CD25IL-2R
CD28
CD27
CD127IL7R
1
0.5
0
-0.5
-1

Figure 9.4 Two distinct dendritic cell populations are identified by CITRUS which are less abundant in NDMM

[A] DC^{16} population expresses CCR7, TIM3 and 2B4. In NDMM the expression of TIM3, and 2B4 is reduced with an increase in PDL1 expression
[B] DC^{TOL} population is strongly PDL1 positive. In NDMM there is loss of DNAM1, TIM3 and gain of PDL1, CD107a and perforin.

In addition to identifying distinct populations within the DC population is was also possible to identify differences in DC phenotype and function between control and NDMM samples. The DC^{16} population was less abundant in NDMM compared to control samples. In NDMM this population also had lower expression of TIM3 (control 5.128, NDMM 2.656 p=0.0122) and 2B4 (control 15.54, NDMM 12.17 p=0.0148) which are expressed by activated DCs. Furthermore an increase in DC^{16} expression of PDL1 (control 7.739, NDMM 17.93 p=0.0349) was seen in NDMM. This suggests that, while overall this is an activated DC population, it is less strongly activated in NDMM and may therefore be less effective at antigen presentation.

The second DC population was also less abundant in myeloma and loss of both TIM3 (control 2.494, NDMM 0.6665 p=0.0165) and DNAM1 (control 4.866, NDMM 3.06 p=0.0165) was seen in the disease state. This was associated with a gain of PDL1 (control 1.732, NDMM 5.357 p=0.0065), CD107a (control 1.616, NDMM 3.696 p=0.0014) and perforin (control 3.857, NDMM 9.554 p=0.0196) expression in NDMM. Perforin expression has been described in a subset of tolerogenic DCs which maintain peripheral tolerance via the deletion of T lymphocytes [211]. The expression of perforin and PDL1 in the absence of strong expression of other markers of DC activation suggest that, in NDMM, this subset has a tolerogenic role and it has therefore been termed DC^{TOL}.

9.4.3 CD8 lymphocytes have distinct cytotoxic and cytokine producing populations with shifts towards a pro-tumour cytokine environment (Figure 9.5)

CIRTUS reproducibly identifies two distinct CD8 positive populations. One of these populations has a cytotoxic effector phenotype ($CD8^{TOX}$) with strong expression of granzyme ($CD8^{TOX}$ 343,7, $CD8^{CYK}$ 44.28, p=<0.0001) and perforin ($CD8^{TOX}$ 119.1, $CD8^{CYK}$ 16.06, p=<0.0001). Interestingly NK cell population cluster closely with this CD8 population, presumably due to their shared cytotoxic phenotype. The second and distinct CD8 population ($CD8^{CYK}$) also has an effector phenotype but is predominantly IL2 producing ($CD8^{TOX}$ 1.066, $CD8^{CYK}$ 1.293, p=0.0010).

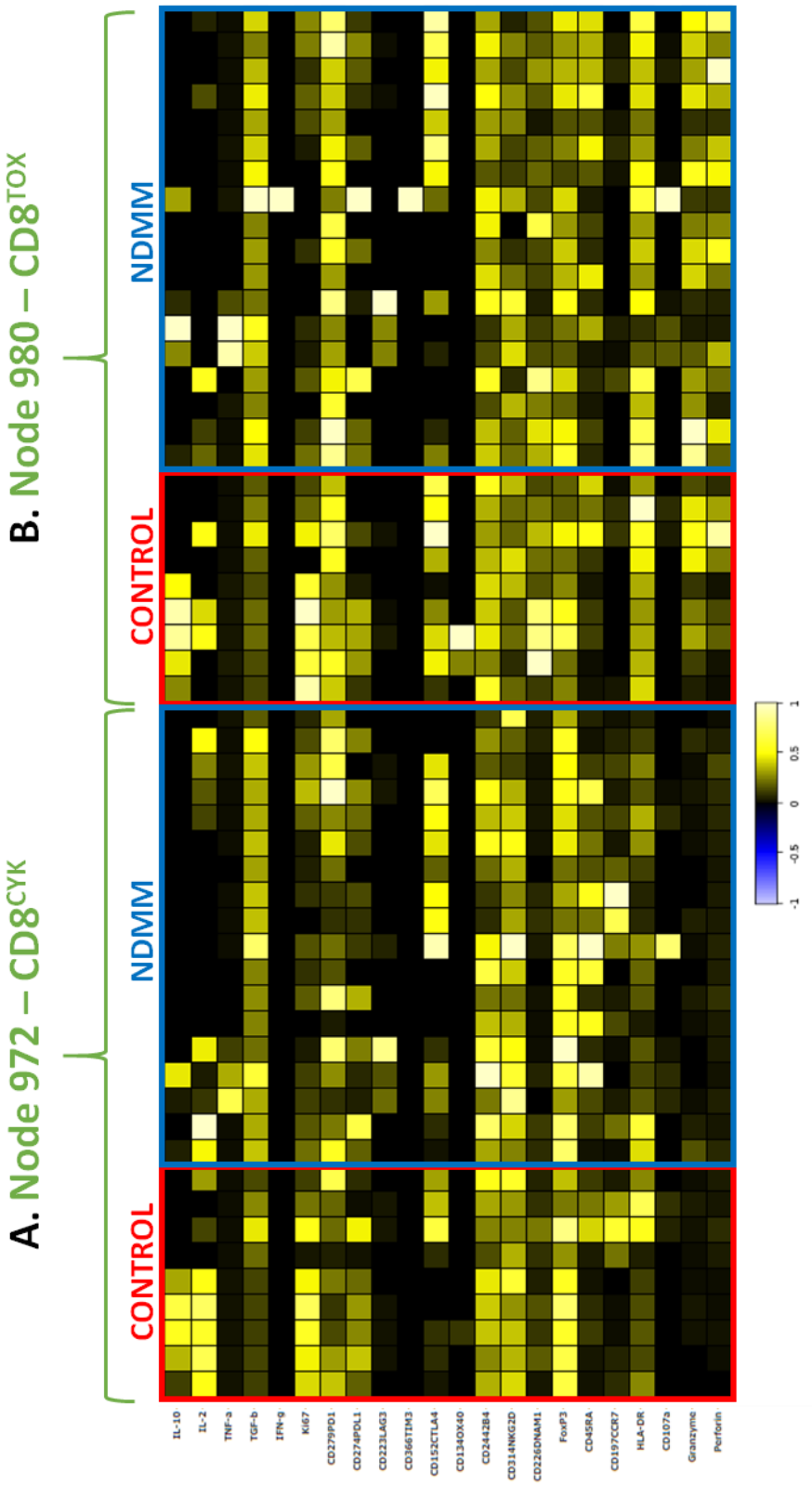

Figure 9.5: CD8 populations as identified by CITRUS

[A] $CD8^{CYK}$ population predominantly expresses IL2 and co-expresses NKG2D. In NDMM this population has lower expression of Ki67 and elevated TGFβ.
[B] $CD8^{TOX}$ population has strong expression of granzyme and perforin and co-expresses DNAM1. In NDMM there is increased expression of TGFb and loss of DNAM1.

A second interesting observation is that the cytotoxic CD8 population co-expresses DNAM1 ($CD8^{TOX}$ 6.559, $CD8^{CYK}$ 3.627, p=<0.0001) while the cytokine producing CD8 population co-expresses NKG2D ($CD8^{TOX}$ 8.968, $CD8^{CYK}$ 14.64, p=<0.0001), suggesting that these co-stimulatory receptors may have a differential response with one promoting a cytokine producing phenotype while the other promotes a cytotoxic response. This has implications for the use of therapeutic agents that target these receptors as it may be possible to modify the CD8 response depending on which co-receptor is targeted.

The CD8 cytokine population is less abundant in NDMM compared to controls. This appears to be due to loss of proliferation as evidences by a fall in Ki67 (control 6.125, NDMM 3.525 p=0.0494) expression in NDMM. This population has an EM/EMRA phenotype as defined by expression of CD45RA and CCR7. In NDMM there is also a shift towards a pro-tumour cytokine prolife with elevated expression of TGFβ (control 9.573, NDMM 20.47 p=0.0022). Although this cell population predominantly expressed NKG2D, expression of DNAM1 is also seen, however this is reduced in NDMM compared to controls (control 5.452, NDMM 2,856 p=0.0096), suggesting a reduction of co-stimulatory potential.

No abundance difference is seen between control and NDMM for the CD8 cytotoxic population. In a similar pattern to the cytokine producing node, an increase in TGFβ (control median 11.63, NDMM 19.29 p=0.0096) and a decrease in DNAM1 (control 9.21, NDMM 5.625 p=0.0080) is seen in NDMM. No difference in granzyme or perforin production is seen between control and NDMM samples. A modest rise in CD107a is seen in NDMM (control 1.061, NDMM 2.687 p=0.0369), the standard deviation, however, is broad (SD NDMM 8.562).

This CITRUS analysis has grouped CD8 lymphocytes primarily according to their functional behaviour while traditional Boolean gating divides them by stage of maturation. Traditional gating did not identify differences in DNAM1 and NKG2D expression between cytotoxic and cytokine producing CD8 populations since it did not classify cells in this way. The pattern of granzyme, perforin and CD107a expression observed in cytotoxic cells identified by CITRUS is very similar to that identified by traditional gating. CITRUS appears to be better at identifying shifts in cytokine producing populations, this is probably because it is able to simultaneously assess the role of multiple cytokines when determining clusters. It was challenging to assess multiple cytokine producing populations using traditional gating techniques which are very dependent on user defined gating and also suffers from reducing population sizes each time a sequential gate is applied.

9.4.4 CD4 lymphocytes with distinct memory and effector phenotype can be identified, with a shift towards a regulatory phenotype (Figure 9.6 and 9.7)

The total CD4 population could be further divided into two distinct populations. The first had a memory phenotype with strong expression of CCR7 ($CD4^{MEM}$ 127.9, $CD4^{EFF}$ 19.23 p=0.0039) while the second had low expression of CCR7 and moderate expression of CD45RA ($CD4^{MEM}$ 5.256, $CD4^{EFF}$ 9.455 p=0.0078) consistent with an effector phenotype. Interestingly the $CD4^{MEM}$ population had stronger expression of a range of cell surface receptors including PDL1 ($CD4^{MEM}$ 19.61, $CD4^{EFF}$ 6.486 p=0.0039), LAG3 ($CD4^{MEM}$ 4.334, $CD4^{EFF}$ 2.754 p=0.0273), TIM3 ($CD4^{MEM}$ 105.9, $CD4^{EFF}$ 39.46 p=0.0039), 2B4 ($CD4^{MEM}$ 3.551, $CD4^{EFF}$ 2.09 p0.0039), DNAM1 ($CD4^{MEM}$ 17.1, $CD4^{EFF}$ 3.995 p0.0039) and PD1 ($CD4^{MEM}$ 63.08, $CD4^{EFF}$ 8.539 p0.0039), while the $CD4^{EFF}$ population had stronger expression of HLA-DR ($CD4^{MEM}$ 38.66, $CD4^{EFF}$ 63.28 p0.0195) suggesting cellular activation, and OX40 ($CD4^{MEM}$ 55.82, $CD4^{EFF}$ 65.57 p0.0039).

When considering differences between control and NDMM, the $CD4^{MEM}$ populations had reduced intensity of expression of OX40 (control median 55.82, NDMM 40.94 p0.0317) and PD1 (control 63.08, NDMM 32.08 p0.0272) in NDMM, while the $CD4^{EFF}$ population had a modest decrease in PD1 (control 8.539, NDMM 6.073 p0.0096) expression in NDMM.

Within the CD4+ cell population an abundance difference was identified by CITRUS in single node with a CD4 effector phenotype. When this node was interrogated further, a loss of Ki67 (control 4.376, NDMM 2.44 p=0.0054) expression was seen in NDMM suggesting that the reduced abundance of this population was due to loss of proliferation. Cells in NDMM also had increased expression of FoxP3 (control 6.041, NDMM 8.436 p=0.0409) and TGFβ (control 6.525, NDMM 12.72 p=0.0027) indicating that this population may have adopted a regulatory function in NDMM.

When compared to traditional gating techniques there does not appear to be an overlap in the changing marker expressions of the identified populations. Using Boolean gating identified loss of DNAM1 and increased TGFβ by CD4 memory subsets with increased PDL1 and TGFβ by CD4 effector subsets. The T regulatory subsets as identified by both techniques demonstrated increased TGFβ expression.

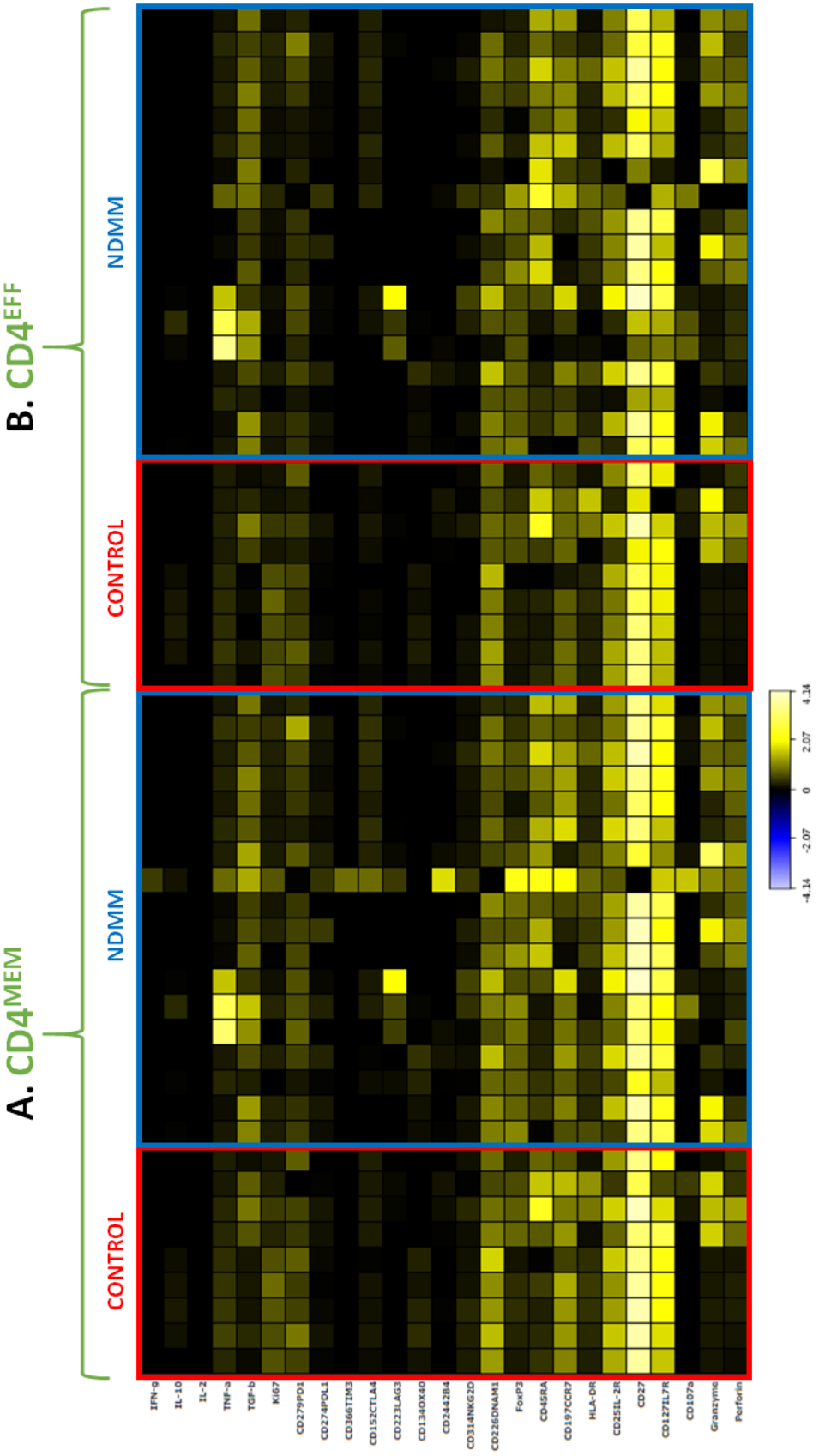
A. CD4MEM
B. CD4EFF
CONTROL
NDMM
CONTROL
NDMM
IFN-g
IL-10
IL-2
TNF-a
TGF-b
Ki67
CD279PD1
CD274PDL1
CD366TIM3
CD152CTLA4
CD223LAG3
CD134OX40
CD244 2B4
CD314NKG2D
CD226DNAM1
FoxP3
CD45RA
CD197CCR7
HLA-DR
CD25IL-2R
CD27
CD127IL7R
CD107a
Granzyme
Perforin
4.14
2.07
0
-2.07
-4.14

Figure 9.6: CD4 lymphocyte populations identified by CITRUS

[A] $CD4^{MEM}$ population has strong expression of CCR7 and also expresses PDL1, LAG3, TIM3, DNAM1 and PD1. In NDMM there is decreased expression of OX40 and PD1.
[B] $CD4^{EFF}$ population expresses CD45RA and also expresses HLA-DR and OX40. In NDMM there is a modest decrease in PD1.

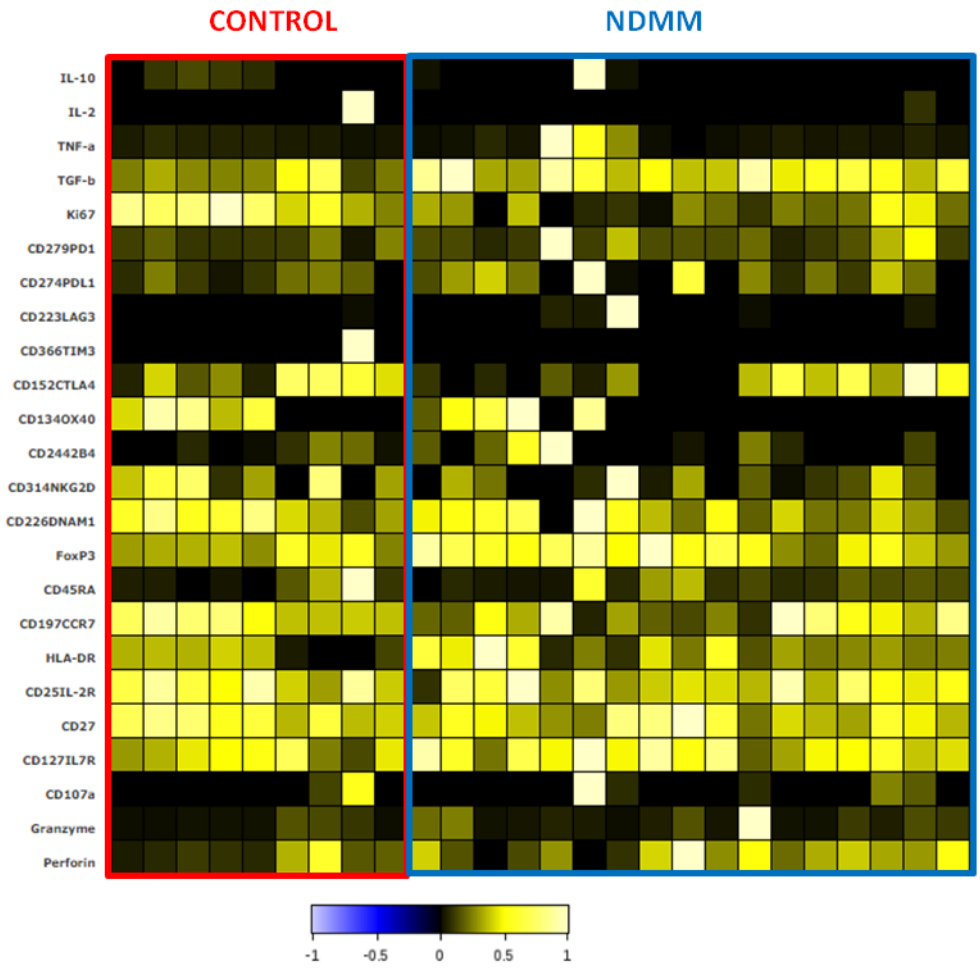

Figure 9.7: CD4 regulatory population

A CD4 effector node was identified which had an abundance difference between control and NDMM. A loss of Ki67 expression was seen in NDMM . Cells in NDMM also had increased expression of FoxP3 and TGFβ.

9.4.5 Natural killer cells have a cytotoxic phenotype and cluster closely to cytotoxic CD8 lymphocytes (Figure 9.8)

NK cells were clustered by CITRUS close to CD8 cytotoxic cells but could be distinguished from the CD8+ population by the absence of CD3 and the presence of CD16 and CD56 expression. No difference in population abundance was seen between control and NDMM.

When the expression of markers by the NK population was compared between control and NDMM, a rise in the NK activating receptor DNAM1 (control 168.7 NDMM 408.3 p=0.0494) was seen in NDMM. This was accompanied by a rise in granzyme (control 207 NDMM 759.2 p=0.0065) but not perforin (control 42.37 NDMM 9.694 p=0.1076) or CD107a (control 6.731, NDMM 4.029 p=0.4523).

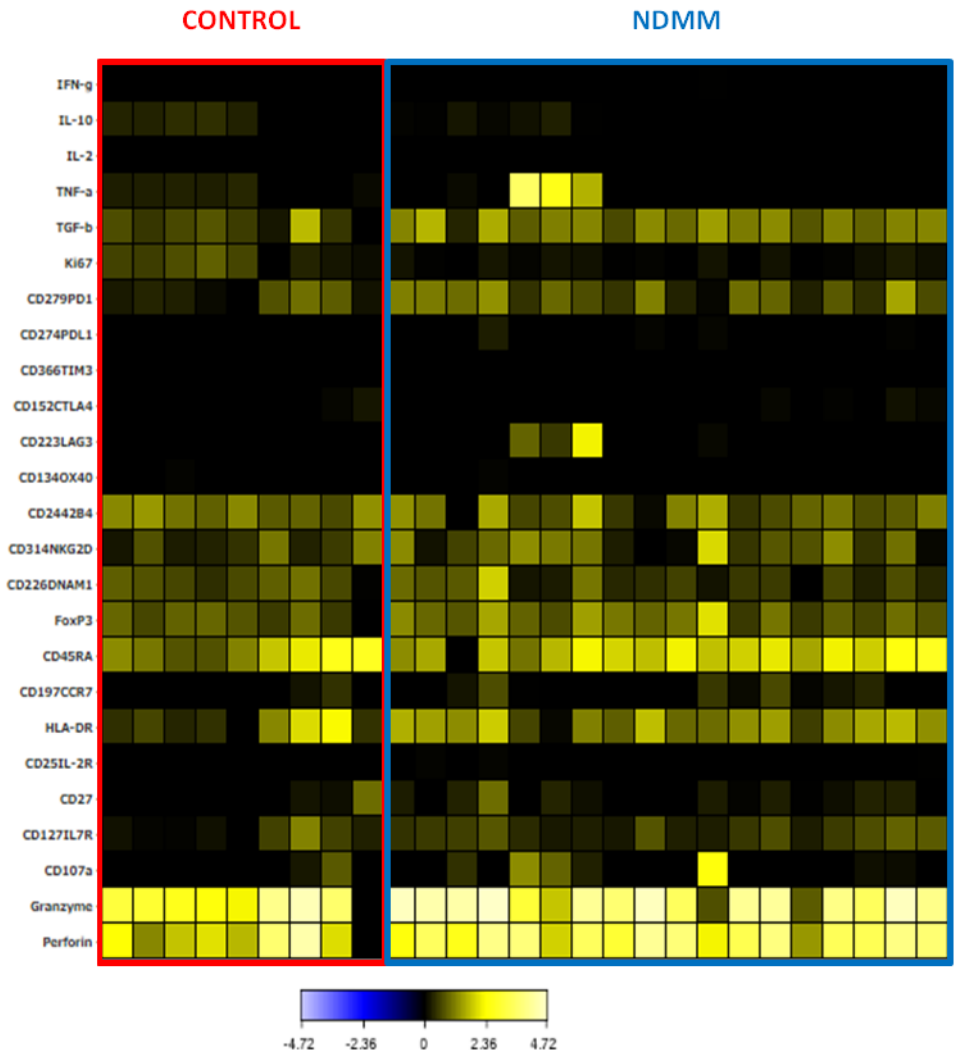

Figure 9.8: Natural killer cells have a cytotoxic phenotype

NK cells have a cytotoxic phenotype. In NDMM an increase in DNAM1 and granzyme but not perforin was seen.

The increased expression of granzyme echoes the intensity increase identified by traditional gating techniques. Since the CITRUS analysis clustered all NK cells into a single node and down-sampling reduces the number of events available for further analysis, it is not possible to explore the NK cell subsets. This is a limitation of clustering techniques when dealing with a large number of different cell types, some of which have large and numerous subpopulations.

9.4.6 B cells are seen in both control and NDMM and cluster in a distinct locations from plasma cells (Figure 9.9)

CD19 and CD20 B cells clustered in a distinct location, which is spatially separate from cells with a malignant plasma phenotype. There was no abundance difference between control and NDMM.

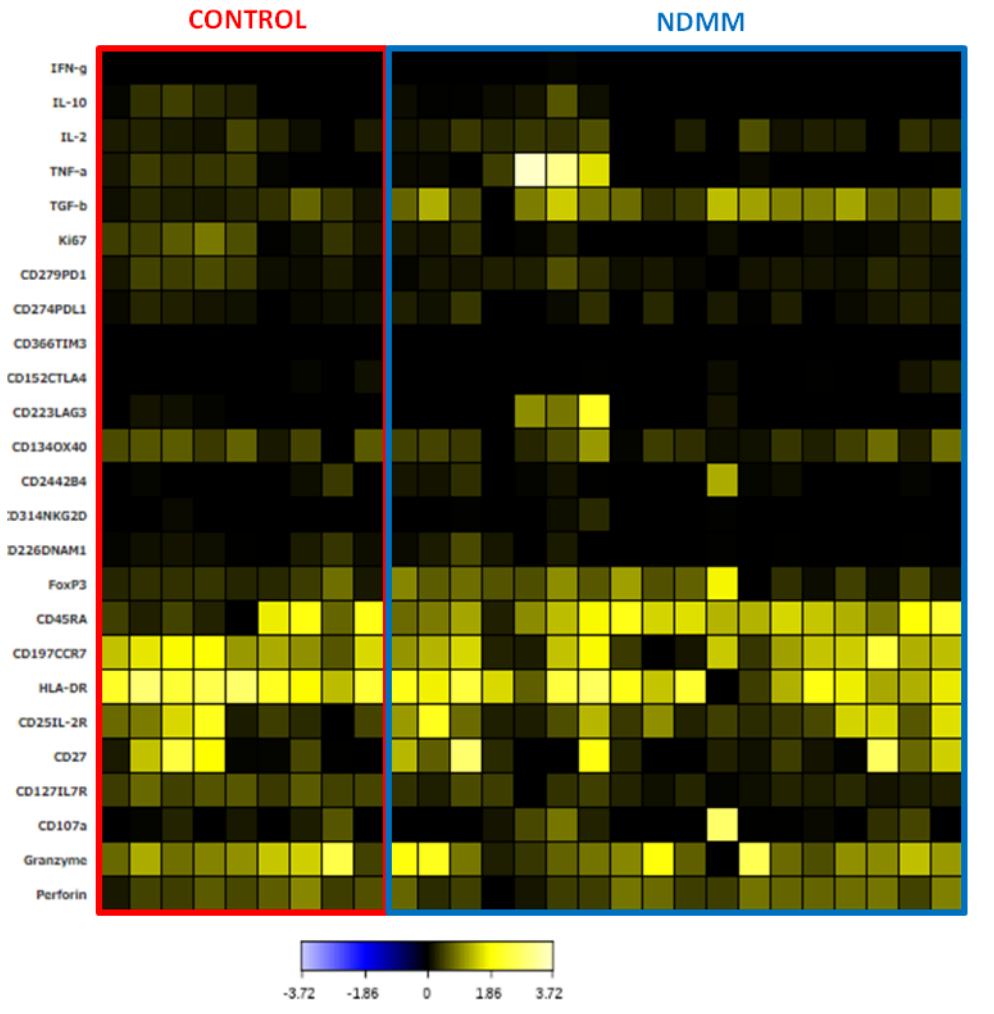

Figure 9.9: B cells populations

B cells were identified in a distinct location from plasma cells. A reduction in PD1 expression was seen in NDMM.

Surprisingly, B cells from individuals with NDMM had lower expression of PD1 (control 725.3 NDMM 407.2 p=0.0165).

When non-myeloma B cells were examined using viSNE and the Boolean gating differences in KI67 and IL2 expression were seen. This is not replicated in this CITRUS data.

9.4.7 Plasma cells from NDMM have a proliferative phenotype with expression of immune regulatory ligands and immune suppressive cytokines (Figure 9.10)

As expected, cells with a malignant plasma cell phenotype, characterised by CD45 negativity, CD38 and CD138 positivity and variable CD56 expression, were significantly less abundant in control samples compared to NDMM.

When malignant plasma cells from individuals with NDMM were compared to the healthy B cell compartment, plasma cells were found to have higher expression of IL10 (B cell 2.222, plasma 6.388 p=0.002) and IL2 (B cell 1.162, plasma 13.52 p=0.0006), PDL1 (B cell 1.933, plasma 3.751 p=0.0013), Ki67 (B cell 0.3075 plasma 9.456 p=<0.0001), CCR7 (B cell 87.06, plasma 1358 p=<0.0001), FoxP3 (B cell 1.815, plasma 5.965 p=<0.0001) and DNAM1 (B cell 7.038 plasma 13.58 p=0.0250) while healthy B cells had higher expression of TIM3 (B cell 48.64 plasma 10.01 p=0.0052) and PD1 (B cell 407.2 plasma 4.699 p=<0.0001). This suggests that the malignant plasma cell compartment has an immune regulatory role via PDL1, IL10 and IL2.

This pattern of proliferation with PDL1, IL2 and IL10 expression is similar to that seen when plasma cells are identified by viSNE gating. Interestingly the TGFβ signal is not seen when the CITRUS algorithm was employed but was strongly expressed by viSNE gating. This is likely to be because CITRUS identified differences between groups while viSNE and Boolean gating focuses on marker expression.

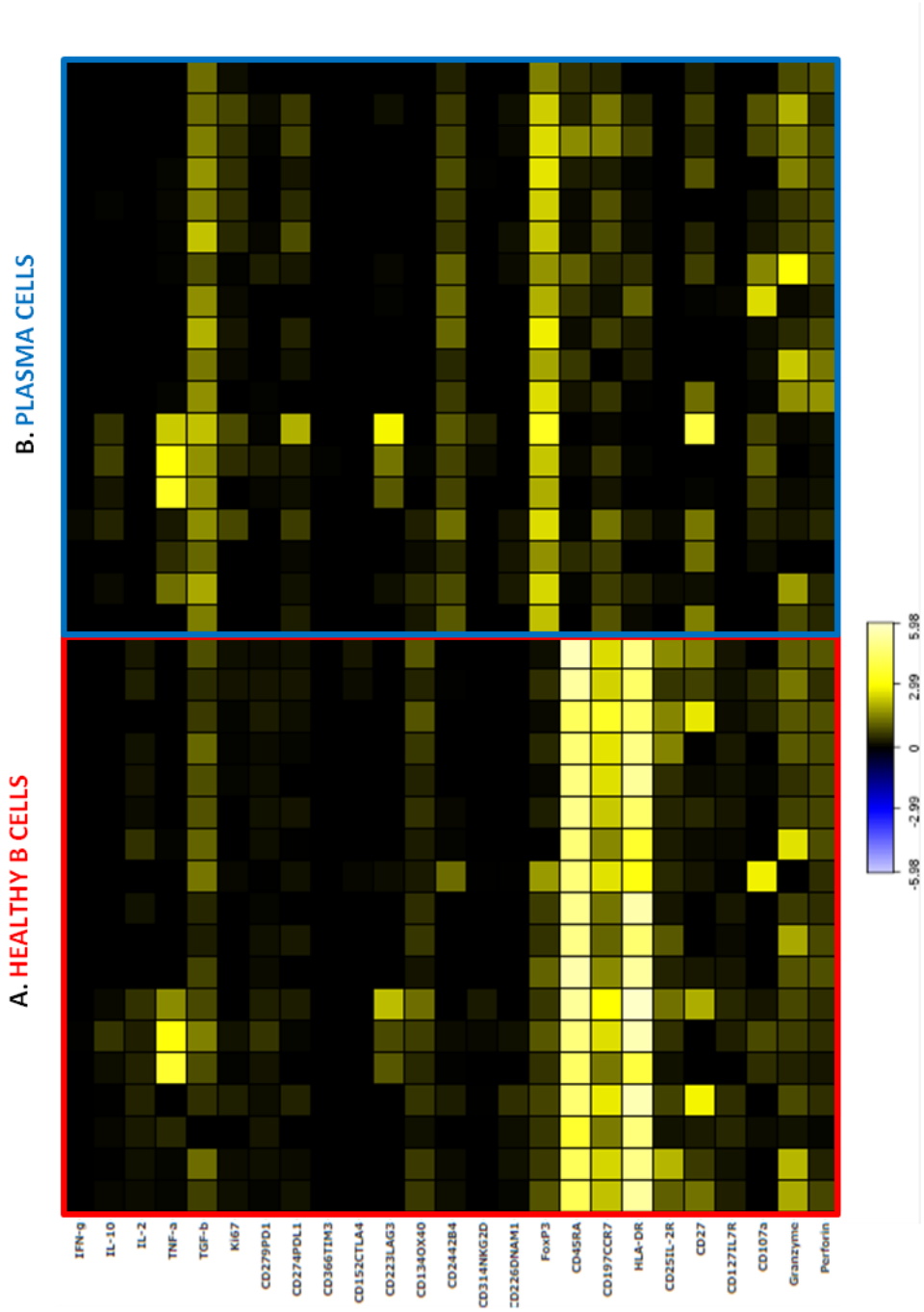

Figure 9.10: Plasma cells from NDMM have a proliferative phenotype with expression of immune regulatory ligands and immune suppressive cytokines when compared to healthy B cell populations

[A] Healthy B cell populations had increased expression of TIM3 and PD1
[B] Plasma cell populations had increased expression of IL10, IL2, PDL1 and Ki67

9.4.8 Immunological fingerprint in NDMM and links with immune surveillance model

Drawing these findings together suggests that an immunological fingerprint is present in NDMM bone marrow samples which distinguishes them from control bone marrow samples (Figure 9.11).

1. Loss of antigen presenting capacity with gain of activity of tolerogenic DCs
2. Loss of cytokine producing CD8 lymphocytes with a shift towards a pro-tumour cytokine profile
3. Loss of a CD4 effector subset with a shift towards a regulatory phenotype

This pattern of expression response is similar to that seen by traditional Boolean gating, with the added information provided by the ability to identify DC populations by CITRUS. It should be remembered however that CITRUS downsamples a small number of events per sample, meaning that some of the populations described contain very few events.

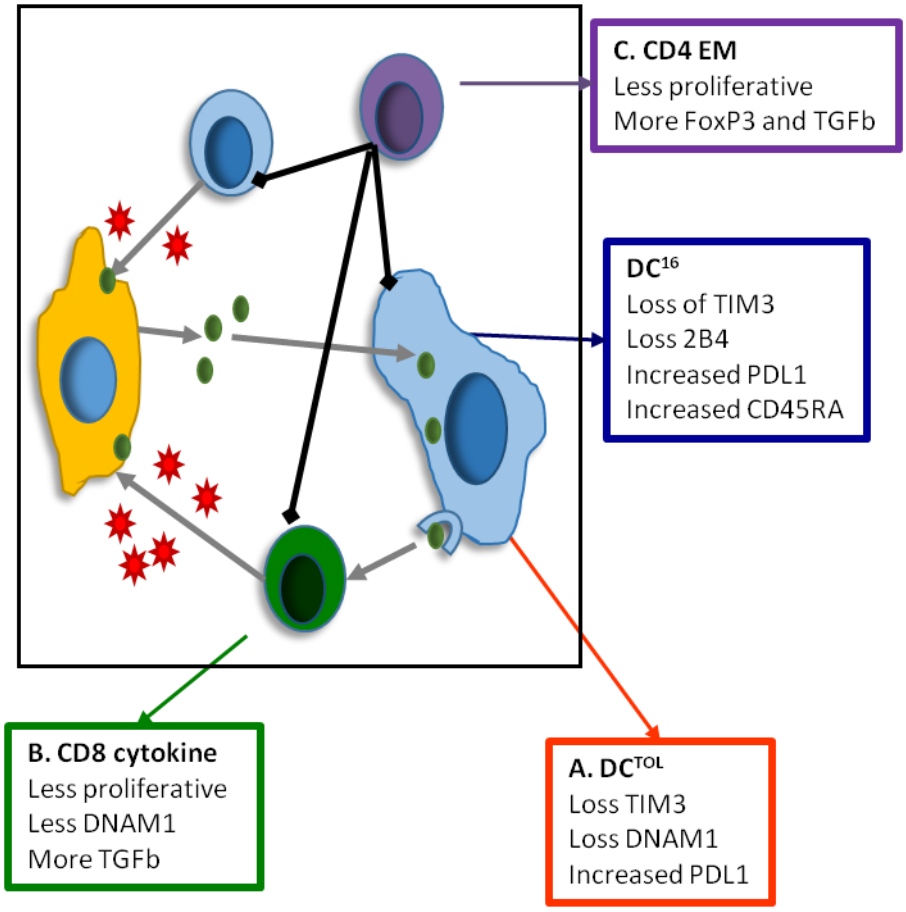

Figure 9.11: Immunological fingerprint in NDMM and links with immune surveillance model
[A] Loss of antigen presenting capacity with gain of activity of tolerogenic DCs
[B] Loss of cytokine producing CD8 lymphocytes with a shift towards a pro-tumour cytokine profile
[C] Loss of a CD4 effector subset with a shift towards a regulatory phenotype

9.4.9 Patterns of population expression and association with survival

I observed a broad range in abundance of key population is myeloma, with some individuals having cell population numbers close to those seen in control samples. This led me to examine whether there was a link between population abundance and ability to control the plasma cell clone. In order to determine whether the level of population abundance resulted in differences in clinical outcome I assessed population size in relation to overall survival duration as well as time to first relapse.

When cell populations with an abundance difference as identified by CITRUS, were considered individually, the size of the CD8 cytokine population positively correlated with duration of survival (p=0.0026, r=0.6643)(Figure 9.12 A). This correlation was not seen for the CD4 population or either DC group.

Next the combined impact of having a larger CD8 cytokine population and a larger DC16 population, considered to be the "active" anti-tumour populations, was assessed. Individuals who had both $CD8^{CYK}$ and DC16 numbers above the NDMM median had better overall survival (Log-rank p=0.0273)(Figure 9.12 B) and time to relapse or death (Log-rank p=0.0366)(Figure 9.12 C) in the first 36 month following diagnosis than those who had either one or neither population numbers above the median. Interestingly 75% (4/6) of those with DC16 and $CD8^{CYK}$ numbers above the median also had DC^{TOL} and CD4 numbers above the median, suggesting that the size of the residual non myeloma immune compartment may be driving this change rather than the cell types which make up the compartment.

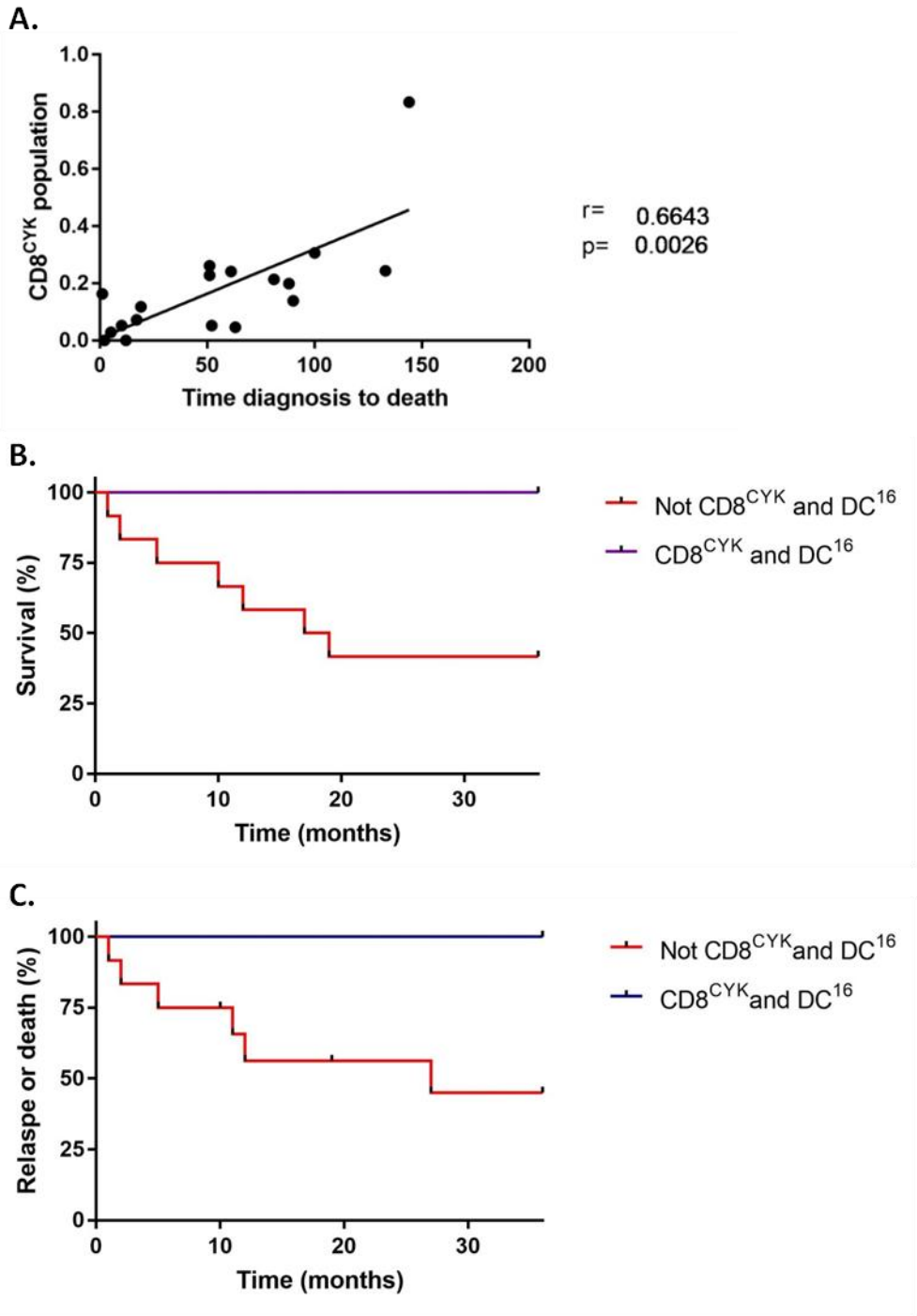

Figure 9.12: Patterns of population expression and association with survival

[A] The size of the $CD8^{CYK}$ population positively correlates with duration of survival

[B] Individuals with both $CD8^{CYK}$ and DC^{16} populations have the median have superior overall survival in the first 36 months following diagnosis

[C] Individuals with both $CD8^{CYK}$ and DC^{16} populations have the median have superior time to relapse or death in the first 36 months following diagnosis

9.5 Summary of results

1. Dendritic cell populations are lost in NDMM and a shift towards tolerogenic activity is seen
2. CD8 lymphocytes have distinct cytotoxic and cytokine producing populations with shifts towards a pro-tumour cytokine environment
3. Differential expression of DNAM1 (cytotoxic) and NKG2D (cytokine) is seen on CD8 subsets
4. CD4 lymphocytes with distinct memory and effector phenotype can be identified with a shift towards a regulatory phenotype
5. Natural killer cells have a cytotoxic phenotype and cluster closely to cytotoxic CD8 lymphocytes
6. Plasma cells from NDMM have a proliferative phenotype with expression of immune regulatory ligands and immune suppressive cytokines
7. Having a larger active anti-tumour immune environment is associated with improved survival and reduced relapse rate.

9.6 Discussion

Using the CITRUS algorithm it is possible to identify a cellular immune signature of NDMM which is characterised by loss of antigen presenting capacity, numerical and functional disturbances in CD8 and CD4 effector populations and a shift towards tolerogenic DC activity.

These multi-cellular changes are expected to have an impact on priming, recruitment and activation of tumour specific lymphocytes and consequently limit direct cellular cytotoxicity toward the malignant clone. This is in keeping with the immunesurveillance model of malignancy and helps to give a global overview of the impact that the presence of malignant plasma cells has on the immune system. It is important to know that these changes are already established at the time point of myeloma diagnosis. This is consistent with previously described metabolomic and genetic profiling of myeloma which also report that these changes are present in both myeloma and MGUS.

The fact that individuals with higher numbers of active anti-tumour immune populations have superior overall and relapse free survival is an important indicator that loss of immunesurveillance has a key role to play in the progression of myeloma and may also influence response to therapy

There are important implications for therapy arising from these findings. Firstly, it may be possible to selectively target and correct these defective immunesurveillance mechanisms at

this early disease state in order to restore immunological control or eradication of the malignant clone and prevent end organ damage. Secondly, established therapies may be effectively suppressing malignant plasma cell growth but failing to restore immune surveillance thereby creating an environment which is primed for relapse. This suggests a role for combined modality therapy targeting both the malignant cell and repairing immunological defects. A number of agents already in use in the treatment of myeloma act via their effects on the immune microenvironment in addition to direct cytotoxic activity. This includes daratumumab and the IMiDs. The addition of checkpoint inhibitors to these existing treatment strategies is an attractive way to attempt to further influence the immune microenvironment in order to control myeloma progression. The role of combined therapies will be discussed further in chapter ten.

9.7 Relevance of work

1. Establishes the presence of a distinct immunological fingerprint in NDMM
2. Identifies immunological features predictive of improved survival

10. Targeting immune checkpoint regulators in relapsed refractory myeloma

10.1 Acknowledgements

The work described in this section was performed as a collaboration between our group at Barts Cancer Institute and Celgene Corporation. Celgene provided access to cryopreserved clinical samples and provided grant support funding for the work performed at BCI.

I designed the mass cytometry panel, performed the optimisation work and performed mass cytometry on the clinical samples. The CITRUS algorithm was run by Mary Young of Celgene. I then performed data interpretation and further data analysis.

10.2 Durvalumab and daratumumab to target the immunological microenvironment in RRMM

As has been established in previous chapters, there is defect in T cell and NK cell function in newly diagnosed multiple myeloma with abnormalities in expression of ligands and receptors in the PD1 axis being particularly marked. This has profound implications for the management of the disease, both in optimising plasma cell clearance and restoring immune surveillance mechanisms.

PD1 and its ligands are known to be expressed across multiple cell populations in myeloma (see chapters 1 and 4-9) and blockade of the PD1 axis has shown clinical efficacy in other tumour types, making this a viable target in myeloma. Single agent activity in myeloma however has been disappointing, whereas combination strategies incorporating IMiDs have demonstrated anti-tumour activity [212]. This provided the rationale for further combination studies incorporating multiple monoclonal antibodies to target protein receptors, such as PDL1 and CD38.

Durvalumab (Astrazeneca) is a human IgG1k monoclonal antibody which recognises PDL1, a ligand for PD1. It has been modified to reduce C1q, CD16, CD32A and CD64 binding [213]. This limits antibody dependent and complement dependent cytotoxicity and therefore maintains PDL1 expression on the cell membrane, permitting blockade of its interaction with PD1. PDL1 inhibitors have been FDA approved for use in advanced urothelial cancer and non-small cell lung cancer. To date there is minimal published data on the use of PDL1 inhibitors in myeloma, however clinical trials in a range of haematological malignancies are on-going.

Daratumumab (Janssen) is a human IgG1k monoclonal antibody which recognises CD38. CD38 is highly expressed on malignant plasma cell but is also expressed on a range of other haematopoetic cell types including erythroid lineages and NK cells [214]. Daratumumab is approved by the European Medicine Agency in the following settings:

1. In combination with bortezomib, melphalan and prednisone for the treatment of adult patients with newly diagnosed multiple myeloma who are ineligible for autologous stem cell transplant
2. As monotherapy for the treatment of adult patients with relapsed and refractory multiple myeloma, whose prior therapy included a proteasome inhibitor and an immunomodulatory agent and who have demonstrated disease progression on the last therapy
3. In combination with lenalidomide and dexamethasone, or bortezomib and dexamethasone, for the treatment of adult patients with multiple myeloma who have received at least one prior therapy.

Daratumumab has a diverse mechanism of action including ADCC, complement dependent cytotoxicity, and antibody dependant cellular phagocytosis [215](Figure 10.1). This induces rapid clearance of CD38 positive cells.

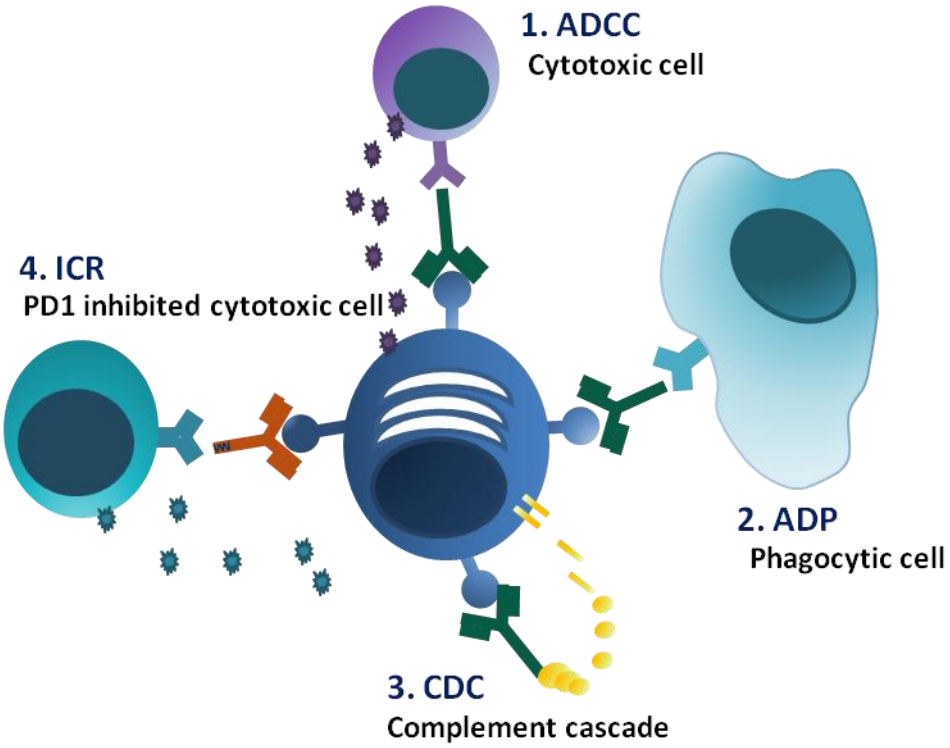

Figure 10.1: Mechnaismsof action of Daratumumab and Durvalumab

Daratumumab has multiple mechanisms of action including antibody dependant recruitment of cytotoxic cells (ADCC), phagocytic cells (ADP) and complement (CDC). Durvalumab has a modified FC domain which limits binding of complement and CD16. It functions by blocking the interaction of PDL1 with PD1 thereby preventing inhibitory signalling to cytotoxic cells (ICR).

Studying the bone marrow of patients who have received the drugs of interest in-vivo, rather than using in-vitro modelling systems, is a more clinically relevant approach to understanding the global immunological activities of these therapeutic agents. In-vitro models may miss

interactions between different immune cells which may influence patient outcome. For example blocking the PD1 axis may result in altered dendritic cells function which, in turn, impacts upon lymphocyte priming and activation. An in-vitro model studying the effect of the drugs on lymphocytes alone would not detect this response.

In-vivo drug assessment also allows us to attempt to determine which patient or disease factors are predictive of response to a certain drug combination as well as whether certain disease features exert a dominant or inhibitory effect over the therapeutic activities of the drugs.

10.3 Aim

To characterise changes in immune subsets following in-vivo treatment with anti-CD38 and anti-PDL1 monoclonal antibodies in patients with relapsed refractory myeloma.

10.4 Specific methodology

10.4.1 Clinical samples and study design

Bone marrow samples were obtained from patients enrolled on the Celgene MEDI4736-MM-003 clinical study (NCT02807454). This was an open label, Phase 2 multi centre, international clinical trial. Bone marrow samples were collected prior to starting treatment and at Cycle 2 Day 15. Daratumumab was administered weekly according to established dosing regimes. Durvalumab was administered once per cycle as established by previous clinical trials. (Figure 10.2) At the time of collection of the second bone marrow samples, patients had received two doses of Durvalumab and six doses of Daratumumab. This study was placed on hold following FDA concerns regarding the safety of PD1 blockade in the setting of myeloma after an excess of deaths was reported in a trial examining Pembrolizumab. This early trial closure limited the number of clinical samples available for analysis. The work was covered under existing ethics approval, as previously described.

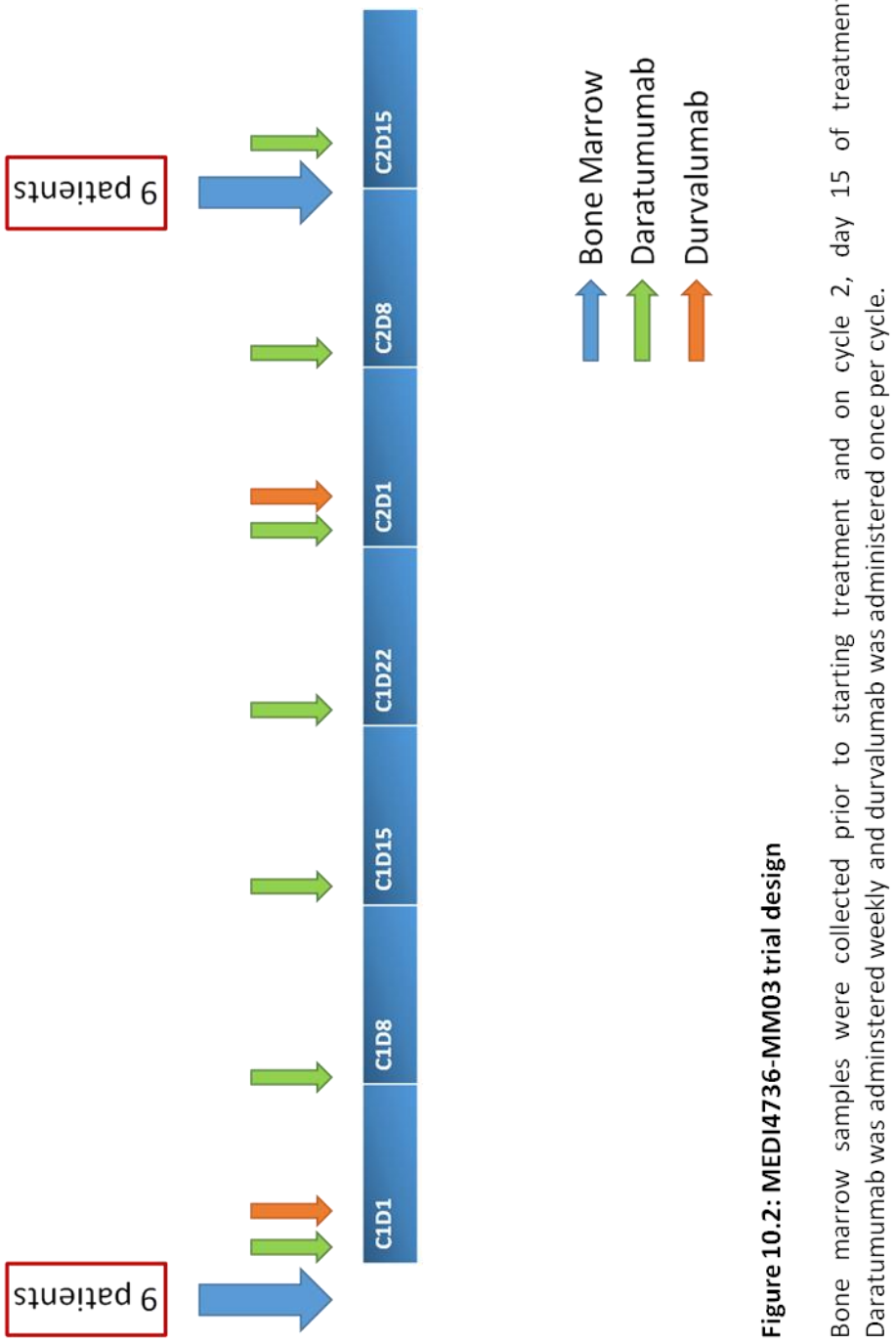

Figure 10.2: MEDI4736-MM03 trial design

Bone marrow samples were collected prior to starting treatment and on cycle 2, day 15 of treatment. Daratumumab was adminstered weekly and durvalumab was administered once per cycle.

10.4.2 Entry and exclusion criteria

Inclusion criteria for the trial included multiply relapsed or double refractory myeloma with measurable burden of disease. Crucially the exclusion criteria included prior exposure to an immune checkpoint inhibitor such as anti-CTLA4 or anti-PD1 mAb, cell based therapies such as CAR-Ts, cancer vaccination and allogenic stem cell transplantation. Furthermore individuals with a history of autoimmune disease or immunodeficiency were also excluded. For the purposes of this work the exclusion of patients whose immune response may be abnormal or

therapeutically modified means that this cohort of patients most closely represents the "normal" activity of the immune system in relapsed refractory myeloma.

It should be noted, however, that both PIs and IMiDs are recognised to exert effects on T cells. As these are now both established treatments for myeloma it is neither possible nor desirable to examine bone marrow samples from relapsed disease which have not been exposed to these agents.

Inclusion criteria	**Exclusion criteria**
3 prior anti myeloma regimen including PI and IMiD or double refractory to PI and IMiD.	Prior exposure to anti-CTLA1, anti-PD1, anti-PDL1 mAbs, cell based therapies or cancer vaccines
Measurable disease	Previous Daratumumab or anti-CD38 therapies
Achieved MR or better to at least 1 prior treatment	Plasmapheresis, major surgery, radiation treatment or systemic anti-myeloma drugs within last 14 days.
Evidence of PD on or within 60 days of most recent treatment	Prior organ or allogeneic stem cell transplantation
Previously received alkylating agent	Prior history of autoimmune disease or immunodeficiency.
ECOG 2 or less	
Prior treatment toxicities resolved or Grade 1 or less	

Table 10.1: Entry and exclusion criteria for MEDI4736-MM-003

Paired bone marrow samples were obtained from 9 patients, mononuclear cells were isolated using gradient density centrifugation with lymphoprep and samples were re-suspended in freezing media (FBS with 10% DMSO) for cryopreservation in liquid nitrogen for storage and transport.

10.4.3 Mass cytometry panel

The previously described mass cytometry panel (chapter 3) was modified to incorporate key markers relating to the PD1 axis and plasma cell ligands with potential therapeutic roles. The new targets incorporated into this panel were PDL2 and B cell maturation antigen (BCMA) which replaced HLA-DR and CD28.

Antigen	Metal	Clone	Source
CD45	89Y	HI30	Fluidigm
IL10	141Pr	JES3-9D7	Biolegend – BCI conjugation
CD19	142Nd	HIB19	Fluidigm
CD274 PDL1	143Nd	29E.2A3	Biolegend – BCI conjugation
CD4	145Nd	RPA-T4	Fluidigm
CD8a	146Nd	RPA-T8	Fluidigm
CD20	147Sm	2H7	Fluidigm
IL2	148Nd	Mq1-17H12	Biolegend – BCI conjugation
CD25	149Sm	2A3	Fluidigm
CD223 LAG3	150Nd	874501	Fluidigm
CD107a	151Eu	H4A3	Fluidigm
TNFa	152Sm	Mab11	Fluidigm
Ki67	153Eu	Ki-67	Biolegend – BCI conjugation
CD3	154Sm	UCHT1	Fluidigm
CD56	155Gd	B159	Fluidigm
CD366 TIM3	156Gd	F38-2E2	Biolegend – BCI conjugation
CD134 OX40	158Gd	ACT35	Fluidigm
CD197	159Tb	G043H7	Fluidigm
PD1	160Gd	EH12.2H7	Biolegend – BCI conjugation
CD38	161Dy	HIT2	Biolegend – BCI conjugation
FoxP3	162Dy	PCH101	Fluidigm
TGFB	163Dy	TW4-6H10	Fluidigm
CD244 2B4	164Dy	C1.7	Biolegend – BCI conjugation
IFNy	165Ho	B27	Fluidigm
CD314 NKG2D	166Er	ON72	Fluidigm
CD27	167Er	L128	Fluidigm
CD138	168Er	DL101	Fluidigm
CD45Ra	169Tm	HI100	Fluidigm
CD152 CTLA4	170Er	14D3	Fluidigm
CD226 DNAM1	171Yb	DX11	Fluidigm
CD279 PDL2*	172Yb	24F.10C12	Fluidigm
Granzyme B	173Yb	GB11	Fluidigm
BCMA*	174Yb	19F2	Fluidigm – Custom conjugation

Perforin	175Lu	B-D48	Fluidigm
CD127	176Yb	A019D5	Fluidigm
CD16	209Bi	3G8	Fluidigm

Table 10.2 Mass cytometry panel. * indicates antibodies which differ from the original panel. PDL2 and BCMA replace CD28 and HLA-DR.

PDL2 is a ligand for PD1 with structural similarity to PDL1. Its tissue expression is more restricted than that of PDL1, with expression predominantly found on DCs, macrophages and bone marrow derived mast cells [216]. As with PDL1, engagement of PDL2 with PD1 suppresses T cell function [216].

BCMA is a member of the TNF receptor superfamily and is expressed on mature B cells [217]. Induction of BCMA signalling via its ligands APRIL and BAFF promote the proliferation and survival of mature plasma cells [217]. These pro-survival signals are also thought to be significant in promoting malignant plasma cell survival in myeloma [217]. The fact that BCMA expression is primarily restricted to mature plasma cells makes BCMA a possible therapeutic target in the management of myeloma [218].

10.4.4 Optimising and troubleshooting mass cytometry panel

Pilot samples were used to ensure that the modified mass cytometry panel was functioning appropriately. This work appeared to identify unexpected expression of BCMA on multiple cell types which do not normally express BCMA. Metal minus one (MMO) and flow cytometry analysis found this to be due to spill over from granzyme B which sits at the +1 position of molecular weight. While signal spillover is rare in mass cytometry when it does occur it is usually due to oxidation of metals with a molecular weight of 1 or 16 less than the channel detecting the spillover (Figure 10.3). As plasma cells are not thought to express granzyme B it is possible to determine BCMA expression on plasma cells but not across the global data set.

10.4.5 Sample preparation

An initial pilot study was performed using six screening bone marrow samples from individuals who did not go on to receive treatment. This identified that cellular viability was poor with a large proportion of cells dying during the thaw process and during overnight resting. To combat this, the previously described thaw procedure was modified. Samples were rapidly thawed in a 37^{o}C waterbath before 1ml of warmed FBS was added dropwise. Resuspended samples were then transferred to 10mls of warmed culture media containing

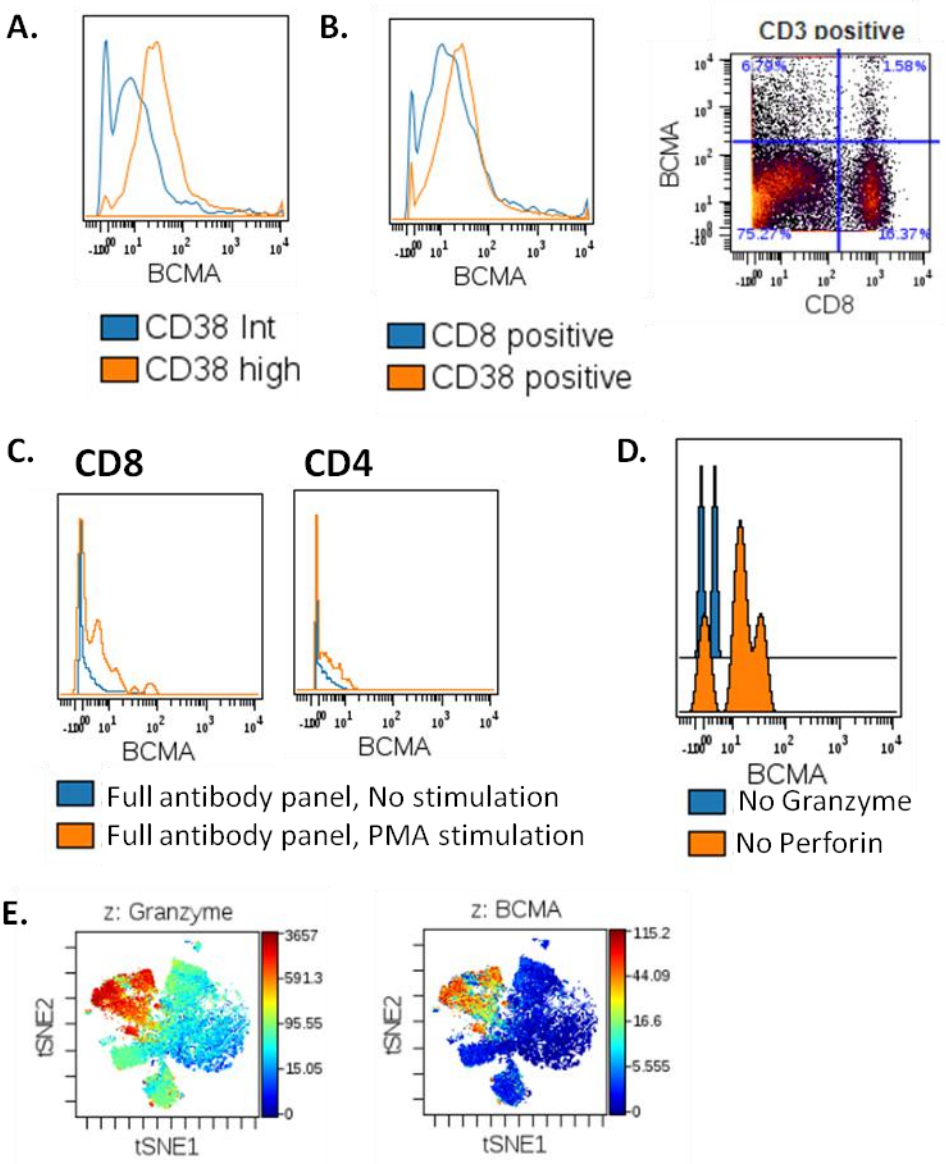

Figure 10.3: Aberrant BCMA expression due to spillover from granzyme channel

[A] Healthy PBMCs were spiked with U266 plasma cells. BCMA intensity was higher on CD38 high cells compared to CD38 intermediate cells, in keeping with expected BCMA distribution.
[B] Unexpected BCMA expression was seen on CD8 positive cells.
[C] Elevated BCMA expression was seen on CD8 cells stained with the full antibody panel and stimulated with PMA. No increase was seen on CD4 cells or unstimulated cells, suggesting the source of the signal was associated with CD8 activation
[D] MMO samples excluding granzyme and perforin were performed as their atomic weight made them potential causes of spillover into the BCMA channel. The BCMA signal was present in the perforin MMO but not the granzyme MMO, confirming that granzyme was responsible for the BCMA signal.
[E] Colocalisation of granzyme and BCMA can be seen on viSNe plots.

10% FBS. Cells were rested for 4 hours in full culture media containing protein transport inhibitor cocktail in a humidified 37^{o}C incubator with 5% CO2.

Cell staining was performed as previously described (Chapter 3). For some samples a second vial was available which was processed and stained in the same way.

10.4.6 Data analysis strategies

Where two vials were available the data was pooled for analysis. Data clean up and gating was performed in Cytobank with mean expression and percent in gate data exported to Microsoft Excel and Graphpad Prism (version 5 and 7.02) for further analysis.

Live single cells were identified using Boolean gating. ViSNE was then used to define key cell populations (Figure 10.4).

A CITRUS analysis was performed on the live cell gate of pre- and on-treatment samples. The selected endpoint was treatment status (pre- versus on-treatment). Algorithm settings were applied as described in chapter 3, in brief, clustering was based on marker abundance, equal sampling was used from each individual (Figure 10.5). The algorithm was run in triplicate.

Statistical analysis was performed using the Wilcoxon test for paired, non-parametric samples.

Assessment of CD38 positive cell clearance is hampered by the fact that the CD38 epitope recognised by Daratumumab overlaps with the epitope recognised by most / all commercially available anti-CD38 monoclonal antibodies. Daratumumab also has a prolonged binding time. The net result is that following treatment with Daratumumab the CD38 epitope may be masked and unavailable for binding by metal-conjugated CD38 antibodies. Currently there are not commercially available antibodies to CD38 which recognise a distinct epitope.

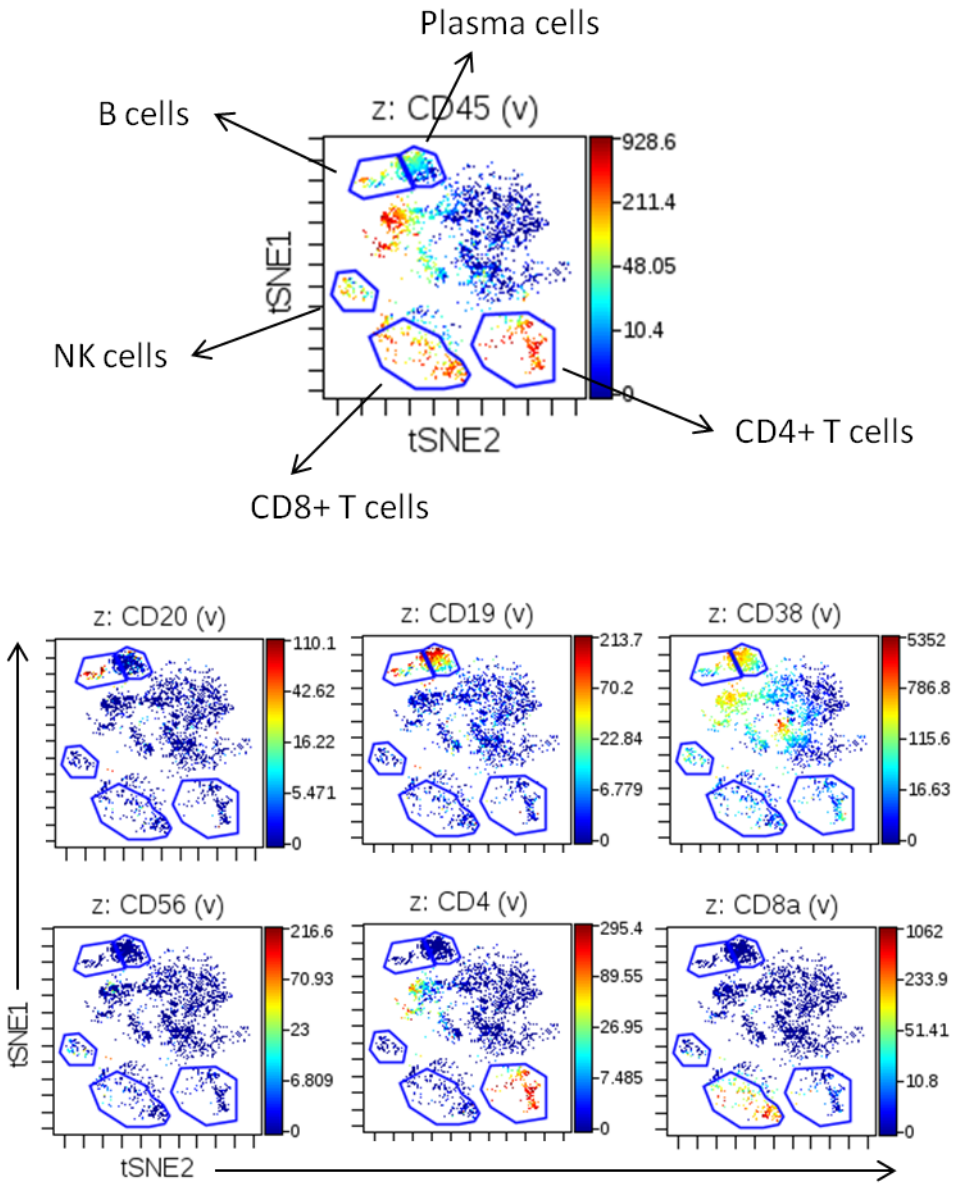

Figure 10.4: Identification of cell populations using viSNE.

Live , single cells were identified by Boolean gating. A viSNE analysis using all markers was then performed and used to identify key populations using established cell phenotypes. A representative pre-treatment sample is shown here. B cells were CD19+CD20+, Plasma cells were CD19+CD38+, NK cells were CD3-CD56+, CD8 cells were CD3+CD8+, CD4 cells were CD3+CD4+.

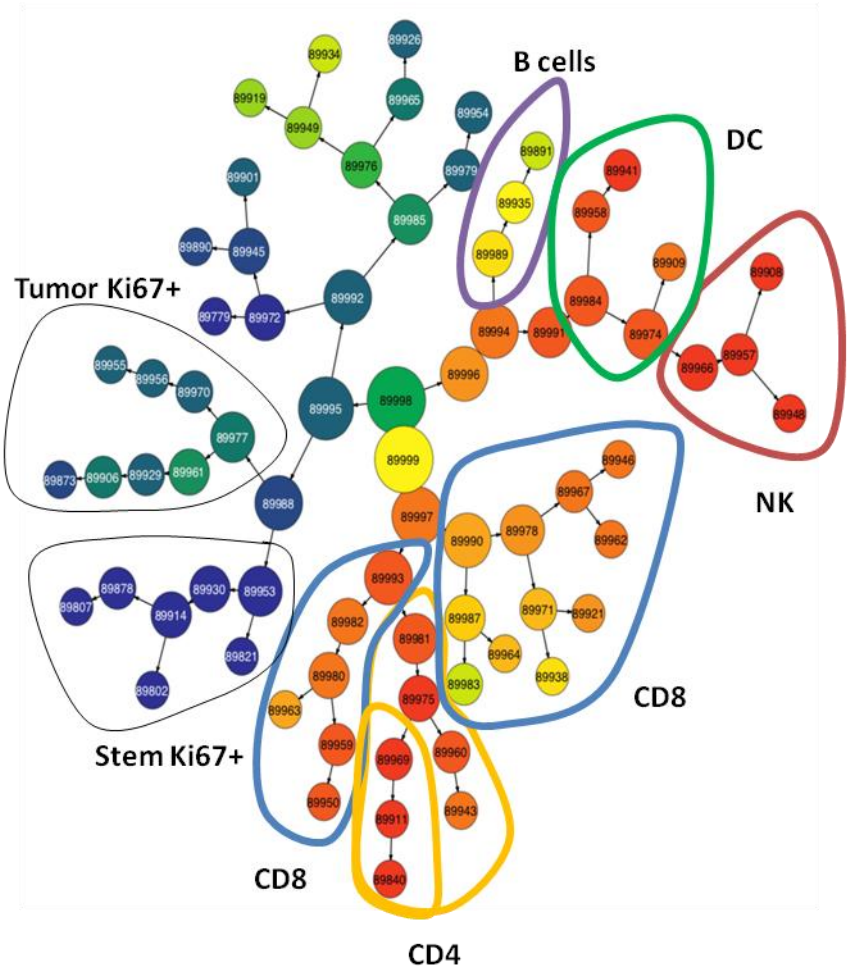

Figure 10.5: Identification of cell populations using CITRUS.

A representative example of the map generated by the CITRUS algorithm with key cell populations identified based on established phenotypes. (Map provided by Mary Young of Celgene)

10.5 Results

10.5.1 CD8 and CD4 lymphocyte numbers rise following treatment with Daratumumab and Durvalumab

Events counts as a proportion of live cells events were examined before treatment and on cycle 2 day 15 (C2D15). When assessed by viSNE gating a relative increase in CD8 (median pre 8%, C2D15 15%, WC p=0.0073) and CD4 (median pre 6.3%, C2D15 11.6% WC p=0.0085) populations was seen while NK (median pre 2.66%, C2D15 0.9% WC p=0.0009) and B cell (median pre 4.82%, C2D15 2.93% WC p=0.0273) populations decreased (Figure 10.6).

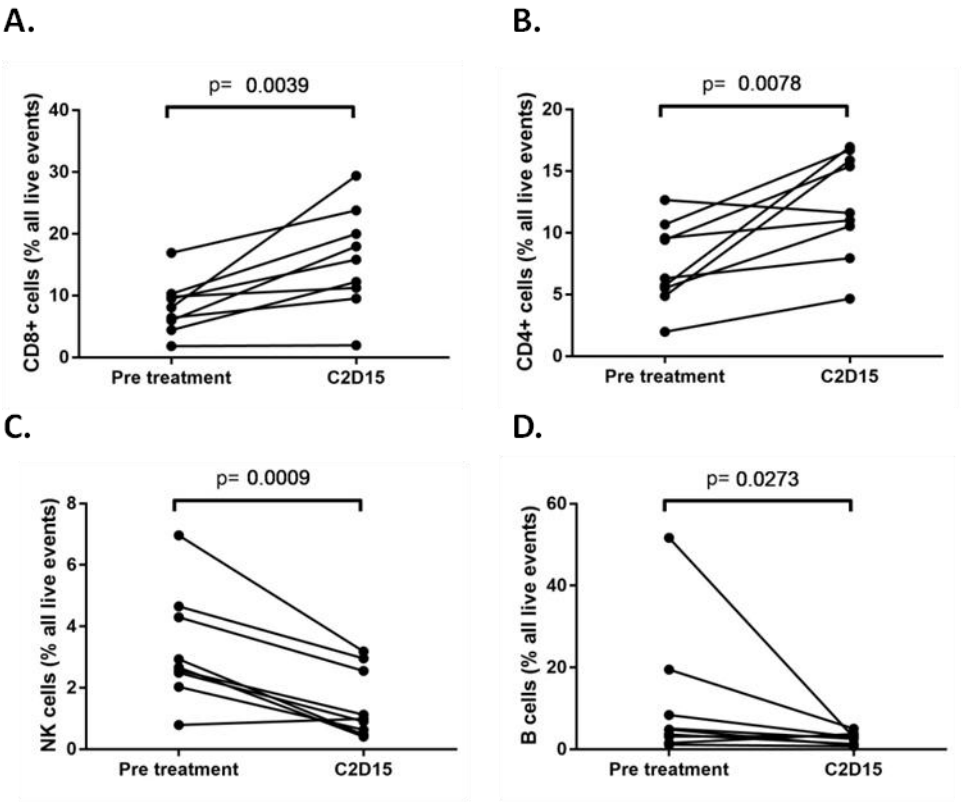

Figure 10.6: Event count by viSNE before treatment and on cycle 2, day 15 of treatment with Daratumumab and Durvalumab

Paired samples were compared using the Wilcoxon test.

[A] An increase in CD8+ T cells is seen (p=0.0039)
[B] An increase in CD4+ T cells is seen (p=0.0078)
[C] A decrease in NK cells is seen (p=0.0009)
[D] A decrease in B cells is seen (p=0.0273)

CITRUS analysis confirmed the fall in NK cells and B cells and also demonstrated a fall in tumour burden and in DC cells, all at an FDR of 0.01. A rise in CD8 populations was seen at an FDR of 0.05 but the rise in CD4 populations could not be demonstrated (Figure 10.7).

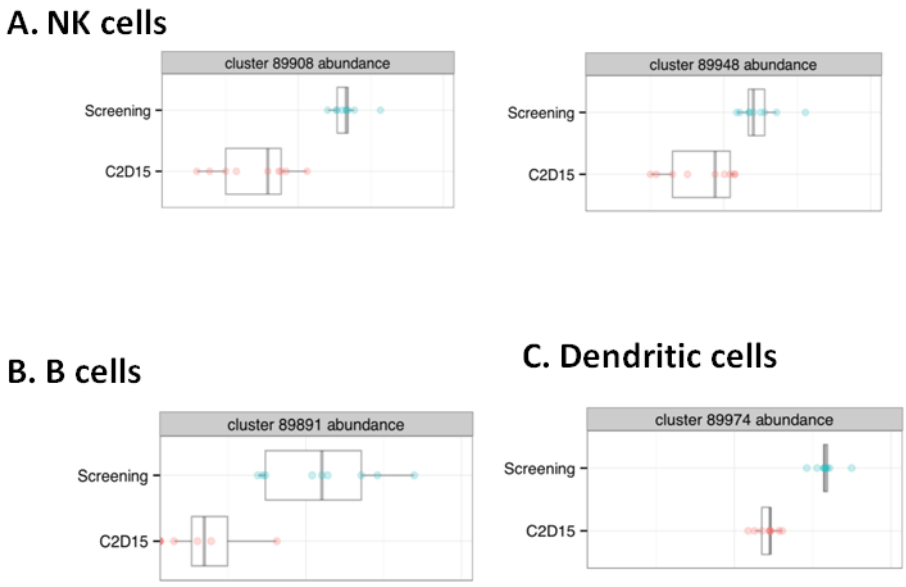

Figure 10.7: Event counts by CITRUS before treatment and on cycle 2, day 15 of treatment with daratumumabaand durvalumab

CITRUS analysis demonstrated a dall in NK, B cells and dendritic cell numbers at an FDR of 0.01.

[A] A fall in the abundance of NK cells in two distinct sub-populations was seen
[B] A fall in B cell abundance was seen
[C] A fall in dendritic cell abundance was seen.

The fall in NK cells and B cells is expected, as both these populations express high levels of CD38 [86] and are therefore depleted by Daratumumab. The apparent rise in CD8 and CD4 may occur due to depletion of these other cell subsets or may be a true rise due to activation and proliferation following inhibition of the PD1 pathway.

10.5.2 CITRUS analysis

10.5.2.1 Population phenotype as identified by CITRUS

Further exploration of the CITRUS analysis demonstrated two distinct NK cell populations, one which expressed IL2 (median MSI naive 4.383, active 5.813 WC p=0.0039), IFNγ (median MSI naive 4.616, active 6.352 WC p=0.0039), TNFα (median MSI naive 5.825, active 86.82 WC p=0.0039) and T-cell immunoglobulin and mucin-domain containing-3 (TIM-3) (median MSI naive 1.425, active 3.001 WC p=0.0039) and can be considered to have an active phenotype, the other did not have active features and is considered naive. The active phenotype also had increased expression of granzyme B (median MSI naive 26.46, active 47.84 WC p=0.0039) and perforin (median MSI naive 11.05, active 11.4 p=0.0078)(Figure 10.8).

Within the dendritic cell population distinct proliferative and non proliferative populations were identified. The proliferative population strongly expressed Ki67 (median MSI proliferative 207.2, non-proliferative 30.4 WC p=0.0156) and co-expressed CCR7 (a marker of tissue DCs) (median MSI proliferative 10.27, non-proliferative 2.161 WC p=0.0078), PDL2 (median MSI proliferative 9.393, non-proliferative 3.423 WC p=0.0078) and, importantly, CD38 (median MSI proliferative 377.9, non-proliferative 50.43 WC p=0.0078) (Figure 10.9).

The B cell node was proliferative (median Ki67 141.8). It expressed very low levels of PDL1 (median MSI 0.9018) and PDL2 (median 1.153)(Figure 10.10).

CD8 populations were the dominant population identified by CITRUS. CD8 expression of Ki67 was lower than for other cell types (median MSI 4.4-24.5) suggesting lack of proliferation. Expression of TGFβ was also seen (median MSI 50.4-76.19). There was varied expression of NKG2D (median MSI 1.286-12.12), 2B4 (median MSI 5.78-46.71), CD107a (median MSI 8.707-12.51), PDL2 (median MSI 15.1-25.89), granzyme (median MSI 779-1521) and perforin (median MSI 218-632) (Figure 10.11).

CD4 lymphocytes, like CD8 lymphocytes, were poorly proliferative (Ki67 median MSI 5.797). PD1 expression was variable (median MSI 1.274-23.33) and cells expressed TGFβ (median MSI 50.27). FoxP3 median MSI expression was 20.56 (Figure 10.12).

Plasma cells were proliferative (Ki67 median MSI 273.4) and had varied expression of IL10 (median MSI 3.908-26.78), LAG3 (median MSI 2.371-40.27) and BCMA (median MSI 3.142-13.28)(Figure 10.13).

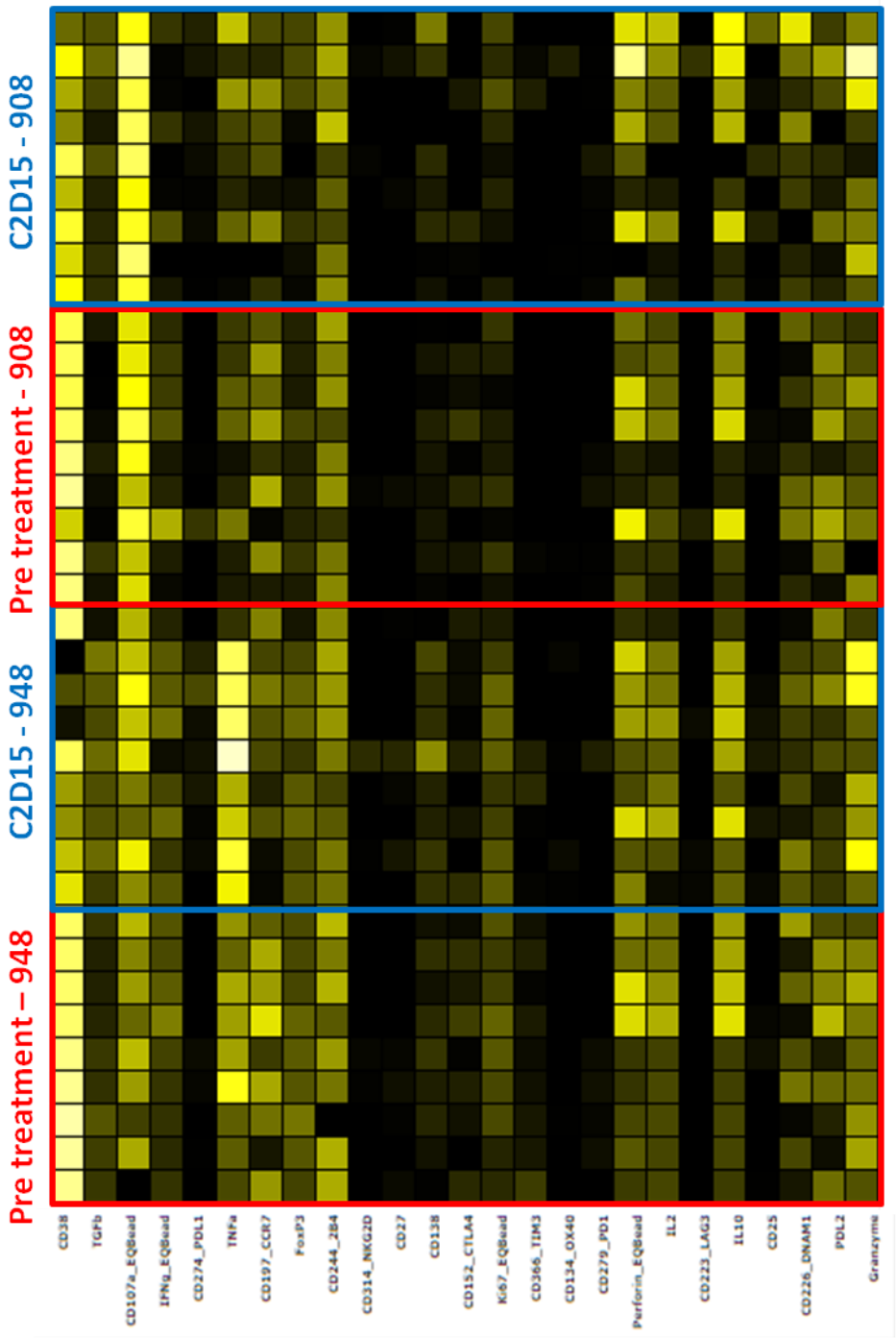

Figure 10.8: Marker expression by NK cell populations identified by CITRUS pre treatment and on cycle 2, day 15 of treatment with durvalumab and daratumumab.

Marker expression is transformed and normalised to the lowest expression per row. Two distinct NK cell populations are seen. Node 948 expresses IL2, IFNγ, TNFα and TIM3 and is considered to have an active phenotype. Node 908 does not have features of cellular activation and is considered naive.

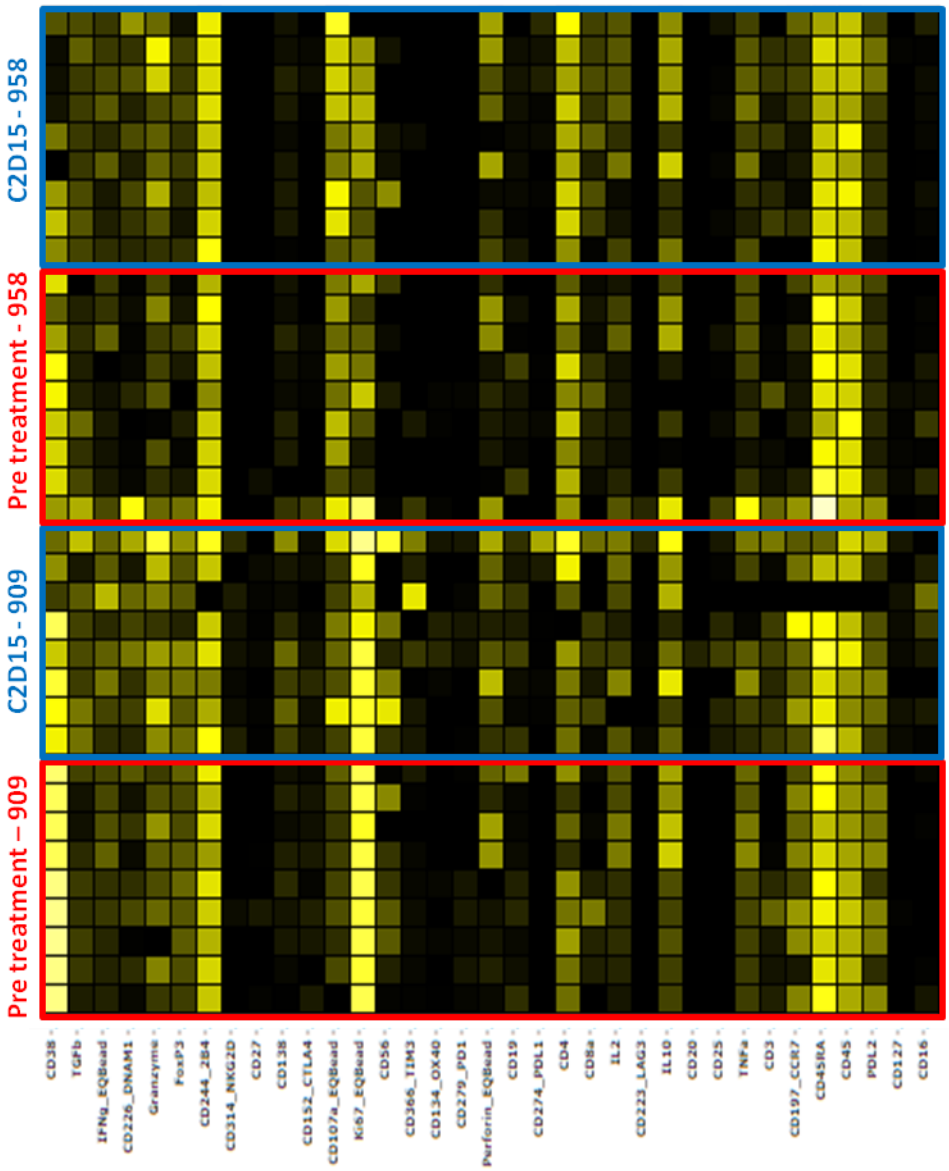

Figure 10.9: Marker expression by DC cell populations identified by CITRUS pre treatment and on cycle 2, day 15 of treatment with durvalumab and daratumumab.

Marker expression is transformed and normalised to the lowest expression per row. Two distinct DC cell populations are seen. Node 909 expresses Ki67 and is considered proliferative. Node 958 is non proliferative. Node 909 co-expresses CCR7, PDL2 and CD38.

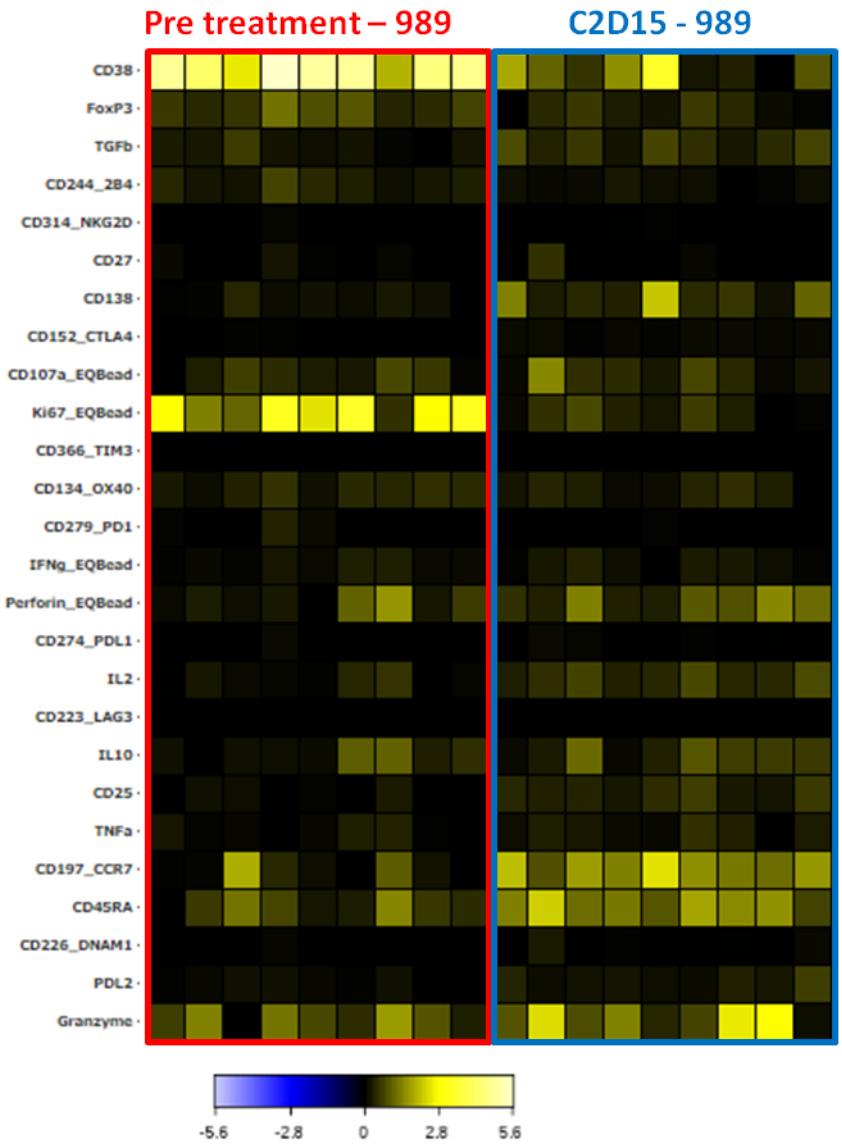

Figure 10.10: Marker expression by B cells identified by CITRUS pre treatment and on cycle 2, day 15 of treatment with durvalumab and daratumumab.

Marker expression is transformed and normalised to the lowest expression per row. Pre treatment B cells express Ki67 and are proliferative.

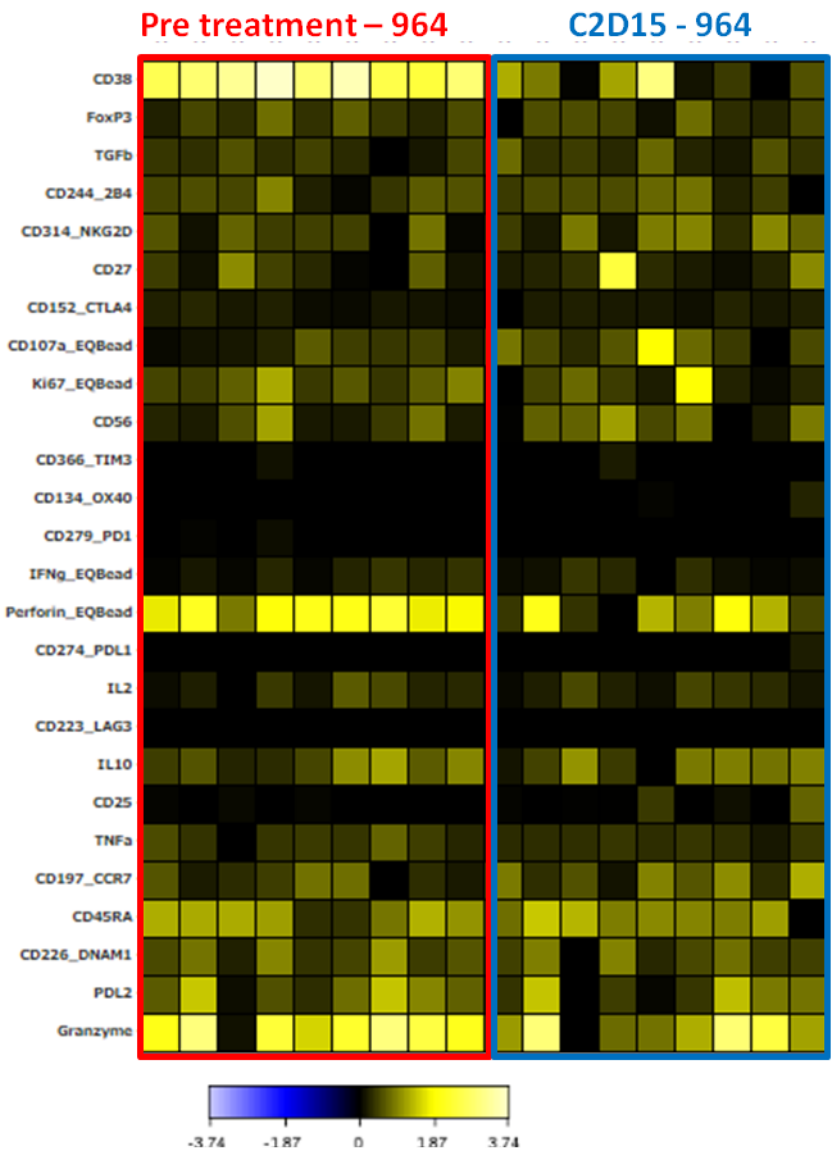

Figure 10.11: Marker expression by CD8 cells identified by CITRUS pre treatment and on cycle 2, day 15 of treatment with durvalumab and daratumumab.

Marker expression is transformed and normalised to the lowest expression per row. Pre treatment CD8 cells express low levels of Ki67. Expression og TGFβ is seen with varied expression of NKG2D, 2B4, CD107a, granzyme and perforin.

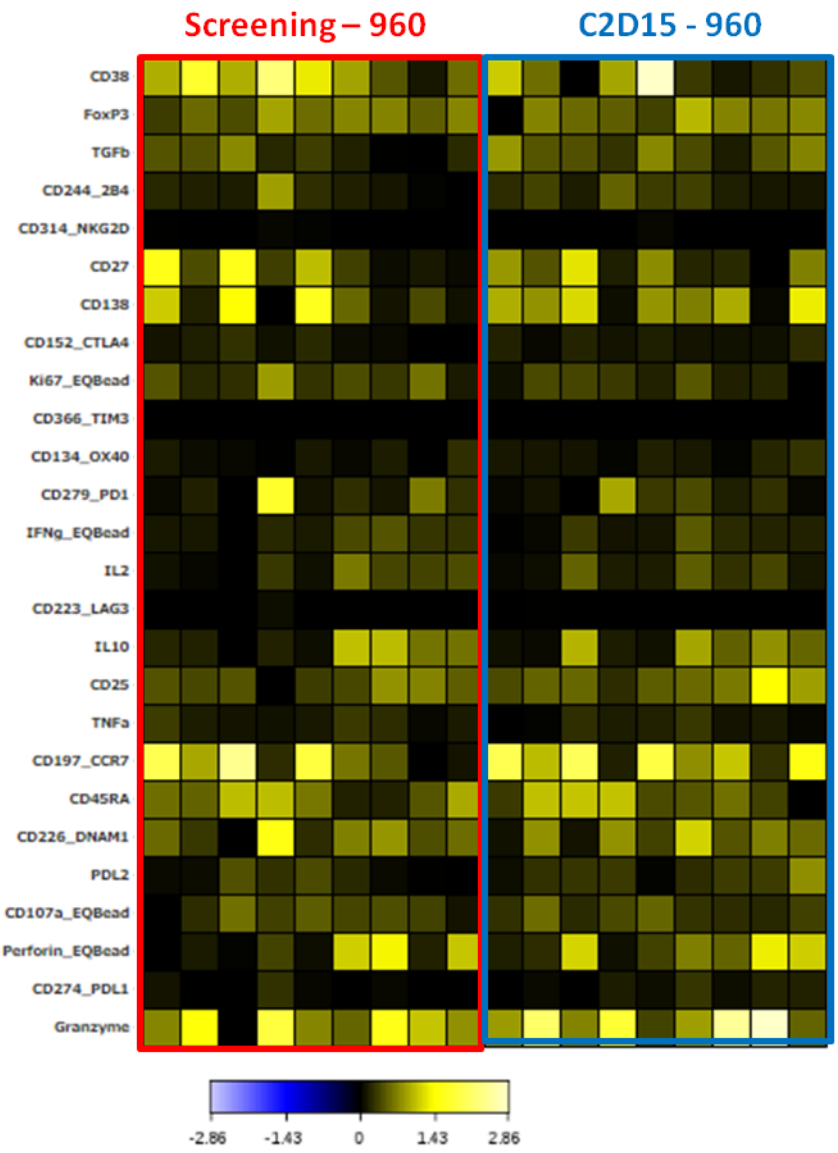

Figure 10.12: Marker expression by CD4 cells identified by CITRUS pre treatment and on cycle 2, day 15 of treatment with durvalumab and daratumumab.

Marker expression is transformed and normalised to the lowest expression per row. Pre treatment CD4 cells express TGFβ with low expression of Ki67 pre treatment.

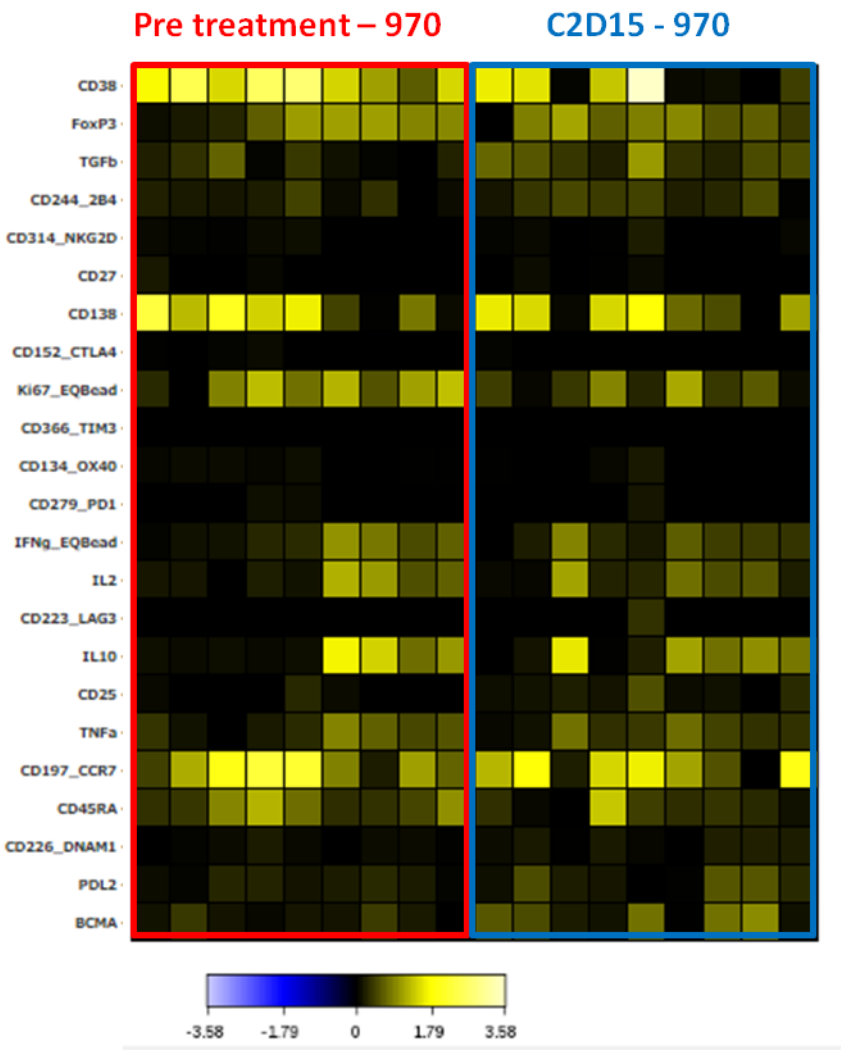

Figure 10.13: Marker expression by plasma cells identified by CITRUS pre treatment and on cycle 2, day 15 of treatment with durvalumab and daratumumab.

Marker expression is transformed and normalised to the lowest expression per row. Pre treatment plasma cells express Ki67. Expression of IL10, LAG3 and BCMA is variable.

10.5.2.2 Functional changes following treatment as identified by CITRUS

Exported marker information from CITRUS was used to assess changes in marker expression at C2D15 in the key populations identified.

When assessed at C2D15, NK cell numbers fall in both the naive and active populations. Those NK cells that remain have an activated phenotype with elevated expression of TNFα (pre MSI 86.82, post 138.7 WC p0.0039) and IFNγ (Pre MSI 6.352, post 11 p0.0195) but interestingly not a rise in markers of cytotoxicity (Figure 10.14).

Within the DCs non-proliferative population, an increase in CD107a (median MSI pre 26.37, post 77.36 p=0.0234) expression is seen, while the proliferative node has an increase in TGFβ (median MSI pre 71.19, post 109.3 p=0.0195) and granzyme (median MSI pre 31.52, post 74.8 p=0.0195) expression (Figure 10.15).

There is a marked decrease in Ki67 (median MSI pre 141.8, post 15.33 p0.0039) in B cell at C2D15, indicating a fall in proliferation. IL2 (median MSI pre 2.42, post 4.581 p0.0078) and TGFβ (median MSI pre 44.78, post 67.57 p0.0039) levels rise (Figure 10.16).

The CD8 population shows a rise in both CD107a (median MSI pre 8.707, post 16.37 p0.0039) and TGFβ (median MSI pre 76.19, post 96.33 p0.0195) (Figure 10.17).

CD4 populations show an increase in TGFβ (median MSI pre 50.27, post 56.16 p=0.0391) on C2D15 (Figure 10.18).

Plasma cells show a C2D15 increase in CD223 - lymphocyte-activation gene 3 (LAG3) (median MSI pre 5.864, post 17.04 p=0.0078) and TGFβ (median MSI pre 56.12, post 71.49 p=0.0078) while BCMA (pre 6.017, post 3.59 p=0.0391) expression falls (Figure 10.19).

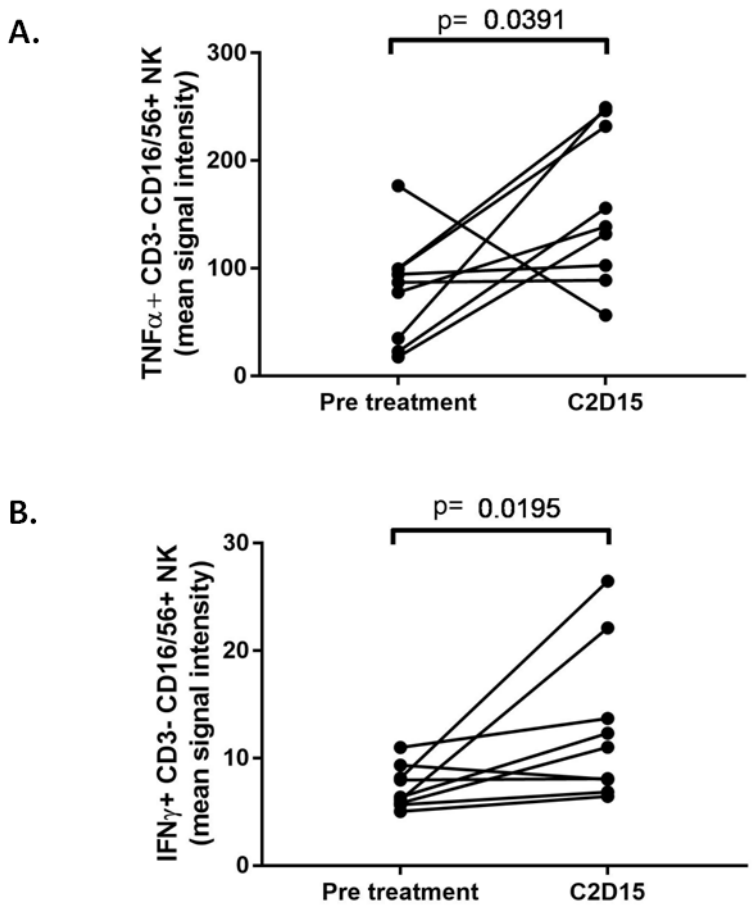

Figure 10.14: Functional changes on NK cells following treatment with daratumumab and durvalumab as assessed by CITRUS analysis.

Paired samples compared using Wilcoxon test.

[A] An increase in NK cell TNFα expression is seen (p=0.0391)
[B] An increase in NK cell IFNγ expression is seen (p=0.0195)

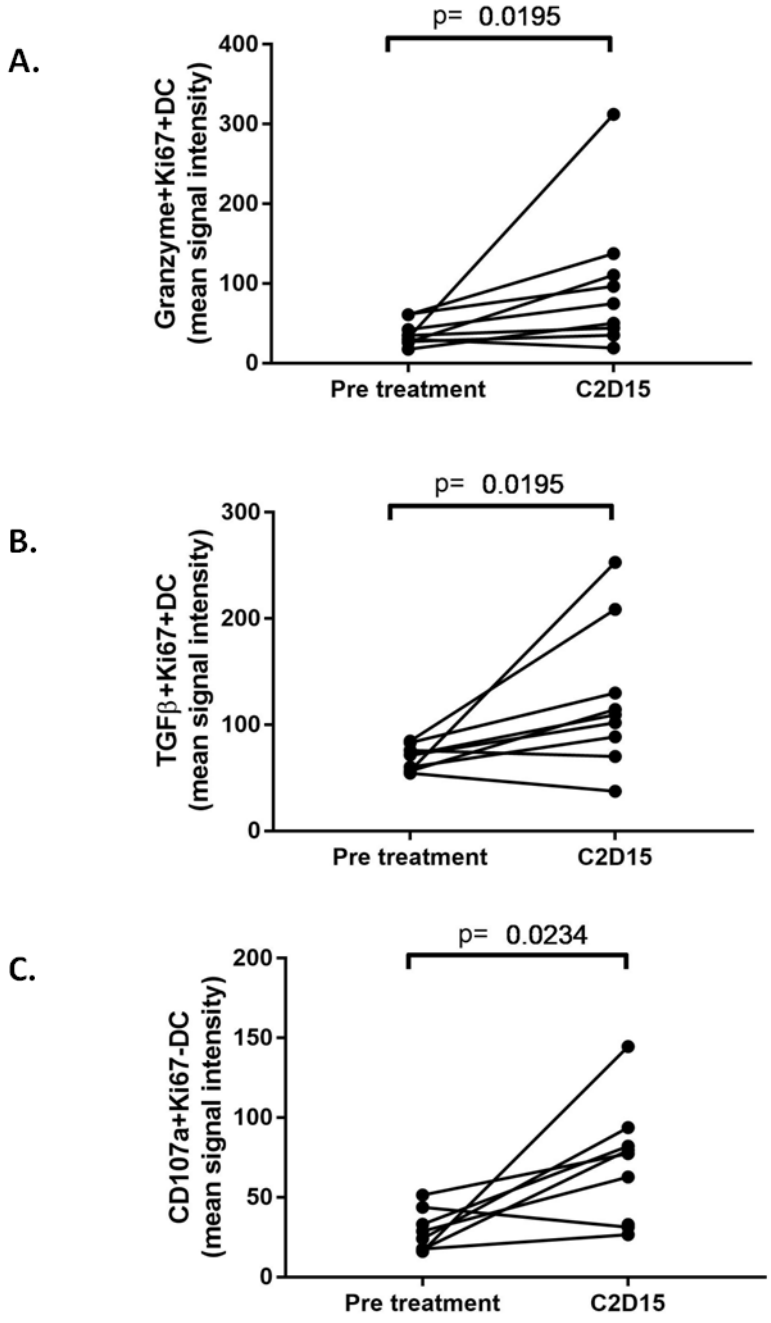

Figure 10.15: Functional changes on DC cells following treatment with daratumumab and durvalumab as assessed by CITRUS analysis.

Paired samples compared using Wilcoxon test.

[A] Increased granzyme expression was seen on the proliferative DC node following treatment (p=0.0195)
[B] Increased TGFβ expression was seen on the proliferative node following treatment (p=0.0195)
[C] Increased expression of CD107a expression was seen on the non-proliferative node following treatment (p=0.0234)

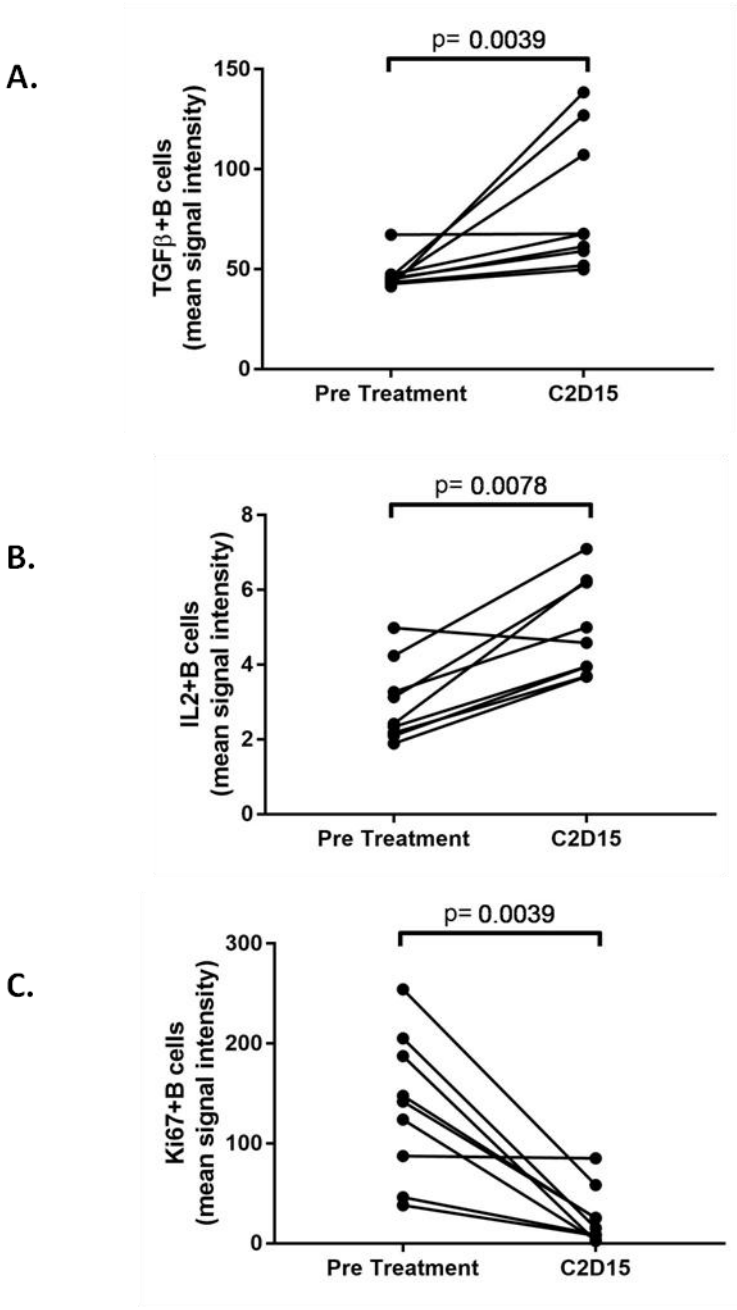

Figure 10.16: Functional changes on B cells following treatment with daratumumab and durvalumab as assessed by CITRUS analysis.

Paired samples compared using Wilcoxon test.

[A] B cell TGFβ expression rises following treatment (p=0.0039)
[B] B cell IL2 expression rises following treatment (p=0.0078)
[C] B cell Ki67 expression falls following treatment (p=0.0039)

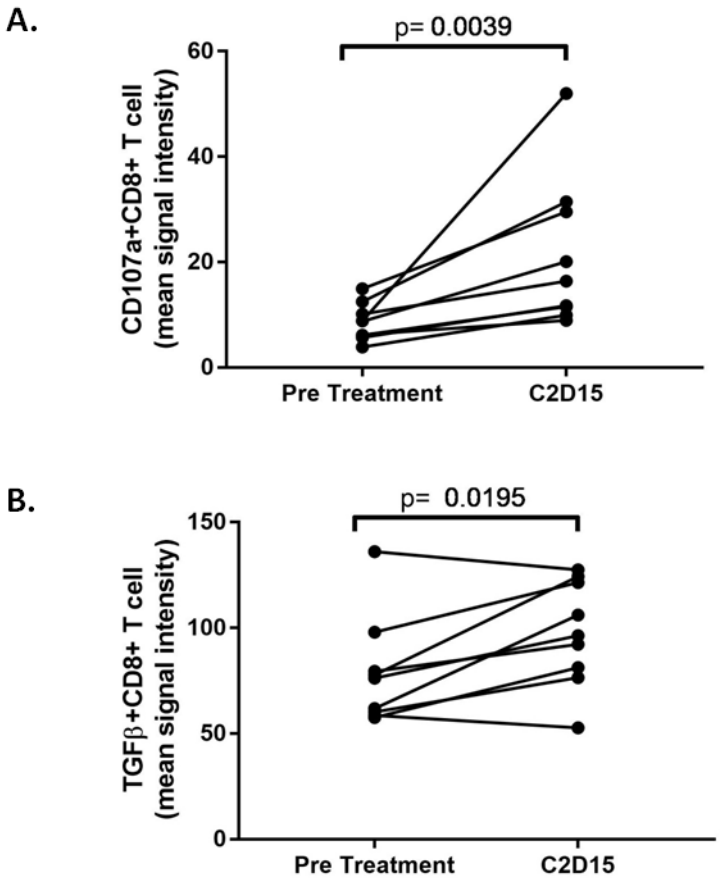

Figure 10.17: Functional changes on CD8 cells following treatment with daratumumab and durvalumab as assessed by CITRUS analysis.

Paired samples compared using Wilcoxon test.

[A] CD8 CD107a levels rise following treatment (p=0.0039)
[B] CD8 TGFβ levels rise following treatment (p=0.0195)

A.

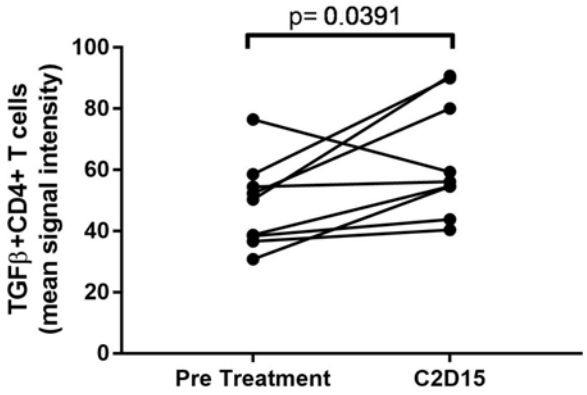

Figure 10.18: Functional changes on CD4 cells following treatment with daratumumab and durvalumab as assessed by CITRUS analysis.

Paired samples compared using Wilcoxon test.

[A] CD4 TGFβ levels rise following treatment (p=0.0391)

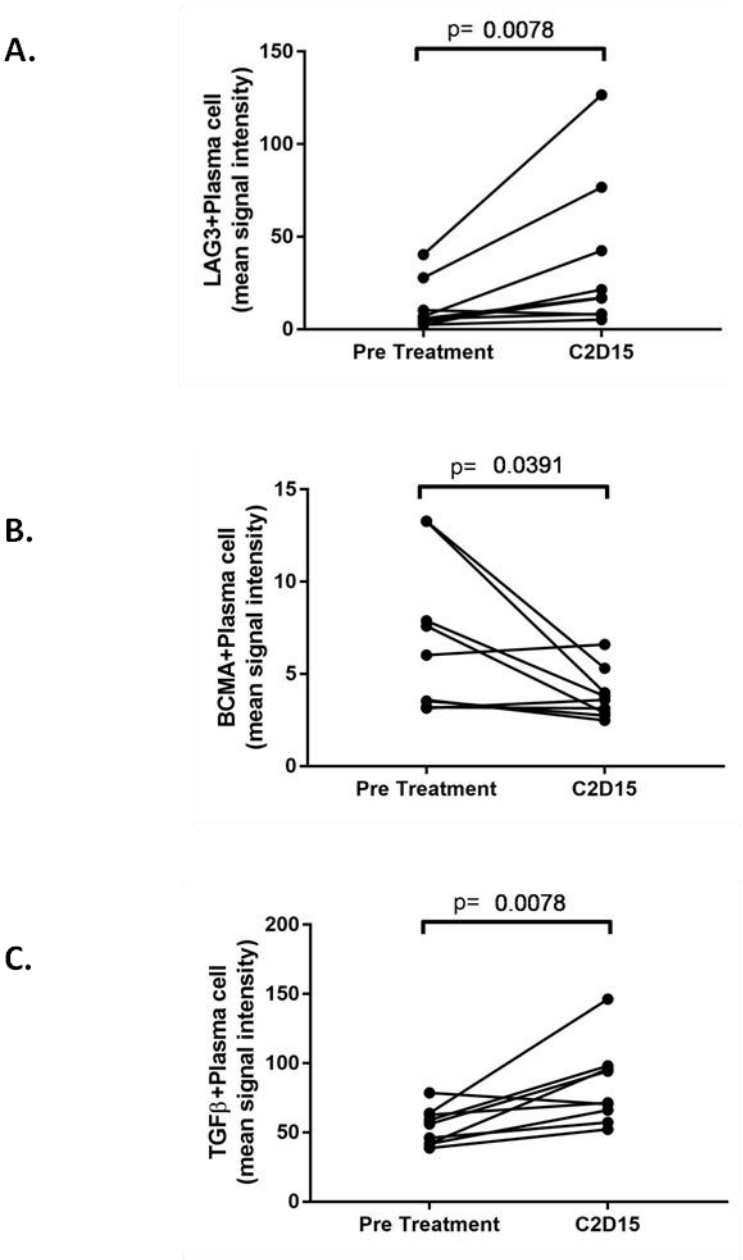

Figure 10.19: Functional changes on plasma cells following treatment with daratumumab and durvalumab as assessed by CITRUS analysis.

Paired samples compared using Wilcoxon test.

[A] Plasma cell LAG3 expression rises following treatment (p=0.0078)
[B] Plasma cell BCMA expression falls following treatment (p=0.0391)
[C] Plasma cell TGFβ expression rises following treatment (p=0.0078)

10.5.3 Analysis from viSNE based gating

When traditional data analysis was applied to viSNE gated populations, changes in functional activity was seen across multiple cell populations on C2D15.

10.5.3.1 CD8 populations have an activation signature consistent with a cytotoxic response following treatment with Daratumumab and Durvalumab

Within CD8 populations there was a rise in granzyme (median pre 52.45%, median post 68.43% WC p=0.0195) and perforin (median pre 24.84%, median post 43.68% WC p=0.0078) expression which was accompanied by a fall in PD1 expression (median pre 19.4%, post 15.49 % WC p=0.0078). Surprisingly, expression of NKG2D, which is expressed by activated CD8 cells, also fell (median pre 68.8%, post 51.27% WC p=0.0273).

The proportion of CD8+CD107a+granzyme+perforin+ cells also rose on CD2D15 (median pre 1.872%, median post 4.403% WC p=0.0273) due to a decrease in the triple negative cell population (median pre 31.7%, post 24.45%, WC p=0.0273).

This pattern of marker expression is consistent with CD8 T cell activation. Increases in granzyme and perforin expression have previously been reported following treatment with Daratumumab [144], however a fall in PD1 expression has not been reported in that setting. It is possible of course that the observed fall in PD1 expression here may be due to Durvalumab.

Within the CD8 subsets, this activation signature was most marked in the EMRA and EM population, although similar changes were also seen in the naïve subset. Additionally naïve cells had an increased expression of CD244 (2B4) (median pre 10.14%, post 29.79 %, WC p=0.0273) while the CM subset became more proliferative on C2D15 (Ki67 median pre 0%, post 11.1% WC p=0.0156)(Figure 10.20).

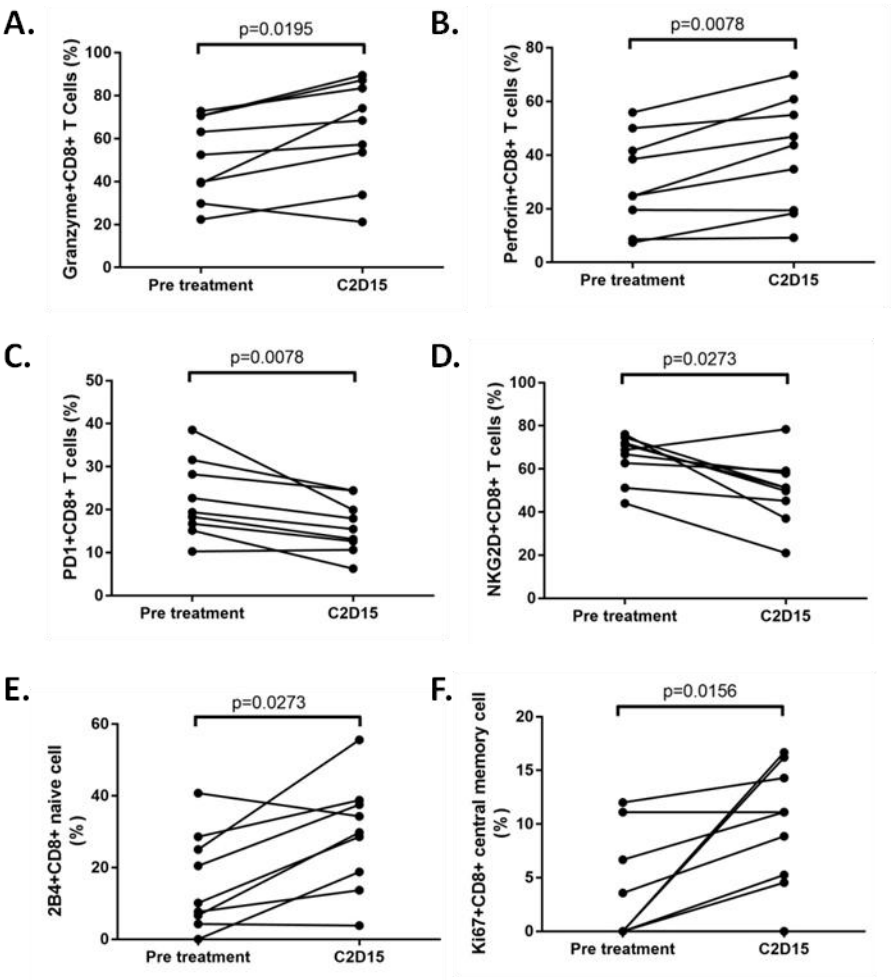

Figure 10.20: Functional changes on CD8 cells following treatment with daratumumab and durvalumab as assessed by viSNE analysis.

Paired samples compared using Wilcoxon test.

[A] CD8 granzyme expression rises following treatment (p=0.0195)
[B] CD8 perforin expression rises following treatment (p=0.0078)
[C] CD8 PD1 expression falls following treatment (p=0.0078)
[D] CD8 NKG2D expression falls following treatment (p=0.0273)
[E] CD8 naive 2B4 expression rises following treatment (p=0.0273)
[F] CD8 central memory Ki67 expression rises following treatment (p=0.0156)

10.5.3.2 T regulatory subsets are less proliferative following treatment with durvalumab and daratumumab

In keeping with changes seen in the CD8 population, the CD4 population also shows a decrease in PD1 (median pre 27.72%, post 21.56% WC p=0.0273) expression which is accompanied by a rise in granzyme (median pre 8.875%, post 17.79% WC p=0.0391). Unsurprisingly, the expression level of granzyme is lower on CD4 population than on CD8. Unlike the CD8 population, however, CD4 cells also show a fall in Ki67 (median pre 9.4%, post 6.55% WC p=0.0078) expression suggesting loss of proliferation. Importantly, this reduction in proliferation (median pre 10.29%, post 2.985% WC p=0.0078) and PD1 expression (median pre 36.36%, post 22.64%, WC p=0.0078) is also seen within the T regulatory subset (Figure 10.21).

10.5.3.3 NK cells show a loss of cytotoxic activity following treatment with daratumumab and durvalumab

Unlike their antigen specific counterparts, NK cells have a fall, not a rise in expression of granzyme (median pre 69.23%, post 48.48%, WC p=0.0078) and perforin (median pre 85.14%, post 73.91% WC p=0.0078) on C2D15. This may be related to the profound depletion of this subset. The activated pattern of cytokine expression seen by CITRUS analysis could not be identified by traditional data analysis techniques (Figure 10.22).

10.5.3.4 B cell populations have a profound reduction in Ki67 expression which is accompanied by a rise in pro-tumour cytokines

B cell population Ki67 expression (median 70.43%, post 5.882% WC p=0.0117) drops significantly following treatment with daratumumab and durvalumab. This is accompanied by a rise in IL2 (median pre 2.273%, post 7.5% WC p=0.0078) and TGFb (median pre 3.235 %, post 15.96% p=0.0273) expression which have previously been reported to support B cell and plasma cell growth (Figure 10.23).

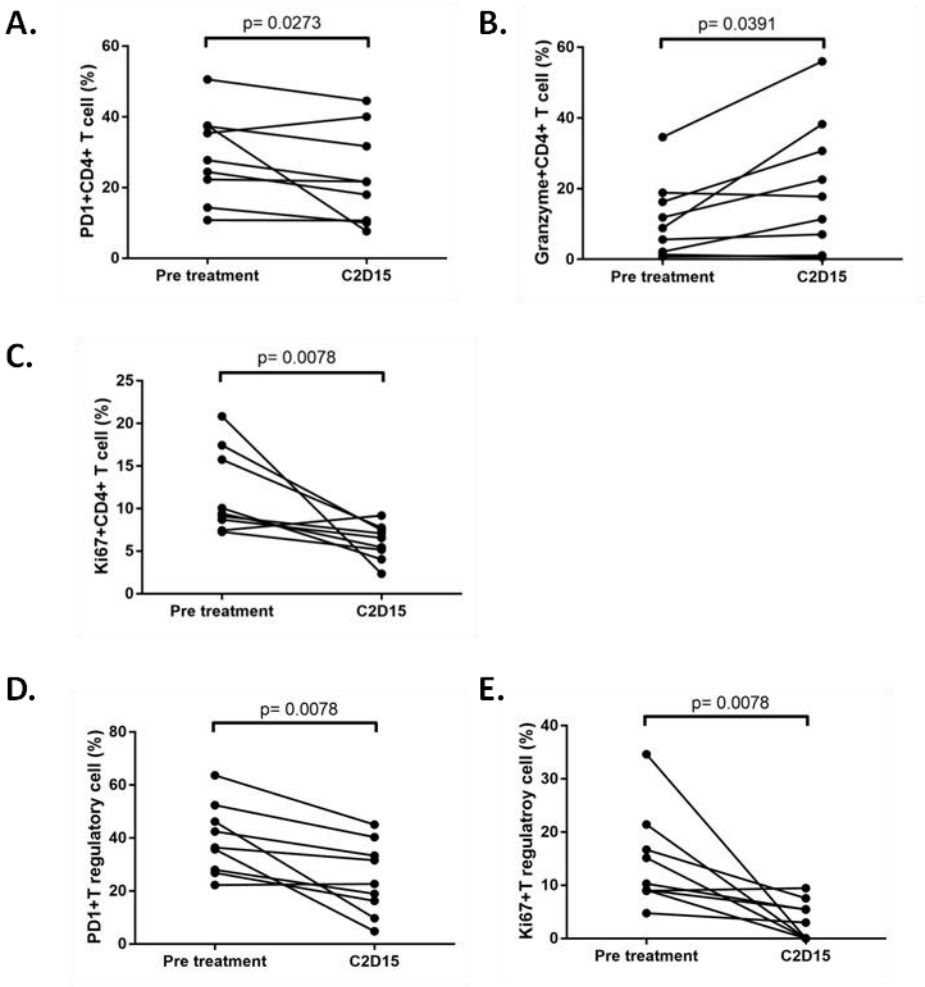

Figure 10.21: Functional changes on CD4 cells following treatment with daratumumab and durvalumab as assessed by viSNE analysis.

Paired samples compared using Wilcoxon test.

[A] CD4 PD1 expression falls following treatment (p=0.0273)
[B] CD4 granzyme expression rises following treatment (p=0.0391)
[C] CD4 Ki67 expression falls following treatment (p=0.0078)
[D] CD4 T regulatory cells PD1 expression falls following treatment (p=0.0078)
[E] CD4 T regulatory cell Ki67 expression falls following tretment (p=0.0078)

A.

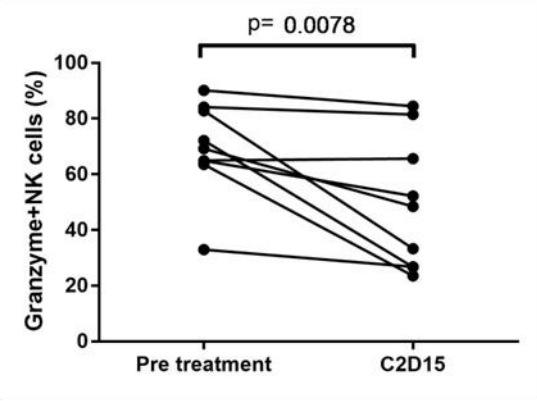

B.

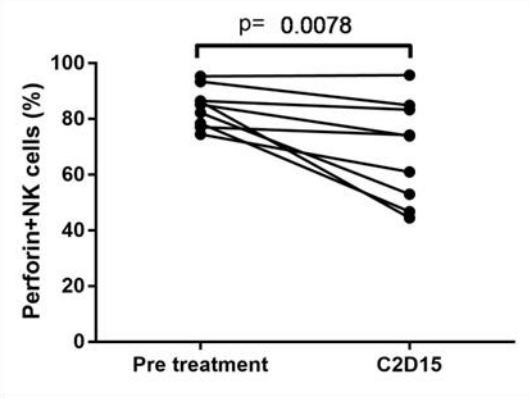

Figure 10.22: Functional changes on NK cells following treatment with daratumumab and durvalumab as assessed by viSNE analysis.

Paired samples compared using Wilcoxon test.

[A] Granzyme expression by NK cells falls following treatment (p=0.0078)
[B] Perforin expression by NK cell falls following treatment (p=0.0078)

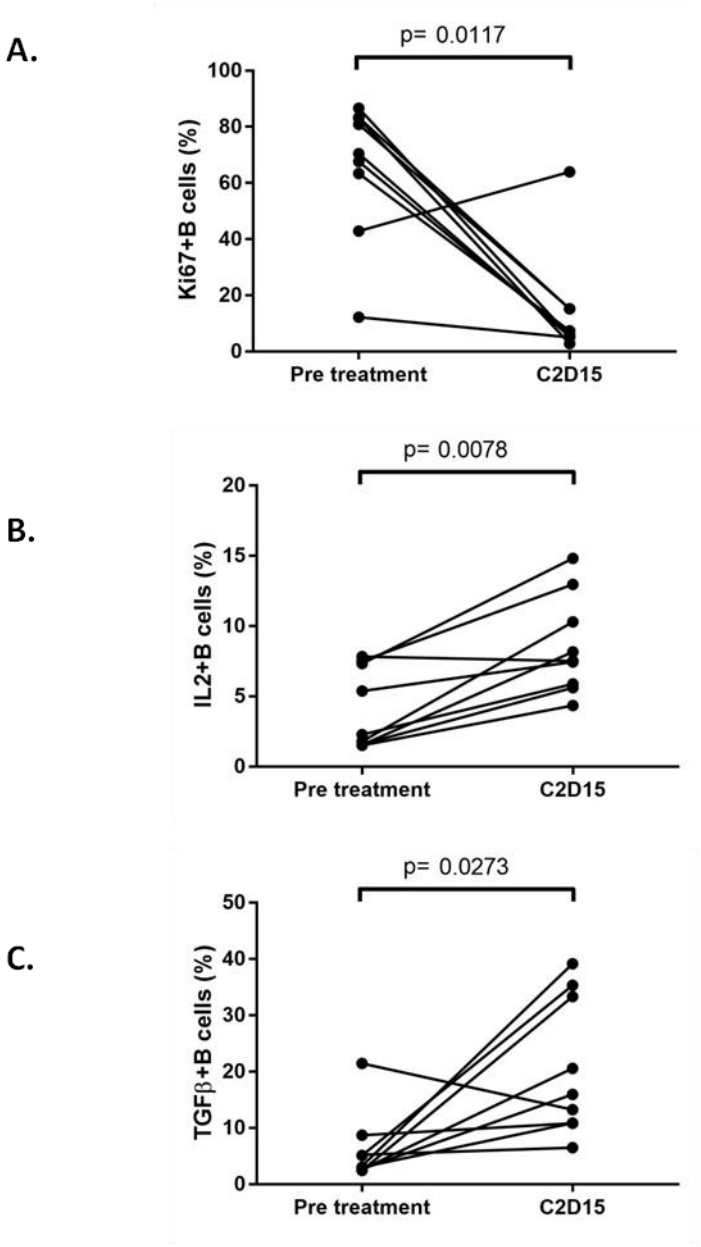

Figure 10.23: Functional changes on B cells following treatment with daratumumab and durvalumab as assessed by viSNE analysis.

Paired samples compared using Wilcoxon test.

[A] B cell Ki67 expression falls following treatment (p=0.0117)
[B] B cell IL2 expression rises following treatment (p=0.0078)
[C] B cell TGFβ expression rises following treatment (p=0.0273)

10.6 Summary of results

1. Following treatment with daratumumab and durvalumab, CD4 and CD8 lymphocyte numbers rise while NK cell and B cell numbers fall.
2. The residual NK cell population is cytokine competent when assessed by CITRUS but shows a loss of cytotoxicity when assessed by viSNE.
3. CD8 populations show an increase in cytotoxic activity with a corresponding fall in PD1 expression
4. CD4 regulatory populations are less proliferative and express less PD1 following treatment
5. B cell subsets have a loss of proliferation accompanied by a rise in pro-tumour cytokine production

10.7 Discussion

This chapter identifies the early immunological changes seen in heavily pre-treated relapsed refractory myeloma patients receiving daratumumab and durvalumab immunotherapy.

A direct comparison between the NDMM and RRMM samples in this work is not possible due to differences in methodology and data analysis techniques. It is clear, however, that PD1 expression persists across multiple cell subsets from the time of myeloma diagnosis to the relapsed refractory setting.

CD8 lymphocytes and NK cells both demonstrate an improvement in functional competency at this early assessment time point. Interestingly CD8 populations show an increase in cytotoxic activity while NK cell show improved cytokine production. This suggests that the NK cell response may be from the $CD56^{bright}$ compartment, which is recognised to be the predominant cytokine producing NK cell subset, however there were insufficient cell numbers in this analysis to confirm that this is the case.

Many of the changes in cell number and function described here have previously been reported in the context of daratumumab therapy [86,144,214]. Importantly the fall in CD8 cells PD1 expression accompanying the increase in cytotoxic activity has not been previously described following daratumumab monotherapy and therefore suggests that this effect is due to the addition of durvalumab.

Since this data has been obtained from an early treatment timepoint it is not yet possible to determine whether these early immunological changes, with the gain of cytotoxic and cytokine production which has the potential to target malignant plasma cells, will translate into clinical efficacy.

10.8 Relevance of work

1. Identifies that dual treatment with daratumumab and durvalumab is associated with an early increase in NK cell and CD8 lymphocyte functional activity
2. Demonstrates a fall in CD8 PD1 expression which has not previously been reported with daratumumab monotherapy

11. General discussion and conclusions

In the preceding chapters I have described the immunological changes across multiple immune subsets seen in newly diagnosed (NDMM) and relapsed refractory (RRMM) multiple myeloma. I have also assessed the impact of combined blockade of CD38 and PDL1 on these defects. I performed this analysis using mass cytometry to maximise the information available.

In the setting of NDMM these immune microenvironment changes include defects in antigen presenting populations, effector and helper lymphocyte populations and NK cells. Importantly these defects are present before treatment has been initiated, have prognostic significance and may be responsible for disease progression from MGUS or asymptomatic myeloma to symptomatic disease.

A recurring theme throughout the chapters of this thesis has been the role of the PD1 axis, with both the receptor PD1 and its ligand PDL1 being upregulated across multiple immune subsets. PD1 expression is known to rise with cellular activation, and is thought to act as a physiological "break" to prevent an uncontrolled immune response leading to unwanted tissue damage or autoimmune disease. This can make the interpretation of PD1 expression data difficult as a healthy, active response to the presence of a malignant cell would be expected to lead to increased PD1 expression. This means that PD1 cannot be used as the sole marker to define cellular exhaustion. This work adds to our understanding of physiological versus pathological PD1 in humans, firstly by demonstrating a functional distinction between $PD1^{int}$ and $PD1^{high}$ expressing CD8 populations, with loss of cytotoxic activity in the $PD1^{high}$ subset, and secondly by identifying functional differences between $PD1^{high}$ CD8 subsets in control and NDMM, with the subset in NDMM having features of exhaustion, indicating that the microenvironmental context is key in determining the behaviour of $PD1^{high}$ expressing CD8 lymphocytes.

The association between expression of PD1 axis receptors and ligands and aberrant functional behaviour in NDMM was also seen in other immune populations. Within the NK cell population increased PD1 expression was observed on the $CD56^{dim}$ subset in NDMM which also demonstrated numerical and functional abnormalities in cytokine production but not cytotoxicity. CD4 lymphocyte populations had increased expression of PDL1 which was not isolated to T regulatory cells and was associated with increased expression of TGFβ expression and reduced proliferation. Plasma cell populations expressed PDL1 and expression levels correlate with TGFβ production. Finally, dendritic cell populations expressed PDL1 and in NDMM were shifted towards a tolerance inducing phenotype.

It was also clear that not all PD1 expressing populations are the same, with populations expressing both PD1 and another checkpoint inhibitor such as LAG3 or TIM3 having distinct patterns of functional behaviour depending on which checkpoint inhibitors were being co-expressed.

Importantly, having features of an active immune response appears to be an important prognostic marker. Within the NK cell subset, NK cell activation correlated with longer duration of survival. Active CD8 cytokine producing population size as identified by CITRUS also correlated with survival, while individuals with both active dendritic cells and CD8 populations also had superior outcomes.

I have also demonstrated that the CD8 subset is able to upregulate markers of cytotoxicity in response to cellular stimulation, suggesting that there is the potential to target these immune defects and restore immunological function at this early disease timepoint.

Since defective immunological response in NDMM correlates with poorer outcome and there is the potential to restore immune function to these cell subsets, this data provides a strong argument for considering multi-lineage immunological damage to represent a form of symptomatic myeloma worthy of treatment. The difficulty remains determining how to identify, in the clinical setting, which patients had sufficient immunological damage to warrant treatment as well as which treatment strategies will be most effective. It may be that drugs targeting the PD1 axis in combination with an immune activating agent such as an IMiD will be an effective strategy at this early disease time point. The issue of identifying which patients will benefit remains unresolved. While a pattern of varied immunological damage affecting multiple cell types can be identified by mass cytometry, this is not a technique which is currently applicable to a clinical setting. Ideally a single marker which can be identified in blood or bone marrow or a simple immunological prognostic score would need to be developed. Possible candidates indentified by this data include PD1 expression, TGFβ expression and markers of NK cell activation. The difficulty, however, remains that myeloma is a diverse disease with different biological and clinical phenotypes and a single strategy to identify and treat those with immunologically symptomatic disease is unlikely to exist. These unanswered questions will be best addressed in the context of a large clinical trial.

Importantly, in the relapsed refractory setting, I have been able to demonstrate that dual treatment with monoclonal antibodies which target the immunological microenvironment in addition to the malignant cell clone are able to generate early functional cytotoxicity and cytokine production signals. While it is not yet known whether this will translate into clinical response it does support the concept that chemotherapy free treatments may be able to

activate immune responses in myeloma and avoid the need for more toxic chemotherapy regimens.

While the field of myeloma therapy has improved considerably in the last decade there still remains a significant treatment and disease morbidity and mortality burden. Since immunological damage is established but demonstrates reversibility at the time of disease diagnosis I would suggest that strategies aimed at restoring immune function at this early disease timepoint should be explored. Simultaneously diminishing tumour burden and restoring immunological control may be one route to curing myeloma.

11.1 Future work

1. Multiparameter phenotyping by mass cytometry of paired blood and bone marrow samples from a large sample of patients with NDMM to determine whether patients with evidence of bone marrow immune dysfunction also have a peripheral blood marker of immune dysfunction which could be used to identify those patients requiring treatment.
2. Sequential multiparameter analysis by mass cytometry of samples from patients with MGUS to identify the immunological changes present as MGUS evolves to myeloma.
3. In-vitro cytotoxicity assays to study the effects of combined immune checkpoint blockade on functional activity of NK cells and CD8 lymphocytes in NDMM in order to identify potentially beneficial therapeutic combinations

12 References

1. Dunn GP, Old LJ, Schreiber RD. The three Es of cancer immunoediting. *Annu Rev Immunol*. 2004;22(4):329-360. doi:10.1146/annurev.immunol.22.012703.104803

2. Chen DS, Mellman I. Oncology meets Immunology : The cancer-immunity cycle. *Immunity*. 2013;39(1):1-10. doi:10.1016/j.immuni.2013.07.012

3. Zitvogel L, Tesniere A, Kroemer G. Cancer despite immunosurveillance: immunoselection and immunosubversion. *Nat Rev Immunol*. 2006;6(10):715-727. doi:10.1038/nri1936

4. Shankaran V, Ikeda H, Bruce AT, et al. IFNγ and lymphocytes prevent primary tumour development and shape tumour immunogenicity. *Nature*. 2001;410(6832):1107-1111. doi:10.1038/35074122

5. Kim R, Emi M, Tanabe K. Cancer immunoediting: From immune surveillance to immune escape. *Immunology*. 2007;121:1-14. doi:10.1016/B978-012372551-6/50066-3

6. Garcia-Lora A, Algarra I, Garrido F. MHC class I antigens, immune surveillance, and tumor immune escape. *J Cell Physiol*. 2003;195(3):346-355. doi:10.1002/jcp.10290

7. Liu J, Hamrouni A, Wolowiec D, et al. Plasma cells from multiple myeloma patients express B7-H1 (PD-L1) and increase expression after stimulation with IFN-γ and TLR ligands via a MyD88-, TRAF6-, and MEK-dependent pathway. *Blood*. 2007;110(1):296-304. doi:10.1182/blood-2006-10-051482

8. Zou W. Regulatory T cells, tumour immunity and immunotherapy. *Nat Rev Immunol*. 2006;6(4):295-307. doi:10.1038/nri1806

9. Cornberg M, Kenney LL, Chen AT, et al. Clonal exhaustion as a mechanism to protect against severe immunopathology and death from an overwhelming CD8T cell response. *Front Immunol*. 2013;4:1-8. doi:10.3389/fimmu.2013.00475

10. Balducci L, Ershler WB. Cancer and ageing: a nexus at several levels. *Nat Rev Cancer*. 2005;5(8):655-662. doi:10.1038/nrc1675

11. Shapiro RS. Malignancies in the setting of primary immunodeficiency: Implications for hematologists/oncologists. *Am J Hematol*. 2011;86(1):48-55. doi:10.1002/ajh.21903

12. Grulich AE, van Leeuwen MT, Falster MO, Vajdic CM. Incidence of cancers in people with HIV / AIDS compared with immunosuppressed transplant recipients: a meta-analysis. *Lancet*. 2007;370:59-67. doi:10.1016/S0140-6736(07)61050-2

13. Buell JF, Gross TG, Woodle ES. Malignancy after transplantation. *Transplantation*. 2005;80(2):S254-S264. doi:10.1097/01.tp.0000186382.81130.ba

14. Fiorino a S, Atac B. Paraproteinemia, plasmacytoma, myeloma and HIV infection. *Leukemia*. 1997;11(12):2150-2156. doi:10.1038/sj.leu.2400875

15. Smyth MJ, Thia KY, Street SE, MacGregor D, Godfrey DI, Trapani JA. Perforin-mediated cytotoxicity is critical for surveillance of spontaneous lymphoma. *J Exp Med*. 2000;192(5):755-760. doi:10.1084/jem.192.5.755

16. Ibrahim EM, Al-Foheidi ME, Al-Mansour MM, Kazkaz GA. The prognostic value of tumor-infiltrating lymphocytes in triple-negative breast cancer: a meta-analysis. *Breast Cancer Res Treat*. 2014;148(3):467-476. doi:10.1007/s10549-014-3185-2

17. Schumacher K, Haensch W, Röefzaad C, Ro C, Schlag PM. Prognostic significance of activated CD8 + T Cell infiltrations within esophageal carcinomas. *Cancer Res*.

2001;61:3932-3936.

18. Eerola A, Soini Y, Pääkkö P. A high humber of tumor-infiltrating lymphocytes are associated with a small tumor size , low tumor stage , and a favorable prognosis in operated small cell lung carcinoma. *Clin Cancer Res*. 2000;6:1875-1881.

19. Park MH, Lee JS, Yoon JH. High expression of CX3CL1 by tumor cells correlates with a good prognosis and increased tumor-infiltrating CD8+ T cells, natural killer cells, and dendritic cells in breast carcinoma. *J Surg Oncol*. 2012;106(4):386-392. doi:10.1002/jso.23095

20. Ishigami S, Natsugoe S, Tokuda K, et al. Clinical impact of intratumoral natural killer cell and dendritic cell infiltration in gastric cancer. *Cancer Lett*. 2000;159:103-108.

21. Villegas FR, Coca S, Villarrubia VG, et al. Prognostic significance of tumor infiltrating natural killer cells subset CD57 in patients with squamous cell lung cancer. *Lung Cancer*. 2002;35(1):23-28. doi:10.1016/S0169-5002(01)00292-6

22. Nakayama S, Yokote T, Akioka T, et al. Infiltration of effector regulatory T cells predicts poor prognosis of diffuse large B-cell lymphoma, not otherwise specified. *Blood Adv*. 2017;1(8):486-493. doi:10.1182/bloodadvances.2016000885

23. Allaoui R, Hagerling C, Desmond E, Warfvinge CF, Jirström K, Leandersson K. Infiltration of γδ T cells, IL-17 + T cells and FoxP3 + T cells in human breast cancer. *Cancer Biomarkers*. 2017;20(4):395-409. doi:10.3233/CBM-170026

24. Hermans C, Anz D, Engel J, Kirchner T, Endres S, Mayr D. Analysis of FoxP3+ T-regulatory cells and CD8+T-Cells in ovarian carcinoma: Location and tumor infiltration patterns are key prognostic markers. *PLoS One*. 2014;9(11):1-9. doi:10.1371/journal.pone.0111757

25. Fu J, Xu D, Liu Z, et al. Increased Regulatory T Cells Correlate With CD8 T-Cell Impairment and Poor Survival in Hepatocellular Carcinoma Patients. *Gastroenterology*. 2007;132(7):2328-2339. doi:10.1053/j.gastro.2007.03.102

26. Barua S, Fang P, Sharma A, et al. Spatial interaction of tumor cells and regulatory T cells correlates with survival in non-small cell lung cancer. *Lung Cancer*. 2018;117(713):73-79. doi:10.1016/j.lungcan.2018.01.022

27. Schietinger A, Greenberg PD. Tolerance and exhaustion: Defining mechanisms of T cell dysfunction. *Trends Immunol*. 2014;35(2):51-60. doi:10.1016/j.it.2013.10.001

28. Wherry EJ, Blattman JN, Murali-Krishna K, van der Most R, Ahmed R. Viral persistence alters CD8 T-cell immunodominance and tissue distribution and results in distinct stages of functional impairment. *J Virol*. 2003;77(8):4911-4927. doi:10.1128/JVI.77.8.4911

29. Wherry EJ, Kurachi M. Molecular and cellular insights into T cell exhaustion. *Nat Rev Immunol*. 2015;15(8):486-499. doi:10.1038/nri3862

30. Riches JC, Davies JK, McClanahan F, et al. T cells from CLL patients exhibit features of T-cell exhaustion but retain capacity for cytokine production. *Blood*. 2013;121(9):1612-1621. doi:10.1182/blood-2012-09-457531

31. McClanahan F, Riches JC, Miller S, et al. Mechanisms of PD-L1/PD-1 mediated CD8 T-cell dysfunction in the context of aging-related immune defects in the Eμ-TCL1 CLL mouse model. *Blood*. 2015;126(2):212-221. doi:10.1182/blood-2015-02-626754

32. McClanahan F, Hanna B, Miller S, et al. PD-L1 checkpoint blockade prevents immune dysfunction and leukemia development in a mouse model of chronic lymphocytic leukemia. *Blood*. 2015;126(2):203-212. doi:10.1182/blood-2015-01-622936

33. The International Agency for Research on Cancer. *WHO Classification of Tumours of Haematopoietic and Lymphoid Tissue (IARC WHO Classification of Tumours)*. 4th Editio. (Swerdlow S, Campo E, Harris NL, et al., eds.). World Health Organization; 2008.

34. Rajkumar SV, Dimopoulos MA, Palumbo A, et al. International Myeloma Working Group updated criteria for the diagnosis of multiple myeloma. *Lancet Oncol*. 2014;15(12):e538-e548. doi:10.1016/S1470-2045(14)70442-5

35. Kristinsson SY, Tang M, Pfeiffer RM, et al. Monoclonal gammopathy of undetermined significance and risk of infections: A population-based study. *Haematologica*. 2012;97(6):854-858. doi:10.3324/haematol.2011.054015

36. Blimark C, Holmberg E, Mellqvist UH, et al. Multiple myeloma and infections: A population-based study on 9253 multiple myeloma patients. *Haematologica*. 2015;100(1):107-113. doi:10.3324/haematol.2014.107714

37. Solomon T, Racheta B, Whitehead S, Coleman MP. *Office for National Statistics Statistical Bulletin: Cancer Survival in England Patients Diagnosed: 2007-2011 and Followed up to 2012*.; 2013.

38. Keats JJ, Chesi M, Egan JB, et al. Clonal competition with alternating dominance in multiple myeloma. *Blood*. 2012;120(5):1067-1077. doi:10.1182/blood-2012-01-405985

39. Riccardi A, Mora O, Tinelli C, et al. Long-term survival of stage I multiple myeloma given chemotherapy just after diagnosis or at progression of the disease: a multicentre randomized study. Cooperative Group of Study and Treatment of Multiple Myeloma. *Br J Cancer*. 2000;82(7):1254-1260. doi:10.1054/bjoc.1999.1087

40. Mateos M-V, Hernández M-T, Giraldo P, et al. Lenalidomide plus Dexamethasone for High-Risk Smoldering Multiple Myeloma. *N Engl J Med*. 2013;369(5):438-447. doi:10.1056/NEJMoa1300439

41. Attal M, Harousseau J, Stoppa A, et al. A prospective, randomized trial of autologous bone marrow transplantation and chemotherapy in multiple myeloma. *N Engl J Med*. 1996;355(2):91-97. doi:10.1056/NEJM199607113350204

42. Bruno B, Rotta M, Patriarca F, et al. A Comparison of Allografting with Autografting for Newly Diagnosed Myeloma. *N Engl J Med*. 2007;356(11):1110-1120. doi:10.1056/NEJMoa065464

43. Gahrton G, Tura S, Ljungman P, et al. Prognostic factors in allogeneic bone marrow transplantation for multiple myeloma. *J Clin Oncol*. 1995;13(6):1312-1322.

44. National Institute for Health and Care Excellence (NICE). *TA311: NICE Guidance on Bortezomib for Induction Therapy in Multiple Myeloma before High-Dose Chemotherapy and Autologous Stem-Cell Transplantation*.; 2014. doi:10.1016/s1470-2045(14)70184-6

45. National Institute for Health and Care Excellence (NICE). *TA228: Bortezomib and Thalidomide for the First Line Treatment of Multiple Myeloma*.; 2011.

46. National Institute for Health and Care Excellence (NICE). *TA129: Bortezomib Monotherapapy for Relapsed for Relapsed Multiple Myeloma*.; 2007. https://www.nice.org.uk/guidance/ta129/resources/bortezomib-monotherapy-for-relapsed-multiple-myeloma-pdf-82598141743045.

47. National Institute for Health and Care Excellence (NICE). *TA573: Daratumumab with Bortezomib and Dexamethasone for Previously Treated Multiple Myeloma*.; 2019.

48. National Institute for Health and Care Excellence (NICE). *TA505: Ixazomib with*

Lenalidomide and Dexamethasone for Treating Relapsed or Refractory Multiple Myeloma.; 2018.

49. National Institute for Health and Care Excellence (NICE). *TA427: Pomalidomide for Relapsed and Refractory Multiple Myeloma Previously Treated with Lenalidomide and Bortezomib*.; 2017.

50. National Institute for Health and Care Excellence (NICE). *TA171: Lenalidomide for the Treatment of Multiple Myeloma in People Who Have Received at Least One Prior Therap*.; 2009.

51. National Institute for Health and Care Excellence (NICE). *TA457: Carfilzomib for Previously Treated Multiple Myeloma*.; 2017. https://www.nice.org.uk/guidance/ta457/resources/carfilzomib-for-previously-treated-multiple-myeloma-pdf-82604850129349.

52. National Institute for Health and Care Excellence (NICE). *TA380: Panobinostat for Treating Multiple Myeloma after at Least 2 Previous Treatments*.; 2016.

53. National Institute for Health and Care Excellence (NICE). *TA510: Daratumumab Monotherap for Treating Relapsed and Refractory Multiple Myeloma*.; 2018.

54. Singh PP, Kumar SK, LaPlant BR, et al. Lenalidomide maintenance therapy In multiple myeloma: A meta-analysis of randomized trials. *Blood*. 2013;122:407.

55. Ludwig H, Durie BGM, McCarthy P, et al. IMWG consensus on maintenance therapy in multiple myeloma. *Blood*. 2012;119(13):3003-3015. doi:10.1182/blood-2011-11-374249

56. Kyle RA, Therneau TM, Rajkumar SV, et al. A long-term study of prognosis in monocloncal gammopathy of undetermined significance. *N Engl J Med*. 2002;346(8):564-569.

57. Dhodapkar M V, Krasovsky J, Osman K, Geller MD. Vigorous premalignancy-specific effector T cell response in the bone marrow of patients with monoclonal gammopathy. *J Exp Med*. 2003;198(11):1753-1757. doi:10.1084/jem.20031030

58. Fonseca R, Bailey RJ, Ahmann GJ, et al. Genomic abnormalities in monoclonal gammopathy of undetermined significance. *Blood*. 2002;100(4):1417-1424. http://www.bloodjournal.org/content/bloodjournal/100/4/1417.full.pdf.

59. Schumacher TN, Schreiber RD. Neoantigens in cancer immunotherapy. *Science (80-)*. 2015;348(6230):69-74. doi:10.1126/science.aaa4971

60. Fratta E, Coral S, Covre A, et al. The biology of cancer testis antigens: Putative function, regulation and therapeutic potential. *Mol Oncol*. 2011;5(2):164-182. doi:10.1016/j.molonc.2011.02.001

61. López-Díaz de Ceria A, Zabalegui N, Rodríguez-Calvillo M, Inogés S, Bendandi M. Anti-idiotype antibodies in cancer treatment. *Oncogene*. 2007;26(25):3594-3602. doi:10.1038/sj.onc.1210371

62. Walz S, Stickel JS, Kowalewski DJ, et al. The antigenic landscape of multiple myeloma : mass spectrometry (re) defines targets for T-cell – based immunotherapy. *Blood*. 2015;126:1203-1214. doi:10.1182/blood-2015-04-640532.S.W.

63. Zheng MM, Zhang Z, Bemis K, et al. The Systemic Cytokine Environment Is Permanently Altered in Multiple Myeloma. *PLoS One*. 2013;8(3):e58504. doi:10.1371/journal.pone.0058504

64. Dianzani U, Pileri A, Boccadoro M, et al. Activated idiotype-reactive cells in suppressor/cytotoxic subpopulations of monoclonal gammopathies: correlation with diagnosis and disease status. *Blood*. 1988;72(3):1064-1068. http://www.ncbi.nlm.nih.gov/pubmed/2970872.

65. Kay NE, Leong TL, Bone N, et al. Blood levels of immune cells predict survival in myeloma patients: results of an Eastern Cooperative Oncology Group phase 3 trial for newly diagnosed multiple myeloma patients. *Blood*. 2001;98(1):23-28. doi:10.1182/blood.V98.1.23

66. Massaia M, Dianzani U, Bianchi A, Camponi A, Boccadoro M, Pileri A. Defective generation of alloreactive cytotoxic T lymphocytes (CTL) in human monoclonal gammopathies. *Clin Exp Immunol*. 1988;73(2):214-218. http://www.ncbi.nlm.nih.gov/pubmed/3263229%5Cnhttp://www.pubmedcentral.nih.gov/articlerender.fcgi?artid=PMC1541589.

67. Bryant C, Suen H, Brown R, et al. Long-term survival in multiple myeloma is associated with a distinct immunological profile, which includes proliferative cytotoxic T-cell clones and a favourable Treg/Th17 balance. *Blood Cancer J*. 2013;3:e148. doi:10.1038/bcj.2013.34

68. Sze DM, Giesajtis G, Brown RD, et al. Clonal cytotoxic T cells are expanded in myeloma and reside in the CD8+ CD57+ CD28- compartment. *Blood*. 2001;98(9):2817-2828.

69. Raitakari M, Brown RD, Sze D, et al. T-cell expansions in patients with multiple myeloma have a phenotype of cytotoxic T cells. *Br J Haematol*. 2000;110(1):203-209. doi:10.1046/j.1365-2141.2000.02131

70. Moss P, Gillespie G, Frodsham P, Bell J, Reyburn H. Clonal populations of CD4+ and CD8+ T cells in patients with multiple myeloma and paraproteinemia. *Blood*. 1996;87(8):3297-3306. http://www.ncbi.nlm.nih.gov/pubmed/8605346.

71. Benson DM, Bakan CE, Mishra A, et al. The PD-1 / PD-L1 axis modulates the natural killer cell versus multiple myeloma effect : a therapeutic target for CT-011 , a novel monoclonal anti – PD-1 antibody. *Blood*. 2010;116(13):2286-2294. doi:10.1182/blood-2010-02-271874

72. Rosenblatt J, Glotzbecker B. PD-1 blockade by CT-011, anti PD-1 antibody, enhances ex-vivo T cell responses to autologous dendritic/myeloma fusion vaccine. *J Immunother*. 2011;34(5):409-418. doi:10.1097/CJI.0b013e31821ca6ce

73. Görgün G, Samur MK, Cowens KB, et al. Lenalidomide enhances immune checkpoint blockade-induced immune response in multiple myeloma. *Clin Cancer Res*. 2015;21(20):4617-4618. doi:10.1158/1078-0432.CCR-15-0200

74. Paley MA, Kroy DC, Odorizzi PM, et al. Progenitor and terminal subsets of CD8+ T cells cooperate to contain chronic viral infection. *Science (80-)*. 2012;338(6111):1220-1225. doi:10.1126/science.1229620

75. Treon SP, Maimonis P, Bua D, et al. Elevated soluble MUC1 levels and decreased anti-MUC1 antibody levels in patients with multiple myeloma. *Blood*. 2000;96(9):3147-3153. http://www.bloodjournal.org/content/96/9/3147.abstract.

76. Beyer M, Kochanek M, Giese T, et al. In vivo peripheral expansion of naive CD4+CD25high FoxP3+ regulatory T cells in patients with multiple myeloma. *Blood*. 2006;107(10):3940-3949. doi:10.1182/blood-2005-09-3671

77. Brimnes MK, Vangsted AJ, Knudsen LM, et al. Increased level of both CD4+FOXP3+ Regulatory t Cells and CD14+HLA-DR-/low myeloid-derived suppressor cells and

decreased level of dendritic cells in patients with multiple myeloma. *Scand J Immunol*. 2010;72(6):540-547. doi:10.1111/j.1365-3083.2010.02463.

78. Feyler S, von Lilienfeld-Toal M, Jarmin S, et al. CD4(+)CD25(+)FoxP3(+) regulatory T cells are increased whilst CD3(+)CD4(-)CD8(-)alphabetaTCR(+) double negative T cells are decreased in the peripheral blood of patients with multiple myeloma which correlates with disease burden. *Br J Haematol*. 2009;144(5):686-695. doi:10.1111/j.1365-2141.2008.07530

79. Giannopoulos K, Kaminska W, Hus I, Dmoszynska A. The frequency of T regulatory cells modulates the survival of multiple myeloma patients: detailed characterisation of immune status in multiple myeloma. *Br J Cancer*. 2012;106(3):546-552. doi:10.1038/bjc.2011.575

80. Muthu Raja KR, Rihova L, Zahradova L, Klincova M, Penka M, Hajek R. Increased T regulatory cells are associated with adverse clinical features and predict progression in multiple myeloma. *PLoS One*. 2012;7(10). doi:10.1371/journal.pone.0047077

81. Muthu Raja KR, Plasil M, Rihova L, Pelcova J, Adam Z, Hajek R. Flow cytometry-based enumeration and functional characterization of CD8 T regulatory cells in patients with multiple myeloma before and after lenalidomide plus dexamethasone treatment. *Cytom Part B - Clin Cytom*. 2014;86(4):220-228. doi:10.1002/cyto.b.21109

82. Coiffier B, Lepage E, Briere J, et al. CHOP chemotherapy plus rituximab compared with CHOP alone in elderly patients with diffuse large-B-cell lymphoma. *N Engl J Med*. 2002;346(4):235-242. doi:10.1056/NEJMoa011795

83. Plesner T, Arkenau HT, Gimsing P, et al. Phase 1/2 study of daratumumab, lenalidomide, and dexamethasone for relapsed multiple myeloma. *Blood*. 2016;128(14):1821-1828. doi:10.1182/blood-2016-07-726729

84. Palumbo A, Chanan-Khan A, Weisel K, et al. Daratumumab, Bortezomib, and Dexamethasone for Multiple Myeloma. *N Engl J Med*. 2016;375(8):754-766. doi:10.1056/NEJMoa1606038

85. Lonial S, Dimopoulos M, Palumbo A, et al. Elotuzumab Therapy for Relapsed or Refractory Multiple Myeloma. *N Engl J Med*. 2015;373(7):621-631. doi:10.1056/NEJMoa1505654

86. Krejcik J, Casneuf T, Nijhof IS, et al. Daratumumab depletes CD38+ immune regulatory cells, promotes T-cell expansion, and skews T-cell repertoire in multiple myeloma. *Blood*. 2016;128(3):384-394. doi:10.1182/blood-2015-12-687749

87. Chapuy CI, Nicholson RT, Aguad MD, et al. Resolving the daratumumab interference with blood compatibility testing. *Transfusion*. 2015;55(6):1545-1554. doi:10.1111/trf.13069

88. Ramadoss NS, Schulman AD, Choi SH, et al. An anti-B cell maturation antigen bispecific antibody for multiple myeloma. *J Am Chem Soc*. 2015;137(16):5288-5291. doi:10.1021/jacs.5b01876

89. Hipp S, Tai Y-T, Blanset D, et al. A novel BCMA/CD3 bispecific T-cell engager for the treatment of multiple myeloma induces selective lysis in vitro and in vivo. *Leukemia*. 2017;31(8):1743-1751. doi:10.1038/leu.2016.388

90. Zou J, Chen D, Zong Y, et al. Immunotherapy based on bispecific T-cell engager with hIgG1 Fc sequence as a new therapeutic strategy in multiple myeloma. *Cancer Sci*. 2015;106(5):512-521. doi:10.1111/cas.12631

91. Greaves P, Gribben JG. The role of B7 family molecules in hematologic malignancy. *Blood*. 2013;121(5):734-744. doi:10.1182/blood-2012-10-385591

92. McClanahan F, Sharp TG, Gribben JG. Catching up with solid tumor oncology: What is the evidence for a prognostic role of programmed cell death-ligand 1/programmed cell death-1 expression in B-cell lymphomas? *Haematologica*. 2016;101(10):1144-1158. doi:10.3324/haematol.2016.145904

93. Lesokhin AM, Ansell SM, Armand P, et al. Nivolumab in patients with relapsed or refractory hematologic malignancy: Preliminary results of a phase Ib study. *J Clin Oncol*. 2016;34(23):2698-2704. doi:10.1200/JCO.2015.65.9789

94. Kearl TJ, Jing W, Gershan JA, Johnson BD. PD-1/PD-L1 blockade after transient lymphodepletion to treat myeloma. *J Immunol*. 2013;190(11):5620-5628. doi:10.1038/jid.2014.371

95. Ray A, Das DS, Song Y, et al. Targeting PD1–PDL1 immune checkpoint in plasmacytoid dendritic cell interactions with T cells, natural killer cells and multiple myeloma cells. *Leukemia*. 2015;29:1441-1444. doi:10.1038/leu.2015.11

96. Miguel JS, Mateos M-V, Shah JJ, et al. Pembrolizumab in Combination with Lenalidomide and Low-Dose Dexamethasone for Relapsed/Refractory Multiple Myeloma (RRMM): Keynote-023. *Blood*. 2015;126:505. http://www.bloodjournal.org/content/126/23/505?sso-checked=true.

97. Ocio EM, Shah J, Jagannath S, et al. Pembrolizumab in combination with pomalidomide and low-dose dexamethasone in refractory or relapsed and refractory multiple myeloma (rrMM): Randomized, phase 3 KEYNOTE-183 study. *Ann Oncol*. 2017;27(Sup 6):313.

98. Mateos M-V, Blacklock H, Schjesvold F, Oriol A, Simpson D, George A. Pembrolizumab plus pomalidomide and dexamethasone for patients with relapsed or refractory multiple myeloma (KEYNOTE-183): a randomised, open-label, phase 3 trial. *Lancet Haematol*. 2019;6(19):459.

99. Usmani SZ, Schjesvold F, Oriol A, Karlin L, Cavo M, Rifkin RM. Pembrolizumab plus lenalidomide and dexamethasone for patients with treatment-naive multiple myeloma (KEYNOTE-185): a randomised, open-label, phase 3 trial. *Lancet Haematol*. 2019;6(9):448.

100. Jing W, Gershan JA, Weber J, et al. Combined immune checkpoint protein blockade and low dose whole body irradiation as immunotherapy for myeloma. *J Immunother cancer*. 2015;3(1):2. doi:10.1186/s40425-014-0043-z

101. Barber A, Zhang T, Megli CJ, Wu J, Meehan KR, Sentman CL. Chimeric NKG2D receptor-expressing T cells as an immunotherapy for multiple myeloma. *Exp Hematol*. 2008;36(10):1318-1328. doi:10.1016/j.exphem.2008.04.010

102. Carpenter RO, Evbuomwan MO, Pittaluga S, et al. B-cell maturation antigen is a promising target for adoptive T-cell therapy of multiple myeloma. *Clin Cancer Res*. 2013;19(8):2048-2060. doi:10.1158/1078-0432.CCR-12-2422

103. Chu J, Deng Y, Benson DM, et al. CS1-specific chimeric antigen receptor (CAR)-engineered natural killer cells enhance in vitro and in vivo antitumor activity against human multiple myeloma. *Leukemia*. 2014;28(4):917-927. doi:10.1038/leu.2013.279

104. Mihara K, Bhattacharyya J, Kitanaka A, et al. T-cell immunotherapy with a chimeric receptor against CD38 is effective in eliminating myeloma cells. *Leukemia*. 2012;26(2):365-367. doi:10.1038/leu.2011.205

105. Gogishvili T, Danhof S, Prommersberger S, et al. SLAMF7-CAR T-cells eliminate myeloma and confer selective fratricide of SLAMF7(+) normal lymphocytes. *Blood*. 2017;130(26):2838-2847. doi:10.1182/blood-2017-04-778423

106. Ali SA, Shi V, Maric I, et al. T cells expressing an anti – B-cell maturation antigen chimeric antigen receptor cause remissions of multiple myeloma. *Blood*. 2016;128(13):1688-1701. doi:10.1182/blood-2016-04-711903

107. Szmania S, Garg TK, Lapteva N, et al. Ex vivo expanded natural killer cells demonstrate robust proliferation in vivo in high-risk relapsed multiple myeloma (MM) patients. *J Immunother*. 2015;38(1):24-36. doi:10.1097/CJI.0000000000000059

108. Leivas A, Perez-Martinez A, Blanchard MJ, et al. Novel treatment strategy with autologous activated and expanded natural killer cells plus anti-myeloma drugs for multiple myeloma. *Oncoimmunology*. 2016;5(12). doi:10.1080/2162402X.2016.1250051

109. Shah N, Martin-Antonio B, Yang H, et al. Antigen Presenting Cell-Mediated Expansion of Human Umbilical Cord Blood Yields Log-Scale Expansion of Natural Killer Cells with Anti-Myeloma Activity. *PLoS One*. 2013;8(10):e76781. doi:10.1371/journal.pone.0076781

110. Alici E, Sutlu T, Björkstrand B, et al. Autologous antitumor activity by NK cells expanded from myeloma patients using GMP-compliant components. *Blood*. 2011;111(6):3155-3162. doi:10.1182/blood-2007-09-110312

111. Carmon L, Avivi I, Kovjazin R, et al. Phase I/II study exploring ImMucin, a pan-major histocompatibility complex, anti-MUC1 signal peptide vaccine, in multiple myeloma patients. *Br J Haematol*. 2015;169(1):44-56. doi:10.1111/bjh.13245

112. Hobo W, Strobbe L, Maas F, et al. Immunogenicity of dendritic cells pulsed with MAGE3, Survivin and B-cell maturation antigen mRNA for vaccination of multiple myeloma patients. *Cancer Immunol Immunother*. 2013;62(8):1381-1392. doi:10.1007/s00262-013-1438-2

113. Hong S, Li H, Qian J, Yang J, Lu Y, Yi Q. Optimizing dendritic cell vaccine for immunotherapy in multiple myeloma: Tumour lysates are more potent tumour antigens than idiotype protein to promote anti-tumour immunity. *Clin Exp Immunol*. 2012;170(2):167-177. doi:10.1111/j.1365-2249.2012.04642

114. Yi Q, Szmania S, Freeman J, et al. Optimizing dendritic cell-based immunotherapy in multiple myeloma: Intranodal injections of idiotype-pulsed CD40 ligand-matured vaccines led to induction of type-1 and cytotoxic T-cell immune responses in patients. *Br J Haematol*. 2010;150(5):554-564. doi:10.1111/j.1365-2141.2010.08286

115. Zahradova L, Mollova K, Ocadlikova D, et al. Efficacy and safety of Id-protein-loaded dendritic cell vaccine in patients with multiple myeloma – Phase II study results. *Neoplasma*. 2012;59(4):440-449.

116. Rosenblatt J, Avivi I, Vasir B, et al. Vaccination with dendritic cell/tumor fusions following autologous stem cell transplant induces immunologic and clinical responses in multiple myeloma patients. *Clin Cancer Res*. 2015;19(13):3640-3648. doi:10.1158/1078-0432.CCR-13-3047

117. Ahmad I, LeBlanc R, Cohen S, et al. Favorable long-term outcome of patients with multiple myeloma using a frontline tandem approach with autologous and non-myeloablative allogeneic transplantation. *Bone Marrow Transplant*. 2016;51(4):529-535. doi:10.1038/bmt.2015.319

118. Gorman J V., Colgan JD. Regulation of T cell responses by the receptor molecule Tim-3.

Immunol Res. 2014;59(1-3):56-65. doi:10.1007/s12026-014-8524-1

119. Triebel F. LAG-3: A regulator of T-cell and DC responses and its use in therapeutic vaccination. *Trends Immunol*. 2003;24(12):619-622. doi:10.1016/j.it.2003.10.001

120. Bardhan K, Anagnostou T, Boussiotis VA. The PD1: PD-L1/2 pathway from discovery to clinical implementation. *Front Immunol*. 2016;7:550. doi:10.3389/fimmu.2016.00550

121. Walker LSK. Treg and CTLA-4: Two intertwining pathways to immune tolerance. *J Autoimmun*. 2013;45:49-57. doi:10.1016/j.jaut.2013.06.006

122. Sugamura K, Ishii N, Weinberg AD. Therapeutic targeting of the effector T-cell co-stimulatory molecule OX40. *Nat Rev Immunol*. 2004;4(6):420-431. doi:10.1038/nri1371

123. López-Soto A, Huergo-Zapico L, Acebes-Huerta A, Villa-Alvarez M, Gonzalez S. NKG2D signaling in cancer immunosurveillance. *Int J Cancer*. 2015;136(8):1741-1750. doi:10.1002/ijc.28775

124. Morisaki T, Onishi H, Katano M. Cancer immunotherapy using NKG2D and DNAM-1 systems. *Anticancer Res*. 2012;32(6):2241-2247.

125. Waggoner SN, Kumar V. Evolving role of 2B4/CD244 in T and NK cell responses during virus infection. *Front Immunol*. 2012;3:1-7. doi:10.3389/fimmu.2012.00377

126. Callahan MK. Immune checkpoint therapy in melanoma. *Cancer J (United States)*. 2016;22(2):73-80. doi:10.1097/PPO.0000000000000183

127. Gide TN, Wilmott JS, Scolyer RA, Long G V. Primary and acquired resistance to immune checkpoint inhibitors in metastatic melanoma. *Clin Cancer Res*. 2018;24(6):1260-1270. doi:10.1158/1078-0432.CCR-17-2267

128. Ramsay AG, Johnson AJ, Lee AM, et al. Chronic lymphocytic leukemia T cells show impaired immunological synapse formation that can be reversed with an immunomodulating drug. *J Clin Invest*. 2008;118(7):2427-2437. doi:10.1172/JC135017

129. Görgün G, Holderried TAW, Zahrieh D, Neuberg D, Gribben JG. Chronic lymphocytic leukemia cells induce changes in gene expression of CD4 and CD8 T cells. *J Clin Investig*. 2005;115(7):1797-1805. doi:10.1172/JCI24176DS1

130. Gassner FJ, Zaborsky N, Catakovic K, et al. Chronic lymphocytic leukaemia induces an exhausted T cell phenotype in the TCL1 transgenic mouse model. *Br J Haematol*. 2015;170(4):515-522. doi:10.1111/bjh.13467

131. Hulspas R, Gorman MRGO, Wood BL, Gratama JW, Sutherland DR. Considerations for the control of background fluorescence in clinical flow cytometry. *Cytom Part B - Clin Cytom*. 2009;76B:355-364. doi:10.1002/cyto.b.20485

132. Feng C, Baranov VI, Winnik MA. Gold-nanoparticle coated La, Tb-encoded PS beads and their application in investigating the performance of the inductively coupled plasma of a mass cytometer. *JAAS*. 2013;28:1475-1484. doi:10.1039/c3ja50149c

133. Fluidigm Corporation. *CyTOF ® 2 Mass Cytometer User Manual*.

134. Bendall SC, Simonds EF, Qiu P, et al. Single-cell mass cytometry of differential immune and drug responses across a human hematopoietic continuum. *Science (80-)*. 2011;332:687-697.

135. Ornatsky O, Bandura D, Baranov V, Nitz M, Winnik MA, Tanner S. Highly multiparametric analysis by mass cytometry. *J Immunol Methods*. 2010;361(1-2):1-20. doi:10.1016/j.jim.2010.07.002

136. Leipold MD, Newell EW, Maecker HT. Multiparameter phenotyping of human PBMCs using mass cytometry. *Methods Mol Biol*. 2015;1343:81-95. doi:10.1007/978-1-4939-2963-4

137. Crowell HL, Zanotelli VRT, Engler S, et al. Compensation of signal spillover in suspension and imaging mass cytometry report compensation of signal spillover in suspension and imaging mass cytometry. *Cell Syst*. 2018;6:612-620. doi:10.1016/j.cels.2018.02.010

138. Finck R, Simonds EF, Jager A, et al. Normalization of mass cytometry data with bead standards. *Cytom Part B - Clin Cytom*. 2013;83A:483-494. doi:10.1002/cyto.a.22271

139. Maecker HT, Trotter J. Flow cytometry controls, instrument setup, and the determination of positivity. *Cytom Part A*. 2006;69A:1037-1042. doi:10.1002/

140. Nicholas KJ, Greenplate AR, Flaherty DK, et al. Multiparameter analysis of stimulated human peripheral blood mononuclear cells : A comparison of mass and fluorescence cytometry. *Cytom Part A*. 2016;89A:271-280. doi:10.1002/cyto.a.22799

141. Levine JH, Simonds EF, Bendall SC, et al. Data-driven phenotypic dissection of AML reveals progenitor- like cells that correlate with prognosis. *Cell*. 2015;162(1):184-197. doi:10.1016/j.cell.2015.05.047

142. Baughn LB, Sachs Z, Noble-Orcutt K, Mitra A, van Ness BG, Linden MA. Phenotypic and functional characterization of a bortezomib resistant multiple myeloma cell line by flow and mass cytometry. *Leuk Lymphoma*. 2017;58(8):1931-1940. doi:10.1080/10428194.2016.1266621.Phenotypic

143. Hansmann L, Blum L, Ju C, Liedtke M, Robinson WH, Davis MM. Mass cytometry analysis shows that a novel memory phenotype B Cell is expanded in multiple myeloma. *Cancer Immunol Res*. 2015;3(6):650-661. doi:10.1158/2326-6066.CIR-14-0236-T

144. Adamns III H, Stevenaert F, Krejcik J, et al. High-parameter mass cytometry (CyTOF) evaluation of relapsed/refractory multiple myeloma (MM) patients treated with daratumumab supports immune modulation as a novel mechanism of action. *Blood*. 2016;128:4521.

145. Strauss-Albee DM, Fukuyama J, Liang EC, et al. Human NK cell repertoire diversity reflects immune experience and correlates with viral susceptibility. *Sci Transl Med*. 2015;7(297):1-6.

146. Qiu P, Simonds EF, Bendall SC, et al. Extracting A Cellular Heirarchy from High-dimensional Cytometry Data with SPADE. *Nat Biotechnol*. 2012;29(10):886-891. doi:10.1038/nbt.1991.Extracting

147. Amir ED, Davis KL, Tadmor MD, et al. viSNE enables visualization of high dimensional single-cell data and reveals phenotypic heterogeneity of leukemia. *Nat Biotechnol*. 2013;31(6):545-552. doi:10.1038/nbt.2594

148. Sean C. Bendall, Nolan GP, Roederer M, Chattopadhyay PK. A Deep Profiler's Guide to Cytometry. *Trends Immunol*. 2013;33(7):323-332. doi:10.1016/j.it.2012.02.010.A

149. Fluidigm Corporation. *Maxpar Panel Designer*.; 2014.

150. Takahashi C, Au-Yeung A, Fuh F, et al. Mass cytometry panel optimization through the designed distribution of signal interference. *Cytom Part A*. 2017;91A:39-47. doi:10.1002/cyto.a.22977

151. Soares A, Govender L, Hughes J, et al. Novel application of Ki67 to quantify antigen-specific in vitro lymphoproliferation. *J Immunol Methods*. 2010;362(1-2):43-50.

doi:10.1016/j.jim.2010.08.007

152. Newell EW, Cheng Y. Mass cytometry: blessed with the curse of dimensionality. *Nat Immunol*. 2016;17(8):890-895. doi:10.1038/ni.3485

153. Bruggner R V, Bodenmiller B, Dill DL, Tibshirani RJ, Nolan GP. Automated identification of stratifying signatures in cellular subpopulations. *Proc Natl Acad Sci U S A*. 2014;111(26):E2770-7. doi:10.1073/pnas.1408792111

154. Bataille R, Jégo G, Robillard N, et al. The phenotype of normal, reactive and malignant plasma cells. Identification of "many and multiple myelomas" and of new targets for myeloma therapy. *Haematologica*. 2006;91(9):1234-1240.

155. Yao W, He JC, Yang Y, et al. The prognostic value of tumor-infiltrating lymphocytes in hepatocellular carcinoma: A systematic review and meta-analysis. *Sci Rep*. 2017;7(1):1-11. doi:10.1038/s41598-017-08128-1

156. Li J, Shayan G, Avery L, et al. Tumor-infiltrating Tim-3+ T cells proliferate avidly except when PD-1 is co-expressed: Evidence for intracellular cross talk. *Oncoimmunology*. 2016;5(10):1-13. doi:10.1080/2162402X.2016.1200778

157. Granier C, Dariane C, Combe P, et al. Tim-3 expression on tumor-infiltrating PD-1+CD8+ T cells correlates with poor clinical outcome in renal cell carcinoma. *Cancer Res*. 2017;77(5):1075-1082. doi:10.1158/0008-5472.CAN-16-0274

158. Li Z, Liu X, Guo R, Wang P. TIM-3 plays a more important role than PD-1 in the functional impairments of cytotoxic T cells of malignant schwannomas. *Tumor Biol*. 2017;39(5):1-10. doi:10.1177/1010428317698352

159. Yang Z, Kim H, Villasboas JC, et al. Expression of Lag-3 defines exhaustion of intratumoral Pd-1 + T Cells and correlates with poor outcome in follicular lymphoma. *Oncotarget*. 2017;8(37):61425-61439. doi:10.1002/hon.2438_128

160. Grosso JF, Goldberg M V, Getnet D, et al. Functionally distinct LAG-3 and PD-1 subsets on activated and chronically stimulated CD8 T cells. *J Immunol*. 2011;182(11):6659-6669. doi:10.4049/jimmunol.0804211.Functionally

161. Bengsch B, Seigel B, Ruhl M, et al. Coexpression of PD-1, 2B4, CD160 and KLRG1 on exhausted HCV-specific CD8+ T cells is linked to antigen recognition and T cell differentiation. *PLoS Pathog*. 2010;6(6):e1000947. doi:10.1371/journal.ppat.1000947

162. Jing W, Gershan JA, Blitzer GC, et al. Adoptive cell therapy using PD-1+ myeloma-reactive T cells eliminates established myeloma in mice. *J Immunother Cancer*. 2017;5(1):1-11. doi:10.1186/s40425-017-0256-z

163. Fernandez-Poma SM, Salas-Benito D, Lozano T, et al. Expansion of tumor-infiltrating CD8+ T cells expressing PD-1 improves the efficacy of adoptive T-cell therapy. *Cancer Res*. 2017;77(13):3672-3684. doi:10.1158/0008-5472.CAN-17-0236

164. Triebel F, Jitsukawa S, Baixeras E, et al. LAG-3, a novel lymphocyte activation gene closely related to CD4. *J Exp Med*. 1990;171:1393-1405.

165. Anderson AC, Joller N, Kuchroo VK. Functions in Immune Regulation. *Immunity*. 2017;44(5):989-1004. doi:10.1016/j.immuni.2016.05.001.Lag-3

166. Gill S, Vasey AE, De Souza A, et al. Rapid development of exhaustion and down-regulation of eomesodermin limit the antitumor activity of adoptively transferred murine natural killer cells. *Blood*. 2012;119(24):5758-5768. doi:10.1182/blood-2012-03-415364

167. Bi J, Tian Z. NK cell exhaustion. *Front Immunol*. 2017;8:1-10. doi:10.3389/fimmu.2017.00760

168. Fauriat C, Long EO, Ljunggren H-G, Bryceson YT. Regulation of human NK-cell cytokine and chemokine production by target cell recognition. *Blood*. 2016;115(11):2167-2177. doi:10.1182/blood-2009-08-238469.A

169. Orange JS. Formation and function of the lytic NK-cell immunological synapse. *Nat Rev Immunol*. 2009;8(9):713-725.

170. Reefman E, Kay JG, Wood SM, et al. Cytokine Secretion Is Distinct from Secretion of Cytotoxic Granules in NK Cells. *J Immunol*. 2010;184(9):4852-4862. doi:10.4049/jimmunol.0803954

171. Medvedev A, Johnsen A, Haux J, et al. Regulation of Fas and Fas-ligand expression in NK cells by cytokines and the involvement of Fas-ligand in NK/LAK cell-mediated cytotoxicity. *Cytokine*. 1997;9(6):394-404.

172. Zamai L, Ahmad M, Bennett IM, Azzoni L, Alnemri ES, Perussia B. Natural Killer (NK) cell–mediated cytotoxicity: Differential use of TRAIL and Fas ligand by immature and mature primary human NK cells. *J Exp Med*. 2002;188(12):2375-2380. doi:10.1084/jem.188.12.2375

173. Zhu Y, Huang B, Shi J. Fas ligand and lytic granule differentially control cytotoxic dynamics of natural killer cell against cancer target. *Oncotarget*. 2016;7(30):47163-47172. doi:10.18632/oncotarget.9980

174. Morvan MG, Lanier LL. NK cells and cancer: You can teach innate cells new tricks. *Nat Rev Cancer*. 2016;16(1):7-19. doi:10.1038/nrc.2015.5

175. Carbone E, Neri P, Mesuraca M, et al. HLA class I, NKG2D, and natural cytotoxicity receptors regulate multiple myeloma cell recognition by natural killer cells. *Blood*. 2015;105(1):251-259. doi:10.1182/blood-2004-04-1422.

176. Bernal M, Garrido P, Jiménez P, et al. Changes in activatory and inhibitory natural killer (NK) receptors may induce progression to multiple myeloma: Implications for tumor evasion of T and NK cells. *Hum Immunol*. 2009;70(10):854-857. doi:10.1016/j.humimm.2009.07.004

177. Von Lilienfeld-Toal M, Frank S, Leyendecker C, et al. Reduced immune effector cell NKG2D expression and increased levels of soluble NKG2D ligands in multiple myeloma may not be causally linked. *Cancer Immunol Immunother*. 2010;59(6):829-839. doi:10.1007/s00262-009-0807-3

178. Fauriat C, Mallet F, Olive D, Costello RT. Impaired activating receptor expression pattern in natural killer cells from patients with multiple myeloma. *Leukemia*. 2006;20(4):732-733. doi:10.1038/sj.leu.2404096

179. El-Sherbiny YM, Meade JL, Holmes TD, et al. The requirement for DNAM-1, NKG2D, and NKp46 in the natural killer cell-mediated killing of myeloma cells. *Cancer Res*. 2007;67(18):8444-8449. doi:10.1158/0008-5472.CAN-06-4230

180. Jurisic V, Srdic T, Konjevic G, Markovic O, Colovic M. Clinical stage-depending decrease of NK cell activity in multiple myeloma patients. *Med Oncol*. 2007;24(3):312-317. doi:10.1007/s12032-007-0007-y

181. Konjević G, Vuletić A, Mirjačić Martinović K, Colović N, Čolović M, Jurišić V. Decreased CD161 activating and increased CD158a inhibitory receptor expression on NK cells underlies impaired NK cell cytotoxicity in patients with multiple myeloma. *J Clin Pathol*.

2016;69(11):1009-1016. doi:10.1136/jclinpath-2016-203614

182. Mace EM, Orange JS. Genetic causes of human NK cell deficiency and their effect on NK cell subsets. *Front Immunol*. 2016;7:1-8. doi:10.3389/fimmu.2016.00545

183. Spinner M, Sanchez L, Hsu A, et al. GATA2 deficiency: A protean disorder of hematopoiesis, lymphatics, and immunity. *Blood*. 2014;123(6):809-821. doi:http://dx.doi.org/10.1182/blood-2013-07-515528

184. Cooper MA, Fehniger TA, Turner SC, et al. Human natural killer cells : a unique innate immunoregulatory role for the CD56 bright subset. *Blood*. 2001;97:3146-3151. doi:10.1182/blood.V97.10.3146

185. Deaglio S, Zubiaur M, Gregorini A, et al. Human CD38 and CD16 are functionally dependent and physically associated in natural killer cells. *Blood*. 2002;99(7):2490-2498. doi:10.1182/blood.V99.7.2490

186. Reid S, Yang S, Brown R, et al. Characterisation and relevance of CD138-negative plasma cells in plasma cell myeloma. *Int J Lab Hematol*. 2010;32(6 PART 1):190-196. doi:10.1111/j.1751-553X.2010.01222.x

187. Ndhlovu LC, Lopez-Verge S, Barbour JD, et al. Tim-3 marks human natural killer cell maturation and suppresses cell-mediated cytotoxicity. *Blood*. 2012;119(16):3734-3743. doi:10.1182/blood-2011-11-392951.

188. Carrega P, Morandi B, Costa R, et al. Natural killer cells infiltrating human nonsmall-cell lung cancer are enriched in CD56 bright CD16 - cells and display an impaired capability to kill tumor cells. *Cancer*. 2008;112(4):863-875. doi:10.1002/cncr.23239

189. Platonova S, Cherfils-Vicini J, Damotte D, et al. Profound coordinated alterations of intratumoral NK cell phenotype and function in lung carcinoma. *Cancer Res*. 2011;71(16):5412-5422. doi:10.1158/0008-5472.CAN-10-4179

190. Vari F, Arpon D, Keane C, et al. Immune evasion via PD-1/PD-L1 on NK cells and monocyte/macrophages is more prominent in Hodgkin lymphoma than DLBCL. *Blood*. 2018;131(16):1809-1819. doi:10.1182/blood-2017-07-796342

191. Alberts B, Johnson A, Lewis J. *Molecular Biology of the Cell*. 4th ed. New York: Garland Science; 2002.

192. Zhu J, Paul WE. CD4 T cells: fates, functions, and faults. *Blood*. 2008;112:1557-1569. doi:10.1182/blood-2008-05-078154.BLOOD

193. Kim H-J, Cantor H. CD4 T-cell subsets and tumor immunity: The helpful and the not-so-helpful. *Cancer Immunol Res*. 2014;2(2):91-98. doi:10.1158/2326-6066.cir-13-0216

194. Prabhala RH, Neri P, Bae JE, et al. Dysfunctional T regulatory cells in multiple myeloma. *Leuk Lymphoma*. 2009;107(1):301-304. doi:10.1182/blood-2005-08-3101

195. Heller KN, Gurer C, Münz C. Virus-specific CD4 + T cells: ready for direct attack. *J Exp Med*. 2006;203(4):805-808. doi:10.1084/jem.20060215

196. Kitano S, Tsuji T, Liu C, et al. Enhancement of tumor-reactive cytotoxic CD4+ T-cell responses after Ipilimumab treatment in four advanced melanoma patients. *Cancer Immunol Res*. 2013;1(4):235-244. doi:10.1158/2326-6066.CIR-13-0068

197. Brown DM, Lampe AT, Workman AM. The differentiation and protective function of cytolytic CD4 T cells in influenza infection. *Front Immunol*. 2016;7:1-8. doi:10.3389/fimmu.2016.00093

198. Spaapen RM, Groen RWJ, Van Den Oudenalder K, et al. Eradication of medullary multiple myeloma by CD4+ cytotoxic human T lymphocytes directed at a single minor histocompatibility antigen. *Clin Cancer Res*. 2010;16(22):5481-5488. doi:10.1158/1078-0432.CCR-10-1340

199. Zhang X, Gao L, Meng K, et al. Characterization of CD4 + T cell-mediated cytotoxicity in patients with multiple myeloma. *Cell Immunol*. 2018;327:62-67. doi:10.1016/j.cellimm.2018.02.009

200. Thiago LS, Perez-Andres M, Balanzategui A, et al. Circulating clonotypic B cells in multiple myeloma and monoclonal gammopathy of undetermined significance. *Haematologica*. 2014;99(1):155-162. doi:10.3324/haematol.2013.092817

201. Pojero F, Casuccio A, Giambanco C, et al. Bone marrow B lymphocytes in multiple myeloma and MGUS: Focus on distribution of naïve cells and memory subsets. *Leuk Res*. 2016;49:51-59.

202. Všianská P, Říhová L, Varmužová T, et al. Analysis of B-cell subpopulations in monoclonal gammopathies. *Clin Lymphoma Myeloma Leuk*. 2015;15(4):e61-71.

203. Bao Y, Cao X. The immune potential and immunopathology of cytokine-producing B cell subsets: A comprehensive review. *J Autoimmun*. 2015;55(1):10-23. doi:10.1016/j.jaut.2014.04.001

204. Sponaas AM, Moharrami NN, Feyzi E, et al. PDL1 expression on plasma and dendritic cells in myeloma bone marrow suggests benefit of targeted anti PD1-PDL1 therapy. *PLoS One*. 2015;10(10):1-8. doi:10.1371/journal.pone.0139867

205. Lino A, Dang V, Lampropoulou V, et al. LAG-3 inhibitory receptor expression identifies immunosuppressive natural regulatory plasma cells. *Immunity*. 2018;49(1):120-133.

206. Salort J De, Sintes J, Llinàs L, Matesanz-Isabel J, Engel P. Expression of SLAM (CD150) cell-surface receptors on human B-cell subsets: from pro-B to plasma cells. *Immunol Lett*. 2011;134(2):129-136.

207. Girolamo D. Expression of TNF-alpha by human plasma cells in chronic inflammation. *J Leukoc Biol*. 1997;61:667-678.

208. Jourdan M, Tarte K, Legouffe E, Brochier J, Rossi J-F, Klein B. Tumor necrosis factor is a survival and proliferation factor for human myeloma cells. *Eur Cytokine Netw*. 1999;10(1):65-70.

209. Ludwig C, Williams DS, Bartlett DB, et al. Alterations in bone marrow metabolism are an early and consistent feature during the development of MGUS and multiple myeloma. *Blood Cancer J*. 2015;5(10):e359-e359file:///C:/Users/FLS/Documents/PhD/0001 P. doi:10.1038/bcj.2015.85

210. Collin M, Mcgovern N, Haniffa M. Human dendritic cell subsets. *Immunology*. 2013;140(1):22-30. doi:10.1111/imm.12117

211. Takenaka M, Quintana F. Tolerogenic dendritic cells. *Semin Immunopathol*. 2017;39(2):113-120.

212. Jelinek T, Hajek R. PD-1/PD-L1 inhibitors in multiple myeloma: The present and the future. *Oncoimmunology*. 2016;5(12):1-11. doi:10.1080/2162402X.2016.1254856

213. Oganesyan V, Gao C, Shirinian L, Wu H, Dall'Acqua WF. Structural characterization of a human Fc fragment engineered for lack of effector functions. *Acta Crystallogr D Biol Crystallogr*. 2008;64(6):700-704.

214. Casneuf T, Xu XS, Iii HCA, et al. Effects of daratumumab on natural killer cells and impact on clinical outcomes in relapsed or refractory multiple myeloma. *Blood Adv*. 2017;1(23):2105. doi:10.1182/bloodadvances.2017006866.

215. Van De Donk NWCJ, Moreau P, Plesner T, et al. Clinical efficacy and management of monoclonal antibodies targeting CD38 and SLAMF7 in multiple myeloma. *Blood*. 2016;127(6):681-696. doi:10.1182/blood-2015-10-646810.infusion-related

216. Keir ME, Butte MJ, Freeman GJ, Sharpe AH. PD-1 and its ligands in tolerance and immunity. *Ann Oncol*. 2008;26:677-704. doi:10.1146/annurev.immunol.26.021607.090331

217. Coquery CM, Erickson LD. Regulatory roles of the Tumor Necrosis Factor receptor BCMA. *Crit Rev Immunol*. 2012;32(4):287-305.

218. Cho S-F, Anderson KC, Tai Y-T. Targeting B Cell Maturation Antigen (BCMA) in multiple myeloma : Potential uses of BCMA-based immunotherapy. *Front Immunol*. 2018;9:1821. doi:10.3389/fimmu.2018.01821